Dissertation
submitted to the
Combined Faculties for the Natural Sciences and for Mathematics
of the Ruperto-Carola University of Heidelberg, Germany
for the degree of
Doctor of Natural Sciences

Put forward by
Msc.-Phys. Univ. Adisorn Adulpravitchai
Born in: Bangkok, Thailand.
Oral Examination: 23 June 2010

A Possible Solution of the Flavor Problem and Radiative Neutrino Masses

Referees:
Prof. Dr. Manfred Lindner
Prof. Dr. Michael G. Schmidt

Zusammenfassung

In dieser Arbeit behandeln wir zwei wichtige Probleme des Standard Modells der Teilchenphysik: das Familien-Problem sowie den Grund für die Kleinheit von Neutrinomassen. Das erste Problem könnte mit der Herkunft nicht-abelscher diskreter Familien-Symmetrien zusammenhängen. Wir diskutieren die Möglichkeit sie von der spontanen Brechung einer kontinuierlichen Familien-Symmetrie, d.h. $SU(2)$ oder $SU(3)$ zu erhalten. Weiter untersuchen wir ihre mögliche Herkunft von einer Orbifold Kompaktifizierung. Wir diskutieren alle diskreten Symmetrien, die man von einem zwei-dimensionalen Orbifold T^2/Z_N erhalten kann. Es sind die Gruppen A_4, S_4, D_4, D_3 und D_6. Wir stellen die Idee vor, die Brechung einer Orbifold GUT mit der von dem Orbifold induzierten Familiensymmetrie zu kombinieren und zeigen die Konstruktion anhand eines sechs-dimensionalen supersymmetrischen $SO(10) \times S_4$ orbifold GUT Modells. Zur Erklärung der zweiten Frage schlagen wir ein Ein-Schleifen Neutrino-Massen Modell im Rahmen links-rechts symmetrischer Modelle vor. Wir beobachteten, daß die Hierarchie von den geladenen Lepton-Massen zu den recht-händigen Neutrino-Massen übertragen wird, was wir als "die radiative Übermittlung der Lepton Familien Hierarchy" bezeichnen. Schließlich, haben wir die phänomenologischen Aspekte des Modells untersucht, wie Lepton Familien Verletzung, Familien Zahl Verletzung und Familien ändernde neutrale Ströme.

Abstract

In this thesis, we discuss two important problems of the Standard Model of Particle Physics (SM), namely the flavor problem and the reason for the smallness of neutrino masses. The first one might be related to the origin of non-abelian discrete flavor symmetries. We discuss the possibility of obtaining them from an underlying continuous flavor symmetry, i.e. $SU(2)$ or $SU(3)$ through spontaneous symmetry breaking. Moreover, we investigate their possible origin from an orbifold compactification. We discuss all non-abelian discrete symmetries, which can arise from an orbifold T^2/Z_N. They are A_4, S_4, D_4, D_3, and D_6. We present the idea of combining the breaking of an orbifold GUT and the flavor symmetry arising from the orbifold. We demonstrate the construction in a 6d SUSY $SO(10) \times S_4$. For the second problem, we propose a one-loop neutrino mass model in the left-right symmetric framework. We observe the transmitted hierarchy from the charged lepton masses to the right-handed neutrino masses, which we call "Radiative Transmission of Lepton Flavor Hierarchy". Finally, we study the phenomenological aspects of the model such as lepton flavor violation (LFV), flavor number violation (FNV), and flavor changing neutral currents (FCNCs).

Contents

Chapter 1

Introduction

The Standard Model of Particle Physics (SM) is a great achievement in explaining the interactions of the fundamental particles. Apart from this achievement, the Standard Model is still not complete because, for instance, it does not include an explanation for gravity, the observation of dark matter, dark energy, the baryon asymmetry of the universe, the hierarchy problem, neutrino masses, and the flavor problem. Therefore, there is the need for the SM to be extended and this usually is addressed as Physics Beyond the Standard Model (BSM).

An important implication of BSM is to explain the origin of neutrino masses [1–3]. Assuming that the neutrino is a Majorana particle, the smallness of the neutrino mass can be explained by the seesaw mechanism [4,5], which introduces in its classical version three right-handed (RH) neutrinos with arbitrary Majorana masses additionally to the SM, resulting in the seesaw formula for the light neutrino mass matrix:

$$M_\nu \;=\; -\, m_D M_R^{-1} m_D^T, \tag{1.1}$$

where m_D and M_R are Dirac and Majorana neutrino mass matrices. An alternative way to obtain the smallness of neutrino masses is to forbid a tree-level mass term for neutrino and generate neutrino masses by radiative corrections only, as done in several models [6–11].

Moreover, the peculiar neutrino mixing, which is quite different from quark mixing, implies an underlying symmetry behind the neutrino mass matrix structure. Several mixing patterns have been proposed to explain the neutrino mixing, such as $\mu - \tau$ symmetry [12], the golden ratio prediction for solar neutrino mixing [13–16], or tri-bimaximal mixing (TBM) [17]. These mixing patterns call for a theoretical explanation.

The flavor problem of the SM has two aspects: The first one is the question of what flavor actually is and why there are only three flavors in the SM. And the second is why the parameters of the flavor sector, the fermion masses and the mixing matrices (especially in the neutrino sector), take the values they do. A popular theoretical explanation is to impose a non-abelian discrete flavor symmetry to explain a certain observed mixing pattern. However, the origin of these flavor symmetries is unclear and there are several attempts to find out the origin of these symmetries.

As the SM is constructed based on two main symmetries, which are gauge and space-time symmetries. The minimal extension of the SM might be to extend the gauge sector by imposing the gauge flavor symmetry and assume its breaking by vacuum expectation values (VEV) of a scalar field. However, breaking a continuous flavor gauge group down to a non-abelian discrete subgroup is a highly non-trivial phenomenological task [18]. In particular, for

such a breaking, large representations of the continuous symmetry are needed [19, 20], which cannot couple directly to the small representations in which the three generations of fermions reside. It is thus worthwhile to consider discrete flavor symmetries arising as extensions of the space-time symmetry. In the context of string theory, string selection rules may lead to a discrete flavor symmetry [21–23]. Moreover, in magnetized extra dimensional models, a discrete flavor symmetry may arise from the localization behavior of zero modes [24, 25]. Alternatively, a discrete symmetry might be a remnant of an orbifold compactification [26–29], which we consider in this thesis.

An interesting aspect of BSM are the Grand Unified Theories (GUTs), in which all SM fermions are embedded into a representation of the GUT group. A GUT can explain the quantization of the SM hypercharge and also the unification of the gauge couplings at a high energy scale, the so-called GUT scale, $M_{GUT} \sim 3 \times 10^{16}$. However, breaking a GUT group down to the SM is a highly non-trivial phenomenological task due to the doublet-triplet splitting problem. In the context of an orbifold compactification, this problem can be solved nicely [30–34]: The gauge symmetry is broken by a non-trivial transformation of the gauge fields under the orbifold parities [35, 36]. A flavor symmetry originating from an orbifold compactification has been studied in an orbifold GUT context [37]. Similarly, it is possible to break a flavor symmetry by a non-trivial transformation of the bulk fermions [38] as well as by Wilson lines [39]. Alternatively, the orbifold compactification can generate the alignment of vacuum expectation values (VEVs) of flavons [40] transmitting the flavor symmetry breaking into the fermion mass matrices.

This thesis is organized as follows: In Chapter 2, we review of aspects of model building. In Chapter 3, we present flavor symmetry models which can explain the neutrino masses and mixing patterns. We also discuss the phenomenology of these models. In Chapter 4, we search for the origin of the non-abelian discrete flavor symmetries, which might arise as subgroups of the continuous symmetries. We restrict ourselves to discuss only the small representations of the flavons which can couple directly to the three generations of fermions at a leading order. From this limited representations, the only non-abelian discrete group which can arise as a residual symmetry is the quaternion group D_2'. However, this group does not have a rich enough structure to predict by itself very specific mixing patterns, such as tri-bimaximal mixing of neutrinos. Therefore, alternative origins of non-abelian discrete symmetries is needed to be investigated, and Chapter 5 is devoted for such the discussion. A non-abelian discrete symmetry can arise as a residual symmetry of the breaking of the Poincaré symmetry in two extra-dimensions by an orbifold compactification. This way is quite promising because the famous non-abelian discrete symmetries such as A_4, S_4, D_4, $D_3 \simeq S_3$, and D_6 which have a rich structure to predict very specific mixing patterns can arise. In Chapter 6, we discuss a flavored orbifold GUT. We show that not only the non-abelian discrete flavor symmetries can arise from the orbifold compactification, but they can be broken by the orbifold as well. Furthermore, this idea can be embedded into a model, in which the GUT group is also broken by the orbifold. We demonstrate this idea in the context of $SO(10) \times S_4$. In Chapter 7, we study a model with an extended scalar sector and a flavor symmetry. The extended scalar sector model leads to lepton flavor violation (LFV) which leads to additional constraints to the parameter space of Physics Beyond the Standard Model. However, when we impose a flavor symmetry to generate a specific structure of the mass matrices, the extended scalar model can be ruled out by the LFV constraint. We demonstrate this idea in the flavor symmetries A_4 and D_4 using the Ma-model as basis, which

is a one-loop neutrino mass model. In Chapter 8, we present a bottom-up one-loop scheme in a left-right symmetric (LR) model, which leads to the effective Ma-model after the LR symmetry is broken. We find the transmission of hierarchies between the charged lepton masses and right-handed neutrino masses. We call this observation, "Radiative Transmission of Lepton Flavor Hierarchies". Moreover, this model has many interesting phenomenological aspects which might be able to show up at the LHC, such as the inert Higgs as a dark matter candidate, new hadronic states, and so on. Finally, we conclude our work in Chapter 9.

This thesis is supplemented by three appendices: In Appendix A, the group theory of non-abelian discrete groups is listed. The mode expansion of a field living on the orbifold is given in Appendix B. In Appendix C, the Higgs sector of models in Chapter 8 is discussed.

Part of this thesis has been published in [18, 29, 41–45].

Chapter 2

Model Building

In this chapter, we briefly discuss some aspects of model building. We first review the Standard Model of Particle Physics. Secondly, we extend the SM to explain the neutrino masses and mixing. Thirdly, we explain the motivation of imposing the flavor symmetries to explain the neutrino mixing patterns. Fourthly, we discuss Supersymmetry (SUSY) as the solution of the hierarchy problem of the scalar sector of the SM. Then we move on to discuss the idea of grand unified theories. Finally, we investigate the ideas of the symmetry breaking from orbifolding.

2.1 Standard Model

In most of this thesis, we will use the left-handed Weyl spinor convention, which is common use in the context of GUTs. Note that only in Chapter 8, we will use the left- and right-handed Dirac spinor convention, which is common use in literature on left-right symmetric model building.
The Standard Model is a Quantum Field Theory based on the gauge symmetry $SU(3)_c \times SU(2)_L \times U(1)_Y$. The SM is a chiral theory, i.e., the left-handed and left-handed conjugate fields transform differently under the gauge group, so that an ordinary Dirac mass term is not allowed by gauge symmetry. In order to give mass to fermions, the left-handed and the left-handed conjugate fermion fields have to couple to a scalar field, the so-called Higgs field, ϕ. When the Higgs field obtains a Vacuum Expectation Value (VEV), the SM gauge group gets broken down to $SU(3)_c \times U(1)_{em}$, and the fermions obtain their masses. The particle content of the SM is given in Table 2.1. Note that the electric charge Q can be written as $Q = T_3 + Y$, where T_3 is the third component of the weak isospin and Y is the hypercharge. The Yukawa couplings of the quarks and charged leptons can be written as

$$\mathcal{L}_Y = y^u_{ij} q^T_i \epsilon \phi u^c_j + y^d_{ij} q^T_i \phi^* d^c_j + y^l_{ij} l^T_i \phi^* e^c_j \,, \tag{2.1}$$

where the Higgs field $\phi = (\phi^+, \phi^0)^T$ transforms under the SM gauge group as $(\underline{\mathbf{1}}, \underline{\mathbf{2}}, +1/2)$ and $\epsilon = i\sigma^2$ is an anti-symmetric 2×2 matrix in $SU(2)_L$ space. After the Higgs obtains its VEV, $\langle \phi \rangle = (0, v)^T$, these Yukawa couplings lead to the fermion mass matrices, $M_{u,d,l} = y^{u,d,l} v$.
In general, the mass matrices are not in a diagonal basis, and therefore we need to transform them into the diagonal basis in which their masses can be read off. A general complex 3×3 matrix as $M_{u,d}$ can be diagonalized by a bi-unitary transformation:

$$U^\dagger_u M_u V_u = \mathrm{diag}(m_u, m_c, m_t) \,, \text{ and } U^\dagger_d M_d V_d = \mathrm{diag}(m_d, m_s, m_b) \,, \tag{2.2}$$

Fields	$(SU(3)_c, SU(2)_L, U(1)_Y)$
$q_i = \begin{pmatrix} u_i \\ d_i \end{pmatrix}$	$(\underline{\mathbf{3}}, \underline{\mathbf{2}}, +1/6)$
u_i^c	$(\bar{\underline{\mathbf{3}}}, \underline{\mathbf{1}}, -2/3)$
d_i^c	$(\bar{\underline{\mathbf{3}}}, \underline{\mathbf{1}}, +1/3)$
$l_i = \begin{pmatrix} \nu_i \\ e_i \end{pmatrix}$	$(\underline{\mathbf{1}}, \underline{\mathbf{2}}, -1/2)$
e_i^c	$(\underline{\mathbf{1}}, \underline{\mathbf{1}}, +1)$

Table 2.1: The particle content of the SM: The index i denotes the i^{th} generation.

where the unitary matrices $U_{u,d}$ and $V_{u,d}$ act on the left-handed and the left-handed conjugate fields, respectively. The matrices $U_{u,d}$ can be calculated from

$$U_u^\dagger M_u M_u^\dagger U_u = \text{diag}(m_u^2, m_c^2, m_t^2) \ , \text{ and } \ U_d^\dagger M_d M_d^\dagger U_d = \text{diag}(m_d^2, m_s^2, m_b^2) \ . \tag{2.3}$$

The CKM matrix, V_{CKM}, originates from the mismatch of these mass bases of the up and down quarks as

$$\mathcal{L} \supset -\frac{g}{\sqrt{2}} u_i^\dagger \sigma^\mu W_\mu^+ (V_{CKM})_{ij} d_j \ , \tag{2.4}$$

where g is the $SU(2)_L$ gauge coupling and $V_{CKM} = U_u^T U_d^*$.
The CKM matrix can be parameterized by three angles, θ_{ij}, and one CP phase, δ as [46]

$$V_{CKM} = \begin{pmatrix} c_{12}c_{23} & s_{12}c_{13} & s_{13}e^{-i\delta} \\ -s_{12}c_{23} - c_{12}s_{23}s_{13}e^{i\delta} & c_{12}c_{23} - s_{12}s_{23}s_{13}e^{i\delta} & s_{23}c_{13} \\ s_{12}s_{23} - c_{12}c_{23}c_{13}e^{i\delta} & -c_{12}s_{23} - s_{12}c_{23}s_{13}e^{i\delta} & c_{23}c_{13} \end{pmatrix} \ , \tag{2.5}$$

where $s_{ij} = \sin\theta_{ij}$ and $c_{ij} = \cos\theta_{ij}$.
The experimental data for quark masses and the CKM matrix is given by [46]

$$\begin{aligned} &m_u = 2.4 \text{ MeV}, \ \ m_c = 1.27 \times 10^3 \text{ MeV}, \ \ m_t = 171.3 \times 10^3 \text{ MeV}, \\ &m_d = 4.75 \text{ MeV}, \ \ m_s = 105 \text{ MeV}, \ \ m_b = 4.20 \times 10^3 \text{ MeV} \\ &\sin\theta_{12}^q = 0.22570, \quad \sin\theta_{23}^q = 0.04150, \quad \sin\theta_{13}^q = 0.00359 \ . \end{aligned} \tag{2.6}$$

2.2 Neutrino Masses and Mixing

Neutrino experiments, which measure differences of square masses as well as mixing angles have shown us that the neutrinos have a tiny mass, and the neutrino mixing shows a very peculiar mixing pattern with two large mixing angles and one small one. The experimental neutrino data is summarized as follows [47]:

$$\begin{aligned} &\Delta m_{21}^2 = \left(7.65^{+0.46}_{-0.40}\right) \cdot 10^{-5} \text{ eV}^2 \quad \text{and} \quad |\Delta m_{31}^2| = \left(2.40^{+0.24}_{-0.22}\right) \cdot 10^{-3} \text{ eV}^2 \\ &\sin^2\theta_{13} \leq 0.040 \ , \quad \sin^2\theta_{23} = 0.50^{+0.13}_{-0.11} \ , \quad \sin^2\theta_{12} = 0.304^{+0.046}_{-0.034} \qquad (2\,\sigma) \ , \end{aligned} \tag{2.7}$$

where Δm_{ij}^2 denotes $m_i^2 - m_j^2$ with $m_{i,j}$ being the neutrino masses. As the sign of Δm_{31}^2 is unknown, it is not clear whether neutrinos follow a normal or an inverted mass ordering.

It has been shown that in the minimal SM there is only one effective dimension-5 operator [48],

$$\mathcal{L}_{\rm dim-5} = \frac{f_{ij}}{2\Lambda}(l_i^T \epsilon\phi)(l_j^T \epsilon\phi) \ , \tag{2.8}$$

which can generate a small neutrino mass given by $f_{ij}v^2/\Lambda$, where Λ is a large effective mass. In fact, there are several ways to realize this operator. A simple way is to introduce three heavy left-handed conjugate neutrinos, ν_i^c, which transform under the SM gauge group as $(\underline{\mathbf{1}}, \underline{\mathbf{1}}, 0)$. This leads to the Yukawa couplings as follow:

$$\mathcal{L}_\nu \supset l_i^T \epsilon\phi \nu_j^c + \frac{1}{2} M_{R,ij} \nu_i^c \nu_j^c \ , \tag{2.9}$$

where $m_D = y^\nu v$ is Dirac mass matrix and M_{ij} is Majorana mass matrix.
Integrating out the heavy left-handed conjugate neutrino leads to a Majorana mass term for the light neutrinos given by

$$M_\nu = -m_D M_R^{-1} m_D^T \ . \tag{2.10}$$

This is known as type-I seesaw mechanism [1–3]. Moreover, if we add a Higgs triplet,

$$\Delta = \begin{pmatrix} \delta^+ & \delta^{++} \\ \delta^0 & -\delta^+ \end{pmatrix} \sim (\underline{\mathbf{1}}, \underline{\mathbf{3}}, +2) \ , \tag{2.11}$$

this leads to the Yukawa coupling

$$\mathcal{L}_\nu \supset y_{ij}^\Delta l_i^T i\sigma^2 \Delta l_j \ . \tag{2.12}$$

After the Higgs triplet obtains a VEV,

$$\Delta = \begin{pmatrix} 0 & 0 \\ v_\Delta & 0 \end{pmatrix} \ , \tag{2.13}$$

this leads to an additional term in Eq.(2.10) as

$$M_\nu = M_{LL} - m_D M_R^{-1} m_D^T \ , \tag{2.14}$$

where $M_{LL} = y^\Delta v_\Delta$, and this situation is known as type-II seesaw mechanism.
As discussed in the quark sector, the charged lepton mass matrix can be diagonalized by a bi-unitary transformation,

$$U_l^\dagger M_l V_l = \mathrm{diag}(m_e, m_\mu, m_\tau) \ , \tag{2.15}$$

where as in the quark sector, U_l can be calculated from

$$U_l^\dagger M_l M_l^\dagger U_l = \mathrm{diag}(m_e^2, m_\mu^2, m_\tau^2) \ . \tag{2.16}$$

In case the neutrino is Dirac type, its mass matrix can be diagonalized by the same way as for the other fermions. However, if the neutrino is Majorana type (their mass matrix is a complex symmetric matrix), it can be diagonalized by a unitary matrix U_ν as,

$$U_\nu^\dagger M_\nu U_\nu^* = \mathrm{diag}(m_1, m_2, m_3) \ , \tag{2.17}$$

where the unitary matrix U_ν can be calculated from $U_\mu^\dagger M_\mu M_\mu^\dagger U_\mu = \mathrm{diag}(m_1^2, m_2^2, m_3^2)$. As in the quark sector, the mismatch of the charged lepton and neutrino bases leads to the lepton mixing matrix given by

$$U_{\rm PMNS} = U_l^T U_\nu^* \ . \tag{2.18}$$

If the neutrino is Dirac type, the $U_{\rm PMNS}$ can be parameterized in the same way as the CKM matrix of the quark sector. However, if the neutrino is of Majorana type, one has to multiply the standard parameterization by two Majorana phases as

$$U_{\rm PMNS} = V \cdot {\rm diag}(e^{i\phi_1}, e^{i\phi_2}, 1) \ , \tag{2.19}$$

where the parameterization of V is given in Eq.(2.5).
In numerical analysis where the mixing matrices are not in the standard parameterization, the mixing angles and the phases can be calculated by [49]

$$\begin{aligned} &\sin(\theta_{13}) = |U_{13}| \ , \ \ \tan(\theta_{12}) = \frac{|U_{12}|}{|U_{11}|} \ , \ \ \tan(\theta_{23}) = \frac{|U_{23}|}{|U_{33}|} \ , \\ &\delta = -{\rm arg}\left(\frac{\frac{U_{11}^* U_{13} U_{31} U_{33}^*}{\cos(\theta_{12})\cos^2(\theta_{13})\cos(\theta_{23})\cos(\theta_{13})} + \cos(\theta_{12})\cos(\theta_{23})\cos(\theta_{13})}{\sin(\theta_{12})\sin(\theta_{23})} \right) \ . \end{aligned} \tag{2.20}$$

In case there are Majorana phases, they can be read off as

$$\phi_1 = -{\rm arg}(e^{i\delta_e} U_{11}^*) \ , \ \text{and} \ \phi_2 = -{\rm arg}(e^{i\delta_e} U_{12}^*) \ , \tag{2.21}$$

where $\delta_e = {\rm arg}(e^{i\delta} U_{13})$.
The CP violation J_{CP} can be calculated by

$$J_{CP} = {\rm Im}(U_{11} U_{12}^* U_{21}^* U_{22}) = {\rm Im}(U_{11} U_{13}^* U_{31}^* U_{33}) = {\rm Im}(U_{22} U_{23}^* U_{32}^* U_{33}) \ . \tag{2.22}$$

There are many proposals to explain the neutrino mixing matrix. Here, we give three interesting proposals which fit nicely with the current experiments:

- $\mu - \tau$ symmetry [12]: $\theta_{23} = \pi/4, \theta_{13} = 0$, and θ_{12} is undetermined.
- Tri-bimaximal mixing [17]: $\theta_{23} = \pi/4, \theta_{13} = 0, (\sin\theta_{12})^2 = 1/3$ (or $\tan\theta_{12} = 1/\sqrt{2}$).
- Golden ratio prediction for solar neutrino mixing [13–16]:
  - (A) $\cot(\theta_{12}) = \varphi$
  - (B) $\cos(\theta_{12}) = \frac{\varphi}{2}$, with the golden ratio $\varphi = \varphi^2 - 1 = \frac{1}{2}(1 + \sqrt{5})$.

$\mu - \tau$ Symmetry

The $\mu - \tau$ symmetry prediction [12] for the neutrino mixing can be obtained from the neutrino mass matrix possessing a $\mu - \tau$ exchange symmetry, i.e., it will not change its form if the second and third columns and rows are exchanged in the charged lepton mass basis.
The corresponding mass matrix reads

$$M_\nu = \begin{pmatrix} a & b & b \\ b & c & d \\ b & d & c \end{pmatrix} \ . \tag{2.23}$$

The neutrino masses are given by

$$m_3 = c - d \ , \ \text{and} \ m_{1,2} = \frac{1}{2}(a + c + d \pm \sqrt{8b^2 + (-a + c + d)^2}) \ . \tag{2.24}$$

This mass matrix leads to maximal atmospheric mixing, $\theta_{23} = \frac{\pi}{4}$, and vanishing θ_{13}. The solar mixing is determined by the parameters in the mass matrix as

$$\tan(2\theta_{12}) = \frac{2\sqrt{2}b}{c+d-a} \,. \tag{2.25}$$

This mass matrix structure can be obtained from non-abelian discrete flavor symmetries, for instance the dihedral groups $D_3 \simeq S_3$ or D_4.

Tri-Bimaximal Mixing

The tri-bimaximal mixing pattern can be parameterized by

$$U_{TBM} = \begin{pmatrix} \frac{2}{\sqrt{6}} & \frac{1}{\sqrt{3}} & 0 \\ -\frac{1}{\sqrt{6}} & \frac{1}{\sqrt{3}} & \frac{1}{\sqrt{2}} \\ -\frac{1}{\sqrt{6}} & \frac{1}{\sqrt{3}} & -\frac{1}{\sqrt{2}} \end{pmatrix} \,. \tag{2.26}$$

The neutrino mass matrix in this case can be written in terms of neutrino masses as

$$\begin{aligned} M_\nu &= U_{TBM} \mathrm{diag}(m_1, m_2, m_3) U_{TBM}^T \,, \\ &= \begin{pmatrix} 2a+b & -a & -a \\ -a & 2a & b-a \\ -a & b-a & 2a \end{pmatrix} \,, \end{aligned} \tag{2.27}$$

where $a = \frac{m_1 - m_2}{3}$ and $b = \frac{m_1 + m_3}{2}$. This mass matrix structure is predictive, since the three mixing angles are fixed from its own structure and it leaves only two free parameters to fit the two neutrino mass square differences given in Eq.(2.7). The underlying flavor symmetries in this case are e.g., S_4 or A_4.

Golden Ratio Prediction for Solar Mixing

There are two proposals that have been made to connect the golden ratio: $\varphi = \varphi^2 - 1 = \frac{1}{2}(1+\sqrt{5})$ to the solar neutrino mixing. The first one is [13–15]

$$\text{(A):} \quad \cot\theta_{12} = \varphi \quad \Rightarrow \sin^2\theta_{12} = \frac{1}{1+\varphi^2} = \frac{2}{5+\sqrt{5}} \quad \simeq 0.276 \,. \tag{2.28}$$

The second possibility is [16]

$$\text{(B):} \quad \cos\theta_{12} = \frac{\varphi}{2} \quad \Rightarrow \sin^2\theta_{12} = \frac{1}{4}(3-\varphi) = \frac{5-\sqrt{5}}{8} \quad \simeq 0.345 \,. \tag{2.29}$$

It can be seen that the both predictions lie within the current 2σ range.
The possibility (A) has first been noted in [13], and was discussed in more detail in [14]. We give an example of the neutrino and charged lepton mass matrices, which can realize (A) as

$$M_\nu = \begin{pmatrix} 0 & a & 0 \\ a & a & 0 \\ 0 & 0 & b \end{pmatrix} \,, \text{ and } M_l = \begin{pmatrix} x & 0 & 0 \\ 0 & y/\sqrt{2} & z/\sqrt{2} \\ 0 & -y/\sqrt{2} & z/\sqrt{2} \end{pmatrix} \,, \tag{2.30}$$

where the solar mixing comes from the neutrino sector, $\cot\theta_{12} = \varphi$, and the atmospheric mixing comes from the charged lepton sector. Note that the flavor symmetry which can realize the prediction in (A) is A_5 symmetry [15], while for (B) the flavor symmetries can be either D_5 or D_{10}, which will be discussed in Section 3.2.

2.3 Flavor Symmetries

As we have seen in the SM, the particle interactions are based on the SM gauge symmetry and the group representations in which the SM fermions reside. Therefore, it might be interesting to apply the same principle to the flavor sector of the SM in which particles in different generations are related by a flavor symmetry.
The flavor symmetry is characterized by being:

- continuous or discrete
- global or local
- abelian or non-abelian.

Continuous flavor symmetries (abelian or non-abelian) such as $U(1)$ [50–52], $SU(2)$ [53, 54], $SO(3)$ [55], and $SU(3)$ [56–58] have been studied in the literature. In case the flavor symmetry is global, there are problems associated with massless Goldstone bosons, when the symmetry is broken spontaneously. However, these problems do not arise in gauge flavor symmetries.

Discrete flavor symmetries are more favored compared to continuous flavor symmetries due to many reasons:

- Their spontaneously breaking does not lead to the massless Goldstone or massive gauge bosons.
- The number of their irreducible representations is finite.
- Non-abelian discrete flavor symmetries can lead to form-diagonalizable neutrino mass matrices, where the mixing parameters are determined by the flavor symmetries, but not the masses.
- Abelian discrete flavor symmetries can be used to forbid or constrain the certain couplings.

The non-abelian discrete flavor symmetries which have been used in the literature for model building are e.g. $D_3 \sim S_3$ [59–81], D_4 [41, 82–84], D_5 [85], D_7 [86], D_{14} [86, 87], A_4 [28, 88–119], $A_5 \sim PSL_2(5)$ [15], T' [120–130], S_4 [131–153], $\Delta(27) \sim (Z_3 \times Z_3') \rtimes Z_3$ [154–158], $PSL_2(7)$ [157, 159, 160], and $T_7 \sim Z_7 \rtimes Z_3$ [161, 162].

2.4 Supersymmetry

Although the SM is very successful, it still suffers from a quadratic divergence in the scalar sector, which is known as the hierarchy problem. There have been many attempts to solve this problem. A popular solution is to introduce a symmetry between bosons and fermions, which is known as Supersymmetry (SUSY). The transformation of fermions to bosons and vice versa are generated by a generator, so-called supercharge Q, with

$$Q|F\rangle = |B\rangle \ , \text{ and } Q|B\rangle = |F\rangle \ . \tag{2.31}$$

From this, we can see that Q must be spinor because both $Q|B\rangle$ and $|F\rangle$ transform like a spinor. The $N = 1$ SUSY algebra of the supercharge is given as follows:

$$\begin{aligned} \{Q_\alpha, \bar{Q}_{\dot{\beta}}\} &= 2(\sigma^\mu)_{\alpha\dot{\beta}} P_\mu \ , \\ \{Q_\alpha, Q_\beta\} &= \{\bar{Q}_\alpha, \bar{Q}_\beta\} = 0 \ , \end{aligned} \tag{2.32}$$

where Q and $\bar{Q}$ are supercharges, and P_μ is the space translation generator. Here, we can see the deep connection between the SUSY generator and the space-time symmetry. In case we extend the space-time symmetry, the SUSY algebra will also be enlarged. For instance, if we begin with $N = 1$ SUSY in a 5-dimensional theory, this will become $N = 2$ SUSY in 4 dimensions [163].

In order to write the supersymmetric Lagrangian, we use the superfield formalism. We define the chiral superfield Φ_i as

$$\Phi_i(y, \theta) = \varphi_i(y) + \sqrt{2}\theta\psi_i(y) + \theta\theta F_i(y), \tag{2.33}$$

where $\varphi_i(y)$ is a scalar component, $\psi_i(y)$ is a (left-handed) Weyl spinor, $F_i(y)$ is an auxiliary field, $y^\mu = x^\mu - i\theta\sigma^\mu\bar{\theta}$, and θ is the Grassmann variable.
We can extend the SM to a supersymmetric version by replacing all SM fields by superfields. Moreover, we need to add another Higgs multiplet to the model because of two main reasons: The first is we need the pair of Higgs chiral multiplets to cancel the gauge anomaly. The second is to give mass to the down quarks and charged leptons since the superpotential is a holomorphic function of chiral superfields and this forbids us to use the charge conjugate of the Higgs as in the SM. Therefore, we work in a two Higgs doublet model (THDM), with Higgs fields $h_{u,d}$. The Yukawa couplings of the minimal supersymmetric standard model (MSSM) read

$$\mathcal{L}_Y = \int d^2\theta \mathrm{W}_Y \ , \tag{2.34}$$

where the superpotential is given by

$$\mathrm{W}_Y = y^u_{ij} q_i^T h_u u_j^c + y^d_{ij} q_i^T h_d d_j^c + y^l_{ij} l_i^T h_d e_j^c + y^\nu_{ij} l_i^T h_u \nu_j^c - \mu h_u h_d \ . \tag{2.35}$$

We note that the SM fields here are chiral superfields.
The F-term of the scalar potential reads

$$V_F = \left| \frac{\partial \mathrm{W}_Y}{\partial \varphi_i} \right| \ , \tag{2.36}$$

where φ_i is the scalar component of a chiral superfield.

2.5 Grand Unified Theories

There are two main hints toward the grand unified theories (GUTs):

- The first is the unified gauge couplings at the GUT scale and
- the second is the explanation of the charge quantization.

Using the Minimal Supersymmetric Standard Model (MSSM) as low energy effective theory and performing the renormalization group evolution of the SM gauge couplings up to the high scale, the SM gauge couplings will meet up at the GUT scale, $M_{\mathrm{GUT}} \sim 3 \times 10^{16}$ GeV. This leads to the suspicion that the SM gauge group might be embedded into a bigger gauge group at the GUT scale. Another hint towards a unified gauge group is the quantization of hypercharge, which satisfies all anomaly constraints. The smallest unified gauge group is $SU(5)$, where quarks and leptons can be grouped into the $\underline{\overline{\mathbf{5}}}$ and $\underline{\mathbf{10}}$ of $SU(5)$. The left-handed conjugate neutrino has to be put in by hand as a singlet under $SU(5)$. However, in

$SU(5)$, the matter content is chosen such that all anomaly constraints are fulfilled. Another attractive candidate for a unified gauge group is the rank-5 $SO(10)$ gauge group, which can group all SM fermions of each flavor including the left-handed conjugate neutrino into a spinor representation, $\underline{\mathbf{16}}$. The seesaw mechanism can be realized naturally due to the existence of the left-handed conjugate neutrino and lead to the smallness of neutrino masses. Furthermore, since the fermions of each flavor are grouped into one $\underline{\mathbf{16}}$ of $SO(10)$, this also explains the quantization of hypercharge.

As $SO(10)$ has rank-5 and the SM gauge group has rank-4, there exist several intermediate symmetries while $SO(10)$ is descending to the SM.
The possible intermediate symmetries are:

- $SU(5)_{GG}$,
- $SU(5) \times U(1)_X$,
- $(SU(5) \times U(1))^{\text{flipped}}$,
- $SU(4) \times SU(2)_L \times SU(2)_R$ [Pati − Salam] ,
- $SU(4) \times SU(2)_L \times U(1)$,
- $SU(3)_c \times SU(2)_L \times SU(2)_R \times U(1)_{B-L}$,

where each breaking chain requires different Higgs representations for its breaking (for a detailed discussion see [164]). We also note that the existence of an intermediate symmetry requires further investigation of the compatibility with gauge coupling unification and proton decay [165].

At the renormalizable level, there are only three types of Higgs representations, i.e. $\underline{\mathbf{10}}_s, \underline{\mathbf{120}}_a$, and $\underline{\overline{\mathbf{126}}}_s$, that can couple to $\Psi_i \sim \underline{\mathbf{16}}_i$ fermions, where i is the flavor index, as can be seen from the following tensor product:

$$\underline{\mathbf{16}} \times \underline{\mathbf{16}} = \underline{\mathbf{10}}_s + \underline{\mathbf{120}}_a + \underline{\mathbf{126}}_s \, . \tag{2.37}$$

The Yukawa couplings read

$$W_Y = y^{10}_{ij} \Psi_i \underline{\mathbf{10}}_s \Psi_j + y^{120}_{ij} \Psi_i \underline{\mathbf{120}}_a \Psi_j + y^{\overline{126}}_{ij} \Psi_i \underline{\overline{\mathbf{126}}}_s \Psi_j \, , \tag{2.38}$$

where the indices a and s refer to the anti-symmetry and symmetry of the Yukawa couplings as

$$y^{10}_{ij} = y^{10}_{ji} \, , \;\; y^{120}_{ij} = -y^{120}_{ji} \, , \text{and} \, , \; y^{\overline{126}}_{ij} = y^{\overline{126}}_{ji} \, . \tag{2.39}$$

Assuming $SO(10)$ is broken through one of the $SU(5)$ breaking chains, the fermion mass matrices can be calculated as [166]

$$M_u = y^{10}_{ij} \langle \underline{\mathbf{5}}(\underline{\mathbf{10}}) \rangle + y^{120}_{ij} \langle \underline{\mathbf{45}}(\underline{\mathbf{120}}) \rangle + y^{\overline{126}}_{ij} \langle \underline{\mathbf{5}}(\underline{\overline{\mathbf{126}}}) \rangle \equiv y^u v_u \tag{2.40}$$

$$M_d = y^{10}_{ij} \langle \underline{\overline{\mathbf{5}}}(\underline{\mathbf{10}}) \rangle + y^{120}_{ij} (\langle \underline{\overline{\mathbf{5}}}(\underline{\mathbf{120}}) \rangle + \langle \underline{\overline{\mathbf{45}}}(\underline{\mathbf{120}}) \rangle) + y^{\overline{126}}_{ij} \langle \underline{\overline{\mathbf{45}}}(\underline{\overline{\mathbf{126}}}) \rangle \equiv y^d v_d \tag{2.41}$$

$$M_l = y^{10}_{ij} \langle \underline{\overline{\mathbf{5}}}(\underline{\mathbf{10}}) \rangle + y^{120}_{ij} (\langle \underline{\overline{\mathbf{5}}}(\underline{\mathbf{120}}) \rangle - 3 \langle \underline{\overline{\mathbf{45}}}(\underline{\mathbf{120}}) \rangle) - 3 y^{\overline{126}}_{ij} \langle \underline{\overline{\mathbf{45}}}(\underline{\overline{\mathbf{126}}}) \rangle \equiv y^l v_d \tag{2.42}$$

$$m_D = y^{10}_{ij} \langle \underline{\mathbf{5}}(\underline{\mathbf{10}}) \rangle + y^{120}_{ij} \langle \underline{\mathbf{5}}(\underline{\mathbf{120}}) \rangle - 3 y^{\overline{126}}_{ij} \langle \underline{\mathbf{5}}(\underline{\overline{\mathbf{126}}}) \rangle \equiv y^\nu v_u \tag{2.43}$$

where we denote the m-dimensional $SU(5)$ component of the n-dimensional representation of $SO(10)$ by $\underline{\mathbf{m}}(\underline{\mathbf{n}})$. We note that the factor -3 is related to the three colors of the down quarks. The Majorana neutrino mass matrices are given by

$$M_R = y_{ij}^{\overline{126}} \langle \underline{\mathbf{1}}(\underline{\overline{\mathbf{126}}}) \rangle \tag{2.44}$$

$$M_{LL} = y_{ij}^{\overline{126}} \langle \underline{\mathbf{15}}(\underline{\overline{\mathbf{126}}}) \rangle. \tag{2.45}$$

If we perform the renormalization group evolution of the quark masses from the Electroweak scale up to the GUT scale, we will find the following approximate relations:

$$m_d \simeq 3m_e \ , \ \ m_s \simeq \frac{1}{3} m_e \ , \ \text{ and } \ \ m_b \simeq m_\tau. \tag{2.46}$$

These relations are known as the Georgi-Jarlskog relations [167]. In order to achieve these relations, one needs the factor of -3 in the (22) component of the charged lepton mass matrix with respect to that of the down quark mass matrix, while all other components are identical in these two mass matrices. A simple example suggested by Georgi and Jarlskog is [167]:

$$M_d = \begin{pmatrix} 0 & a_d & 0 \\ a_d & b_d & 0 \\ 0 & 0 & c_d \end{pmatrix}, M_l = \begin{pmatrix} 0 & a_d & 0 \\ a_d & -3b_d & 0 \\ 0 & 0 & c_d \end{pmatrix}. \tag{2.47}$$

As the coupling of $\underline{\mathbf{120}}$ and $\underline{\overline{\mathbf{126}}}$ gives exactly the factor of -3 in the charged lepton mass matrix with respect to the down quark mass matrix, we may assume that the (22) component is dominated by the Higgs, $\underline{\mathbf{120}}$ or $\underline{\overline{\mathbf{126}}}$, while the other components of these two mass matrices are dominated by the Higgs, $\underline{\mathbf{10}}$.

Alternatively, if we do not want to use large representations such as $\underline{\mathbf{120}}$ or $\underline{\overline{\mathbf{126}}}$, instead we can use small representations such as $\underline{\mathbf{16}}, \underline{\overline{\mathbf{16}}}, \underline{\mathbf{45}}$, or $\underline{\mathbf{54}}$, which couple to the fermion Ψ_i via non-renormalizable interactions. The coupling $\Psi_i \underline{\mathbf{10}} \Psi_j$ leads to a symmetric mass matrix: $M_u = M_d = m_D = M_l$ at the GUT scale. The Majorana masses of the left-handed (conjugate) neutrinos can be obtained from the non-renormalizable interaction, $\Psi_i \underline{\overline{\mathbf{16}}}\ \underline{\overline{\mathbf{16}}} \Psi_j$, which acts like $\Psi_i \underline{\overline{\mathbf{126}}} \Psi_j$ in the renormalizable case. The Georgi-Jarlskog relations can be achieved by the non-renormalizable interaction, $\Psi_i \underline{\mathbf{45}}\ \underline{\mathbf{10}} \Psi_j$.

Despite the success of SUSY GUTs, there is a generic problem, namely, the doublet-triplet splitting problem. The mass of the doublet Higgs is at the Electroweak scale, while neither a colored triplet Higgs nor proton decay have been observed and therefore its mass has to be close to the GUT scale. Dimopolous and Wilczek proposed a mechanism [168] to achieve a mass splitting using the VEV of the adjoint representation, $\langle \underline{\mathbf{45}} \rangle$ in the $B - L$ direction

$$\langle \underline{\mathbf{45}} \rangle = i\sigma^2 \otimes \text{diag}(a, a, a, 0, 0). \tag{2.48}$$

Chacko and Mohapatra [169] proposed another mechanism leading to a VEV structure of the Dimopoulos-Wilczek type, that is

$$\langle \underline{\mathbf{45}} \rangle = i\sigma^2 \otimes \text{diag}(0, 0, 0, b, b). \tag{2.49}$$

We note that a solution which uses $\underline{\mathbf{126}}$ instead of $\underline{\mathbf{45}}$ to achieve the splitting was proposed by Lee and Mohapatra [170].

2.6 Symmetry Breaking from Orbifolding

In this section, we will discuss how the symmetry can be broken by an orbifold compactification. We will give an example in a 5-dimensional theory (5d theory) for simplicity. We note that the same principle can be applied for a (4+n)-dimensional theory. A more detail discussion can be found in [163, 171].
We first consider a complex scalar field ϕ living in 5d, $x^M = (x^\mu, x^5)$. The action of the massless scalar field is given by

$$S = \int d^5x \frac{1}{2}\partial_M\phi^*\partial^M\phi = \int d^4x dy \frac{1}{2}(\partial_\mu\phi^*\partial^\mu\phi + \partial_5\phi^*\partial^5\phi), \tag{2.50}$$

where here we denote $x^5 = y$ for simplicity. The fifth dimension is compactified on a circle S^1 by the identification of

$$y \to y + 2\pi R, \tag{2.51}$$

where R is the size of the extra-dimension. The Lorentz symmetry $SO(1,4)$ is broken down to $SO(1,3)$ by this compactification. The scalar field can be written in term of a mode expansion as

$$\phi(x,y) = \sum_{n=-\infty}^{\infty} \phi^{(n)}(x^\mu)e^{iny/R} \,. \tag{2.52}$$

Using this mode expansion and integrating out y, the action can be written as

$$S = -\frac{2\pi R}{2}\int d^4x \sum_{n=-\infty}^{\infty}(\partial_\mu\phi^{(n)*}\partial^\mu\phi^{(n)} + \frac{n^2}{R^2}\phi^{(n)*}\phi^{(n)}) \,, \tag{2.53}$$

where the factor $2\pi R$ can be absorbed into the scalar field without loss of generality. Now, we consider an orbifold S^1/Z_2 by modding out a Z_2 group from this circle. The orbifold can be obtained by the identification of

$$y \to -y \,. \tag{2.54}$$

The scalar field is forced to be an eigenstate of this Z_2 parity,

$$\phi(x,-y) = \eta\phi(x,y), \tag{2.55}$$

where $\eta = \pm$. Its eigenstates can be written as

$$\begin{aligned} \phi_+(x,y) &= \sum_{n=-\infty}^{\infty} \phi_+^{(n)}(x^\mu)\cos ny/R \,, \\ \phi_-(x,y) &= \sum_{n=-\infty}^{\infty} \phi_-^{(n)}(x^\mu)\sin ny/R \,, \end{aligned} \tag{2.56}$$

where ϕ_+, ϕ_- are the Z_2 even and odd eigenstates. Here, we can see that the Z_2 even state contains a zero mode, while the odd one does not. If we consider the effective theory below the compactification scale $1/R$, we can forget about the non-zero modes because they are decoupled. Therefore, the particle content of the low energy effective theory contains only the set of zero modes.

Now let us move on to consider an abelian gauge theory in 5d. The action of the gauge field A_M reads

$$\begin{aligned} S &= -\frac{1}{4g_5^2}\int d^5x F_{MN}F^{MN} \\ &= -\frac{1}{4g_5^2}\int d^4xdy(F_{\mu\nu}F^{\mu\nu} + 2(\partial_\mu A_5 - \partial_5 A_\mu)^2) \ , \end{aligned} \tag{2.57}$$

where g_5 is a gauge coupling in 5d.
By the compactification on the circle S^1 as before in Eq.(2.51), A_5 is decoupled and becomes a scalar field in the 4d effective theory. The fields, A_μ and A_5 can be written in the terms of the mode expansion as

$$\begin{aligned} A_\mu(x,y) &= \sum_{n=-\infty}^{\infty} A_\mu^{(n)}(x^\mu)e^{iny/R} \ , \\ A_5(x,y) &= \sum_{n=-\infty}^{\infty} A_5^{(n)}(x^\mu)e^{iny/R} \ , \end{aligned} \tag{2.58}$$

with the Hermiticity condition $A_M^{(n)*} = A_M^{(-n)}$.
Integrating out y, we obtain the 4d effective theory as follows

$$S = -\frac{2\pi R}{4g_5^2}\int d^4x \sum_{n=-\infty}^{\infty} F_{\mu\nu}^{(n)}F^{(n)\mu\nu} + 2\frac{2\pi R}{4g_5^2}\int d^4x[\partial_\mu A_5^{(n)} - i\frac{n}{R}A_\mu^{(n)}]^2, \tag{2.59}$$

where the first term is a tower of kinetic terms with the 4d gauge coupling $g_4^2 = \frac{g_5^2}{2\pi R}$, and the second term gives the mass terms for the non-zero modes $n \neq 0$.
In general for non-abelian gauge symmetries, the gauge field is in the adjoint representation of the gauge group,

$$A_M \equiv A_M^a T^a \ , \quad \text{and} \quad F_{MN} \equiv \partial_M A_N - \partial_N A_M + [A_M, A_N] \ . \tag{2.60}$$

Under the parity transformation given in Eq.(2.54), the gauge field, $A_\mu(x,y)$, transforms as

$$A_\mu(x,-y) = PA_\mu(x,y)P^{-1} \ , \tag{2.61}$$

while $A_5(x,y)$ and $\phi(x,y)$ transform as

$$\begin{aligned} A_5(x,-y) &= -PA_5(x,y)P^{-1} \ , \\ \phi(x,-y) &= P\phi(x,y). \end{aligned} \tag{2.62}$$

As an example to see how the symmetry can be broken by the orbifold, we consider a $SU(3)$ gauge symmetry in 5d with a scalar field ϕ in the fundamental (triplet) representation. The generators of $SU(3)$ are the Gell-Mann matrices λ^a, where $a = 1-8$. For $P = \mathrm{diag}(1,1,-1)$, we obtain

$$\begin{aligned} \lambda^a &\rightarrow P\lambda^a P^{-1} = \lambda^a \ , \ \ \mathrm{a} = 1,2,3, \text{ and } 8 \ , \\ \lambda^{\hat{a}} &\rightarrow P\lambda^{\hat{a}} P^{-1} = -\lambda^{\hat{a}} \ , \ \ \hat{\mathrm{a}} = 4,5,6,7 \ . \end{aligned} \tag{2.63}$$

The generators $\lambda_{1,2,3}$ belong to the $SU(2)$ subgroup and λ_8 belongs to the $U(1)$ subgroup. Hence $SU(2) \times U(1)$ remains unbroken and the non-zero modes, which do not belong to $SU(2) \times U(1)$, are decoupled from the low energy effective theory. Moreover, the scalar triplet is decomposed into a doublet and singlet under $SU(2) \times U(1)$, where only the doublet survives at low energy.

The relation given in Eq.(2.63) can be restated as the condition for the unbroken generators as

$$[A_\mu^a \lambda^a, P] = 0 \ . \quad \text{(no summation)} \tag{2.64}$$

We note that this principle can be applied to other gauge groups such as $SU(5)$ [30–34], or $SO(10)$ [172–181] and the doublet-triplet splitting can be solved nicely by an appropriate choice of orbifold parities.

Chapter 3

Flavor symmetry models

In this chapter, we present the flavor models which predict the neutrino mixing. The first model is constructed based on the dihedral group D_4, which predicts $\mu - \tau$ symmetry in the neutrino mass matrix leading to maximal atmospheric mixing $\theta_{23} = \pi/4$ and $\theta_{13} = 0$. The second model uses the dihedral group D_{10} to predict the golden ratio for solar neutrino mixing.

3.1 A SUSY D_4 model for $\mu - \tau$ symmetry

Since the maximal atmospheric mixing θ_{23} and the vanishing of the θ_{13} can be explained from the neutrino mass matrix which has the $\mu - \tau$ symmetry (see Section 2.2), it might be interesting to find the theoretical explanation of such the mass matrix structure. As discussed in Section 2.3, a popular approach is to impose the non-abelian discrete flavor symmetry. In this section, we impose the non-abelian discrete flavor symmetry D_4 to explain the origin of the $\mu - \tau$ symmetry in the neutrino mass matrix. We note that our model is the supersymmeterized version of the model presented by Grimus and Lavoura (GL) in [182], where we extend the flavor group, which is $D_4 \times Z_2^{(\text{aux})}$ in the original model, to $D_4 \times Z_5$. An additional difference is the absence of left-handed conjugate neutrinos. Despite these changes, the model is the same as the GL model, since θ_{23} maximal and $\theta_{13} = 0$ arise through the same mismatch of D_4 preserved subgroups, D_2 in the charged lepton and Z_2 in the neutrino sector.

3.1.1 Group Theory of D_4

Before discussing the model, we briefly review some basic features of the dihedral group D_4. Its order is eight, and it has five irreducible representations which we denote as $\underline{\mathbf{1_i}}$, $\mathbf{i} = 1, ..., 4$ and $\underline{\mathbf{2}}$. All of them are real and only $\underline{\mathbf{2}}$ is faithful[1]. The group is generated by the two generators A and B which can be chosen to be [183]

$$\mathrm{A} = \begin{pmatrix} i & 0 \\ 0 & -i \end{pmatrix} \quad \text{and} \quad \mathrm{B} = \begin{pmatrix} 0 & 1 \\ 1 & 0 \end{pmatrix} \tag{3.1}$$

[1] A representation is faithful if each distinct group element is associated with a different matrix representation. Otherwise it is unfaithful.

	classes				
	$\mathcal{C}_1$	$\mathcal{C}_2$	$\mathcal{C}_3$	$\mathcal{C}_4$	$\mathcal{C}_5$
G	1	A	A^2	B	A B
$^\circ\mathcal{C}_i$	1	2	1	2	2
$^\circ h_{\mathcal{C}_i}$	1	4	2	2	2
$\underline{\mathbf{1_1}}$	1	1	1	1	1
$\underline{\mathbf{1_2}}$	1	1	1	-1	-1
$\underline{\mathbf{1_3}}$	1	-1	1	1	-1
$\underline{\mathbf{1_4}}$	1	-1	1	-1	1
$\underline{\mathbf{2}}$	2	0	-2	0	0

Table 3.1: Character table of the group D_4. $\mathcal{C}_i$ are the classes of the group, $^\circ\mathcal{C}_i$ is the order of the i^{th} class, i.e. the number of distinct elements contained in this class, $^\circ h_{\mathcal{C}_i}$ is the order of the elements S in the class $\mathcal{C}_i$, i.e. the smallest integer (> 0) for which the equation $S^{\,^\circ h_{\mathcal{C}_i}} = 1$ holds. Furthermore the table contains one representative for each class $\mathcal{C}_i$ given as product of the generators A and B of the group.

for $\underline{\mathbf{2}}$. Note that A is a complex matrix, although $\underline{\mathbf{2}}$ is a real representation. For $(a_1, a_2)^T \sim \underline{\mathbf{2}}$ therefore $(a_2^\star, a_1^\star)^T$ transforms as $\underline{\mathbf{2}}$ under D_4. The generators of the one-dimensional representations can be found in the character table, displayed in Table 3.1. The generators fulfill the relations

$$A^4 = 1, \qquad B^2 = 1, \quad \text{and} \quad ABA = B\,. \tag{3.2}$$

The product rules for $\underline{\mathbf{1_i}}$ are the following

$$\underline{\mathbf{1_i}}\times\underline{\mathbf{1_i}} = \underline{\mathbf{1_1}}\ ,\ \ \underline{\mathbf{1_1}}\times\underline{\mathbf{1_i}} = \underline{\mathbf{1_i}}\ \text{ for }\ \mathbf{i} = 1, ..., 4\ ,\ \ \underline{\mathbf{1_2}}\times\underline{\mathbf{1_3}} = \underline{\mathbf{1_4}}\ ,\ \ \underline{\mathbf{1_2}}\times\underline{\mathbf{1_4}} = \underline{\mathbf{1_3}}\ ,\ \text{and}\ \ \underline{\mathbf{1_3}}\times\underline{\mathbf{1_4}} = \underline{\mathbf{1_2}}\ .$$

For $s_i \sim \underline{\mathbf{1_i}}$ and $(a_1, a_2)^T \sim \underline{\mathbf{2}}$ we find

$$\begin{pmatrix} s_1 a_1 \\ s_1 a_2 \end{pmatrix} \sim \underline{\mathbf{2}}\ ,\quad \begin{pmatrix} s_2 a_1 \\ -s_2 a_2 \end{pmatrix} \sim \underline{\mathbf{2}}\ ,\quad \begin{pmatrix} s_3 a_2 \\ s_3 a_1 \end{pmatrix} \sim \underline{\mathbf{2}}\ ,\ \text{and}\quad \begin{pmatrix} s_4 a_2 \\ -s_4 a_1 \end{pmatrix} \sim \underline{\mathbf{2}}\ .$$

The product $\underline{\mathbf{2}} \times \underline{\mathbf{2}}$ decomposes into the four singlets which read for $(a_1, a_2)^T$, $(b_1, b_2)^T \sim \underline{\mathbf{2}}$:

$$a_1 b_2 + a_2 b_1 \sim \underline{\mathbf{1_1}}\ ,\quad a_1 b_2 - a_2 b_1 \sim \underline{\mathbf{1_2}}\ ,\quad a_1 b_1 + a_2 b_2 \sim \underline{\mathbf{1_3}}\ ,\ \text{and}\quad a_1 b_1 - a_2 b_2 \sim \underline{\mathbf{1_4}}\ .$$

More general formulae for generators, Kronecker products and Clebsch Gordan coefficients can be found, for example, in [120, 184]. Notice that our group basis does not coincide with the one chosen by GL in [182]. Therefore, the mass matrices shown below have a different appearance, especially the charged lepton mass matrix is not diagonal in our basis. However, the prediction of the mixing angles does not depend on the chosen group basis.

All subgroups of D_4 are abelian: $Z_2 \cong D_1$, Z_4 and $D_2 \cong Z_2 \times Z_2$. We are interested in Z_2 subgroups which are generated by $B\,A^m$ with $m = 0, ..., 3$ and in the D_2 subgroup generated by A^2 and BA. In order to see that $B\,A^m$ gives a Z_2 group, note that

$$(B\,A^m)^2 = B\,A^m B\,A^m = B\,A^{m-1} B\,A^{m-1} = \cdots = B^2 = 1$$

holds, due to Eq.(3.2). Similarly, one finds for A^2 and BA:

$$(A^2)^2 = A^4 = 1 \quad \text{and} \quad (BA)^2 = BABA = B^2 = 1$$

by using again the generator relations. Obviously, A^2 and BA are not equal (in general) and thus they generate different Z_2 subgroups. Additionally, we have to check that A^2 and BA commute

$$A^2BA = A^3BA^2 = A^4BA^3 = BAA^2 \ .$$

This shows that A^2 and BA generate a $Z_2 \times Z_2$ group, which is isomorphic to a D_2 group. The other non-trivial element of the D_2 group is BA^3. Thus, one could also use the two elements A^2 and BA^3 to generate this D_2 group. However, we follow the convention to use A^2 and the element BA^p with p being the smallest possible natural number as generators. The Z_2 symmetry given through BA^m is left unbroken by a non-vanishing VEV of a singlet transforming as $\underline{\mathbf{1_3}}$ if m is even and of one transforming as $\underline{\mathbf{1_4}}$ for m being odd. Additionally, it will be left intact by the fields $\psi_{1,2}$ forming a doublet, if their VEVs have the following structure:

$$\begin{pmatrix} \langle\psi_1\rangle \\ \langle\psi_2\rangle \end{pmatrix} \propto \begin{pmatrix} e^{-\frac{\pi i m}{2}} \\ 1 \end{pmatrix} . \tag{3.3}$$

For preserving the D_2 group generated by A^2 and BA, only singlets in $\underline{\mathbf{1_4}}$ are allowed to have a non-vanishing VEV. Especially, no fields forming a doublet under D_4 should acquire a VEV. Clearly, in all cases singlets in the trivial representation of D_4, $\underline{\mathbf{1_1}}$, are allowed to have a non-vanishing VEV. Note also that in none of the cases a field transforming as $\underline{\mathbf{1_2}}$ can acquire a non-zero VEV. Since we concentrate on the D_2 subgroup induced by A^2 and BA, the Z_2 subgroup has to be generated by BA^m, with m being even in order not to be a subgroup of the D_2 group. Only then the mismatch between the two subgroups is achieved. The choice of m, $m = 0$ or $m = 2$, depends on the relative sign between $\langle\psi_1\rangle$ and $\langle\psi_2\rangle$ for two fields $\psi_{1,2} \sim \underline{\mathbf{2}}$.

3.1.2 The Model at Leading Order

We augment the Minimal Supersymmetric Standard Model (MSSM) by the flavor symmetry $D_4 \times Z_5$. The non-trivial breaking of D_4 is responsible for maximal atmospheric mixing and vanishing θ_{13}, while Z_5 is necessary to separate the charged lepton and the neutrino sector. The model contains three left-handed lepton doublets l_i, the three left-handed conjugate charged leptons e_i^c, the MSSM Higgs doublets $h_{u,d}$, and two sets of flavons $\{\chi_e, \varphi_e\}$, and $\{\chi_\nu, \varphi_\nu, \psi_{1,2}\}$ which break D_4 in the charged lepton and the neutrino sector, respectively. The transformation properties of these fields are collected in Table 3.2.

Fermion Masses

The invariance of the charged lepton and neutrino mass terms under the flavor group $D_4 \times Z_5$ requires the presence of at least one flavon. Thus, charged lepton masses are generated by non-renormalizable operators only. In a model which treats quarks as well, this allows the explanation of the small τ mass compared to the top quark mass without relying on a large value of $\tan\beta = \langle h_u\rangle/\langle h_d\rangle = v_u/v_d$. The neutrinos receive Majorana masses through the dimension-5 operator $l h_u l h_u/\Lambda$, which can be made invariant under the flavor group by

Field	l_1	$l_{2,3}$	e_1^c	$e_{2,3}^c$	h_u	h_d	χ_e	φ_e	χ_ν	φ_ν	$\psi_{1,2}$
D_4	$\underline{\mathbf{1_1}}$	$\underline{\mathbf{2}}$	$\underline{\mathbf{1_1}}$	$\underline{\mathbf{2}}$	$\underline{\mathbf{1_1}}$	$\underline{\mathbf{1_1}}$	$\underline{\mathbf{1_1}}$	$\underline{\mathbf{1_4}}$	$\underline{\mathbf{1_1}}$	$\underline{\mathbf{1_3}}$	$\underline{\mathbf{2}}$
Z_5	ω	ω	1	1	ω^3	ω	ω^3	ω^3	ω^2	ω^2	ω^2

Table 3.2: Particle content of the model. l_i denotes the three left-handed lepton $SU(2)_L$ doublets, e_i^c are the left-handed conjugate charged leptons, and $h_{u,d}$ are the MSSM Higgs doublets. The flavons χ_e, φ_e, χ_ν, φ_ν, and $\psi_{1,2}$ only transform under $D_4 \times Z_5$. The phase factor ω is $e^{\frac{2\pi i}{5}}$.

coupling it to a flavon. The part of the superpotential giving lepton masses reads at Leading Order (LO):

$$\begin{aligned} \mathrm{W}_l &= y_1^e \chi_e l_1 e_1^c \frac{h_d}{\Lambda} + y_2^e \chi_e (l_2 e_3^c + l_3 e_2^c)\frac{h_d}{\Lambda} + y_3^e \varphi_e (l_2 e_2^c - l_3 e_3^c)\frac{h_d}{\Lambda} \\ &+ y_1 \chi_\nu l_1 l_1 \frac{h_u^2}{\Lambda^2} + y_2 l_1 (l_2\psi_2 + l_3\psi_1)\frac{h_u^2}{\Lambda^2} + y_2 (l_2\psi_2 + l_3\psi_1) l_1 \frac{h_u^2}{\Lambda^2} + y_3 \varphi_\nu (l_2 l_2 + l_3 l_3)\frac{h_u^2}{\Lambda^2} \\ &+ y_4 \chi_\nu (l_2 l_3 + l_3 l_2)\frac{h_u^2}{\Lambda^2} \,, \end{aligned} \tag{3.4}$$

where Λ is the cutoff scale of the theory whose order of magnitude is determined by the scale of the light neutrino masses, see below. For the moment we assume that the flavons χ_e and φ_e acquire the VEVs

$$\langle \varphi_e \rangle = u_e \quad \text{and} \quad \langle \chi_e \rangle = w_e \,. \tag{3.5}$$

As discussed in Section 3.1.1, these VEVs break D_4 down to D_2 generated by A^2 and BA in the charged lepton sector. The VEVs of the flavons that couple only to neutrinos at LO are of the form

$$\langle \varphi_\nu \rangle = u \,, \quad \langle \chi_\nu \rangle = w \,, \quad \begin{pmatrix} \langle \psi_1 \rangle \\ \langle \psi_2 \rangle \end{pmatrix} = v \begin{pmatrix} 1 \\ 1 \end{pmatrix}, \tag{3.6}$$

and therefore they leave a Z_2 subgroup, generated by B, unbroken. As mentioned, the equality of the VEVs of $\langle \psi_1 \rangle$ and $\langle \psi_2 \rangle$ is crucial. As we will discuss further, the vacuum structure in Eq.(3.5) and Eq.(3.6) is a natural result of the minimization of the flavon potential. We obtain the following fermion mass matrices when inserting the flavon VEVs and $\langle h_{u,d} \rangle = v_{u,d}$:

$$M_l = \frac{v_d}{\Lambda} \begin{pmatrix} y_1^e w_e & 0 & 0 \\ 0 & y_3^e u_e & y_2^e w_e \\ 0 & y_2^e w_e & -y_3^e u_e \end{pmatrix} \quad \text{and} \quad M_\nu = \frac{v_u^2}{\Lambda^2} \begin{pmatrix} y_1 w & y_2 v & y_2 v \\ y_2 v & y_3 u & y_4 w \\ y_2 v & y_4 w & y_3 u \end{pmatrix} . \tag{3.7}$$

Thereby, the left-handed fields are on the left-hand and the left-handed conjugate fields on the right-hand side for M_l. The matrix $M_l\, M_l^\dagger$ is diagonalized by the unitary matrix U_l, i.e. $U_l^\dagger\, M_l\, M_l^\dagger\, U_l$ is diagonal. U_l acts on the left-handed charged lepton fields and is given by

$$U_l = \begin{pmatrix} 1 & 0 & 0 \\ 0 & e^{i\pi/4}/\sqrt{2} & e^{-i\pi/4}/\sqrt{2} \\ 0 & e^{-i\pi/4}/\sqrt{2} & e^{i\pi/4}/\sqrt{2} \end{pmatrix} . \tag{3.8}$$

For the masses of the charged leptons we find

$$m_e = \frac{v_d}{\Lambda} |y_1^e w_e| \,, m_\mu = \frac{v_d}{\Lambda} |y_3^e u_e + i y_2^e w_e| \,, \quad \text{and} \quad m_\tau = \frac{v_d}{\Lambda} |y_3^e u_e - i y_2^e w_e| \,. \tag{3.9}$$

In order to arrive at non-degenerate masses for the μ and the τ lepton, either $y_3^e u_e$ or $y_2^e w_e$ has to be complex indicating CP violation in the Yukawa couplings and/or flavon VEVs. For m_τ being around 2 GeV, we find that for small $\tan\beta$ - corresponding to v_d of the order of 100 GeV - the ratio of the flavon VEVs u_e and w_e over the cutoff scale Λ should fulfill [2]

$$\frac{u_e}{\Lambda}\,,\frac{w_e}{\Lambda} \sim \lambda_c^2 \approx 0.04 \tag{3.10}$$

with λ_c being the Cabibbo angle. The smallness of the ratio m_e/m_τ is in this model only explained by the assumption of a small enough coupling y_1^e. Similarly, m_μ/m_τ enforces a certain cancellation between the two contributions $y_3^e u_e$ and $iy_2^e w_e$ in m_μ. In [182] these problems have been solved by the assumption that the electron couples to a Higgs field different from those coupling to the μ and the τ lepton, and by an additional symmetry which leads to $m_\mu = 0$ if unbroken.

The neutrino mass matrix in the charged lepton mass basis (indicated by a prime ($'$)) reads

$$M_\nu' = U_l^\dagger M_\nu U_l^* = \frac{v_u^2}{\Lambda^2}\begin{pmatrix} y_1 w & y_2 v & y_2 v \\ y_2 v & y_4 w & y_3 u \\ y_2 v & y_3 u & y_4 w \end{pmatrix}. \tag{3.11}$$

As M_ν' is $\mu-\tau$ symmetric, it immediately follows that the lepton mixing angle θ_{13} vanishes and θ_{23} is maximal. The solar mixing angle θ_{12} is not predicted, but in general expected to be large. Also the Majorana phases $\phi_{1,2}$ are not constrained. The lepton mixing matrix is of the form

$$U_{PMNS} = \mathrm{diag}(e^{i\gamma_1}, e^{i\gamma_2}, e^{i\gamma_3}) \cdot \begin{pmatrix} \cos\theta_{12} & \sin\theta_{12} & 0 \\ -\frac{\sin\theta_{12}}{\sqrt{2}} & \frac{\cos\theta_{12}}{\sqrt{2}} & -\frac{1}{\sqrt{2}} \\ -\frac{\sin\theta_{12}}{\sqrt{2}} & \frac{\cos\theta_{12}}{\sqrt{2}} & \frac{1}{\sqrt{2}} \end{pmatrix} \cdot \mathrm{diag}(e^{i\beta_1}, e^{i\beta_2}, e^{i\beta_3})\,. \tag{3.12}$$

The Majorana phases $\phi_{1,2} = \alpha_{1,2}/2$ can be extracted from U_{PMNS} by bringing it into the standard form [46]. Due to the additional factor 1/2, the phases $\phi_{1,2}$ vary between 0 and π. Assuming that all flavon VEVs are of the same size, the estimate in Eq.(3.10) also holds for the VEVs of the flavons χ_ν, φ_ν, and $\psi_{1,2}$. For small $\tan\beta$, i.e. $v_u \approx v_d \approx 100$ GeV, a light neutrino mass scale between $\sqrt{|\Delta m_{31}^2|} \approx 0.05$ eV and 1 eV fixes the range of the cutoff scale Λ to be

$$4\cdot 10^{11}\ \mathrm{GeV} \lesssim \Lambda \lesssim 8\cdot 10^{12}\ \mathrm{GeV}\,. \tag{3.13}$$

As it will be shown further, we can assume that CP is only violated spontaneously in this model by imaginary VEVs w_e and w of χ_e and χ_ν. Thus, apart from w_e and w, all other parameters, i.e. couplings and VEVs, are real in what follows. According to Eq.(3.9), an imaginary w_e allows the μ and the τ lepton masses to be non-degenerate. In the neutrino sector only the VEV w of χ_ν is imaginary, whereas all other entries in M_ν' are real, so that the matrix in Eq.(3.11) can be written as

$$M_\nu' = \frac{v_u^2}{\Lambda}\frac{v}{\Lambda}\begin{pmatrix} i\,s & t & t \\ t & i\,x & z \\ t & z & i\,x \end{pmatrix}, \tag{3.14}$$

[2] Although not excluded, there is no obvious reason to assume that there is a large hierarchy among the different flavon VEVs. In general, these are correlated through the parameters of the flavon potential.

where we have defined the real parameters

$$s = y_1 \frac{\mathrm{Im}(w)}{v} \ , \quad t = y_2 \ , \quad x = y_4 \frac{\mathrm{Im}(w)}{v} \ , \quad \text{and} \quad z = y_3 \frac{u}{v} \ . \tag{3.15}$$

Mismatch of Subgroups

In the following, we discuss how the subgroup mismatch plays an important role for the prediction of the neutrino mixing. To elucidate the reason why the two subgroups preserved in the charged lepton and the neutrino sector have to be different, i.e. the Z_2 subgroup present in the neutrino sector should not be a subgroup of the D_2 group of the charged lepton sector, observe that $M_l\, M_l^\dagger$ as well as $M_\nu\, M_\nu^\dagger$ for M_l and M_ν given in Eq.(3.7) can be written in the following form

$$M_i\, M_i^\dagger = \begin{pmatrix} A_i & B_i\, e^{i\,\beta_i} & B_i\, e^{i\,(\beta_i + \phi_i\,\mathrm{j})} \\ B_i\, e^{-i\,\beta_i} & C_i & D_i\, e^{i\phi_i\,\mathrm{j}} \\ B_i\, e^{-i\,(\beta_i+\phi_i\,\mathrm{j})} & D_i\, e^{-i\,\phi_i\,\mathrm{j}} & C_i \end{pmatrix}, \qquad i = l, \nu \ . \tag{3.16}$$

This form is achieved for M_l (M_ν) as long as at least one Z_2 group, originating from $\mathrm{B\,A}^m$, is conserved in the charged lepton (neutrino) sector. A matrix of this type is diagonalized by

$$U_i = \begin{pmatrix} e^{i\,\beta_i} & 0 & 0 \\ 0 & 1 & 0 \\ 0 & 0 & e^{-i\,\phi_i\,\mathrm{j}} \end{pmatrix} U_{\max}\, U_{12}(\theta_i)\, U(\alpha_k^i), \tag{3.17}$$

where

$$U_{\max} = \begin{pmatrix} 1 & 0 & 0 \\ 0 & \frac{1}{\sqrt{2}} & -\frac{1}{\sqrt{2}} \\ 0 & \frac{1}{\sqrt{2}} & \frac{1}{\sqrt{2}} \end{pmatrix} \ , \quad U_{12}(\theta_i) = \begin{pmatrix} \cos\theta_i & \sin\theta_i & 0 \\ -\sin\theta_i & \cos\theta_i & 0 \\ 0 & 0 & 1 \end{pmatrix} \ , \quad U(\alpha_k^i) = \begin{pmatrix} e^{i\,\alpha_1^i} & 0 & 0 \\ 0 & e^{i\,\alpha_2^i} & 0 \\ 0 & 0 & e^{i\,\alpha_3^i} \end{pmatrix} . \tag{3.18}$$

In [86,184] it has been shown that the quantities ϕ_i and j are related to the group theoretical indices of the flavor symmetry. j is the representation index of the doublet, under which two of the three left-handed lepton generations transform. Thus, it is the same for charged leptons and neutrinos. ϕ_i can be expressed as

$$\phi_i = \frac{2\,\pi}{n}\, m_i \ , \tag{3.19}$$

where n is the index of the group D_n and $m_{l\,(\nu)}$ the index of the preserved subgroup in the charged lepton (neutrino) sector that has a generator of the form $\mathrm{B\,A}^{m_{l\,(\nu)}}$. $m_{l\,(\nu)}$ is an integer number between zero and $(n-1)$. The parameters A_i, ..., D_i and the phase β_i are real functions of the matrix entries of $M_i\, M_i^\dagger$, whose actual form is not needed here. The phases α_k^i are irrelevant for the diagonalization of $M_i\, M_i^\dagger$, but are necessary for the diagonalization of the neutrino mass matrix M_ν alone. The angle θ_i can be expressed through the parameters A_i, ..., D_i as follows:

$$\tan 2\theta_i = \frac{2\sqrt{2}\, B_i}{C_i + D_i - A_i} \ . \tag{3.20}$$

The general form of the PMNS matrix is then

$$U_{PMNS} = U_l^T\, U_\nu^\star = U(\alpha_k^l)\, U_{12}^T(\theta_l)\, U_{\max}^T \begin{pmatrix} e^{i\,(\beta_l-\beta_\nu)} & 0 & 0 \\ 0 & 1 & 0 \\ 0 & 0 & e^{-i\,(\phi_l-\phi_\nu)\,\mathrm{j}} \end{pmatrix} U_{\max}\, U_{12}(\theta_\nu)\, U(-\alpha_{\tilde{k}}^\nu)\ . \tag{3.21}$$

This form already shows that it is essential to have a non-trivial phase $e^{-i\,(\phi_l-\phi_\nu)\,\mathrm{j}}$ in order to guarantee that the maximal mixing in the $2-3$ sector is not cancelled. For the third column of U_{PMNS}, which determines the mixing angles θ_{13} and θ_{23}, we find

$$\begin{aligned} &|(U_{PMNS})_{e3}| = |\sin((\phi_l-\phi_\nu)\,\mathrm{j}/2)\,\sin\theta_l|\ , \quad |(U_{PMNS})_{\mu 3}| = |\sin((\phi_l-\phi_\nu)\,\mathrm{j}/2)\,\cos\theta_l|\ , \\ &|(U_{PMNS})_{\tau 3}| = |\cos((\phi_l-\phi_\nu)\,\mathrm{j}/2)|\ . \end{aligned} \tag{3.22}$$

Using that we preserve a Z_2 symmetry generated by B in the neutrino sector and a D_2 group generated by B A (according to our convention for the generators of the group D_2 introduced in Section 3.1.1) in the charged lepton sector gives for ϕ_ν and ϕ_l:

$$\phi_\nu = 0 \quad \text{and} \quad \phi_l = \frac{\pi}{2}\ . \tag{3.23}$$

j is trivially one, since D_4 only contains one irreducible two-dimensional representation $\underline{\mathbf{2}}$. As the elements $(1,k)$ and $(k,1)$ with $k=2,3$ in M_l vanish, see Eq.(3.7), the parameter B_l in Eq.(3.16) is zero (and also $\beta_l = 0$) and thus $\theta_l = 0$ as well, according to Eq.(3.20). This results in

$$|(U_{PMNS})_{e3}| = 0\ , \quad |(U_{PMNS})_{\mu 3}| = |(U_{PMNS})_{\tau 3}| = \frac{1}{\sqrt{2}}\ , \tag{3.24}$$

giving maximal atmospheric mixing and vanishing θ_{13}. A few things are interesting to notice: In principle four different cases might occur. These arise from whether the subgroups D_2 and Z_2 contain the same element BA^m or not, and from whether the D_2 subgroup is unbroken in the charged lepton sector or only a Z_2 subgroup is preserved. The first issue determines whether m_l equals m_ν or not, i.e. whether $|\phi_l - \phi_\nu|$ is zero or not. The second one is responsible for (non-)zero θ_l. We can see from Eq.(3.22) that for no mismatch of the subgroups θ_{13} as well as θ_{23} vanish, in contrast to what is observed in Nature. So the mismatch of the two subgroups is necessary. If θ_l is zero, i.e. the subgroup present in the charged lepton sector is a D_2 group, $\theta_{13} = 0$ and θ_{23} maximal will follow. If, however, only a smaller Z_2 group is present in the charged lepton sector, neither θ_{13} being zero nor θ_{23} being maximal holds. Then only the PMNS matrix element $|(U_{PMNS})_{\tau 3}|$ is fixed by group theory.

Finally, the matrix U_l given in Eq.(3.8) will equal the matrix shown in Eq.(3.17), if we additionally set the phases to $\alpha_1^l = 0$, $\alpha_2^l = \pi/4$, and $\alpha_3^l = 3\pi/4$.

One might ask the question what actually determines the size of the solar mixing angle θ_{12} in this context. For $\theta_l = 0$, we find from Eq.(3.21) that

$$|(U_{PMNS})_{e1}| = |\cos\theta_\nu| \quad \text{and} \quad |(U_{PMNS})_{e2}| = |\sin\theta_\nu|\ , \tag{3.25}$$

which shows that θ_{12} is given by θ_ν. Since this angle would vanish, if a D_2 group instead of a Z_2 group (with generator BA^m) was present in the neutrino sector, one might interpret the size of the solar mixing angle as hint to how strongly a D_2 group is broken in the neutrino sector.

Phenomenology

In the following we analyze the phenomenology of this model. For the eigenvalues of $M'_\nu M'^\dagger_\nu$ we find

$$m^2_{2,1} = \tfrac{1}{2}\left(\tfrac{v_u^2}{\Lambda}\right)^2\left(\tfrac{v}{\Lambda}\right)^2\left[s^2+4t^2+x^2+z^2 \pm \sqrt{(s-x)^2(8t^2+(s+x)^2)+2(4t^2+x^2-s^2)z^2+z^4}\right]$$
$$\text{and} \quad m^2_3 = \left(\tfrac{v_u^2}{\Lambda}\right)^2\left(\tfrac{v}{\Lambda}\right)^2\left(x^2+z^2\right) . \tag{3.26}$$

This assignment of the eigenvalues is unambiguous, since $m_2^2 > m_1^2$ is experimentally known and the eigenvalue corresponding to the eigenvector $(0,1,-1)^T$ can only be m_3^2. The solar mixing angle θ_{12} is found to depend on s, t, x, and z in the following way

$$\tan 2\theta_{12} = \frac{2\sqrt{2}\,|t|\,\sqrt{(s-x)^2+z^2}}{x^2+z^2-s^2} . \tag{3.27}$$

Before discussing the general case with unconstrained parameters s, t, x, and z we comment on the special case in which z vanishes, since then the model contains three real parameters which can be determined by the three experimental quantities Δm^2_{21}, $|\Delta m^2_{31}|$, and θ_{12}. According to Eq.(3.15) either y_3 or u have to vanish for $z=0$ to hold. Assuming that y_3 is zero however has to be regarded as fine-tuning. In contrast to that, a vanishing VEV u can be explained either through the absence of the flavon φ_ν from the model or through a flavon potential which only allows configurations with $u=0$ to be minima. The neutrino mass m_3 is then proportional to $|x|$. From Eq.(3.26) and Eq.(3.27) we can derive for $z=0$:

$$m_3^2 = -\frac{1}{4}\frac{\cos^4\theta_{12}}{\sin^2\theta_{12}}\frac{(\Delta m^2_{21}+\Delta m^2_{31}(\tan^4\theta_{12}-1))^2}{\Delta m^2_{31}(1+\tan^2\theta_{12})-\Delta m^2_{21}} . \tag{3.28}$$

Neglecting the solar mass square difference we can simplify this expression to

$$m_3^2 \approx -\Delta m^2_{31}\cot^2 2\theta_{12} . \tag{3.29}$$

Eq.(3.29) shows that $\Delta m^2_{31} < 0$, i.e. the neutrinos have to have an inverted hierarchy. Note that similar results can also be found in [185]. A relation analogous to Eq.(3.28) can be found for $|m_{ee}|$ measured in $0\nu\beta\beta$ decay experiments. Note that $|m_{ee}|$ is proportional to $|s|$ due to Eq.(3.14) and can be written in terms of m_3, $\tan\theta_{12}$ and the mass square differences as

$$|m_{ee}|^2 = m_3^2\frac{(\Delta m^2_{21}(1-2\tan^2\theta_{12})+\Delta m^2_{31}(\tan^4\theta_{12}-1))^2}{(\Delta m^2_{21}+\Delta m^2_{31}(\tan^4\theta_{12}-1))^2} . \tag{3.30}$$

In the limit of vanishing solar mass splitting we find

$$|m_{ee}| \approx m_3 . \tag{3.31}$$

Taking the best-fit values $\Delta m^2_{21} = 7.65\cdot 10^{-5}\,\text{eV}^2$, $\Delta m^2_{31} = -2.40\cdot 10^{-3}\,\text{eV}^2$, and $\sin^2\theta_{12} = 0.304$ [47, 186] we obtain $s \approx 0.02075$, $t \approx 0.03502$, $x \approx 0.02146$ [3] for $v_u \approx 100\,\text{GeV}$, $\Lambda \approx 4\cdot 10^{11}\,\text{GeV}$, and $v/\Lambda \approx \lambda_c^2 \approx 0.04$. The neutrino masses are $m_1 \approx 0.05348$ eV, $m_2 \approx 0.05419$ eV and $m_3 \approx 0.02146$ eV. Their sum $\sum m_i \approx 0.1291$ eV lies below the upper bound required from cosmological data [187]. $|m_{ee}|$ equals 0.02075 eV which might be detectable in the far future [188]. The two Majorana phases $\phi_{1,2}$ are $\phi_1 = \pi/2$ and $\phi_2 = 0$. For tritium β decay,

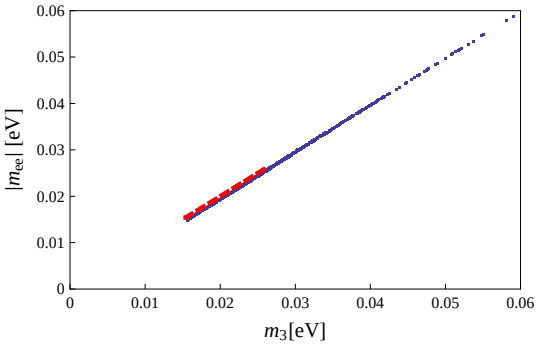

Figure 3.1: $|m_{ee}|$ plotted against m_3 for $z \neq 0$. The dashed (red) line indicates the results for $z = 0$. Mass square differences and the solar mixing angle are in the allowed 2σ ranges [47, 186]. As one can see, $|m_{ee}|$ and m_3 have nearly the same value. Additionally, one finds that m_3 has a lower bound around 0.015 eV. For $z = 0$ we also find an upper bound on m_3.

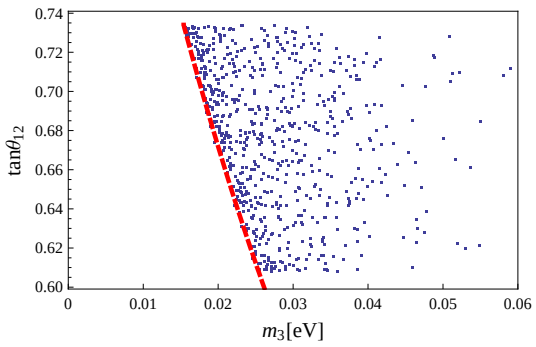

Figure 3.2: $\tan\theta_{12}$ plotted against m_3 for non-vanishing z. Again the dashed (red) line indicates $z = 0$ (assuming the best-fit value for the atmospheric mass square difference) and gives a lower bound for $z \neq 0$. Apart from that, the results for $\tan\theta_{12}$ are only constrained by the requirement that they are within the experimental 2σ ranges [47, 186], $0.61 \lesssim \tan\theta_{12} \lesssim 0.73$.

we find $m_\beta \approx 0.05370$ eV which is about a factor of four smaller than the expected sensitivity of the KATRIN experiment [189, 190].

Turning to the general case with $z \neq 0$ we first observe that also in this case the light neutrinos have to have an inverted hierarchy. To see this, let us assume that the matrix in Eq.(3.14) would allow the neutrinos to be normally ordered, i.e. $m_3 > m_1$ as well as $m_3 > m_2$. From $m_3^2 - m_2^2 > 0$ it follows

$$x^2 + z^2 - s^2 - 4t^2 - \sqrt{(s-x)^2(8t^2 + (s+x)^2) + 2(4t^2 + x^2 - s^2)z^2 + z^4} > 0 \,. \tag{3.32}$$

From this we can deduce

$$x^2 + z^2 > s^2 + 4t^2 \quad \text{and} \quad 16t^2(t^2 + x(s-x) - z^2) > 0 \,. \tag{3.33}$$

Rearranging the first inequality and taking $t \neq 0$ (otherwise θ_{12} would be zero) for the second one, we get

$$x^2 - s^2 > 4t^2 - z^2 \quad \text{and} \quad t^2 - z^2 > x(x-s) \,. \tag{3.34}$$

The sum of these inequalities leads to

$$s(x-s) > 3t^2 > 0 \,. \tag{3.35}$$

From Eq.(3.35) we see that s and x have the same sign, while $x^2 > s^2$, hence $x(x-s) > s(x-s)$. Combining Eq.(3.34) and Eq.(3.35), we find $t^2 - z^2 > 3t^2$, an obvious contradiction. Thus, the neutrinos cannot be normally ordered as assumed by $m_3^2 > m_2^2$. Instead we always have $m_2^2 > m_3^2$, which is only possible in case of an inverted hierarchy. Note that it is a priori not clear that also m_1 is larger than m_3, since the sizes of the mass square differences have to be tuned such that $\Delta m_{21}^2 \ll |\Delta m_{31}^2|$. In fact, Δm_{21}^2 is given by

$$\Delta m_{21}^2 = \left(\frac{v_u^2}{\Lambda}\right)^2 \left(\frac{v}{\Lambda}\right)^2 \sqrt{(s-x)^2(8t^2 + (s+x)^2) + 2(4t^2 + x^2 - s^2)z^2 + z^4} \,. \tag{3.36}$$

[3] Actually we find four solutions which all lead to the same absolute values, but to different signs for s, t and x, with the constraint that s and x have the same sign.

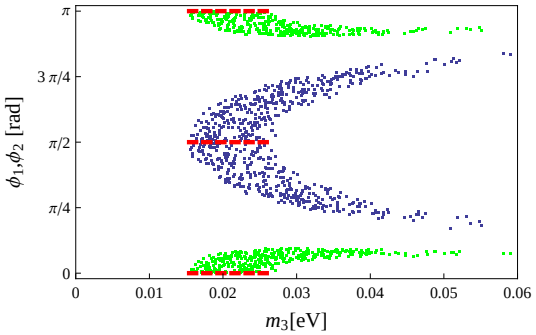

Figure 3.3: The Majorana phases ϕ_1 (blue/darker gray) and ϕ_2 (green/lighter gray) plotted against the lightest neutrino mass m_3 for non-vanishing z. The values for $z = 0$, $\phi_1 = \frac{\pi}{2}$, $\phi_2 = 0$, are displayed by dashed (red) lines. Notice that the results for $z \neq 0$ are centered around these values. The measured quantities, Δm^2_{21}, $|\Delta m^2_{31}|$ and θ_{12}, are within the 2σ ranges [47, 186].

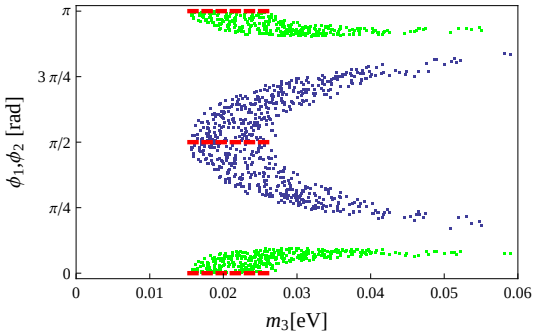

Figure 3.4: Phase difference $\phi_1 - \phi_2$ against m_3 for $z \neq 0$. The case $z = 0$, $|\phi_1 - \phi_2| = \pi/2$, is given by the dashed (red) lines. As one can see, $|\phi_1 - \phi_2|$ is restricted to the interval $[\pi/2, 3\pi/4]$ for $m_3 \lesssim 0.06$ eV. Its deviation from $\pi/2$ increases with increasing m_3. Again, the mass square differences and θ_{12} are within the experimentally allowed 2σ ranges [47, 186].

It vanishes, if $z = 0$ and $s = x$. Thus, $\Delta m^2_{21} \ll |\Delta m^2_{31}|$ will hold, if these equalities are nearly met. As noted, the vanishing of z can be made a natural result of the model. The near equality $s \approx x$, however, has to be regarded as a certain tuning of the couplings y_1 and y_4, see Eq.(3.15).

We have studied the general case $z \neq 0$ numerically. To fix the light neutrino mass scale we adjust the resulting solar mass square difference to its best-fit value. At the same time the atmospheric mass square difference and the mixing angle θ_{12} have to be within their allowed 2σ ranges [47, 186]. First, we note that our numerical results confirm that z in general has to be smaller than the parameters s, t, and x, and that s and x have to have nearly the same value. In Figure 3.1 we plot $|m_{ee}|$ against the lightest neutrino mass m_3. As one can see, the approximate equality of $|m_{ee}|$ and m_3, deduced for $z = 0$ in Eq.(3.31), still holds for $z \neq 0$. The dashed (red) line is the result for $z = 0$. One finds that m_3 has a minimal value around 0.015 eV, i.e. m_3 cannot vanish, and for $z = 0$ it also has a maximal one around 0.027 eV. These two bounds can be found as well by using Eq.(3.29). The non-vanishing of $m_3 \approx |m_{ee}|$ agrees with the findings in the literature that $|m_{ee}|$ is required to be larger than 0.01 eV, if neutrinos follow an inverted hierarchy [191–193]. Figure 3.2 shows that the relation in Eq.(3.29), which is fulfilled to a good accuracy for $z = 0$, gives a lower bound for $z \neq 0$ in the $\tan\theta_{12} - m_3$ plane and no further constraints on the solar mixing angle can be derived. Note that we have used the best-fit value of the atmospheric mass square difference for the dashed (red) line in Figure 3.2. Finally, we plot the Majorana phases ϕ_1 and ϕ_2 in Figure 3.3 against the lightest neutrino mass m_3. As one can see, the phase ϕ_1 (blue/darker gray) varies between $\pi/8$ and $7\pi/8$, while ϕ_2 (green/lighter gray) either lies in the interval $[0, \pi/8]$ or $[7\pi/8, \pi]$ for small values of m_3, i.e. $m_3 \lesssim 0.06$ eV. The dashed (red) lines indicate again the values of ϕ_1 and ϕ_2 achieved in the limit $z = 0$. As the difference $\phi_1 - \phi_2$ of the two Majorana phases is the only quantity which can be realistically determined by future experiments [188] through

$$|m_{ee}| = |m_1 \cos^2\theta_{12} e^{2i(\phi_1 - \phi_2)} + m_2 \sin^2\theta_{12}| \,, \tag{3.37}$$

we also plot $\phi_1 - \phi_2$ against m_3 in Figure 3.4. This plot shows that the phase difference has to lie in the rather narrow ranges $[-3\pi/4, -\pi/2]$ or $[\pi/2, 3\pi/4]$ for small values of m_3. As one can see, the deviations from $|\phi_1 - \phi_2| = \pi/2$ ($z = 0$ case) become larger for larger values of m_3.

Flavon Superpotential

In the following we discuss the flavon superpotential and show that the VEV structure assumed in (Eq.(3.5) and) Eq.(3.6) naturally arises, as does the spontaneous CP violation. In constructing the superpotential we work along the lines of [28, 103, 104, 117, 118]. For this purpose, we generalize R-parity to a $U(1)_R$ symmetry under which the "matter fields" transform with charge $+1$, while the fields h_u and h_d and the flavons are uncharged and another type of fields, the driving fields, have charge $+2$. We note that the flavons and the driving fields transform trivially under the Standard Model gauge group, but non-trivially under the flavor symmetry. The set needed for constructing the potential consists of $\chi_e^0 \sim (\underline{\mathbf{1}}_{\mathbf{1}}, \omega^4)$, $\sigma^0 \sim (\underline{\mathbf{1}}_{\mathbf{4}}, \omega)$, and $\chi_\nu^0 \sim (\underline{\mathbf{1}}_{\mathbf{1}}, \omega)$ under (D_4, Z_5). Since all terms of the superpotential have to have $U(1)_R$ charge $+2$, the driving fields cannot couple to the fermions and can only appear linearly in the flavon superpotential. The renormalizable $D_4 \times Z_5$ invariant superpotential for flavons and driving fields reads

$$\begin{aligned} \mathrm{W}_f &= a\,\chi_e^0\,\chi_e^2 + b\,\chi_e^0\,\varphi_e^2 \\ &\quad + c\,\sigma^0\,(\psi_1^2 - \psi_2^2) + d\,\chi_\nu^0\,\psi_1\,\psi_2 + e\,\chi_\nu^0\,\varphi_\nu^2 + f\,\chi_\nu^0\,\chi_\nu^2 \,. \end{aligned} \tag{3.38}$$

Assuming that the flavons acquire their VEVs in the supersymmetric limit, we can use the F-terms of the driving fields to determine the vacuum structure of the flavons. The equations

$$\frac{\partial \mathrm{W}_f}{\partial \chi_e^0} = a\,\chi_e^2 + b\,\varphi_e^2 = 0 \,, \tag{3.39a}$$

$$\frac{\partial \mathrm{W}_f}{\partial \sigma^0} = c\,(\psi_1^2 - \psi_2^2) = 0 \,, \tag{3.39b}$$

$$\frac{\partial \mathrm{W}_f}{\partial \chi_\nu^0} = d\,\psi_1\,\psi_2 + e\,\varphi_\nu^2 + f\,\chi_\nu^2 = 0 \,, \tag{3.39c}$$

result in

$$\langle \chi_e \rangle = \pm i \sqrt{\frac{b}{a}}\,\langle \varphi_e \rangle \,, \quad \langle \psi_1 \rangle = \pm \langle \psi_2 \rangle \,, \quad \langle \chi_\nu \rangle = \pm i \sqrt{\frac{d\,\langle \psi_1 \rangle\,\langle \psi_2 \rangle + e\,\langle \varphi_\nu \rangle^2}{f}} \,, \tag{3.40}$$

which can be re-written as

$$w_e = \pm i \sqrt{\frac{b}{a}}\,u_e \,, \quad \langle \psi_1 \rangle = \pm v \,, \quad w = \pm i \sqrt{\frac{d\,\langle \psi_1 \rangle\,\langle \psi_2 \rangle + e\,u^2}{f}} \,. \tag{3.41}$$

Note that the VEVs $\langle \varphi_e \rangle = u_e$, $\langle \psi_2 \rangle = v$, and $\langle \varphi_\nu \rangle = u$ are unconstrained by the potential. Note further that the choice of sign in all cases is independent in Eq.(3.40) and Eq.(3.41). For the discussion of the preserved subgroup structure it is anyway only relevant whether $\langle \psi_1 \rangle = \langle \psi_2 \rangle$ or $\langle \psi_1 \rangle = -\langle \psi_2 \rangle$. For $\langle \psi_1 \rangle = \langle \psi_2 \rangle$ as used in Eq.(3.6) we conserve a subgroup Z_2 of D_4 generated by B, whereas the relation $\langle \psi_1 \rangle = -\langle \psi_2 \rangle$ indicates that the Z_2 subgroup

generated by BA^2 is left unbroken. This Z_2 group is also not a subgroup of the D_2 group conserved in the charged lepton sector. Thus, the subgroups of the charged lepton and the neutrino sector will be misaligned in both cases. In this paper we only consider the case of $\langle\psi_1\rangle = \langle\psi_2\rangle = v$. Eq.(3.41) shows then that the VEVs w_e and w necessarily have to be imaginary, so that CP is spontaneously violated, if the parameters $a, ..., f$ and the VEVs u_e, v, and u are chosen to be positive.

We remark that, due to the $U(1)_R$ symmetry, a μ-term $\mu h_u h_d$ is forbidden in our model and has to be generated by some other mechanism. This feature is shared by all models using a $U(1)_R$ symmetry. In the derivation of Eq.(3.39), terms of the form $\chi_\nu^0 h_u h_d$ which couple a driving field to the MSSM Higgs fields can be safely neglected. They also cannot induce a μ-term, since only vanishing VEVs are allowed for the driving fields, if the parameters $a, ..., f$ and the flavon VEVs are non-zero, as they are in our case. Finally, note that we find flat directions in this potential in the case of spontaneous CP violation under discussion here. These are however expected to be lifted by the inclusion of the NLO corrections as well as through soft supersymmetry breaking terms. Such nearly flat directions might be of interest for inflation [194].

3.1.3 Next-to-Leading Order Corrections

In order to determine how our results are corrected at NLO, we take into account the effects of operators which are suppressed by one more power of the cutoff scale Λ compared to the LO. Such contributions to the fermion masses include two instead of only one flavon. In the flavon superpotential we add terms consisting of one driving field and three flavons. It turns out that there are actually no contributions to the fermion masses from two-flavon insertions due to the Z_5 symmetry. Hence, the only NLO corrections we need to consider are those of the flavon superpotential, which lead to a shift in the flavon VEVs parameterized as

$$\langle\chi_e\rangle = w_e + \delta w_e \ , \ \ \langle\chi_\nu\rangle = w + \delta w \ , \ \text{ and } \ \ \langle\psi_1\rangle = v + \delta v \ . \tag{3.42}$$

The VEVs $\langle\varphi_e\rangle = u_e$, $\langle\varphi_\nu\rangle = u$, and $\langle\psi_2\rangle = v$ which are not determined at LO remain unconstrained also at NLO. The natural size of the VEV shifts is

$$\frac{\delta\text{VEV}}{\text{VEV}} \sim \lambda_c^2 \ . \tag{3.43}$$

As will be discussed below, the shifts δw and δw_e are in general complex, whereas the shift δv in the VEV $\langle\psi_1\rangle$ is real for this type of spontaneous CP violation.

Fermion Masses

The VEV shifts induce corrections to the lepton mass matrices given in Eq.(3.7) when the shifted VEVs are inserted into the LO terms, see Eq.(3.4). In case of the charged lepton masses only the VEV of χ_e is shifted. Such a shift is, however, not relevant, since it can be absorbed into the Yukawa couplings y_1^e and y_2^e. [4] Especially, U_l is still given by Eq.(3.8). The form of the neutrino mass matrix is changed through the shifts of the VEVs as

$$M_\nu = \frac{v_u^2}{\Lambda^2}\begin{pmatrix} y_1(w+\delta w) & y_2 v & y_2(v+\delta v) \\ y_2 v & y_3 u & y_4(w+\delta w) \\ y_2(v+\delta v) & y_4(w+\delta w) & y_3 u \end{pmatrix} \ . \tag{3.44}$$

[4] These then become complex which however does not affect our results.

Note that δw cannot simply be absorbed into w, since δw is complex, whereas w is imaginary. In the charged lepton mass basis the matrix in Eq.(3.44) reads

$$M'_\nu = \frac{v_u^2}{\Lambda^2} \begin{pmatrix} y_1(w+\delta w) & y_2(v+e^{i\pi/4}\delta v/\sqrt{2}) & y_2(v+e^{-i\pi/4}\delta v/\sqrt{2}) \\ y_2(v+e^{i\pi/4}\delta v/\sqrt{2}) & y_4(w+\delta w) & y_3 u \\ y_2(v+e^{-i\pi/4}\delta v/\sqrt{2}) & y_3 u & y_4(w+\delta w) \end{pmatrix} . \quad (3.45)$$

To evaluate the shifts in the neutrino masses and to discuss the deviations of the mixing angles from their LO values, especially θ_{13} from zero and θ_{23} from maximal, we parameterize the Majorana neutrino mass matrix as

$$M'_\nu = \frac{v_u^2}{\Lambda}\frac{v}{\Lambda} \begin{pmatrix} i\,s\,(1+\alpha\,\epsilon) & t\,(1+e^{i\pi/4}\,\epsilon) & t\,(1+e^{-i\pi/4}\,\epsilon) \\ t\,(1+e^{i\pi/4}\,\epsilon) & i\,x\,(1+\alpha\,\epsilon) & z \\ t\,(1+e^{-i\pi/4}\,\epsilon) & z & i\,x\,(1+\alpha\,\epsilon) \end{pmatrix} \quad (3.46)$$

with s, t, x, and z as given in Eq.(3.15) and [5]

$$\alpha\,\epsilon = \frac{\delta w}{w} \ , \ \ \alpha = \alpha_r + i\,\alpha_i \ , \ \text{ and } \ \ \epsilon = \frac{1}{\sqrt{2}}\,\frac{\delta v}{v} \approx \lambda_c^2 \approx 0.04 \ . \quad (3.47)$$

The neutrino masses and mixing parameters resulting from Eq.(3.46) can then be calculated in an expansion in the small parameter ϵ. We observe that the mass shift of m_3^2 would vanish for δw being zero. Its explicit form is

$$(m_3^{\rm NLO})^2 = (m_3^{\rm LO})^2 + 2\left(\frac{v_u^2}{\Lambda}\right)^2\left(\frac{v}{\Lambda}\right)^2 x(\alpha_r\,x + \alpha_i\,z)\,\epsilon \ , \quad (3.48)$$

with $(m_3^{\rm LO})^2$ given in Eq.(3.26). Similarly, the masses m_1^2 and m_2^2 undergo shifts proportional to ϵ. A simple expression can however only be found for the sum $m_1^2 + m_2^2$:

$$(m_1^{\rm NLO})^2 + (m_2^{\rm NLO})^2 = (m_1^{\rm LO})^2 + (m_2^{\rm LO})^2 + 2\left(\frac{v_u^2}{\Lambda}\right)^2\left(\frac{v}{\Lambda}\right)^2 (2\sqrt{2}\,t^2 + \alpha_r\,(s^2+x^2) - \alpha_i\,x\,z)\,\epsilon \ . \quad (3.49)$$

$(m_{1,2}^{\rm LO})^2$ can be found in Eq.(3.26). The mixing angle θ_{13} no longer vanishes and we find

$$\sin\theta_{13} \approx \left|\frac{t\,x}{t^2+(s-x)x-z^2}\right|\,\epsilon \ . \quad (3.50)$$

For θ_{23} we get

$$\tan\theta_{23} \approx 1 + \sqrt{2}\,\frac{x\,z}{t^2+(s-x)x-z^2}\,\epsilon \ . \quad (3.51)$$

The deviation from maximal atmospheric mixing can also be expressed through

$$|\cos 2\theta_{23}| \approx \sqrt{2}\,\left|\frac{x\,z}{t^2+(s-x)x-z^2}\right|\,\epsilon \approx \sqrt{2}\,\left|\frac{z}{t}\right|\,\sin\theta_{13} \ . \quad (3.52)$$

From both formulae one can deduce that in the case $z = 0$ the corrections to maximal atmospheric mixing are not of the order ϵ, but only arise at $\mathcal{O}(\epsilon^2)$. Contrary to this, θ_{13} will still receive corrections of order ϵ, if $z = 0$. The solar mixing angle θ_{12}, which is not fixed to

[5] We assume that ϵ is positive.

a precise value in this model, also gets corrections of order ϵ. We note that the smallness of $|s-x|$ and z, required by the smallness of Δm^2_{21}, might lead to a disturbance of the expansion in the parameter ϵ.

A correlation between $\cos 2\theta_{23}$ and $\sin\theta_{13}$ depending only on physical quantities, Δm^2_{ij}, ..., and not on the parameters of the model, s, t, ..., can be obtained by an analytic consideration which is done analogously to the study performed in [67]. Clearly, the matrix in Eq.(3.45) is no longer $\mu-\tau$ symmetric. However, we find the following remnants of this symmetry:

$$(M'_\nu)_{e\mu} = (M'_\nu)^*_{e\tau} \quad \text{and} \quad (M'_\nu)_{\mu\mu} = (M'_\nu)_{\tau\tau} \; . \tag{3.53}$$

This shows that $\mu-\tau$ symmetry is only broken by phases, but not by the absolute values of the matrix elements. This leads to

$$\begin{aligned}
0 &= |(M'_\nu)_{e\mu}|^2 + |(M'_\nu)_{\mu\mu}|^2 - |(M'_\nu)_{e\tau}|^2 - |(M'_\nu)_{\tau\tau}|^2 \; , \\
0 &= (M'_\nu M'^\dagger_\nu)_{\mu\mu} - (M'_\nu M'^\dagger_\nu)_{\tau\tau} = \sum_{j=1}^{3} m_j^2 (|(U_{PMNS})_{\mu j}|^2 - |(U_{PMNS})_{\tau j}|^2) \; , \\
0 &= \Big((\sin^2\theta_{12} - \sin^2\theta_{13}\cos^2\theta_{12})\, m_1^2 + (\cos^2\theta_{12} - \sin^2\theta_{13}\sin^2\theta_{12})\, m_2^2 - \cos^2\theta_{13}\, m_3^2 \Big) \cos(2\theta_{23}) \\
&\quad - \Delta m^2_{21} \sin 2\theta_{12} \sin 2\theta_{23} \cos\delta \sin\theta_{13} \; .
\end{aligned} \tag{3.54}$$

Since $\sin\theta_{13} \sim \mathcal{O}(\epsilon)$ and $\cos 2\theta_{23} \sim \mathcal{O}(\epsilon)$ is already known, we can linearize this equation and obtain (using best-fit values for the physical quantities and the fact that neutrinos have an inverted hierarchy in this model)

$$\cos 2\theta_{23} \approx -\frac{\Delta m^2_{21} \sin 2\theta_{12}}{\Delta m^2_{32} + \Delta m^2_{21} \sin^2\theta_{12}} \cos\delta \sin\theta_{13} \approx 0.03 \cos\delta \sin\theta_{13} \; . \tag{3.55}$$

Eq.(3.55) can be used to estimate the largest possible deviation from maximal mixing. For $\sin\theta_{13}$ being at its $2\,\sigma$ limit of 0.2 and $|\cos\delta| = 1$, $|\cos 2\theta_{23}|$ still has to be less than 6×10^{-3}, which is well within the $1\,\sigma$ error. Finally, we note that Eq.(3.55) must be consistent with Eq.(3.52), and thus we again find that z ought to be small.

Flavon Superpotential

The corrections to the flavon superpotential stem from terms involving one driving field and three flavons. These terms are non-renormalizable and suppressed by the cutoff scale Λ. We find

$$\begin{aligned}
\Delta \mathrm{W}_f = \quad & \frac{k_1}{\Lambda}\,\chi^0_e\,\chi^3_\nu + \frac{k_2}{\Lambda}\,\chi^0_e\,\chi_\nu\,\varphi^2_\nu + \frac{k_3}{\Lambda}\,\chi^0_e\,\chi_\nu\psi_1\psi_2 + \frac{k_4}{\Lambda}\,\chi^0_e\,\varphi_\nu\,(\psi_1^2+\psi_2^2) \\
& + \frac{k_5}{\Lambda}\,\sigma^0\,\varphi_e\,\chi^2_e + \frac{k_6}{\Lambda}\,\sigma^0\,\varphi^3_e + \frac{k_7}{\Lambda}\,\chi^0_\nu\,\chi^3_e + \frac{k_8}{\Lambda}\,\chi^0_\nu\,\chi_e\varphi^2_e \, .
\end{aligned} \tag{3.56}$$

Assuming that CP is only spontaneously violated forces all k_i to be real. We calculate the F-terms of $\mathrm{W}_f + \Delta\mathrm{W}_f$ for the driving fields using that the VEVs can be parameterized as

$$\langle\chi_e\rangle = w_e + \delta w_e \; , \quad \langle\chi_\nu\rangle = w + \delta w \; , \quad \text{and} \quad \langle\psi_1\rangle = v + \delta v \; . \tag{3.57}$$

The VEVs $\langle\varphi_e\rangle = u_e$, $\langle\varphi_\nu\rangle = u$, and $\langle\psi_2\rangle = v$ are not determined at LO. We assume that only terms containing up to one VEV shift or the suppression factor $1/\Lambda$, but not both, are relevant. The F-terms then lead to

$$2\,a\,w_e\,\delta w_e + \frac{1}{\Lambda}(k_1\,w^3 + k_2\,u^2\,w + k_3\,v^2\,w + 2\,k_4\,u\,v^2) = 0\;, \tag{3.58a}$$

$$2\,c\,v\,\delta v + \frac{u_e}{\Lambda}(k_5\,w_e^2 + k_6\,u_e^2) = 0\;, \tag{3.58b}$$

$$d\,v\,\delta v + 2\,f\,w\,\delta w + \frac{w_e}{\Lambda}(k_7\,w_e^2 + k_8\,u_e^2) = 0\;. \tag{3.58c}$$

Here we have chosen the solutions with + in Eq.(3.41). The explicit forms of the shifts read

$$\delta v = -\frac{1}{2\,c}\,\frac{u_e}{v\,\Lambda}\,(k_5\,w_e^2 + k_6\,u_e^2)\;, \tag{3.59a}$$

$$\delta w = \frac{1}{4\,c\,f}\,\frac{1}{w\,\Lambda}\,(d\,(k_5 w_e^2 + k_6 u_e^2)\,u_e - 2\,c\,(k_7\,w_e^2 + k_8\,u_e^2)\,w_e)\;, \tag{3.59b}$$

$$\delta w_e = -\frac{1}{2\,a}\,\frac{1}{w_e\,\Lambda}\,(k_1\,w^3 + k_2\,u^2\,w + k_3\,v^2\,w + 2\,k_4\,u\,v^2)\;. \tag{3.59c}$$

As one can see, for our type of spontaneous CP violation, δv is real, whereas δw_e and δw turn out to be complex in general. As can be read off from Eq.(3.59), all shifts are generically of order

$$\frac{\delta\mathrm{VEV}}{\mathrm{VEV}} \sim \lambda_c^2 \quad \text{for} \quad \mathrm{VEV} \sim \lambda_c^2\,\Lambda\;. \tag{3.60}$$

Finally, note that the free parameters $\langle\varphi_e\rangle = u_e$, $\langle\varphi_\nu\rangle = u$, and $\langle\psi_2\rangle = v$ are still undetermined.

3.2 A SUSY D_{10} model for Golden Ratio prediction

As discussed in Chapter 2, there are two possibilities to link the solar neutrino mixing with the golden ratio $\varphi = \varphi^2 - 1 = \frac{1}{2}\,(1+\sqrt{5})$:

- (A) $\cot(\theta_{12}) = \varphi$
- (B) $\cos(\theta_{12}) = \frac{\varphi}{2}$

In [15], it has shown the connection between (A) and the non-abelian discrete group A_5. The reason for A_5 being the candidate symmetry is because this group is isomorphic to the rotational group of the icosahedron and its geometrical features can be linked to the golden ratio. For instance, the 12 vertices of an icosahedron with edge-length 2 have Cartesian coordinates $(0, \pm 1, \pm\varphi)$, $(\pm 1, \pm\varphi, 0)$, and $(\pm\varphi, 0, \pm 1)$. A peculiar feature of $\cot\theta_{12} = \varphi$ is that the angle gives also $\tan 2\theta_{12} = 2$, and this can be obtained from a simple matrix proportional to [14]

$$M_\nu \propto \begin{pmatrix} 0 & 1 \\ 1 & 1 \end{pmatrix}. \tag{3.61}$$

This matrix is invariant under a Z_2 symmetry generated by [14]

$$S = \frac{1}{\sqrt{5}}\begin{pmatrix} -1 & 2 \\ 2 & 1 \end{pmatrix}, \tag{3.62}$$

where invariance is fulfilled when $S^T\, M_\nu\, S = M_\nu$.

Now we concentrate on the possible theoretical origin of the golden ratio prediction (B). We stress that flavor models based on the symmetry group D_{10} are natural candidates to generate $\theta_{12} = \pi/5$. The dihedral group D_{10} is the rotational symmetry group of a decagon and the exterior angle in a decagon is nothing but $\pi/5$, or 36 degrees. We remark that also D_5, the rotational symmetry group of a regular pentagon, could be possible. In a regular pentagon the length of a diagonal is φ times the length of a side. The triangle formed by the diagonal and two sides has one angle of 108° (the internal angle) and two angles with 36° each. However, here we focus on D_{10} because it turns out that the vacuum alignment we need in our model is simplified due to the larger number of representations in D_{10}. Note that just as considering A_5 for the golden ratio prediction (A) was motivated by geometrical considerations, the use of the (mathematically simpler) pentagon or decagon symmetry group is here motivated by prediction (B).

3.2.1 Golden Ratio Prediction and Dihedral Groups

We have seen that there is a simple Z_2 under which a mass matrix generating $\cot\theta_{12} = \varphi$ is invariant, see Eq.(3.61) and Eq.(3.62). The second golden ratio proposal (B) corresponds to $\tan 2\theta_{12} = \sqrt{1+\varphi^2}/(\varphi-1)$, and therefore it diagonalizes a less straightforward matrix. Nevertheless, in this case one can make use of Z_2 invariance as well, however the charged lepton sector has also to be taken into account. We will first discuss this for the simplified 2-flavor case with symmetric mass matrices, before making the transition to dihedral groups and then to the explicit model based on D_{10} that we will construct.

The generators of the Z_2 under which the neutrino mass matrix M_ν and the charged lepton mass matrix M_l have to be invariant are

$$S_{\nu,l} = \begin{pmatrix} 0 & e^{-i\phi_{\nu,l}} \\ e^{i\phi_{\nu,l}} & 0 \end{pmatrix}, \tag{3.63}$$

respectively. The matrices M_ν and M_l are invariant when they have the following structure:

$$\begin{aligned} M_{\nu,l} = \begin{pmatrix} A_{\nu,l}\, e^{i\phi_{\nu,l}} & B_{\nu,l} \\ B_{\nu,l} & A_{\nu,l}\, e^{-i\phi_{\nu,l}} \end{pmatrix} &= \begin{pmatrix} e^{i\phi_{\nu,l}} & 0 \\ 0 & 1 \end{pmatrix} \begin{pmatrix} A_{\nu,l} & B_{\nu,l} \\ B_{\nu,l} & A_{\nu,l} \end{pmatrix} \begin{pmatrix} 1 & 0 \\ 0 & e^{-i\phi_{\nu,l}} \end{pmatrix} \\ &\equiv P_{\nu,l} \begin{pmatrix} A_{\nu,l} & B_{\nu,l} \\ B_{\nu,l} & A_{\nu,l} \end{pmatrix} Q_{\nu,l}\,. \end{aligned} \tag{3.64}$$

The inner matrix can be written as

$$\begin{pmatrix} A_{\nu,l} & B_{\nu,l} \\ B_{\nu,l} & A_{\nu,l} \end{pmatrix} = \tilde{U}_{\nu,l}^T\, \mathrm{diag}(A_{\nu,l} - B_{\nu,l}\ ,\ A_{\nu,l} + B_{\nu,l})\, \tilde{U}_{\nu,l}\,, \text{ where } \tilde{U}_{\nu,l} = \begin{pmatrix} -\frac{1}{\sqrt{2}} & \frac{1}{\sqrt{2}} \\ \frac{1}{\sqrt{2}} & \frac{1}{\sqrt{2}} \end{pmatrix}. \tag{3.65}$$

The total diagonalization matrices of M_ν and M_l are $U_{\nu,l} = P_{\nu,l}\, \tilde{U}_{\nu,l}$ and the physical mixing matrix is their product $U = U_l^\dagger\, U_\nu = \tilde{U}_l^\dagger\, P_l^\dagger\, P_\nu\, \tilde{U}_\nu$. The 11-element is found to be

$$|U_{e1}|^2 = \left| \cos\frac{1}{2}(\phi_\nu - \phi_l) \right|^2 . \tag{3.66}$$

The fact that a non-trivial phase matrix lies in between the two maximal rotations $\tilde{U}_l^\dagger$ and $\tilde{U}_\nu$ is crucial. Obviously, at this stage any mixing angle could be generated. However, the

observation made in [86, 184, 195, 196] was that the phase factors in Eq.(3.63) can be linked to group theoretical flavor model building with dihedral groups D_n. To make the connection from Eq.(3.66) to dihedral groups, we note that the flavor symmetry D_n has 2-dimensional representations $\mathbf{\underline{2}_j}$, with $\mathrm{j} = 1, \ldots, \frac{n}{2} - 1$ ($\mathrm{j} = 1, \ldots, \frac{n-1}{2}$) for integer (odd) n, generated by

$$A = \begin{pmatrix} e^{2\pi i \frac{\mathrm{j}}{n}} & 0 \\ 0 & e^{-2\pi i \frac{\mathrm{j}}{n}} \end{pmatrix} \text{ and } B = \begin{pmatrix} 0 & 1 \\ 1 & 0 \end{pmatrix}. \tag{3.67}$$

Z_2 subgroups are generated by

$$B\,A^k = \begin{pmatrix} 0 & e^{-2\pi i \frac{\mathrm{j}}{n} k} \\ e^{2\pi i \frac{\mathrm{j}}{n} k} & 0 \end{pmatrix} \tag{3.68}$$

with integer k. This is just the required form of a Z_2 generator in Eq.(3.63). It is now possible to construct models in which the two fermions transform under the representation $\mathbf{\underline{2}_j}$ of D_n, and D_n is broken such that M_ν is left invariant under $B\,A^{k_\nu}$ and M_l is left invariant under $B\,A^{k_l}$ [86,184,195,196]. Consequently, the relation in Eq.(3.66) is obtained and we can identify

$$|U_{e1}|^2 = \left| \cos \pi \frac{\mathrm{j}}{n} \left(k_\nu - k_l\right) \right|^2 . \tag{3.69}$$

Hence, a natural candidate to implement the requested value of $\pi/5$ is, e.g., D_{10}. This is no surprise given the observation that we made at the beginning of this section, namely that $\pi/5$ is the exterior angle of a decagon and that D_{10} is its rotational symmetry group.

3.2.2 The Model at Leading Order

Fermion Masses

We continue with an explicit model: We work in the framework of the MSSM without explicitly introducing left-handed conjugate neutrinos. Majorana masses for the light neutrinos are thus generated by an effective operator coupling to two Higgs VEVs. We augment the MSSM by a flavor symmetry $D_{10} \times Z_5$. The symmetry D_{10} is used for our prediction of the solar mixing angle, while the auxiliary Abelian symmetry Z_5 separates the charged lepton and neutrino sectors. Due to the flavor symmetry, no renormalizable Yukawa couplings are allowed for the charged leptons and the dimension 5 operator giving mass to the neutrinos vanishes as well. Mass for the leptons is generated by coupling them to gauge singlet flavons, which acquire VEVs and thereby break the flavor group. The charged lepton masses are thus generated by dimension-5 operators, whereas the neutrino masses are generated by dimension 6 operators[6].

The transformation properties of the MSSM leptons and Higgs fields, as well as the representations under which the flavons transform, are given in Table 3.3. The multiplication table and the Clebsch-Gordan coefficients of D_{10} are given in Appendix A.2. Note that the fermions and the flavons that couple to them are all in unfaithful representations[7] of D_{10}

[6] In a model including quarks, this may explain $m_\tau \ll m_t$ without invoking a large $\tan\beta$.

[7] A representation is unfaithful if at least two distinct group elements are mapped to the same matrix representation.

Field	$l_{1,2}$	l_3	$e^c_{1,2}$	e^c_3	$h_{u,d}$	σ^e	$\chi^e_{1,2}$	$\xi^e_{1,2}$	$\rho^e_{1,2}$	σ^ν	$\varphi^\nu_{1,2}$	$\chi^\nu_{1,2}$	$\xi^\nu_{1,2}$
D_{10}	$\underline{\mathbf{2_4}}$	$\underline{\mathbf{1_1}}$	$\underline{\mathbf{2_2}}$	$\underline{\mathbf{1_1}}$	$\underline{\mathbf{1_1}}$	$\underline{\mathbf{1_1}}$	$\underline{\mathbf{2_2}}$	$\underline{\mathbf{2_3}}$	$\underline{\mathbf{2_4}}$	$\underline{\mathbf{1_1}}$	$\underline{\mathbf{2_1}}$	$\underline{\mathbf{2_2}}$	$\underline{\mathbf{2_3}}$
Z_5	ω	ω	ω^2	ω^2	1	ω^2	ω^2	ω^2	ω^2	ω^3	ω^3	ω^3	ω^3

Table 3.3: Particle content of the D_{10} model: l_i are the three left-handed lepton doublets, e^c_i are the left-handed conjugate charged lepton singlets, and $h_{u,d}$ are the MSSM Higgs doublets. Furthermore we have flavons σ^e, $\chi^e_{1,2}$, $\xi^e_{1,2}$, $\rho^e_{1,2}$, σ^ν, $\varphi^\nu_{1,2}$, $\chi^\nu_{1,2}$, and $\xi^\nu_{1,2}$, which only transform under $D_{10}\times Z_5$. The phase $\omega = e^{\frac{2\pi i}{5}}$ is the fifth unit root.

(i.e., in $\underline{\mathbf{2_2}}$ and $\underline{\mathbf{2_4}}$), so that here a D_5 structure would have sufficed. However, the full D_{10} structure is needed to achieve the desired vacuum alignment.

We can continue by constructing the Yukawa superpotential, giving the leading order terms for both charged lepton and neutrino masses:

$$\begin{aligned}
\mathrm{W}_l &= y^e_1\,(l_1\,e^c_2\,\chi^e_2 + l_2\,e^c_1\,\chi^e_1)\,\frac{h_d}{\Lambda} + y^e_2\,(l_1\,e^c_1\,\rho^e_1 + l_2\,e^c_2\,\rho^e_2)\,\frac{h_d}{\Lambda} + y^e_3\,(l_3\,e^c_1\,\chi^e_2 + l_3\,e^c_2\,\chi^e_1)\,\frac{h_d}{\Lambda} \\
&+ y^e_4\,(l_1\,e^c_3\,\rho^e_2 + l_2\,e^c_3\,\rho^e_1)\,\frac{h_d}{\Lambda} + y^e_5\,l_3\,e^c_3\,\sigma^e\,\frac{h_d}{\Lambda} \\
&+ y^\nu_1\,l_1\,l_2\,\sigma^\nu\,\frac{h_u^2}{\Lambda^2} + y^\nu_1\,l_2\,l_1\,\sigma^\nu\,\frac{h_u^2}{\Lambda^2} + y^\nu_2\,(l_1\,l_1\,\chi^\nu_1 + l_2\,l_2\,\chi^\nu_2)\,\frac{h_u^2}{\Lambda^2} + y^\nu_3\,l_3\,l_3\,\sigma^\nu\,\frac{h_u^2}{\Lambda^2}\,.
\end{aligned} \tag{3.70}$$

As we will show below, introducing appropriate driving fields and minimizing the flavon superpotential leads to the following VEVs for the flavons:

$$\begin{pmatrix} \langle\chi^e_1\rangle \\ \langle\chi^e_2\rangle \end{pmatrix} = v_e \begin{pmatrix} 1 \\ e^{\frac{2\pi i k}{5}} \end{pmatrix},\quad \begin{pmatrix} \langle\xi^e_1\rangle \\ \langle\xi^e_2\rangle \end{pmatrix} = w_e \begin{pmatrix} 1 \\ e^{\frac{3\pi i k}{5}} \end{pmatrix},\quad \begin{pmatrix} \langle\rho^e_1\rangle \\ \langle\rho^e_2\rangle \end{pmatrix} = z_e \begin{pmatrix} 1 \\ e^{\frac{4\pi i k}{5}} \end{pmatrix}, \tag{3.71}$$

where k is an odd integer between 1 and 9, and

$$\begin{pmatrix} \langle\varphi^\nu_1\rangle \\ \langle\varphi^\nu_2\rangle \end{pmatrix} = v_\nu \begin{pmatrix} 1 \\ 1 \end{pmatrix},\quad \begin{pmatrix} \langle\chi^\nu_1\rangle \\ \langle\chi^\nu_2\rangle \end{pmatrix} = w_\nu \begin{pmatrix} 1 \\ 1 \end{pmatrix},\quad \begin{pmatrix} \langle\xi^\nu_1\rangle \\ \langle\xi^\nu_2\rangle \end{pmatrix} = z_\nu \begin{pmatrix} 1 \\ 1 \end{pmatrix}. \tag{3.72}$$

The VEVs of the singlet flavons, $\langle\sigma^e\rangle = x_e$ and $\langle\sigma^\nu\rangle = x_\nu$, are assumed to be also non-vanishing. The VEV structure then leads to the following mass matrices:

$$\begin{aligned}
M_l &= \frac{\langle h_d\rangle}{\Lambda} \begin{pmatrix} y^e_2\,z_e & y^e_1\,v_e\,e^{\frac{2\pi i k}{5}} & y^e_4\,z_e\,e^{\frac{4\pi i k}{5}} \\ y^e_1\,v_e & y^e_2\,z_e\,e^{\frac{4\pi i k}{5}} & y^e_4\,z_e \\ y^e_3\,v_e\,e^{\frac{2\pi i k}{5}} & y^e_3\,v_e & y^e_5\,x_e \end{pmatrix}, \\
m_\nu &= \frac{\langle h_u\rangle^2}{\Lambda^2} \begin{pmatrix} y_2\,w_\nu & y_1\,x_\nu & 0 \\ \cdot & y_2\,w_\nu & 0 \\ \cdot & \cdot & y_3\,x_\nu \end{pmatrix}.
\end{aligned} \tag{3.73}$$

To see that indeed the golden ratio prediction is obtained from the above two matrices, note that for the choice $k = 3$ the relevant matrix $M_l\,M_l^\dagger$ takes the form

$$M_l\,M_l^\dagger = \begin{pmatrix} A & B\,e^{-2i\phi} & D\,e^{i(\delta-\phi)} \\ B\,e^{2i\phi} & A & D\,e^{i(\delta+\phi)} \\ D\,e^{-i(\delta-\phi)} & D\,e^{-i(\delta+\phi)} & G \end{pmatrix},\ \text{where } \phi = \frac{4\pi}{5}\,. \tag{3.74}$$

The quantities A, B, D, G are real and positive, δ is a phase. To obtain the golden ratio prediction for the solar mixing angle, we have to set in Eq.(3.71) and Eq.(3.73) $k = 3$ or $k = 7$. From the other possibilities, $k = 1$ or $k = 9$ would give a solar mixing angle of $\frac{2\pi}{5}$, while $k = 5$ would give a vanishing solar mixing angle. This small number of degeneracies cannot be resolved by the flavon potential. Looking at the last matrix $M_l\, M_l^\dagger$ in Eq.(3.74), one immediately recognizes the Z_2-invariance of the upper left 12-block, which is just the invariance we were seeking for, see Eq.(3.64). To be precise, the D_{10} was broken in a way that $M_l\, M_l^\dagger$ is left invariant under $B\, A^3$, while the neutrino mass matrix M_ν is left invariant under $B\, A^0 = B$. Inserting this in Eq.(3.69), where we have to set j = 4 because the first and second left-handed lepton doublets transform as $\underline{\mathbf{2}}_\mathbf{4}$, we expect $|U_{e1}|^2 = |\cos\frac{6}{5}\pi|^2$, which is indeed equivalent to an angle of $\pi/5$. We will explicitly check this in the following. Diagonalizing $M_l\, M_l^\dagger$ with the relation $U_l^\dagger\, M_l\, M_l^\dagger\, U_l = \mathrm{diag}(m_e^2,\, m_\mu^2,\, m_\tau^2)$ is achieved with the matrix

$$U_l = \mathrm{diag}(e^{-2i\phi}, 1, e^{-i(\phi+\delta)}) \begin{pmatrix} -\sqrt{\frac{1}{2}} & \sqrt{\frac{1}{2}} & 0 \\ \sqrt{\frac{1}{2}} & \sqrt{\frac{1}{2}} & 0 \\ 0 & 0 & 1 \end{pmatrix} \begin{pmatrix} 1 & 0 & 0 \\ 0 & \cos\theta_{23} & \sin\theta_{23} \\ 0 & -\sin\theta_{23} & \cos\theta_{23} \end{pmatrix} . \tag{3.75}$$

The diagonal phase matrix on the left is crucial. The rotation angle in the 23-axis is given by

$$\tan 2\theta_{23} = \frac{2\sqrt{2}\, D}{G - A - B} , \tag{3.76}$$

and the charged lepton masses are given by

$$\begin{gathered} m_e^2 = A - B \ , \quad m_{\mu,\tau}^2 = \tfrac{1}{2}\left[(A + B + G) \pm w\,(A + B - G)\right] , \\ \text{where } w = \sqrt{1 + 8\, D^2/(A + B - G)^2} . \end{gathered} \tag{3.77}$$

The neutrino mass matrix is diagonalized via $U_\nu^\dagger\, M_\nu\, U_\nu^* = M_\nu^{\mathrm{diag}}$, where

$$U_\nu = \begin{pmatrix} -\sqrt{\frac{1}{2}} & \sqrt{\frac{1}{2}} & 0 \\ \sqrt{\frac{1}{2}} & \sqrt{\frac{1}{2}} & 0 \\ 0 & 0 & 1 \end{pmatrix} P . \tag{3.78}$$

The eigenvalues have in general non-trivial phases which are taken into account in the diagonal matrix P, and their absolute values are

$$m_1 = \frac{\langle h_u\rangle^2}{\Lambda^2}|y_2\, w_\nu - y_1\, x_\nu| \ , \quad m_2 = \frac{\langle h_u\rangle^2}{\Lambda^2}|y_2\, w_\nu + y_1\, x_\nu| \ , \quad m_3 = \frac{\langle h_u\rangle^2}{\Lambda^2}|y_3\, x_\nu| . \tag{3.79}$$

We note that the model makes no predictions about the neutrino masses or their ordering. Nevertheless, one can easily convince oneself that the number of free parameters in the model is enough to fit the neutrino and charged lepton masses, as well as the large atmospheric neutrino mixing angle θ_{23}. The model does in general not predict θ_{23} to be maximal, which is not an issue given the fact that it is the lepton mixing parameter with the largest allowed range. However, maximal mixing is compatible with the model. We have $\theta_{23} = \pi/4$ when $G = A + B$, in which case $m_{\mu,\tau}^2 = A + B \mp \sqrt{2}\, D$ and m_e^2 as in Eq.(3.77). There is no more

Field	ψ^{0e}	$\varphi^{0e}_{1,2}$	$\xi^{0e}_{1,2}$	$\psi^{0\nu}$	$\chi^{0\nu}_{1,2}$	$\xi^{0\nu}_{1,2}$
D_{10}	$\underline{\mathbf{1}}_\mathbf{3}$	$\underline{\mathbf{2}}_\mathbf{1}$	$\underline{\mathbf{2}}_\mathbf{3}$	$\underline{\mathbf{1}}_\mathbf{4}$	$\underline{\mathbf{2}}_\mathbf{2}$	$\underline{\mathbf{2}}_\mathbf{3}$
Z_5	ω	ω	ω	ω^4	ω^4	ω^4

Table 3.4: Transformation properties of the driving fields under $D_{10} \times Z_5$. Again ω is the fifth unit root $e^{\frac{2\pi i}{5}}$.

predictivity that can be traced due to the fact that there is a comparably large number of flavons required in order to make the model work. This is the price one unfortunately has to pay if one insists in the rather peculiar value of θ_{12}. Given the fact that current data allows for this very interesting possibility, one should nevertheless pursue the task of constructing models leading to it. The final PMNS matrix can be calculated from Eq.(2.18) as $U = U_l^T\, U_\nu^*$. One finds that U_{e3} is vanishing and that atmospheric neutrino mixing is governed by $\tan 2\theta_{23}$ given by Eq.(3.76). As mentioned above, the PMNS matrix has a non-trivial phase matrix including ϕ in between the two maximal 12-rotations, one of which stems from U_l, the other from U_ν. As discussed above, this is the origin of the required result. Indeed, the 12-element of U is

$$|U_{e2}|^2 = \sin^2\phi = \sin^2\pi/5\,, \tag{3.80}$$

and due to $U_{e3} = 0$ this is just $\sin^2\theta_{12}$. We have thus achieved our goal of predicting $\theta_{12} = \pi/5$.

Flavon Superpotential

To obtain the necessary vacuum alignment in the flavon potential, we need to introduce a $U(1)_R$ and driving fields as discussed in Section 3.1. The transformation properties of the driving fields are given in Table 3.4. The flavon superpotential can then be divided into two parts

$$\mathrm{W}_f = \mathrm{W}_{f,e} + \mathrm{W}_{f,\nu}\,, \tag{3.81}$$

where $\mathrm{W}_{f,e}$ and $\mathrm{W}_{f,\nu}$ are responsible for the vacuum alignment of the flavons contributing to the charged lepton and neutrino masses, respectively. We begin by considering the charged lepton part:

$$\begin{aligned}\mathrm{W}_{f,e} \;=\;& a_e\,(\chi_1^e\,\xi_1^e + \chi_2^e\,\xi_2^e)\,\psi^{0e} + b_e\,(\chi_1^e\,\xi_2^e\,\varphi_1^{0e} + \chi_2^e\,\xi_1^e\,\varphi_2^{0e}) + c_e\,(\xi_1^e\,\rho_2^e\,\varphi_1^{0e} + \xi_2^e\,\rho_1^e\,\varphi_2^{0e}) \\ & + d_e\,(\xi_2^e\,\xi_1^{0e} + \xi_1^e\,\xi_2^{0e})\,\sigma^e + f_e\,(\xi_1^e\,\rho_1^e\,\xi_1^{0e} + \xi_2^e\,\rho_2^e\,\xi_2^{0e})\,.\end{aligned} \tag{3.82}$$

As the flavor symmetry is broken at a high scale, the scalar potential can be minimized in the supersymmetric limit. Hence, we can determine the supersymmetric minimum of the

potential by setting the F-terms of the driving fields to zero:

$$\begin{aligned}
\frac{\partial \mathrm{W}_{f,e}}{\partial \psi^{0e}} &= a_e\,(\chi_1^e\,\xi_1^e + \chi_2^e\,\xi_2^e) = 0\,, \\
\frac{\partial \mathrm{W}_{f,e}}{\partial \varphi_1^{0e}} &= b_e\,\chi_1^e\,\xi_2^e + c_e\,\xi_1^e\,\rho_2^e = 0\,, \\
\frac{\partial \mathrm{W}_{f,e}}{\partial \varphi_2^{0e}} &= b_e\,\chi_2^e\,\xi_1^e + c_e\,\xi_2^e\,\rho_1^e = 0\,, \\
\frac{\partial \mathrm{W}_{f,e}}{\partial \xi_1^{0e}} &= d_e\,\xi_2^e\sigma^e + f_e\,\xi_1^e\,\rho_1^e = 0\,, \\
\frac{\partial \mathrm{W}_{f,e}}{\partial \xi_2^{0e}} &= d_e\,\xi_1^e\,\sigma^e + f_e\,\xi_2^e\,\rho_2^e = 0\,.
\end{aligned}$$

Similarly, from the neutrino part

$$\begin{aligned}
\mathrm{W}_{f,\nu} &= a_\nu\,(\chi_1^\nu\,\xi_1^\nu - \chi_2^\nu\,\xi_2^\nu)\,\psi^{0\nu} + b_\nu\,(\varphi_1^\nu\,\chi_1^\nu\,\xi_2^{0\nu} + \varphi_2^\nu\,\chi_2^\nu\,\xi_1^{0\nu}) + c_\nu\,(\xi_2^\nu\,\xi_1^{0\nu} + \xi_1^\nu\,\xi_2^{0\nu})\,\sigma^\nu \\
&\quad + d_\nu\,(\varphi_1^\nu\,\xi_2^\nu\,\chi_1^{0\nu} + \varphi_2^\nu\,\xi_1^\nu\,\chi_2^{0\nu}) + f_\nu\,((\varphi_1^\nu)^2\,\chi_2^{0\nu} + (\varphi_2^\nu)^2\,\chi_1^{0\nu}) + g_\nu\,(\chi_2^\nu\,\chi_1^{0\nu} + \chi_1^\nu\,\chi_2^{0\nu})\,\sigma^\nu\,,
\end{aligned} \tag{3.83}$$

we obtain a minimum of the potential by setting the F-terms of the driving fields to zero:

$$\begin{aligned}
\frac{\partial \mathrm{W}_{f,\nu}}{\partial \psi^{0\nu}} &= a_\nu\,(\chi_1^\nu\,\xi_1^\nu - \chi_2^\nu\,\xi_2^\nu) = 0\,, \\
\frac{\partial \mathrm{W}_{f,\nu}}{\partial \chi_1^{0\nu}} &= d_\nu\,\varphi_1^\nu\,\xi_2^\nu + f_\nu\,(\varphi_2^\nu)^2 + g_\nu\,\chi_2^\nu\,\sigma^\nu = 0\,, \\
\frac{\partial \mathrm{W}_{f,\nu}}{\partial \chi_2^{0\nu}} &= d_\nu\,\varphi_2^\nu\,\xi_1^\nu + f_\nu\,(\varphi_1^\nu)^2 + g_\nu\,\chi_1^\nu\,\sigma^\nu = 0\,, \\
\frac{\partial \mathrm{W}_{f,\nu}}{\partial \xi_1^{0\nu}} &= b_\nu\,\varphi_2^\nu\,\chi_2^\nu + c_\nu\,\xi_2^\nu\,\sigma^\nu = 0\,, \\
\frac{\partial \mathrm{W}_{f,\nu}}{\partial \xi_2^{0\nu}} &= b_\nu\,\varphi_1^\nu\,\chi_1^\nu + c_\nu\,\xi_1^\nu\,\sigma^\nu = 0\,.
\end{aligned}$$

As advocated above, these two sets of equations are uniquely solved by the VEV configurations given in Eq.(3.71) and Eq.(3.72), where we have set a possible relative phase in the doublet of VEVs of the flavons in the charged lepton sector to zero. This can be done without loss of generality, as only the phase difference between the two sectors is phenomenologically relevant. We have also assumed that none of the parameters in the superpotential vanish. For the charged lepton sector, the flavon VEVs w_e and x_e are free parameters (which we take to be non-zero), while

$$v_e = e^{\frac{4\pi i k}{5}}\,\frac{c_e\,d_e\,x_e}{b_e\,f_e}\,, \quad z_e = e^{\frac{8\pi i k}{5}}\,\frac{d_e\,x_e}{f_e}\,. \tag{3.84}$$

Similarly v_ν and x_ν are free parameters (again taken to be non-vanishing) and

$$w_\nu = -\frac{c_\nu\,f_\nu\,x_\nu\,v_\nu^2}{c_\nu\,g_\nu\,x_\nu^2 - b_\nu\,d_\nu\,v_\nu^2}\,, \quad z_\nu = \frac{b_\nu\,f_\nu\,v_\nu^3}{c_\nu\,g_\nu\,x_\nu^2 - b_\nu\,d_\nu\,v_\nu^2}\,. \tag{3.85}$$

The driving fields themselves are only allowed to have vanishing VEVs, as can be inferred from considering the F-terms of the flavons. Note, that since we cannot make the cutoff

scale Λ arbitrarily large, we need to take into account NLO corrections to both, the Yukawa and flavon superpotentials. We also should be careful in what regards potentially dangerous FCNCs induced by the flavons. All this could be taken into account by carefully studying the mass spectrum of the scalars. Given the sizable number of fields this is not an easy task, but fortunately it suffices to make some general estimates, which agree well quantitatively with a lengthy explicit calculation in a similar model [87]: The τ lepton mass, see Eq.(3.77), is of order $\langle f\rangle\, v/\Lambda$, where $\langle f\rangle$ is a flavon VEV, v the Higgs VEV ($\simeq 10^2$ GeV), and Λ is the cutoff scale. The neutrino mass, see Eq.(3.79), is of order $\langle f\rangle\, v^2/\Lambda^2$. With the charged lepton τ mass $\simeq$ GeV and the neutrino mass $\simeq 0.1$ eV, it follows that $\Lambda \simeq 10^{12}$ GeV and $\langle f\rangle \simeq 10^{10}$ GeV. Now we can estimate that the flavon mass is also of order of $\langle f\rangle$. NLO corrections to the potential, and therefore to the neutrino and charged lepton mass matrices, are of order $\langle f\rangle/\Lambda \simeq 10^{-2}$ and therefore under control. Any potentially dangerous flavor changing neutral currents are also suppressed by the heavy mass scale $\langle f\rangle$.

In this chapter, we have constructed two flavor models which can explain neutrino mixing patterns such as $\mu-\tau$ symmetry and the golden ratio prediction of the solar mixing. The first model was based on D_4 flavor symmetry, which predicts the $\mu-\tau$ symmetry. We have performed a phenomenological analysis under the assumption of a certain type of spontaneous CP violation suggested by the minimization of the potential. As a result, the neutrinos had to have an inverted hierarchy. The quantity $|m_{ee}|$, measured in $0\nu\beta\beta$ decay, is almost equal to the lightest neutrino mass m_3. Furthermore, we have found that m_3 cannot vanish and has a lower bound around 0.015 eV. The Majorana phases ϕ_1 and ϕ_2 are restricted to a certain range at least for small m_3. In contrast to that, the solar mixing angle θ_{12} can take all values allowed by experiments. We have also analyzed the NLO terms in this model and have shown that they only induce shifts in the VEVs of the flavons, but no additional terms in the Yukawa sector. The shifts yield deviations from the LO results, $\theta_{13}=0$ and $\theta_{23}=\pi/4$. Comparing these deviations we see that although both of them could in principle be of order $\epsilon \approx \lambda_c^2 \approx 0.04$, the smallness of the parameter z, necessary to arrive at mass square differences and θ_{12} within the 2σ ranges, leads to the fact that θ_{23} is much closer to $\pi/4$ than θ_{13} is close to zero. The second model explains the connection between the golden ratio prediction of solar mixing and the dihedral group. We have found out that the suitable flavor group is either D_5 or D_{10}. We have explicitly constructed the flavor model based on D_{10} group because the vacuum alignment we need in our model is simplified due to the larger number of representations in D_{10}.

Chapter 4

Non-Abelian Discrete Groups from The Breaking of Continuous Flavor Symmetries

As discussed in the last chapter, we see how non-abelian discrete flavor symmetries play an important role for neutrino mixing predictions. In this chapter, we intend to embed these symmetries into a continuous gauge symmetry. The idea of embedding a discrete flavor symmetry in a larger continuous group has been discussed in the literature, for example in [137]. However, no complete model exists, in the sense that there is no explanation for the underlying symmetry breaking dynamics. In order to obtain a complete model, we have to determine the scalar representations that break the gauge symmetry as well as their VEV structure. If we limit ourselves to the three generations of fermions, we need to consider only the gauge symmetries, $SU(2)$ or $SU(3)$, as all other semi-simple Lie groups do not have two- or three-dimensional representations. We do not need to discuss an $SO(3)$ separately, since the $SO(3)$ gauge theory can simply be considered as an $SU(2)$ theory with a limited representation content. In the case of flavor symmetry $SU(2)$, the fermions will transform as $\underline{\mathbf{2}}+\underline{\mathbf{1}}$ or $\underline{\mathbf{3}}$. For the flavor symmetry $SU(3)$, the fermions will transform as $\underline{\mathbf{3}}$ and $\bar{\underline{\mathbf{3}}}$. We note that the flavor symmetries considered here commute with the SM gauge group.

In order to break a gauge flavor symmetry spontaneously, we need a set of scalar fields which transforms non-trivially under the gauge flavor symmetry and they acquire the VEVs in a certain direction leading to the breaking of the gauge symmetry down to a subgroup. We limit ourselves to discuss only the representations of the scalar fields which can couple to the three generations of the fermions at the leading order as can be seen from the tensor products:
For $SU(2)$,

$$\begin{aligned}
&\underline{\mathbf{2}}\times\underline{\mathbf{2}}=\underline{\mathbf{1}}+\underline{\mathbf{3}}\,,\\
&\underline{\mathbf{2}}\times\underline{\mathbf{3}}=\underline{\mathbf{2}}+\underline{\mathbf{4}}\,,\\
&\underline{\mathbf{3}}\times\underline{\mathbf{3}}=\underline{\mathbf{1}}+\underline{\mathbf{3}}+\underline{\mathbf{5}}\,,
\end{aligned} \tag{4.1}$$

and for $SU(3)$,

$$\begin{aligned} \underline{\mathbf{3}} \times \underline{\mathbf{3}} &= \bar{\underline{\mathbf{3}}} + \underline{\mathbf{6}} \,, \\ \bar{\underline{\mathbf{3}}} \times \bar{\underline{\mathbf{3}}} &= \underline{\mathbf{3}} + \bar{\underline{\mathbf{6}}} \,, \\ \underline{\mathbf{3}} \times \bar{\underline{\mathbf{3}}} &= \underline{\mathbf{1}} + \underline{\mathbf{8}} \,. \end{aligned} \tag{4.2}$$

To determine whether a certain VEV structure conserves a subgroup of the flavor symmetry $SU(2)$ or $SU(3)$, we test which elements of the flavor symmetry leave the VEV invariant. We will assume a minimal scalar content for any representation, i.e. real scalars for real representations, complex scalars for pseudo-real and complex representations. We then check for each representation, which subgroups are conserved by the VEV of a scalar field transforming under this representation. We also consider combinations of VEVs, but only where such a combination could lead to a non-abelian subgroup.

This chapter is organized as follows: In Section 4.1, we discuss the breaking of the flavor symmetry $SU(2)$ with the two-, three-, four-, and five-dimensional representations. In Section 4.2, we discuss the breaking of the flavor symmetry $SU(3)$ by the three-, six-, and eight-dimensional representations.

4.1 Flavor Symmetry $SU(2)$

4.1.1 Breaking with The Two-Dimensional (Doublet) Representation

In the two-dimensional representation of SU(2), the group elements are mapped onto 2×2 unitary matrices with unit determinant. Thereby each group element has two eigenvalues λ_1 and λ_2. They must obey the constraint that $\lambda_1\lambda_2 = 1$, as the product of the eigenvalues is just the determinant. Hence, if one of the eigenvalues is 1, so will be the other one. The only 2×2 matrix with two eigenvalues of 1 is obviously the unit matrix. Hence, the identity element is the only element of the group that can leave a doublet VEV invariant. We conclude from this that the VEV of a scalar transforming as a doublet of $SU(2)$ always breaks the entire group. This will of course not change if we add further scalars of any sort.

4.1.2 Breaking with The Three-Dimensional (Triplet) Representation

The triplet is the fundamental representation of $SO(3)$, and an unfaithful representation of $SU(2)$. The group elements are mapped onto 3×3 orthogonal matrices with unit determinant. These can be thought of as rotations in three-dimensional Euclidean space. If such a rotation leaves a vector invariant, the vector must be parallel (or, obviously, antiparallel) to the axis of rotation. Hence, any given triplet VEV will conserve the subgroup formed by the rotations around the axis defined by the VEV. Thus the VEV of any triplet will break $SU(2)$ down to Spin(2), the double covering of $SO(2)$, which is in fact isomorphic to $SO(2)$ and $U(1)$.

Note that there is one $SO(2)$ for each possible axis, i.e. infinitely many $SO(2)$'s that are all mutually disjoint (up to the identity element). If we introduce two triplets, their VEVs will either be linearly dependent, or not. If they are linearly dependent, they will break to the same subgroup. If they are linearly independent, they will break to disjoint subgroups, hence fully breaking $SO(3)$. As the triplet is an unfaithful representation of $SU(2)$, we will always conserve a subgroup Z_2 under which all components of the triplet transform trivially, while both components of the doublet transform non-trivially.

Another way to see how $SU(2)$ is broken down to $U(1)$ by the triplet is to write its VEV in term of a traceless Hermitian 2×2 matrix V, which transforms under $SU(2)$ as

$$V \to V' = UVU^\dagger \,, \tag{4.3}$$

where U is a special unitary matrix. We are looking for the subgroup of $SU(2)$ formed by those elements U which leave V invariant, i.e. for which $V = V'$. This set is just the set of all matrices U that commute with V. What does it mean if U commutes with V? Let $\vec{v_i}$ be the eigenvector V associated with the eigenvalue λ_i, which are nondegenerate. Then

$$V(U\vec{v_i}) = U(V\vec{v_i}) = \lambda_i(U\vec{v_i}). \tag{4.4}$$

Hence $U\vec{v_i}$ is also an eigenvector of V with eigenvalue λ_i. As this eigenvalue is non-degenerate $U\vec{v_i}$ must linearly depend on $\vec{v_i}$. Therefore $\vec{v_i}$ is also an eigenvector of U. This holds for both eigenvectors of V. We can thereby specify the subgroup conserved by this VEV: It is the set of all U having the same set of eigenvectors as V. The most general form of a group element is then

$$U = \begin{pmatrix} \vec{v_1} & \vec{v_2} \end{pmatrix} \begin{pmatrix} e^{i\alpha} & 0 \\ 0 & e^{-i\alpha} \end{pmatrix} \begin{pmatrix} \vec{v_1} & \vec{v_2} \end{pmatrix}^\dagger . \tag{4.5}$$

This representation is clearly unitarily equivalent to a diagonal representation, i.e. it reduces to two representations of $U(1)$. Therefore we can see that $SU(2)$ is broken down to $U(1)$.

We conclude from this that if we use three-dimensional representations to break $SU(2)$, we either leave a $U(1) \cong SO(2)$ symmetry or a Z_2 invariant. In particular, no non-abelian subgroups can be conserved. We therefore do not need to consider combining a triplet VEV with a VEV of a different representation.

4.1.3 Breaking with The Four-Dimensional (Tetraplet) Representation

As the $\underline{\mathbf{4}}$ of $SU(2)$ arises from the product of a vector and a spinor, it can be written as a 3×2 complex matrix, with one spinor index and one vector index. There must be further constraints, as such a matrix has 6 complex degrees of freedom. To find them, we take a look at the Clebsch Gordan coefficients.

Writing the $\underline{\mathbf{4}}$ as a matrix, it acts on a spinor and transforms it into a vector. As the Clebsch Gordan coefficients are normally given in spherical coordinates we start with these, later switching back to Cartesian coordinates, where the scalar product of two vectors is simply a matrix multiplication. In spherical coordinates, we can give the four degrees of freedom of the $\underline{\mathbf{4}}$ as ϕ_1 (m=$\frac{3}{2}$), ϕ_2 (m=$\frac{1}{2}$), ϕ_3 (m=$-\frac{1}{2}$), and ϕ_4 (m=$-\frac{3}{2}$). Correspondingly we write the two components of the spinor, which we want to transform into a vector, as ψ_1 (m=$\frac{1}{2}$) and ψ_2 (m=$-\frac{1}{2}$). Using the Clebsch Gordan coefficients for $SU(2)$ [46], we find that they combine in the following way to form a vector:

$$\frac{1}{2}(\sqrt{3}\phi_1\psi_2 - \phi_2\psi_1) \quad (m = \ \ 1) \,, \tag{4.6}$$

$$\frac{1}{\sqrt{2}}(\phi_2\psi_2 - \phi_3\psi_1) \quad (m = \ \ 0) \,, \tag{4.7}$$

$$\frac{1}{2}(\phi_3\psi_2 - \sqrt{3}\phi_4\psi_1) \quad (m = -1) \,. \tag{4.8}$$

Switching to Cartesian coordinates, this corresponds to a vector

$$\begin{pmatrix} \frac{1}{2\sqrt{2}}[(\phi_2 - \sqrt{3}\phi_4)\psi_1 + (\phi_3 - \sqrt{3}\phi_1)\psi_2] \\ \frac{i}{2\sqrt{2}}[-(\phi_2 + \sqrt{3}\phi_4)\psi_1 + (\phi_3 + \sqrt{3}\phi_1)\psi_2)] \\ \frac{1}{\sqrt{2}}(\phi_2\psi_2 - \phi_3\psi_1) \end{pmatrix} . \tag{4.9}$$

This vector arises from multiplying a spinor with the following matrix:

$$\frac{1}{\sqrt{2}} \begin{pmatrix} \frac{1}{2}(\phi_2 - \sqrt{3}\phi_4) & \frac{1}{2}(\phi_3 - \sqrt{3}\phi_1) \\ -\frac{i}{2}(\phi_2 + \sqrt{3}\phi_4) & \frac{i}{2}(\phi_3 + \sqrt{3}\phi_1) \\ -\phi_3 & \phi_2 \end{pmatrix} , \tag{4.10}$$

or, in another simpler parameterization

$$V = \begin{pmatrix} a & b \\ c & d \\ -b + id & a + ic \end{pmatrix} , \tag{4.11}$$

where a, b, c, and d are complex. This is then the most general form for the VEV of a $\underline{\mathbf{4}}$. It transforms in the following way:

$$V \to V' = OVU^\dagger , \tag{4.12}$$

as it has one vector and one spinor indices. O and U are of course not independent, but describe a rotation of the same magnitude around the same axis. It can be checked by explicit calculation that V' can be parameterized in the same way as V for an arbitrary rotation.

Again we can reformulate the condition of invariance as a condition on the eigensystem. Demanding the invariance $V' = V$, it leads to the condition:

$$OV = VU . \tag{4.13}$$

We first observe that we can deduce from Eq.(4.12) the following two equations:

$$VV^\dagger = OVV^\dagger O^T , \tag{4.14}$$

$$V^\dagger V = UV^\dagger VU^\dagger , \tag{4.15}$$

from which we immediately deduce that the eigenvectors of $VV^\dagger$ (i.e. the left singular vectors of V, denoted by $\vec{u_i}$) must also be eigenvectors of O (with the usual ambiguities for degenerate singular and eigenvalues), and the right singular vectors of V, denoted by $\vec{w_i}$, must be eigenvectors of U. Using this knowledge, we find that

$$VU\vec{w_i} = V\mu_i\vec{w_i} = \sigma_i\mu_i\vec{u_i} , \tag{4.16}$$

for $i = 1, 2$, μ_i being the eigenvalues of U and σ_i being the singular values of V. Using the condition in Eq.(4.13), We also have

$$VU\vec{w_i} = OV\vec{w_i} = O\sigma_i\vec{u_i} = \lambda_i\sigma_i\vec{u_i} , \tag{4.17}$$

with λ_i being the eigenvalues of O. From the last two equations, we can deduce that $\lambda_i = \mu_i$. As O and U are rotations by the same angle θ, their eigenvalues are $e^{\pm i\theta}$ and 1 for O, and

$e^{\pm i\frac{\theta}{2}}$ for U. How can they be made to coincide? Apart from the trivial case of both being the unit matrix, we are only left with the possibility of identifying the exponential eigenvalues, which is only possible for $\theta = \pm\frac{4\pi}{3}$. The final left singular vector $\vec{u_3}$ is then the eigenvector of O corresponding to the eigenvalue 1, i.e. it defines the axis of rotation. If it is real, we will then break to all rotations around that axis, with the angles given above. This is a Z_3 subgroup of $SU(2)$. If the axis is complex (and real and imaginary parts are not linearly dependent), no such elements will exist and $SU(2)$ will be fully broken.

Will the subgroup be enlarged if V has degenerate singular values? We first take the case $\sigma = \sigma_1 = \sigma_2 \neq 0$. $\vec{u_3}$ is still an eigenvector of O, the $\vec{u_i}$ and $\vec{w_i}$ however need not be eigenvectors of O and U, respectively. Rather we have

$$VU\vec{w_i} = V(\alpha_i\vec{w_1} + \beta_i\vec{w_2}) = \sigma(\alpha_i\vec{u_1} + \beta_i\vec{u_2}) \,, \tag{4.18}$$

$$VU\vec{w_i} = OV\vec{w_i} = \sigma O\vec{u_i} = \sigma(\alpha_i'\vec{u_1} + \beta_i'\vec{u_2}) \,, \tag{4.19}$$

from which we can immediately infer that $\alpha_i = \alpha_i'$ and $\beta_i = \beta_i'$. This means that again their eigenvalues need to coincide, and we again break to Z_3 or nothing. Finally, we need to consider the case, where one of the non-trivial singular values is zero, $\sigma_2 = 0$. In this case O and U need only coincide in one eigenvalue, but this condition is already strong enough to constrain the elements in the same way, i.e. giving Z_3 as the conserved subgroup. We thus find that a VEV for the four-dimensional representation of $SU(2)$ can never lead to the conservation of a non-abelian subgroup.

4.1.4 Breaking with The Five-Dimensional (Quintuplet) Representation

The VEV V of a scalar transforming under the five-dimensional representation can be written as a 3×3 traceless, real symmetric matrix. It transforms under $SU(2)$ as

$$V \to V' = OVO^T \,, \tag{4.20}$$

with O being a special orthogonal matrix. Again the question of invariance can be reduced to a question of commutation and hence to coincident eigenspace. We note that the condition for the invariance of V is:

$$OV = VO \,. \tag{4.21}$$

For a VEV with nondegenerate eigenvalues the general form of elements in the conserved subgroup is

$$O = \begin{pmatrix} \vec{v_1} & \vec{v_2} & \vec{v_3} \end{pmatrix} \begin{pmatrix} (-1)^n & 0 & 0 \\ 0 & (-1)^m & 0 \\ 0 & 0 & (-1)^{n+m} \end{pmatrix} \begin{pmatrix} \vec{v_1} & \vec{v_2} & \vec{v_3} \end{pmatrix}^T \,, \tag{4.22}$$

with n, m integers (as V is symmetric it can be diagonalized by a real orthogonal matrix, and hence O will have only real eigenvectors and therefore only real eigenvalues). After a similarity transformation this is a representation of $Z_2 \times Z_2 \cong D_2$. However, since we actually break $SU(2)$ with an unfaithful representation, we actually conserve the double-valued group D_2'. The $SU(2)$ doublet will transform as a doublet in this group as well, while the triplet, as can be seen from the matrix above, decomposes into the three non-trivial one-dimensional

representations. D_2' [1] has no non-abelian subgroups, so we will not consider a combination of this VEV with others.

Next we consider VEVs V with two degenerate eigenvalues. The elements of the conserved subgroup must still have $\vec{v_3}$ as an eigenvector with a real eigenvalue. There are, however, two cases here. The first case is to assign the eigenvalue 1 to $\vec{v_3}$. These are all elements having $\vec{v_3}$ as axis of rotation. They form $SO(2)$ subgroup. Another case is to assign the eigenvalue (-1) to $\vec{v_3}$. The eigenvectors of V are now no longer uniquely defined. If $\vec{v_1}$ and $\vec{v_2}$ are two orthonormal eigenvectors of V corresponding to the same eigenvalue, we can find an arbitrary orthonormal basis of the corresponding eigenspace as $(c\vec{v_1} + s\vec{v_2})$ and $(-s\vec{v_1} + c\vec{v_2})$, where s and c are the sine and cosine, respectively, of some undefined angle. The elements of the preserved subgroup reads

$$Y \begin{pmatrix} (-1)^n & 0 & 0 \\ 0 & (-1)^{n+1} & 0 \\ 0 & 0 & -1 \end{pmatrix} Y^T, \tag{4.23}$$

using $Y \equiv \begin{pmatrix} (c\vec{v_1} + s\vec{v_2}) & (-s\vec{v_1} + c\vec{v_2}) & \vec{v_3} \end{pmatrix}$. By multiplying Eq.(4.23) on the right by

$$\begin{pmatrix} \vec{v_1} & \vec{v_2} & \vec{v_3} \end{pmatrix}, \tag{4.24}$$

and on the left by its transpose, we perform a unitary transformation and end up with

$$\begin{pmatrix} (-1)^n(c^2 - s^2) & 2cs(-1)^n & 0 \\ 2cs(-1)^n & (-1)^n(s^2 - c^2) & 0 \\ 0 & 0 & -1 \end{pmatrix}. \tag{4.25}$$

Since the above matrix must still have a unit determinant, we know that the upper left 2×2 matrix must have determinant (-1) and must also be orthogonal. Combining the two sets of elements, we find that our representation is reducible, reducing to the defining representation of $O(2)$ and the one-dimensional representation, where each element is mapped onto its determinant. As our original group was $SU(2)$, we are actually breaking to the double covering of $O(2)$, which is the group Pin(2). Combining several such VEVs, they can coincide in the non-degenerate eigenvector, in which case Pin(2) is conserved, the non-degenerate eigenvector of one can lie in the degenerate eigenspace of the other, in which case the conserved subgroup is D_2', or their eigenbasis could be unrelated, in which case only Z_2 is conserved.

There are thus only two non-abelian groups which can be the residual subgroup of $SU(2)$ after breaking with the VEV of a five-dimensional representation: The group D_2' for non-degenerate eigenvalues and the group Pin(2) for degenerate eigenvalues. Some of these results can also be found in [197].

4.2 Flavor Symmetry $SU(3)$

4.2.1 Breaking with The Three-Dimensional (Triplet) Representation

In the three-dimensional representation of $SU(3)$, the group elements are mapped onto 3×3 unitary matrices with unit determinant. Therefore, each element will have three eigenvalues

[1] The dihedral group D_2 being an abelian group has four one-dimensional irreducible representations. The order of D_2 is 4. The double valued counterpart of the dihedral group D_2 is D_2'. D_2' has four one- and one two-dimensional irreducible representations. The order of D_2' is 8. D_2' is the simplest non-abelian double valued dihedral group and is also called the quaternion group. For more information see [184].

λ_1, λ_2, and λ_3. If one of these eigenvalues, λ_1, is 1, then the other two eigenvalues will have to fulfill $\lambda_2\lambda_3 = 1$, since the matrix has a unit determinant. This means that if λ_2 is also equal to 1, then $\lambda_3 = 1$ as well. That is, the only element with more than one eigenvalue equal to 1 is the identity element, the only element with three 1 eigenvalues.
This means that each element which is not the identity will have at most one eigenvector corresponding to an eigenvalue of 1. For a simple example, the matrix

$$\begin{pmatrix} e^{i\phi} & 0 & 0 \\ 0 & e^{-i\phi} & 0 \\ 0 & 0 & 1 \end{pmatrix} \tag{4.26}$$

will have the eigenvector

$$\begin{pmatrix} 0 \\ 0 \\ 1 \end{pmatrix} \tag{4.27}$$

corresponding to an eigenvalue of 1. As no direction in three-dimensional complex space is favored, there will exist for each complex 3-vector non-trivial group elements having this vector as an eigenvector with eigenvalue 1. These elements form the subgroup conserved by a VEV proportional to that eigenvector. As each non-trivial element has at most one such eigenvector, these subgroups will all be disjoint.

What is the subgroup conserved by such a VEV? We can already guess that it will be $SU(2)$, but this can be motivated by considering the group of elements that leave invariant a vector $\vec{v}$. We then make a unitary similarity transformation

$$U \to U' = \begin{pmatrix} \vec{x} & \vec{y} & \vec{v} \end{pmatrix}^\dagger U \begin{pmatrix} \vec{x} & \vec{y} & \vec{v} \end{pmatrix} , \tag{4.28}$$

where U is an element of the group and $\vec{x}$ and $\vec{y}$ are arbitrary mutually orthogonal vectors that are also orthogonal to $\vec{v}$. We obtain

$$U' = \begin{pmatrix} U'_{2\times 2} & 0 \\ 0 & 1 \end{pmatrix} . \tag{4.29}$$

As U' is unitary by itself and also has unit determinant, we see that the three-dimensional representation reduces to the two-dimensional one plus the one-dimensional representation of $SU(2)$. Since all the $SU(2)$ subgroups are disjoint, introducing two or more triplet scalars either breaks to an $SU(2)$ (in case their VEVs are linearly dependent) or it will break the entire $SU(3)$ group (if they are not).

What about anti-triplets? The arguments are the same as for the triplets, if we consider them separately, as the two representations can only be distinguished if they show up together. But even if we introduce scalars transforming as triplets and scalars transforming as anti-triplets, we do not find any new subgroups: The reason is the same as above, each scalar VEV breaks to a specific $SU(2)$ and they are all disjoint. The only thing we observe is that if we introduce a scalar triplet and a scalar anti-triplet, they will break to the same $SU(2)$ if the VEV of the triplet is proportional to the complex conjugated VEV of the anti-triplet. If this is not the case, they will break to disjoint $SU(2)$'s, i.e. they will fully break $SU(3)$.

We conclude that an arbitrary collection of scalar triplets and anti-triplets either conserves an $SU(2)$ subgroup of our original $SU(3)$ symmetry, or it fully breaks that symmetry.

4.2.2 Breaking with The Six-Dimensional (Sixtet) Representation

Writing the VEV of the six-dimensional representation as a complex, symmetric 3×3 matrix V, it transforms under $SU(3)$ in the following way:

$$V \to V' = UVU^T \ . \tag{4.30}$$

Demanding invariance can then be rewritten as the condition

$$UV = VU^* \ . \tag{4.31}$$

We now note that V need not necessarily be diagonalizable. However, since V is complex and symmetric can be written in the form

$$W^T V W = V_{\text{diag}} \ , \tag{4.32}$$

with W being unitary [198]. We can write $W \equiv (\vec{w_1}, \vec{w_2}, \vec{w_3})$. The $\vec{w_i}$'s are then singular vectors of V obeying the relation

$$V\vec{w_i} = \sigma_i \vec{w_i}^* \ , \tag{4.33}$$

with σ_i being the diagonal elements of V_{diag}, i.e. the singular values of V. The condition of Eq.(4.31) then leads to

$$V(U^*\vec{w_i}) = UV\vec{w_i} = \sigma_i U \vec{w_i}^* = \sigma_i (U^*\vec{w_i})^* \ . \tag{4.34}$$

If V has three distinct singular values, this means that all $\vec{w_i}$ need to be eigenvectors of U^*. Also, the corresponding eigenvalue of U^* needs to be real. Therefore the discussion is the same as for the five-dimensional representation of $SO(3)$: The conserved subgroup is D_2. If V has two degenerate singular values, then U^* should act on the corresponding singular space with only real coefficients, that is it should be block-diagonalizable to give an orthogonal 2×2 submatrix. The conserved subgroup will then be $O(2)$. As V need not to be traceless, we encounter the additional case of three degenerate singular values. Here U^* needs to act on all singular vectors with real coefficients, so the conserved subgroup in this case is $SO(3)$. Of these subgroups only the last two are non-abelian and need to be considered in combination with other VEVs.

We demanded above that the eigenvalues of U need to be real. This condition stems from Eq.(4.33): If $\vec{w_i}$ obeys that relation, then $\alpha\vec{w_i}$ will only obey the same relation if α is real or, alternatively σ_i must be zero. Thereby VEVs with zero eigenvalues are algebraically special: The group elements preserving such a VEV can have complex eigenvalues corresponding to the singular vectors of V with singular value 0. A special unitary matrix cannot have only one non-real eigenvalue. Hence the case of interest is a VEV with two zero eigenvalues. In this case, the singular vectors of V are no longer uniquely defined. If $\vec{w_1}$ and $\vec{w_2}$ are two orthonormal singular vectors of V corresponding to the same singular values, we can find an arbitrary orthonormal basis of the corresponding vector space as $(a\vec{w_1} + b\vec{w_2})$ and $(-\bar{b}\vec{w_1} + \bar{a}\vec{w_2})$, with a and b being two complex numbers obeying $|a|^2 + |b|^2 = 1$. Defining $X_w \equiv \begin{pmatrix} (a\vec{w_1} + b\vec{w_2}) & (-\bar{b}\vec{w_1} + \bar{a}\vec{w_2}) & \vec{w_3} \end{pmatrix}$, we can therefore write any matrix in $SU(3)$ that commutes with V in the following form:

$$X_w \begin{pmatrix} e^{i\alpha} & 0 & 0 \\ 0 & e^{i(m\pi - \alpha)} & 0 \\ 0 & 0 & (-1)^m \end{pmatrix} X_w^\dagger \ , \tag{4.35}$$

where the eigenvalue corresponding to the non-zero singular value is real.
To reduce this representation, we do a unitary equivalence transformation by multiplying on the right by

$$\begin{pmatrix} \vec{w_1} & \vec{w_2} & \vec{w_3} \end{pmatrix} , \tag{4.36}$$

and on the left with the Hermitian conjugate. The resulting matrix is

$$\begin{pmatrix} |a|^2 e^{i\alpha} + |b|^2 e^{i(m\pi-\alpha)} & a\bar{b}(e^{i\alpha} - e^{i(m\pi-\alpha)}) & 0 \\ \bar{a}b(e^{i\alpha} - e^{i(m\pi-\alpha)}) & |a|^2 e^{i(m\pi-\alpha)} + |b|^2 e^{i\alpha} & 0 \\ 0 & 0 & (-1)^m \end{pmatrix} , \tag{4.37}$$

where it can be factorized as

$$\begin{pmatrix} i^m & 0 & 0 \\ 0 & i^m & 0 \\ 0 & 0 & (-1)^m \end{pmatrix} \begin{pmatrix} x_w & y_w & 0 \\ -y_w^* & x_w^* & 0 \\ 0 & 0 & 1 \end{pmatrix} , \tag{4.38}$$

where

$$x_w = |a|^2 e^{i\frac{(2\alpha-m\pi)}{2}} + |b|^2 e^{-i\frac{(2\alpha-m\pi)}{2}} , \tag{4.39}$$

$$y_w = 2iab^* \sin\left(\frac{2\alpha - m\pi}{2}\right) . \tag{4.40}$$

These two matrices commute. The first matrix is the representation of Z_4. If we observe that $|x_w|^2 + |y_w|^2 = 1$, we will see that the second matrix furnishes a representation of $SU(2)$. Therefore, the conserved subgroup here is $SU(2) \times Z_4$, where the first two generations form a doublet of $SU(2)$ and a faithful representation of Z_4, while the third generation is a singlet of $SU(2)$ and an unfaithful, non-trivial representation of Z_4. We also note that we have the correct number of free parameters: The absolute value of a (or b), the phase of ab^*, and the phase difference $(2\alpha - m\pi)$.

What if we combine two six-dimensional VEVs? If they coincide in all three singular vectors, the subgroup will be determined by the VEV with less degenerate eigenvalues. If they have only one singular vector in common, we break to the subgroup of elements having two degenerate real eigenvalues, which is Z_2. If they have no singular vectors in common, we will break $SU(3)$ fully. Zero eigenvalues will only be relevant if the VEVs coincide in all three singular vectors anyway, and the zero eigenvalues correspond to the same eigenspace. In this case the full subgroup $SU(2) \times Z_4$ is conserved.

We thus have three non-abelian groups that can be conserved by a sextet VEV, $O(2)$ for two degenerate singular values, $SO(3)$ for three degenerate singular values, and $SU(2) \times Z_4$ for two zero eigenvalues.

What if both a $\underline{\mathbf{6}}$ and a triplet acquire a VEV? If the triplet VEV is not a singular vector of the $\underline{\mathbf{6}}$, then $SU(3)$ will be fully broken. What if it is a singular vector? If V has two degenerate singular values, the triplet can correspond to the non-degenerate singular value. In this case, the determinant of the 2×2 submatrix will be fixed to be one, and the conserved subgroup is $SO(2)$ or $U(1)$. If the triplet VEV corresponds to a degenerate singular value, the degeneracy will become irrelevant and the subgroup is Z_2. If V has three degenerate singular values, the triplet, which is in the defining representation of $SO(3)$, will break that subgroup in the usual way down to $U(1)$, or it will fully break it, if the real and imaginary parts of the triplet VEV are not parallel. If we combine a V with two zero singular values with a

triplet VEV, we again have two possibilities: The triplet VEV can correspond to the non-zero singular value. In this case m is fixed to be 0 or 2, and we break down to $SU(2)$ (the former Z_4 element can just be multiplied into the $SU(2)$ element, without changing the determinant). If the triplet VEV is a singular vector of V corresponding to a zero singular value, we will have to take a closer look. The $SU(2)$ element in Eq.(4.38) has eigenvalues $e^{\pm i\frac{(2\alpha-m\pi)}{2}}$. So, without loss of generality, we must now demand $(i)^m e^{i\frac{(2\alpha-m\pi)}{2}} = 1$. The resulting element then has in addition two eigenvalues of (-1), corresponding to fixed vectors. The conserved subgroup is then Z_2.

4.2.3 Breaking with The Eight-dimensional (Octet) Representation

We can write the VEV of a scalar transforming under the adjoint representation of $SU(3)$ as a traceless Hermitian 3×3 matrix V. It then transforms under $SU(3)$ in the following way:

$$V \to V' = UVU^\dagger, \tag{4.41}$$

where U is a special unitary matrix. As V is traceless, we need to consider two distinct cases: Either V has three distinct eigenvalues, or it has two degenerate eigenvalues λ, the third eigenvalue being (-2λ). The only possible VEV with three degenerate eigenvalues is the zero matrix, i.e. a vanishing VEV, which naturally does not break $SU(3)$.

Again, we can reformulate the condition of invariance as a condition on the eigensystem. We note that the condition for the invariance of V reads

$$UV = VU\ . \tag{4.42}$$

In the case of a V with three distinct eigenvalues, the most general form for an element of the conserved subgroup is

$$U = \begin{pmatrix} \vec{v_1} & \vec{v_2} & \vec{v_3} \end{pmatrix} \begin{pmatrix} e^{i\alpha} & 0 & 0 \\ 0 & e^{i\beta} & 0 \\ 0 & 0 & e^{-i(\alpha+\beta)} \end{pmatrix} \begin{pmatrix} \vec{v_1} & \vec{v_2} & \vec{v_3} \end{pmatrix}^\dagger . \tag{4.43}$$

This representation is clearly unitarily equivalent to a diagonal representation, i.e. it reduces to three representations of $U(1)$. As α and β are, however, independent, there will actually be two distinct $U(1)$ groups. Therefore an adjoint VEV with three distinct eigenvalues breaks $SU(3)$ down to $U(1)\times U(1)$. Note that such a VEV can never conserve a non-abelian subgroup of $SU(3)$ and we do not need to consider it any further.

We now proceed to VEVs V having two degenerate eigenvalues. The eigenvectors of V are now no longer uniquely defined. If $\vec{v_1}$ and $\vec{v_2}$ are two orthonormal eigenvectors of V corresponding to the same eigenvalue, we can find an arbitrary orthonormal basis of the corresponding eigenspace as $(a\vec{v_1} + b\vec{v_2})$ and $(-\bar{b}\vec{v_1} + \bar{a}\vec{v_2})$, with a and b being two complex numbers obeying $|a|^2 + |b|^2 = 1$. Defining $X_v \equiv \begin{pmatrix} (a\vec{v_1} + b\vec{v_2}) & (-\bar{b}\vec{v_1} + \bar{a}\vec{v_2}) & \vec{v_3} \end{pmatrix}$, we can therefore write any matrix in SU(3) that commutes with V in the following form:

$$X_v \begin{pmatrix} e^{i\alpha} & 0 & 0 \\ 0 & e^{i\beta} & 0 \\ 0 & 0 & e^{-i(\alpha+\beta)} \end{pmatrix} X_v^\dagger\ . \tag{4.44}$$

To reduce this representation, we do a unitary equivalence transformation by multiplying on the right by

$$\begin{pmatrix} \vec{v_1} & \vec{v_2} & \vec{v_3} \end{pmatrix} , \tag{4.45}$$

and on the left with the Hermitian conjugate. The resulting matrix is

$$\begin{pmatrix} |a|^2 e^{i\alpha} + |b|^2 e^{i\beta} & a\bar{b}(e^{i\alpha} - e^{i\beta}) & 0 \\ \overline{a}b(e^{i\alpha} - e^{i\beta}) & |a|^2 e^{i\beta} + |b|^2 e^{i\alpha} & 0 \\ 0 & 0 & e^{-i(\alpha+\beta)} \end{pmatrix} . \tag{4.46}$$

We now show that this is a representation of $SU(2) \times U(1)$. To do this we factorize the matrix Eq.(4.46):

$$\begin{pmatrix} e^{i\frac{(\alpha+\beta)}{2}} & 0 & 0 \\ 0 & e^{i\frac{(\alpha+\beta)}{2}} & 0 \\ 0 & 0 & e^{-i(\alpha+\beta)} \end{pmatrix} \begin{pmatrix} x_v & y_v & 0 \\ -y_v^* & x_v^* & 0 \\ 0 & 0 & 1 \end{pmatrix} , \tag{4.47}$$

where

$$x_v = |a|^2 e^{i\frac{(\alpha-\beta)}{2}} + |b|^2 e^{-i\frac{\alpha-\beta}{2}} , \tag{4.48}$$

$$y_v = 2iab^* \sin\left(\frac{\alpha-\beta}{2}\right) . \tag{4.49}$$

These two matrices commute. The first matrix is the representation of U(1), with the first two generations transforming in the same way, and the third with double and opposite charge. Since $|x_v|^2 + |y_v|^2 = 1$, the second matrix is a representation of SU(2), under which the first two generations form a doublet and the third generation is a singlet. We also note that we have the correct number of free parameters: The absolute value of a (or b), the phase of ab^*, and the phase difference $(\alpha - \beta)$.

We consider the case of two adjoint VEVs, where both VEVs have degenerate eigenvalues. First of all, their non-degenerate eigenvalues could correspond to the same eigenvector. In this case, they will naturally break to the same subgroup. Then we could have the case, where the non-degenerate eigenvalue of the second VEV corresponds to an eigenvector lying in the eigenspace of the degenerate eigenvalue of the first VEV. This, in a way, singles out a basis of that eigenspace and thereby coincides with the VEV of an octet with three distinct eigenvalues, i.e. conserves a subgroup $U(1) \times U(1)$. Therefore, if there is no relation between the eigenvectors of the two VEVs, we will only conserve the subgroup Z_3, corresponding to the three third roots of unity, which can never be broken by adjoint scalars.

Combining a degenerate adjoint VEV with a triplet VEV, we find three possibilities: First, the triplet VEV can coincide with the non-degenerate eigenvector. In this case $e^{-i(\alpha+\beta)}$ must be equal to 1 and we break down to the same $SU(2)$ conserved by the triplet VEV alone. If the triplet VEV lies in the degenerate eigenspace, we will break the $SU(2)$ conserved by the octet VEV and will be left with only a residual $U(1)$. If the triplet VEV is not an eigenvector of the adjoint VEV we will again break the entire group. Thus, the only new non-abelian subgroup of $SU(3)$ we can conserve with the VEV of a scalar transforming under the adjoint representation will be the subgroup $SU(2) \times U(1)$, if the VEV has two degenerate eigenvalues.

We proceed further by combining a VEV of an adjoint with a VEV of a $\underline{\mathbf{6}}$. The adjoint VEV must have two degenerate eigenvalues, as only then we have the possibility of conserving a non-abelian subgroup. If there does not exist a basis of singular vectors for the sixtet

VEV, which is also a basis of eigenvectors for the octet VEV, $SU(3)$ will be fully broken. In particular, the eigenvector of the octet VEV corresponding to the non-degenerate eigenvalue, $\vec{v_3}$, must always be a singular vector of the sextet VEV. If the sixtet VEV has two degenerate singular values, $\vec{v_3}$ can correspond to the non-degenerate singular value. In this case, the conserved subgroup is $O(2)$. If $\vec{v_3}$ corresponds to a degenerate singular value, the degeneracy will become irrelevant and the subgroup is D_2. If the sixtet VEV has three degenerate singular values, one of the degeneracies will become irrelevant and we break down to $O(2)$. In the case of a sextet VEV with two zero eigenvalues, we again have two possibilities: $\vec{v_3}$ can correspond to the non-zero singular value. In this case nothing changes, and $SU(2) \times Z_4$ is still the conserved subgroup. If $\vec{v_3}$ is an eigenvector of the sixtet VEV corresponding to a zero eigenvalue, a specific basis will be singled out for the elements of the conserved subgroup. It is thus only determined by the possible eigenvalues, and cannot be non-abelian. In this case it will be $U(1) \times Z_2$. Thus, no new non-abelian subgroups can be attained by combining the VEVs of these different $SU(3)$ representations.

The results of this chapter can be summarized in one sentence: The only non-abelian discrete subgroup that can be conserved by VEVs of the small representations (dimension equal or less than five and eight, respectively) of $SU(2)$ and $SU(3)$ is the group D_2', which has been used as a flavor symmetry [199], but does not have a rich enough structure to predict by itself very specific mixing patterns, such as tri-bimaximal mixing for neutrinos [184]. We note that in case we use a more complicate representation such as the seven-dimensional representation, we can obtain A_4 as the subgroup of $SO(3)$ [19, 20]. However, since this representation cannot couple directly to the three generations of the SM fermions, further generations of the fermions are required leading to difficulties with phenomenology because we need to make these fermions heavy in order to avoid being observed at present collider experiments. Therefore, it seems that the assumption of the origin of non-abelian discrete flavor symmetries from the breaking of continuous flavor symmetries is disfavored and another hypothetical origin will be needed, which we will discuss in the next chapter.

Chapter 5

Non-Abelian Discrete Flavor Symmetries from T^2/Z_N Orbifolds

Two main types of symmetries are needed to construct the Lagrangian of the Standard Model: Space-time and gauge symmetry. In fact, it is a much simpler task to add an additional gauge group to the SM than extending the space-time symmetry. However, as discussed in the last chapter, breaking a continuous flavor gauge group down to a non-abelian discrete subgroup is a highly non-trivial phenomenological task. Therefore, it is worthwhile to consider discrete flavor symmetries arising as extensions of the space-time symmetry.

An extension of the space-time symmetry can only be achieved by an extension of space-time itself. Hence, we need to work in an extra-dimensional framework. Such an extension of space-time will enlarge the Poincaré symmetry. If the n extra dimensions are compactified on an orbifold, the space-time symmetry will in general not be the full $(4+n)$-dimensional Poincaré symmetry. However, depending on the exact compactification, there may be residual discrete symmetries, which can then play the role of a flavor symmetry.

This idea was first explored in [28], where two extra dimensions have been assumed. This can be considered as the minimal number in this setup, as one extra dimension does not lead to non-abelian symmetries. For a specific 2-dimensional orbifold it was shown there, that the residual Poincaré symmetry is the group S_4, the group of permutations of four distinct objects (if discrete symmetries, such as parity, are not taken into account, i.e. if we only consider proper Lorentz transformations, the residual symmetry will be A_4). A_4 and S_4 are both popular and phenomenologically successful as flavor symmetries, especially for predicting tri-bimaximal neutrino mixing. In this chapter, we generalize the discussion of [28] by considering all possible 2-dimensional orbifolds and calculating the resulting symmetry. As it turns out, the resulting flavor symmetries are, in addition to A_4 and S_4, the three dihedral groups D_4, $D_3 \cong S_3$, and $D_6 \cong D_3 \times Z_2$, all of which have been widely used as flavor symmetries.

Another way of obtaining discrete flavor symmetries from orbifolds is inspired by string theory and uses string selection rules [22]. We will not use this approach and will only use regular field theory on the orbifold. However, as discussed in [22], the two approaches do not contradict each other: If we have an orbifold possessing an inherent discrete symmetry, such as the ones we discuss in this chapter, and then also impose the string selection rules, we will end up with an enlarged flavor symmetry.

This chapter is organized as follows. In Section 5.1 we discuss the possible 2-dimensional orbifolds and review how discrete symmetries can be extracted from them. We also explain,

why a 1-dimensional orbifold is not sufficient to obtain a non-abelian flavor symmetry. In Section 5.2 we discuss orbifold by orbifold which symmetry group arises from it. In Section 5.3 we discuss the relation between flavor group representations and brane fields constrained to the fixed points in a certain twisted sector.

5.1 Orbifolding

We work in a 6-dimensional framework, where the two extra dimensions are compactified on an orbifold T^2/Z_N [163]. The coordinates in the two extra dimensions are denoted by (x_5, x_6).

A 2-dimensional torus T^2 is obtained by identifying the opposite sides of a parallelogram:

$$\begin{aligned} (x_5, x_6) &\rightarrow (x_5, x_6) + \vec{e}_1 \ , \\ (x_5, x_6) &\rightarrow (x_5, x_6) + \vec{e}_2 \ , \end{aligned} \tag{5.1}$$

where $\vec{e}_1 = (1, 0)$, $\vec{e}_2 = C(\cos(\alpha), \sin(\alpha))$ are the basis vectors of the torus. We can always choose $\vec{e}_1$ to point along the x_5 axis and to be normalized, leaving two free parameters defining $\vec{e}_2$, C and α, the length and the angle with respect to the x_5 axis. In this torus, the origin $(0, 0)$ is identified with all points of the form

$$a\vec{e}_1 + b\vec{e}_2 \ , \tag{5.2}$$

where a, b are integers.

Aside from the torus basis, the orbifold is further defined by the abelian group Z_N, which is modded out of the torus. This means that we further identify points related by a rotation around the origin through integer multiples of an angle ϕ, with $N\phi = 2\pi$. The choice of Z_N is strictly constrained, as we discuss in the following [183]. The group Z_N is generated by one element, which corresponds to a rotation by the angle ϕ. Its matrix representation in the Cartesian x_5-x_6 basis is thus

$$\omega = \begin{pmatrix} \cos(\phi) & -\sin(\phi) \\ \sin(\phi) & \cos(\phi) \end{pmatrix} . \tag{5.3}$$

Since the origin does not change under the rotation, all the points which are identified with the origin in the torus should be rotated to points which are also identified with the origin, i.e.

$$\omega(a\vec{e}_1 + b\vec{e}_2) = a'\vec{e}_1 + b'\vec{e}_2 \ , \tag{5.4}$$

where a, a', b, and b' are all integers.

Instead of using Cartesian coordinates we can use the torus basis $\vec{e}_1, \vec{e}_2$. The matrix representation of the generating element in this basis reads

$$\hat{\omega} = \begin{pmatrix} n_1 & n_2 \\ n_3 & n_4 \end{pmatrix} , \tag{5.5}$$

where $\hat{\omega} = U\omega U^{-1}$ and U is the similarity transformation relating the Cartesian and the torus bases to each other. In this basis we have

$$\begin{pmatrix} n_1 & n_2 \\ n_3 & n_4 \end{pmatrix} \begin{pmatrix} a \\ b \end{pmatrix} = \begin{pmatrix} a' \\ b' \end{pmatrix} . \tag{5.6}$$

Due to the fact that a, b, a', b' are integers, the n_i's must also be integers. And since the trace is a basis-independent quantity, we have

$$2\cos(\phi) = Tr\omega = Tr\hat{\omega} = n_1 + n_4 \ , \tag{5.7}$$

which implies that $2\cos(\phi)$ is an integer and thus $\cos(\phi) = -1, -1/2, 0, 1/2, 1$ corresponding to $\phi = \pi, 2\pi/3, \pi/2, \pi/3, 2\pi$. This directly leads to a constraint for the Z_N, and we are only allowed to choose $N = 1, 2, 3, 4, 6$. This then also leads to a constraint concerning our choice of torus basis vectors, since the rotational symmetry Z_N needs to be consistent with the symmetry of the torus. When modding out Z_2, this is no constraint, as any basis is consistent with reflections. For Z_3 and Z_6, we can only take the relative angle between the basis vectors to be 60, 120, or 150 degrees. All three possibilities give the same orbifold. Here, we choose the 60° lattice with basis vectors $(\vec{e}_1 = (1,0), \vec{e}_2 = (1/2, \sqrt{3}/2))$ [1]. Finally, when modding out Z_4, the only possibility is a 90° lattice, with both basis vectors normalized to a length of 1.

We thus only have to discuss four different cases: T^2/Z_2, T^2/Z_3, T^2/Z_4, and T^2/Z_6. For the last three cases the orbifold is uniquely defined, while for the first case we need to additionally discuss the effect of choosing a specific basis.

From these four orbifolds, we can then extract the residual Poincaré symmetry, which will in all cases be a non-abelian discrete symmetry. This is done in the following way: After choosing the orbifold, we determine the fixed points. A fixed point is a point for which a rotation by an integer multiple of ϕ is equivalent to a lattice translation. These points are potential candidates for the localization of 3-branes [2] and thus the Standard Model fermions can be taken to be brane fields, which are non-vanishing only at the fixed points. The fixed points are divided into several twisted sectors, where the mth twisted sector contains those fixed points for which a rotation by $m\phi$ corresponds to a lattice translation. A given fixed point can lie in several twisted sectors.

We assume all fixed points to be physically equivalent. This then means that the remnant translation and rotation symmetries are those which result only in a permutation of the fixed points, i.e., only map fixed points to other fixed points. These remnant symmetry operations are the elements of the residual Poincaré symmetry, and all that remains to be done is to find the underlying group structure.

One can then immediately see, why we do not need to consider the 1-dimensional orbifold S^1/Z_N: It has only two fixed points, and thus any symmetry group which permutes them will be a subgroup of the permutation group for two distinct objects, $S_2 \simeq Z_2$, which is abelian. Since we want to obtain a non-abelian discrete symmetry, we need to consider at least a 2-dimensional orbifold.

5.2 Symmetries from Orbifolding

In our discussion we parameterize the two extra dimensions by one complex number $z \equiv x_5 + ix_6$. Analogously to Eq.(5.1), the torus T^2 is obtained by identifying the points in the

[1] The other two equivalent possibilities are the $SU(3)$ lattice with $(\vec{e}_1 = (1,0), \vec{e}_2 = (-1/2, \sqrt{3}/2))$ and the G_2 lattice with $(\vec{e}_1 = (1,0), \vec{e}_2 = (-3/2, \sqrt{3}/2))$.

[2] A 3-brane has three spatial dimensions.

complex plane related by

$$z \rightarrow z+1 \ , \tag{5.8}$$
$$z \rightarrow z+\gamma \ , \tag{5.9}$$

where the complex numbers $(1,\gamma)$ correspond to the basis vectors $(\vec{e}_1,\vec{e}_2)$.

5.2.1 T^2/Z_2

If we mod out a Z_2 reflection symmetry, γ can be arbitrary in general. However, in order to obtain a non-abelian symmetry, we have only two possibilities: The first one is $\gamma = e^{i\pi/3}$, which gives us an S_4 flavor symmetry, or an A_4 symmetry if only proper Lorentz transformations and translations (i.e. no discrete parities) are considered. The other possible basis is $\gamma = e^{i\pi/2} = i$.

Case 1: $\gamma = e^{i\pi/3}$

This orbifold is shown in Figure 5.1. The Z_2 parity is defined by

$$z \rightarrow -z \ . \tag{5.10}$$

The fixed points are given by $(z_1,z_2,z_3,z_4) = (1/2,(1+\gamma)/2,\gamma/2,0)$. Considering only proper Lorentz transformations and translations, the fixed points are permuted by two translation operations S_i, and the rotation T_R,

$$S_1 : z \rightarrow z+1/2, \tag{5.11}$$
$$S_2 : z \rightarrow z+\gamma/2, \tag{5.12}$$
$$T_R : z \rightarrow \omega z, \tag{5.13}$$

where $\omega = \gamma^2$. We can write down these operations in terms of the interchange of the fixed points as following,

$$\begin{aligned} S_1[(14)(23)] : (z_1,z_2,z_3,z_4) &\rightarrow (z_4,z_3,z_2,z_1) \ , \\ S_2[(12)(34)] : (z_1,z_2,z_3,z_4) &\rightarrow (z_2,z_1,z_4,z_3) \ , \\ T_R[(123)(4)] : (z_1,z_2,z_3,z_4) &\rightarrow (z_3,z_1,z_2,z_4) \ . \end{aligned} \tag{5.14}$$

From these elements we can define two generators of A_4 as

$$S = [(14)(23)], \tag{5.15}$$
$$T = [(123)(4)], \tag{5.16}$$

satisfying the generator relations,

$$\begin{aligned} S^2 &= 1 \ , \\ T^3 &= 1 \ , \\ (ST)^3 &= 1 \ . \end{aligned} \tag{5.17}$$

In case we consider the full Poincaré group, there will be two additional parities,

$$P : z \rightarrow z^*, \tag{5.18}$$
$$P' : z \rightarrow -z^*, \tag{5.19}$$

which can be written in terms of the interchange of the fixed points as

$$P[(23)(1)(4)] : (z_1, z_2, z_3, z_4) \rightarrow (z_1, z_3, z_2, z_4) \ , \tag{5.20}$$
$$P'[(23)(1)(4)] : (z_1, z_2, z_3, z_4) \rightarrow (z_1, z_3, z_2, z_4) \ . \tag{5.21}$$

In terms of the interchange of the fixed points, these two parities are equivalent. Combining these parities with the operators given in Eq.(5.14), we end up with the S_4 flavor symmetry generated by

$$S = [(12)(34)][(23)(1)(4)] = [(1243)], \tag{5.22}$$
$$T = [(123)(4)], \tag{5.23}$$

satisfying the generator relations

$$\begin{aligned} S^4 &= 1 \ , \\ T^3 &= 1 \ , \\ (ST^2)^2 &= 1 \ . \end{aligned} \tag{5.24}$$

Case 2: $\gamma = e^{i\pi/2} = i$

This orbifold is shown in Figure 5.2. The Z_2 parity is defined by

$$z \rightarrow -z \ . \tag{5.25}$$

The fixed points are then given by $(z_1, z_2, z_3, z_4) = (1/2, (1+i)/2, i/2, 0)$. They are permuted by the two translation operations

$$S_1 : z \rightarrow z + 1/2 \ , \tag{5.26}$$
$$S_2 : z \rightarrow z + i/2 \ . \tag{5.27}$$

Moreover, the fixed points are also permuted by the rotation

$$T_R : z \rightarrow \omega z \ , \tag{5.28}$$

where $\omega = e^{i\pi/2} = i$. One can also write these operations explicitly in terms of the interchange of the fixed points,

$$S_1[(14)(23)] : (z_1, z_2, z_3, z_4) \rightarrow (z_4, z_3, z_2, z_1) \ , \tag{5.29}$$
$$S_2[(12)(34)] : (z_1, z_2, z_3, z_4) \rightarrow (z_2, z_1, z_4, z_3) \ , \tag{5.30}$$
$$T_R[(13)(2)(4)] : (z_1, z_2, z_3, z_4) \rightarrow (z_3, z_2, z_1, z_4) \ . \tag{5.31}$$

From these elements we can define two generators,

$$A = [(13)(2)(4)][(14)(23)] = [(1432)] \ , \tag{5.32}$$
$$B = [(12)(34)] \ , \tag{5.33}$$

satisfying the generator relations,

$$\begin{aligned} A^4 &= 1 \ , \\ B^2 &= 1 \ , \\ ABA &= B \ . \end{aligned} \tag{5.34}$$

This describes the dihedral group D_4, the symmetry group of the square. The group theory of D_4 is discussed in Section 3.1.1. Note that this group is not enlarged if we include parity transformations.

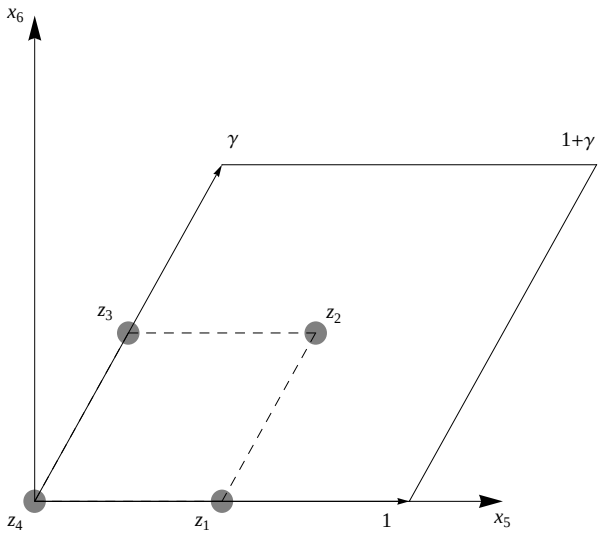

Figure 5.1: The orbifold T^2/Z_2 in case 1 with basis vectors $\vec{e_1}$, $\vec{e_2}$ and fixed points z_i. The polygon formed by the fixed points, corresponding to the discrete symmetries A_4 or S_4, are shown with dashed lines.

5.2.2 T^2/Z_3

When modding out Z_3 we consider, without loss of generality, only the torus with a 60° lattice, as already mentioned in Section 5.1. This corresponds to the choice $\gamma = e^{i\pi/3}$. This orbifold is shown in Figure 5.2. The operation of the generator of the Z_3 symmetry is given by

$$z \to e^{i2\pi/3} z \ . \tag{5.35}$$

The corresponding fixed points are $(z_1, z_2, z_3) = (0, i/\sqrt{3}, 1/2 + i/2\sqrt{3})$. The translation operations permuting these fixed points are

$$S_1 : z \ \to \ z + (1/2 + i/2\sqrt{3}) \ , \tag{5.36}$$
$$S_2 : z \ \to \ z + i/\sqrt{3} \ . \tag{5.37}$$

Moreover, the fixed points are also permuted by the rotation with respect to the origin

$$T_R : z \ \to \ \omega z \ , \tag{5.38}$$

where $\omega = e^{i\pi/3} = i$. Again, one can also write the symmetry operations in terms of a permutation of the fixed points,

$$S_1[(321)] : (z_1, z_2, z_3) \ \to \ (z_2, z_3, z_1) \ , \tag{5.39}$$
$$S_2[(123)] : (z_1, z_2, z_3) \ \to \ (z_3, z_1, z_2) \ , \tag{5.40}$$
$$T_R[(23)] : (z_1, z_2, z_3) \ \to \ (z_1, z_3, z_2) \ . \tag{5.41}$$

A possible parity transformation would be equivalent to the rotation T_R and thus does not need to be considered separately. We can formulate two generators

$$A \ = \ [(321)] \ , \tag{5.42}$$
$$B \ = \ [(321)][(23)] = [(13)] \ , \tag{5.43}$$

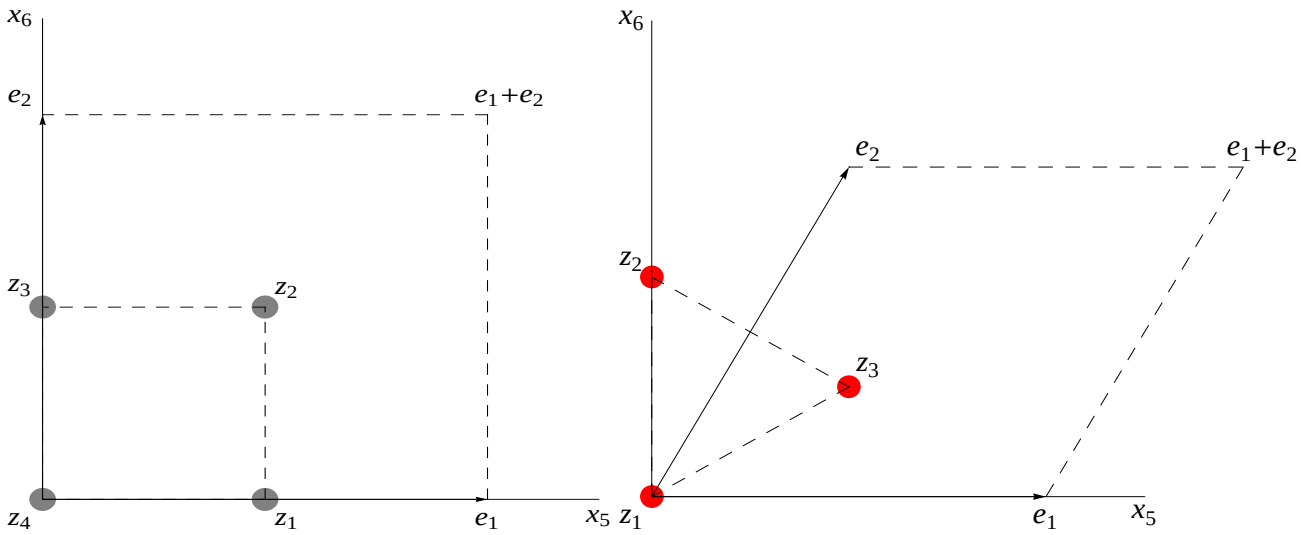

Figure 5.2: The orbifolds T^2/Z_2 in case 2 (left) and T^2/Z_3 (right) with basis vectors $\vec{e_1}$, $\vec{e_2}$ and fixed points z_i. The square (left) and the triangle (right) formed by the fixed points, corresponding to the discrete symmetries D_4 and D_3 respectively, are shown with dashed lines.

satisfying the generator relations

$$\begin{aligned} A^3 &= 1\,, \\ B^2 &= 1\,, \\ ABA &= B\,. \end{aligned} \tag{5.44}$$

This describes the dihedral group D_3, the symmetry group of the triangle, which is isomorphic to S_3, the permutation group of three distinct objects. As it is a dihedral group, its group theory can be found in Appendix A.1.

5.2.3 T^2/Z_4

When modding out the abelian group Z_4, we have only one consistent choice of basis, $\gamma = e^{i\pi/2} = i$. The torus is the same one we used for T^2/Z_2 to obtain the D_4 symmetry, as one can also see in Figure 5.3. In fact, the fixed points will also be the same and we will thus obtain the same flavor symmetry. This is due to the fact that we obtain all fixed points of the orbifold T^2/Z_4 in the second twisted sector, where we only consider the squared generator of Z_4. This corresponds to a Z_2 subgroup of Z_4 and is thus fully equivalent to our discussion for T^2/Z_2 with a 90° lattice. The first twisted sector only contains the fixed points z_2 and z_4; as both of them also appear in the second twisted sector, no new fixed points and thus no new residual translational or rotational symmetry operations arise due to the larger abelian group, Z_4. Thus, the unique symmetry we obtain is D_4.

5.2.4 T^2/Z_6

As for T^2/Z_3 we use the 60° lattice, i.e. $\gamma = e^{i\pi/3}$. The orbifold is shown in Figure 5.3. The operation of the Z_6 symmetry for the first twisted sector is defined by

$$z \to e^{i2\pi/6} z\,. \tag{5.45}$$

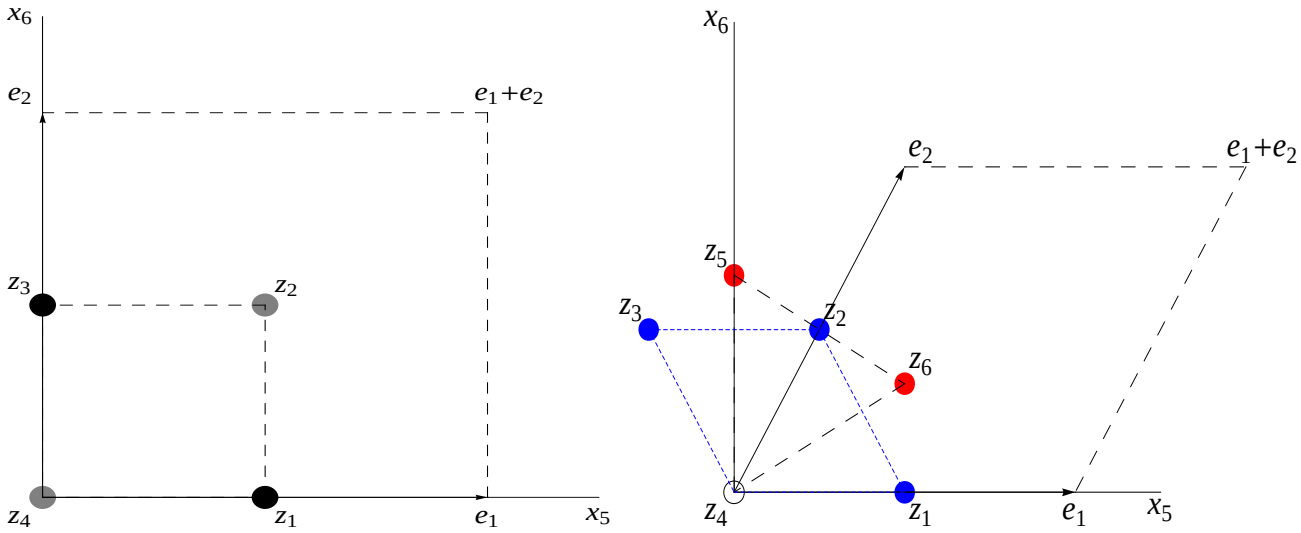

Figure 5.3: The orbifolds T^2/Z_4 (left) and T^2/Z_6 (right) with basis vectors $\vec{e_1}$, $\vec{e_2}$ and fixed points z_i. On the left, the fixed points which are both in the first and the second twisted sector are designated by gray points, those fixed points which are only in the second twisted sector are designated by black points. On the right, the fixed point which is in all twisted sectors is represented by a circle, those fixed points which are only in the second twisted sector are designated by red (lighter gray) points, while those fixed points which are only in the third twisted sector are given by blue (darker gray) points.

For the first twisted sector, we have only one fixed point which is $z_4 = 0$. For the second twisted sector, the operation of the Z_6 symmetry reads

$$z \to e^{i2\pi/3} z \ . \tag{5.46}$$

The fixed points of the second twisted sector are $(z_4, z_5, z_6) = (0, i/\sqrt{3}, 1/2(1 + i/\sqrt{3})$ which are the same as in the case of T^2/Z_3.
For the third twisted sector, finally, the operation of Z_6 symmetry is written as

$$z \to -z \ . \tag{5.47}$$

The fixed points in this sector thus are $(z_1, z_2, z_3, z_4) = (1/2, 1/4 + i\sqrt{3}/4, -1/4 + i\sqrt{3}/4, 0)$. Combining all fixed points $(z_1, z_2, z_3, z_4, z_5, z_6)$, we find that the fixed points are only permuted by residual rotation operations, i.e. translation symmetry is fully broken. These rotations are

$$T_{R1} : z \ \to \ e^{i\pi/3} z \ , \tag{5.48}$$
$$T_{R2} : z \ \to \ e^{i2\pi/3} z \ . \tag{5.49}$$

Moreover, if we assume the full Poincaré symmetry, we will also have two parity operations acting on the fixed points

$$P_1 : z \ \to \ z^*, \tag{5.50}$$
$$P_2 : z \ \to \ -z^*, \tag{5.51}$$

where z^* denotes the complex conjugation of z.

We can write all of these symmetry operations in terms of a permutation of the fixed points as

$$\begin{aligned} T_{R1}[(123)(56)] : (z_1, z_2, z_3, z_4, z_5, z_6) &\rightarrow (z_3, z_1, z_2, z_4, z_6, z_5) \ , & (5.52) \\ T_{R2}[(132)] : (z_1, z_2, z_3, z_4, z_5, z_6) &\rightarrow (z_2, z_3, z_1, z_4, z_5, z_6) \ , & (5.53) \\ P_1[(23)(56)] : (z_1, z_2, z_3, z_4, z_5, z_6) &\rightarrow (z_1, z_3, z_2, z_4, z_6, z_5) \ , & (5.54) \\ P_2[(23)] : (z_1, z_2, z_3, z_4, z_5, z_6) &\rightarrow (z_1, z_3, z_2, z_4, z_5, z_6) \ . & (5.55) \end{aligned}$$

From these operators, we can form the generators

$$\begin{aligned} A &= [(123)(56)] \ , & (5.56) \\ B &= [(23)] \ , & (5.57) \end{aligned}$$

satisfying the generator relations,

$$\begin{aligned} A^6 &= 1 \ , \\ B^2 &= 1 \ , \\ ABA &= B \ . & (5.58) \end{aligned}$$

This defines the group $D_6 \cong D_3 \times Z_2 \cong S_3 \times Z_2$. If we do not include the parity operations, we will effectively lose the generator B. The flavor symmetry then has only one generator and is the abelian group Z_6.

5.3 Group Representations

To construct a full model, one now needs to assign the fermion generations to representations of these flavor groups. The orbifold fixed points are interpreted as 3-branes, on which the fermion fields are localized. The flavor symmetry operations which permute the fixed points then act non-trivially on the fermion fields. Irreducible representations correspond to relations among the field values at different fixed points; these relations are invariant under symmetry operations. In general, this means that one or more fermion generations transforming under an irreducible representation of the flavor group will be "smeared out" over all available fixed points. All representations can be reproduced in this way, and the origin of the flavor group from orbifolding thus does not offer any restrictions on the choice of representations. Also, all representations will correspond in general to the field(s) being non-vanishing at all fixed points. Thus, although the flavor symmetry as a whole has a straightforward interpretation in the geometry of the orbifold, the different representations do not.

This is at least a bit different for the last orbifold we have discussed, T^2/Z_6. The resulting flavor symmetry was D_6, which is isomorphic to $D_3 \times Z_2$. We observe that all symmetry operations leave the origin, the fixed point z_4, invariant. Thus, a field which is localized at the origin will transform trivially under the flavor symmetry. In addition the subgroup D_3 generated by A^2 and B leaves the fixed points z_5 and z_6, i.e. the fixed points of the second twisted sector, invariant. Fields localized only on these two fixed points thus transform non-trivially only under the Z_2 factor of the flavor group. Similarly, the fixed points of the third twisted sector, z_1, z_2, and z_3 are not permuted by the group element A^3, which generates Z_2. Fields localized in this sector will thus only transform non-trivially under the D_3 factor of the flavor group. Fields transforming non-trivially both under D_3 and Z_2 will

necessarily be non-vanishing in both the second and the third twisted sector. For more details on the representation theory of D_6 and the transformation properties of representations under subgroups, see [184].

The orbifold T^2/Z_6 thus is so appealing that different representations correspond to different localizations in the orbifold and therefore have a more intuitive interpretation in terms of the orbifold geometry. However, also here all representations can be reproduced, and the orbifold origin of the flavor symmetry does not offer further input as to which representations to use for model building.

We have discussed all possible non-abelian discrete symmetries arising from 2-dimensional orbifolds. In this context the flavor symmetries arise as a remnant symmetry of the full 6-dimensional space-time symmetry. This remnant symmetry can then be interpreted as the permutation symmetry of the orbifold fixed points. These fixed points, in turn, are taken to be 3-branes, on which the three generations of Standard Model fermions reside. The flavor symmetry then has a straightforward interpretation in terms of the geometry of the orbifold. As in crystallography, the number of possible lattice structures and symmetry groups is strictly limited for orbifolds. The resulting flavor symmetries are all crystallographic point groups, as was to be expected. The possible flavor groups we obtain are S_4, A_4, S_3, D_4, and $D_6 \simeq D_3 \times Z_2$, where the first two have already been discussed in [28]. All of these groups have been widely used as phenomenologically successful flavor symmetries.

Chapter 6

Flavored Orbifold GUT

In the last chapter, it has been shown that a non-abelian discrete flavor symmetry can arise as a result of an orbifold compactification. In order to give a prediction for the neutrino mixing, the flavor symmetry has to be broken by a certain VEV alignment of flavons. To obtain a viable VEV alignment of flavons often requires a complicated structure in the flavon superpotential (see the discussion in Chapter 3). However, in the orbifold context, the VEV alignment of the flavons can be easily obtained from orbifolding without dealing with a complicated flavon superpotential [40]. Moreover, an orbifold compactification of a GUT can lead to its breaking and nicely solve, e.g., the doublet-triplet splitting problem [30–34]. Recently, the idea of combining the flavor symmetry originating from an orbifold compactification with an orbifold GUT has been studied [37].

In this chapter, we propose the idea of combining the breaking of a GUT by boundary conditions on an orbifold with the breaking of the flavor symmetry arising from the orbifold. We demonstrate this idea with a simple model in the context of a 6d SUSY SO(10) orbifold GUT with an S_4 flavor symmetry. We assume that the orbifold parities act on gauge, SUSY as well as flavor space. Hence, the zero modes are determined by the overall parity.

6.1 Flavor Symmetry from Orbifolding

We study the breaking of an SO(10) GUT and its flavor symmetry on the $T^2/(Z_2^I \times Z_2^{PS} \times Z_2^{GG})$ orbifold (see Figure 6.1) with radii $R = R_5 = R_6$, which we choose such that $2\pi R = 1$ for simplicity. The orbifold is defined by

$$T_1 : z \to z + 1, \qquad T_2 : z \to z + \gamma, \qquad Z : z \to -z. \tag{6.1}$$

where $z = x^5 + ix^6$ and $\gamma = e^{i\pi/3}$. As has been shown in the last chapter, the breaking of Poincaré symmetry from 6d to 4d through compactification on the orbifold leads to a remnant S_4 flavor symmetry. We note that the additional modding out of groups, Z_2^{PS}, Z_2^{GG}, does not change the structure of the orbifold. Concretely, the orbifold has four fixed points, $(z_1, z_2, z_3, z_4) = (1/2, (1+\gamma)/2, \gamma/2, 0)$, which are permuted by two translation operations S_i, the rotation T_R, and two parity operations $P^{(\prime)}$:

$$\begin{aligned} &S_1 : z \to z + 1/2, \qquad S_2 : z \to z + \gamma/2, \qquad T_R : z \to \gamma^2 z, \\ &P : z \to z^*, \qquad P' : z \to -z^* \,. \end{aligned} \tag{6.2}$$

One can also write these operations explicitly in terms of interchange of the fixed points, $S_1[(14)(23)]$, $S_2[(12)(34)]$, $T_R[(123)(4)]$, $P[(23)(1)(4)]$, and $P'[(23)(1)(4)]$. From these elements we can define the two generators of S_4 as $S = S_2P$ and $T = T_R$ satisfying the generator relation, $S^4 = T^3 = (ST^2)^2 = 1$. The localization of a brane field defines its representation of S_4. The generators S, T can be represented by the matrices,

$$S = \begin{pmatrix} 0 & 0 & 1 & 0 \\ 1 & 0 & 0 & 0 \\ 0 & 0 & 0 & 1 \\ 0 & 1 & 0 & 0 \end{pmatrix}, \quad T = \begin{pmatrix} 0 & 0 & 1 & 0 \\ 1 & 0 & 0 & 0 \\ 0 & 1 & 0 & 0 \\ 0 & 0 & 0 & 1 \end{pmatrix}, \tag{6.3}$$

acting on the brane field $\psi(x^\mu) = (\psi_1, \psi_2, \psi_3, \psi_4)^T$, where $\psi_i = \psi(x^\mu, z_i)$ is a field localized at the fixed point z_i. We denote this basis as localization basis. The characters of S and T show that the four dimensional representation generated by $\langle S, T\rangle$ can be decomposed as

$$\underline{\mathbf{4}} = \underline{\mathbf{3_1}} \oplus \underline{\mathbf{1_1}} \ , \tag{6.4}$$

and the explicit unitary transformation is

$$S \to U^\dagger S U = \begin{pmatrix} S_3^{fl} & \\ & 1 \end{pmatrix}, \quad T \to U^\dagger T U = \begin{pmatrix} T_3^{fl} & \\ & 1 \end{pmatrix} \quad \text{with} \quad U = \begin{pmatrix} (\alpha_{ij}) & (\beta_i) \end{pmatrix} \tag{6.5}$$

$$\text{and} \qquad (\alpha_{ij}) = \begin{pmatrix} -\frac{1}{2\sqrt{3}} & \frac{1}{\sqrt{3}} & \frac{1}{\sqrt{3}} \\ -\frac{1}{2\sqrt{3}} & \frac{\omega}{\sqrt{3}} & \frac{\omega^2}{\sqrt{3}} \\ -\frac{1}{2\sqrt{3}} & \frac{\omega^2}{\sqrt{3}} & \frac{\omega}{\sqrt{3}} \\ \frac{\sqrt{3}}{2} & 0 & 0 \end{pmatrix}, \qquad (\beta_i) = \begin{pmatrix} \frac{1}{2} \\ \frac{1}{2} \\ \frac{1}{2} \\ \frac{1}{2} \end{pmatrix}, \tag{6.6}$$

where $\omega = e^{2\pi i/3}$ and S_3^{fl}, T_3^{fl} are the three-dimensional generators of S_4 acting on a triplet $\underline{\mathbf{3_1}}$ in flavor basis. The transformation of a brane field $\psi(x)$ is accordingly related to the flavor basis $\psi^{fl}(x^\mu) = U^\dagger \psi(x^\mu)$, as well as the Clebsch-Gordan coefficients. The first three components of ψ^{fl} form a triplet $\underline{\mathbf{3_1}}$ and the last one forms a singlet $\underline{\mathbf{1_1}}$. The representations $\underline{\mathbf{1_2}}$ and $\underline{\mathbf{3_2}}$ are obtained analogously by using the freedom to change the phase of each brane field in a symmetry transformation. Concretely, by replacing S with $(-S)$, we obtain a representation of S_4 which decomposes as $\langle -S, T\rangle = \underline{\mathbf{3_2}} \oplus \underline{\mathbf{1_2}}$. Similarly, the $\underline{\mathbf{2}}$ of S_4 can be obtained from the four dimensional representation $\langle S := T_R^2 P T_R, T := T_R^2\rangle = \underline{\mathbf{2}} \oplus \underline{\mathbf{1_1}} \oplus \underline{\mathbf{1_1}}$. Bulk fields $B_K(x^\mu, z)$ are coupled to brane fields $\psi_i(x^\mu)$ in localization basis and form a trivial singlet via

$$J(x^\mu) = \int \mathrm{d}z \sum_i \alpha_{iK} B_K(x^\mu, z) \psi_i(x^\mu) \delta(z - z_i) \ , \tag{6.7}$$

as it is described explicitly in [28]. We assume that (bulk) flavons obtain a constant VEV in the following. Furthermore, we will work in the flavor basis with irreducible representations only and omit the superscript ^{fl} for simplicity in the following.

6.2 Symmetry Breaking by Boundary Conditions

6.2.1 Gauge Symmetry Breaking

In order to demonstrate how the flavor structure can be obtained and broken appropriately from an orbifold, we implement it in a 6d SO(10) model with a breaking of gauge symmetry

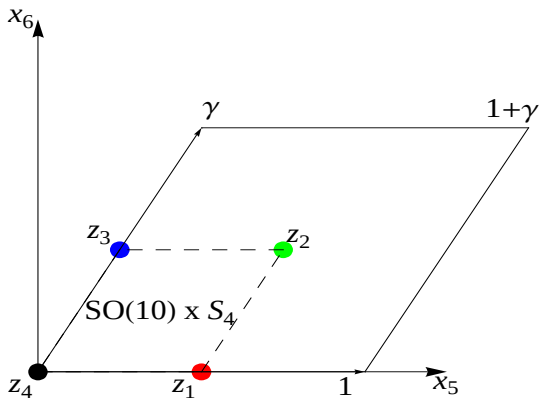

Figure 6.1: The Orbifold $T^2/(Z_2^I \times Z_2^{PS} \times Z_2^{GG})$ with its four fixed points (z_1, z_2, z_3, z_4). The symmetry of interchanging the fixed points forms the discrete group S_4.

and $N = 2$ SUSY down to $N = 1$ SUSY, which nicely leads to a splitting of the doublet and triplet components in $H_{u,d}$ similar to [177,200]. We neglect the anomaly cancellation [201,202] for the purpose of this study.

If we begin with $N = 1$ SUSY in 6d, it will give $N = 2$ SUSY in 4d. The gauge vector multiplet, $(V_M, \lambda_{1,2})$, can be decomposed in terms of one vector and one chiral multiplets of the unbroken N=1 SUSY in 4d as

$$V = (V_\mu, \lambda_1) \ , \quad \Sigma = (V_{5,6}, \lambda_2) \ , \tag{6.8}$$

where V and Σ transform in the adjoint representation of $SO(10)$.

The gauge fields transform under the orbifold parities as

$$\begin{aligned} P_I V(x^\mu, -z) P_I^{-1} &= \eta_I V(x^\mu, z) \ , \\ P_{PS} V(x^\mu, -z + z_1) P_{PS}^{-1} &= \eta_{PS} V(x^\mu, z + z_1) \ , \\ P_{GG} V(x^\mu, -z + z_3) P_{GG}^{-1} &= \eta_{GG} V(x^\mu, z + z_3) \ , \end{aligned} \tag{6.9}$$

where the matrices $P_I = I$, P_{PS}, and P_{GG} act on the gauge space and are given by [176]

$$P_{PS} = \begin{pmatrix} -\sigma^0 & 0 & 0 & 0 & 0 \\ 0 & -\sigma^0 & 0 & 0 & 0 \\ 0 & 0 & -\sigma^0 & 0 & 0 \\ 0 & 0 & 0 & \sigma^0 & 0 \\ 0 & 0 & 0 & 0 & \sigma^0 \end{pmatrix} \ , \ P_{GG} = \begin{pmatrix} \sigma^2 & 0 & 0 & 0 & 0 \\ 0 & \sigma^2 & 0 & 0 & 0 \\ 0 & 0 & \sigma^2 & 0 & 0 \\ 0 & 0 & 0 & \sigma^2 & 0 \\ 0 & 0 & 0 & 0 & \sigma^2 \end{pmatrix} \ , \tag{6.10}$$

where σ^0 is the 2×2 unity matrix, while σ^2 is one of the Pauli matrices. The parities of the gauge field V are chosen as $\eta_I = \eta_{PS} = \eta_{GG} = +1$, while for Σ, we choose the parities $\eta_I = \eta_{PS} = \eta_{GG} = -1$. The first parity (corresponding to fixed point z_4) is used to break $N = 2$ SUSY to $N = 1$ SUSY [176,203], and the remaining two parities are used to break the gauge symmetry. The zero modes of the gauge fields, V and Σ, are given in Table 6.1.

The GUT scale M_{GUT} is determined by the compactification scale. The unbroken gauge group of the effective 4d theory is $G_{SM'} = SU(3) \times SU(2) \times U(1)_Y \times U(1)_X$, which is given by

$G_{SM'}$	G_{GG}	G_{PS}	$(V_\mu,\, \lambda_1)$			$(V_{5,6},\, \lambda_2)$		
			Z_2^I	Z_2^{GG}	Z_2^{PS}	Z_2^I	Z_2^{GG}	Z_2^{PS}
$(\underline{\boldsymbol{8}}, \underline{\boldsymbol{1}}, 0)_0$	$\underline{\mathbf{24}}_0$	$(\underline{\mathbf{15}}, \underline{\mathbf{1}}, \underline{\mathbf{1}})$	+	+	+	−	−	−
$(\underline{\mathbf{3}}, \underline{\mathbf{2}}, \text{-}5)_0$	$\underline{\mathbf{24}}_0$	$(\underline{\mathbf{6}}, \underline{\mathbf{2}}, \underline{\mathbf{2}})$	+	+	−	−	−	+
$(\underline{\bar{\mathbf{3}}}, \underline{\mathbf{2}}, 5)_0$	$\underline{\mathbf{24}}_0$	$(\underline{\mathbf{6}}, \underline{\mathbf{2}}, \underline{\mathbf{2}})$	+	+	−	−	−	+
$(\underline{\boldsymbol{1}}, \underline{\boldsymbol{3}}, 0)_0$	$\underline{\mathbf{24}}_0$	$(\underline{\mathbf{1}}, \underline{\mathbf{3}}, \underline{\mathbf{1}})$	+	+	+	−	−	−
$(\underline{\boldsymbol{1}}, \underline{\boldsymbol{1}}, 0)_0$	$\underline{\mathbf{24}}_0$	$(\underline{\mathbf{1}}, \underline{\mathbf{1}}, \underline{\mathbf{3}})$	+	+	+	−	−	−
$(\underline{\mathbf{3}}, \underline{\mathbf{2}}, 1)_{+4}$	$\underline{\mathbf{10}}_{+4}$	$(\underline{\mathbf{6}}, \underline{\mathbf{2}}, \underline{\mathbf{2}})$	+	−	−	−	+	+
$(\underline{\bar{\mathbf{3}}}, \underline{\mathbf{1}}, -4)_{+4}$	$\underline{\mathbf{10}}_{+4}$	$(\underline{\mathbf{15}}, \underline{\mathbf{1}}, \underline{\mathbf{1}})$	+	−	+	−	+	−
$(\underline{\mathbf{1}}, \underline{\mathbf{1}}, 6)_{+4}$	$\underline{\mathbf{10}}_{+4}$	$(\underline{\mathbf{1}}, \underline{\mathbf{1}}, \underline{\mathbf{3}})$	+	−	+	−	+	−
$(\underline{\bar{\mathbf{3}}}, \underline{\mathbf{2}}, -1)_{-4}$	$\underline{\overline{\mathbf{10}}}_{-4}$	$(\underline{\mathbf{6}}, \underline{\mathbf{2}}, \underline{\mathbf{2}})$	+	−	−	−	+	+
$(\underline{\mathbf{3}}, \underline{\mathbf{1}}, 4)_{-4}$	$\underline{\overline{\mathbf{10}}}_{-4}$	$(\underline{\mathbf{15}}, \underline{\mathbf{1}}, \underline{\mathbf{1}})$	+	−	+	−	+	−
$(\underline{\mathbf{1}}, \underline{\mathbf{1}}, -6)_{-4}$	$\underline{\overline{\mathbf{10}}}_{-4}$	$(\underline{\bar{\mathbf{1}}}, \underline{\mathbf{1}}, \underline{\mathbf{3}})$	+	−	+	−	+	−
$(\underline{\boldsymbol{1}}, \underline{\boldsymbol{1}}, 0)_0$	$\underline{\mathbf{1}}_0$	$(\underline{\mathbf{15}}, \underline{\mathbf{1}}, \underline{\mathbf{1}})$	+	+	+	−	−	−

Table 6.1: Parity assignments for the components $V_M^A = \frac{1}{2}\mathrm{tr}(T^A V_M)$ of the $\underline{\mathbf{45}}$-plet of SO(10). $G_{SM'} = SU(3) \times SU(2) \times U(1)_Y \times U(1)_X$, $G_{GG} = SU(5) \times U(1)$, and $G_{PS} = SU(4) \times SU(2) \times SU(2)$. [176]

the intersection of the SO(10) subgroups at the fixed points. The remaining $\mathrm{U}(1)_X$ is broken by the left-handed conjugate neutrino mass term.
Moreover, the Higgs fields also transform under the orbifold parities as

$$\begin{aligned} P_I H(x^\mu, -z) &= \eta_I H(x^\mu, z)\ , \\ P_{PS} H(x^\mu, -z + z_1) &= \eta_{PS} H(x^\mu, z + z_1)\ , \\ P_{GG} H(x^\mu, -z + z_3) &= \eta_{GG} H(x^\mu, z + z_3)\ , \end{aligned} \tag{6.11}$$

where we choose $\eta^I = 1$ for all Higgs fields. We choose parities as $\eta_{PS} = \eta_{GG} = 1$ for H_d, and $\eta_{PS} = 1, \eta_{GG} = -1$ for H_u in order to obtain the two Higgs $SU(2)$ doublets of the SUSY SM as the zero modes, while the color Higgs triplets are massive, and their masses are at the GUT scale. This gives a solution to the doublet-triplet splitting problem. Furthermore, we choose the parities for the Higgs fields $\Delta_{1,2}$ as $\eta_{PS,1} = -1, \eta_{GG,1} = -1$, and $\eta_{PS,2} = 1, \eta_{GG,2} = -1$, respectively. These lead to Majorana mass terms for the neutrinos. The zero modes of the Higgs fields, $\underline{\mathbf{10}}$, and $\underline{\overline{\mathbf{16}}}$ are summarized in Table 6.2. The mode expansion of the fields can be found in Appendix B. We note that all flavons have positive gauge parities.

6.2.2 Flavor Symmetry Breaking

The mechanism to obtain the VEV alignment of the flavon fields has been firstly discussed in [40]. By assigning parities to the flavons living in the bulk, one can single out a zero mode

SO(10)	$\underline{\mathbf{10}}$							
G_{PS}	$(\underline{\mathbf{1}},\underline{\mathbf{2}},\underline{\mathbf{2}})$		$(\underline{\mathbf{1}},\underline{\mathbf{2}},\underline{\mathbf{2}})$		$(\underline{\mathbf{6}},\underline{\mathbf{1}},\underline{\mathbf{1}})$		$(\underline{\mathbf{6}},\underline{\mathbf{1}},\underline{\mathbf{1}})$	
G_{GG}	$\underline{\overline{\mathbf{5}}}_{-2}$		$\underline{\mathbf{5}}_{+2}$		$\underline{\overline{\mathbf{5}}}_{-2}$		$\underline{\mathbf{5}}_{+2}$	
$G_{SM'}$	$(\underline{\mathbf{1}},\underline{\mathbf{2}},-1/2)_{-2}$		$(\underline{\mathbf{1}},\underline{\mathbf{2}},+1/2)_{+2}$		$(\underline{\bar{\mathbf{3}}},\underline{\mathbf{1}},+1/3)_{-2}$		$(\underline{\mathbf{3}},\underline{\mathbf{1}},-1/3)_{+2}$	
	Z_2^{PS}	Z_2^{GG}	Z_2^{PS}	Z_2^{GG}	Z_2^{PS}	Z_2^{GG}	Z_2^{PS}	Z_2^{GG}
H_d	+	+	+	−	−	+	−	−
H_u	+	−	+	+	−	−	−	+
SO(10)	$\underline{\overline{\mathbf{16}}}$							
G_{PS}	$(\underline{\bar{\mathbf{4}}},\underline{\mathbf{2}},\underline{\mathbf{1}})$		$(\underline{\bar{\mathbf{4}}},\underline{\mathbf{2}},\underline{\mathbf{1}})$		$(\underline{\mathbf{4}},\underline{\mathbf{1}},\underline{\mathbf{2}})$		$(\underline{\mathbf{4}},\underline{\mathbf{1}},\underline{\mathbf{2}})$	
G_{GG}	$\underline{\overline{\mathbf{10}}}_{+1}$		$\underline{\mathbf{5}}_{-3}$		$\underline{\overline{\mathbf{10}}}_{+1}$		$\underline{\mathbf{5}}_{-3},\underline{\mathbf{1}}_{+5}$	
$G_{SM'}$	$(\underline{\bar{\mathbf{3}}},\underline{\mathbf{2}},-1/6)_{+1}$		$(\underline{\mathbf{1}},\underline{\mathbf{2}},+1/2)_{-3}$		$(\underline{\mathbf{3}},\underline{\mathbf{1}},+2/3)_{+1}$ $\oplus(\underline{\mathbf{1}},\underline{\mathbf{1}},-1)_{+1}$		$(\underline{\mathbf{3}},\underline{\mathbf{1}},-1/3)_{-3}$ $\oplus(\underline{\mathbf{1}},\underline{\mathbf{1}},0)_{+5}$	
	Z_2^{PS}	Z_2^{GG}	Z_2^{PS}	Z_2^{GG}	Z_2^{PS}	Z_2^{GG}	Z_2^{PS}	Z_2^{GG}
$\bar{\Delta}_1$	−	−	−	+	+	−	+	+
$\bar{\Delta}_2$	+	−	+	+	−	−	−	+

Table 6.2: Parity assignments for the bulk $\underline{\mathbf{10}}$ and $\underline{\overline{\mathbf{16}}}$ hypermultiplets. [202]

and determine the flavon VEVs by their transformations under the orbifold parities. We assume that flavons transform non-trivially,

$$P_1\phi(x^\mu,-z) = \eta_1\,\phi(x^\mu,z), \tag{6.12a}$$
$$P_2\phi(x^\mu,-z+z_1) = \eta_2\,\phi(x^\mu,z+z_1), \tag{6.12b}$$
$$P_3\phi(x^\mu,-z+z_3) = \eta_3\,\phi(x^\mu,z+z_3), \tag{6.12c}$$

where the $P_{1,2,3} = Z, T_1Z, T_2Z$ can be formed by combining the translation operators $T_{1,2}$ and parity operator Z acting on flavor space. The first parity (corresponding to fixed point z_4) is used to break $N=2$ SUSY to $N=1$ SUSY [176, 203] and the remaining two parities are used to generate the VEV alignment of the flavons by singling out the appropriate zero modes.

The VEV alignment of flavons plays an important role in predicting neutrino mixing angles. Here, we give a simple example to demonstrate it in an extension of SM by the flavor symmetry S_4. Assuming the neutrino mass is generated by an effective dimension-5 operator, the relevant term in the Lagrangian will be given by

$$\mathcal{L}_\nu = \frac{(L^T\epsilon H_u)(L^T\epsilon H_u)}{\Lambda}\Big(\frac{y_a\phi_\nu + y_b\eta_\nu}{\Lambda_f}\Big), \tag{6.13}$$

where the fields transform under S_4 as $L,\phi_\nu \sim \underline{\mathbf{3_1}}$ and $\eta_\nu \sim \underline{\mathbf{1_1}}$ [204]. When the triplet obtains the VEV $\langle\phi_\nu\rangle \sim (1,1,1)^T v$, the neutrino mass matrix reads

$$m_\nu = m_0\begin{pmatrix} 2a+b & -a & -a \\ . & 2a & b-a \\ . & . & 2a \end{pmatrix}, \tag{6.14}$$

$\mathcal{C}_2$	$\underline{\mathbf{3_i}}$	$\mathcal{C}_4$	$\underline{\mathbf{3_1}}$	$\underline{\mathbf{3_2}}$	$\underline{\mathbf{2}}$
EV	1	EV	-1	1	1
S^2	$\begin{pmatrix}1 & 1 & 1\end{pmatrix}$	TST	$\begin{pmatrix}-2 & 1 & 1\end{pmatrix}$		$\begin{pmatrix}1 & 1\end{pmatrix}$
TS^2T^2	$\begin{pmatrix}1 & \omega^2 & \omega\end{pmatrix}$	T^2S	$\begin{pmatrix}-2 & \omega^2 & \omega\end{pmatrix}$		$\begin{pmatrix}1 & \omega\end{pmatrix}$
$S^2TS^2T^2$	$\begin{pmatrix}1 & \omega & \omega^2\end{pmatrix}$	ST^2	$\begin{pmatrix}-2 & \omega & \omega^2\end{pmatrix}$		$\begin{pmatrix}1 & \omega^2\end{pmatrix}$
		$TSTS^2$	$\begin{pmatrix}0 & -1 & 1\end{pmatrix}$		$\begin{pmatrix}1 & 1\end{pmatrix}$
		STS^2	$\begin{pmatrix}0 & -\omega^2 & \omega\end{pmatrix}$		$\begin{pmatrix}1 & \omega\end{pmatrix}$
		S^2TS	$\begin{pmatrix}0 & -\omega & \omega^2\end{pmatrix}$		$\begin{pmatrix}1 & \omega^2\end{pmatrix}$

Table 6.3: Eigenvector structure of the elements of the conjugacy classes $\mathcal{C}_{2,4}$ in representation $\underline{\mathbf{2}}$ and $\underline{\mathbf{3_i}}$, where S, T are generators of S_4 in the notation given in Appendix A.4 and $\omega = \mathrm{e}^{2\pi i/3}$. EV denotes a/the non-degenerate eigenvalue.

with $a = y_a \langle \phi_\nu \rangle / \Lambda_f$, $b = y_b \langle \eta_\nu \rangle / \Lambda_f$, as well as $m_0 = \langle H_u \rangle^2 / \Lambda$ which can be diagonalized by the tri-bimaximal mixing matrix.

In general, the flavon VEV alignment is determined by a possibly complicated flavon potential (see the flavon potential discussion in Chapter 3). However, in an orbifold context, the VEV alignment can be obtained from the fixed points of the action of parity operators on the fields, i.e., the simultaneous eigenvectors of the set of orbifold parity operators. Therefore, the flavon potential can remain simple. Parity operators can be formed by elements of order two of the flavor group [40]. Hence, the eigenvalues are ± 1. The elements of order two in S_4 are in the conjugacy classes $\mathcal{C}_2$ and $\mathcal{C}_4$. VEVs originating from the same set of parity operators are orthogonal. Since the parity operators can be chosen differently for different representations of S_4, VEVs of fields in different representations do not have to be orthogonal.

In the following, we discuss the eigenvalue and -vector structure of the elements of S_4. The non-degenerate eigenvalues of a conjugacy class can be inferred from the corresponding character, which is the sum of the eigenvalues. The eigenvalues or the representation $\underline{\mathbf{2}}$ of the conjugacy class $\mathcal{C}_2$ are degenerate and equal to 1. Hence, it is not possible to single out only one zero mode. The eigenvalues for the conjugacy class $\mathcal{C}_4$ are non-degenerate and the eigenvectors to the eigenvalue 1 are shown in Table 6.3. They differ only by a phase factor $\omega = e^{2\pi i/3}$. As can be seen, the eigenvectors of the non-degenerate eigenvalues of S^2, TST, and $TSTS^2$, respectively, form a tri-bimaximal mixing matrix. Hence, by choosing two of the three elements as parity operators, we can obtain a neutrino mass matrix which leads to a tri-bimaximal mixing matrix. The corresponding combinations with factors of ω lead to the same mixing angles but different phases. Any other combination of two arbitrary distinct elements leads to one single zero mode which is orthogonal to both given eigenvectors. The structure for the representation $\underline{\mathbf{3_2}}$ can be easily obtained from the structure of $\underline{\mathbf{3_1}}$, as they are related by $S \leftrightarrow -S$.

Concretely, in order to obtain the VEV alignment for the triplet $\underline{\mathbf{3_1}}$, we choose

$$P_1 = 1\,, \qquad P_2 = TST\,, \qquad P_3 = TSTS^2\,, \tag{6.15}$$

$$\text{i.e.}\quad P_2 = \frac{1}{3}\begin{pmatrix} -1 & 2 & 2 \\ 2 & 2 & -1 \\ 2 & -1 & 2 \end{pmatrix}\ , \qquad\qquad P_3 = \begin{pmatrix} 1 & 0 & 0 \\ 0 & 0 & 1 \\ 0 & 1 & 0 \end{pmatrix}\ ,$$

where S, T are generators of S_4 in the notation given in Appendix A.4. P_2 and P_3 are simultaneously diagonalized by the unitary matrix U

$$U = \begin{pmatrix} \frac{1}{\sqrt{3}} & \frac{2}{\sqrt{6}} & 0 \\ \frac{1}{\sqrt{3}} & -\frac{1}{\sqrt{6}} & \frac{1}{\sqrt{2}} \\ \frac{1}{\sqrt{3}} & -\frac{1}{\sqrt{6}} & -\frac{1}{\sqrt{2}} \end{pmatrix}\ , \qquad \begin{aligned} U^\dagger P_2 U &= \text{diag}(1,\,-1,\,1)\ , \\ U^\dagger P_3 U &= \text{diag}(1,\,1,\,-1)\ , \end{aligned} \tag{6.16}$$

Hence, a field $\phi_{\eta_1\eta_2\eta_3} \sim \underline{\mathbf{3_1}}$ where η_i denotes the parities introduced in Eq.(6.12), can have the following possible VEV configurations:

$$\langle \phi_{+++} \rangle = \begin{pmatrix} 1 & 1 & 1 \end{pmatrix}^T / \sqrt{3} \left\langle \tilde{\phi}_{+++} \right\rangle\ , \tag{6.17a}$$

$$\langle \phi_{+-+} \rangle = \begin{pmatrix} 2 & -1 & -1 \end{pmatrix}^T / \sqrt{6} \left\langle \tilde{\phi}_{+-+} \right\rangle\ , \tag{6.17b}$$

$$\langle \phi_{++-} \rangle = \begin{pmatrix} 0 & 1 & -1 \end{pmatrix}^T / \sqrt{2} \left\langle \tilde{\phi}_{++-} \right\rangle\ , \tag{6.17c}$$

with $\tilde{\phi}_i$ denoting the single zero mode of ϕ_i, and lead to a viable neutrino mass matrix Eq.(6.14).

In order to obtain the VEV alignment for the triplet $\underline{\mathbf{3_2}}$, we choose the parity operators in flavor space as

$$P_1 = 1\ , \qquad\qquad P_2 = STS^2\ , \qquad\qquad P_3 = TSTS^2\ , \tag{6.18}$$

$$\text{i.e.}\quad P_2 = \begin{pmatrix} -1 & 0 & 0 \\ 0 & 0 & -\omega \\ 0 & -\omega^2 & 0 \end{pmatrix}, \qquad\qquad P_3 = \begin{pmatrix} -1 & 0 & 0 \\ 0 & 0 & -1 \\ 0 & -1 & 0 \end{pmatrix}\ .$$

Obviously, there is only one zero mode and the VEV alignment of $\chi^i_{1,0,0}$ is given by

$$\left\langle \chi^i_{1,0,0} \right\rangle = \begin{pmatrix} 1 & 0 & 0 \end{pmatrix}^T \left\langle \tilde{\chi}^i_{1,0,0} \right\rangle\ . \tag{6.19}$$

Similarly, the VEV alignment of the doublets can be achieved by choosing the parities

$$P_1 = 1\ , \quad P_{2,3} = TST = TSTS^2 = S = \begin{pmatrix} 0 & 1 \\ 1 & 0 \end{pmatrix}\ , \tag{6.20}$$

which result in two possible VEV alignments,

$$\langle \varphi_{1,\pm 1} \rangle = (1, \pm 1)^T / \sqrt{2}\, \langle \tilde{\varphi}_{1,\pm 1} \rangle\ . \tag{6.21}$$

Note that the VEVs $(1,0)^T$ or $(0,1)^T$ cannot be achieved for the doublet in this basis of S_4.

Field	$SO(10)$	S_4	Z_N	Z_N	$\eta_I\eta_1$	$\eta_{PS}\eta_2$	$\eta_{GG}\eta_3$
ψ	$\underline{\mathbf{16}}$	$\underline{\mathbf{3_2}}$	0	0			
Ψ_u	$\underline{\mathbf{16}}$	$\underline{\mathbf{1_1}}$	0	1			
$\bar{\Psi}_u$	$\overline{\underline{\mathbf{16}}}$	$\underline{\mathbf{1_1}}$	0	-1			
Ψ_d	$\underline{\mathbf{16}}$	$\underline{\mathbf{1_1}}$	1	0			
$\bar{\Psi}_d$	$\overline{\underline{\mathbf{16}}}$	$\underline{\mathbf{1_1}}$	-1	0			
H_u	$\underline{\mathbf{10}}$	$\underline{\mathbf{1_1}}$	0	-2	$+$	$+$	$-$
H_d	$\underline{\mathbf{10}}$	$\underline{\mathbf{1_1}}$	-2	0	$+$	$+$	$+$
$\chi^u_{1,0,0}$	$\underline{\mathbf{1}}$	$\underline{\mathbf{3_2}}$	0	1	$+$	$-$	$-$
$\chi^d_{1,0,0}$	$\underline{\mathbf{1}}$	$\underline{\mathbf{3_2}}$	1	0	$+$	$-$	$-$
Φ	$\underline{\mathbf{45}}$	$\underline{\mathbf{1_1}}$	2	2	$+$	$+$	$+$
$\varphi_{1,1,1}$	$\underline{\mathbf{1}}$	$\underline{\mathbf{3_1}}$	0	2	$+$	$+$	$+$
$\varphi_{2,-1,-1}$	$\underline{\mathbf{1}}$	$\underline{\mathbf{3_1}}$	0	2	$+$	$-$	$+$
$\varphi_{0,1,-1}$	$\underline{\mathbf{1}}$	$\underline{\mathbf{3_1}}$	0	2	$+$	$+$	$-$
$\varphi_{1,1}$	$\underline{\mathbf{1}}$	$\underline{\mathbf{2}}$	0	2	$+$	$+$	$+$
$\varphi_{1,-1}$	$\underline{\mathbf{1}}$	$\underline{\mathbf{2}}$	0	2	$+$	$-$	$-$
$\bar{\Delta}_1$	$\overline{\underline{\mathbf{16}}}$	$\underline{\mathbf{1_1}}$	0	0	$+$	$-$	$-$
$\bar{\Delta}_2$	$\overline{\underline{\mathbf{16}}}$	$\underline{\mathbf{1_1}}$	2	2	$+$	$+$	$-$
$\phi_{1,1,1}$	$\underline{\mathbf{1}}$	$\underline{\mathbf{3_1}}$	-4	-4	$+$	$+$	$+$
ϕ_1	$\underline{\mathbf{1}}$	$\underline{\mathbf{1_1}}$	-4	-4	$+$	$+$	$+$

Table 6.4: Particle content of the model. Bulk fields are classified by three orbifold parities in addition to the symmetry groups.

6.3 Model: $SO(10) \times S_4$

In the following, we sketch a model that is based on the previous discussion. Besides the gauge field, we introduce a $\underline{\mathbf{16}}$ brane field ψ, which leads to the SM matter, the bulk Higgs fields $H_{u,d} \sim \underline{\mathbf{10}}$ generating fermion masses and breaking electroweak symmetry, the bulk Higgs fields $\bar{\Delta}_i \sim \overline{\underline{\mathbf{16}}}$ giving Majorana mass terms for neutrinos, and the bulk Higgs field $\Phi \sim \underline{\mathbf{45}}$ leading to the Georgi-Jarlskog factor [167]. Furthermore, there are heavy vector-like fermions $\Psi_{u,d} + \bar{\Psi}_{u,d}$ on the brane, and the flavon fields χ_i, φ_i, as well as ϕ_i in the bulk. We denote the flavon fields according to their VEV alignment, i.e., $\langle \phi_{x,y,z} \rangle \propto (x,\, y,\, z)^T$. The complete particle content is presented in Table 6.4. The transformation with respect to the orbifold parities determines the zero modes of the bulk fields. The leading order terms of the superpotential read

$$\mathrm{W_{LO}} = \sum_{i=u,d} y_i(\psi\chi^i_{1,0,0})\bar{\Psi}_i + y'_i\Psi_i H_i \Psi_i + M^i_\Psi \bar{\Psi}_i \Psi_i \,. \tag{6.22}$$

After the heavy vector-like fields are integrated out at the scale $M_\Psi^{u,d}$, they lead to the effective terms

$$\mathrm{W}_{\text{eff}} \supset \sum_{i=u,d} \frac{(y_i y_i')^2}{M_\Psi^{i2}} (\psi \chi^i_{1,0,0})(\psi \chi^i_{1,0,0}) H_i \ , \tag{6.23}$$

which will generate the third generation masses after the flavons obtain a VEV [152,205]. Besides the terms generating the third generation charged fermions masses, there are subleading terms from effective operators,

$$\mathrm{W}_{\text{NLO}} = \sum_{\varphi' s} \frac{y_i^u}{\Lambda} \varphi_i \psi H_u \psi + \sum_{\varphi' s} \frac{y_i^d}{\Lambda^2} \varphi_i \Phi \psi H_d \psi + \frac{y_{\chi^u}}{\Lambda^2} (\chi^u)^2 \psi H_u \psi + \frac{y_{\chi^d}}{\Lambda^2} (\chi^d)^2 \psi H_d \psi \ , \tag{6.24}$$

where Λ with $R^{-1} < \Lambda < M_{pl}$ [1] is the cutoff scale of this model. They contribute subdominantly to the mass matrices and lead to the masses of the first two generations as well as the mixing angles. The third term can be neglected, as its contribution to the up-type quark masses is subdominant to the first one. After exchanging the first and third generation, the charged fermion mass matrices are described by

$$M_u = m_t' \begin{pmatrix} A^u & C^u & D^u \\ . & B^u & E^u \\ . & . & 1 - 2\,C^u \end{pmatrix} , \tag{6.25a}$$

$$M_d = m_b' \begin{pmatrix} A^d & C^d - F^d & D^d \\ . & B^d & E^d \\ . & . & 1 - 2\,C^d + 2\,F^d \end{pmatrix} , \tag{6.25b}$$

$$M_l = m_b' \begin{pmatrix} 3\,A^d & 3\,C^d - F^d & 3\,D^d \\ . & 3\,B^d & 3\,E^d \\ . & . & 1 - 6\,C^d + 2\,F^d \end{pmatrix} , \tag{6.25c}$$

where $m_{t,b}' = y_{u,d}^2 y_{u,d}'^2 \left\langle \chi^{u,d}_{1,0,0} \right\rangle^2 \langle H_i \rangle \,/\, \left(M_\Psi^{u,d} \right)^2$. The coefficients $A^i, \ldots, F^i$ can be easily inferred from Eq.(6.24) by inserting the flavon VEVs. Note that the top mass m_t is approximately given by m_t' and the bottom mass by $m_b \approx m_b'$ as well as $m_\tau \approx m_b'$. In order to obtain the Georgi-Jarlskog relations [167] at the GUT scale, $m_e \simeq m_d/3$, $m_\mu \simeq 3$, $m_s, m_\tau \simeq m_b$, we assume that $A^i, C^i, D^i, E^i \ll F^d < B^i < 1$. Hence, the Cabibbo angle θ_c is approximately given by $\sin\theta_c = -F^d/B^d$.

Neutrino masses are generated by the terms

$$\mathrm{W}_\nu = \frac{y_R}{\Lambda} \psi \bar{\Delta}_1 \bar{\Delta}_1 \psi + \left(\frac{y^\nu_{1,1,1}}{\Lambda^2} \phi_{1,1,1} + \frac{y^\nu_1}{\Lambda^2} \phi_1 \right) \psi \bar{\Delta}_2 \bar{\Delta}_2 \psi \ . \tag{6.26}$$

The first term generates left-handed conjugate neutrinos masses, which contribute to the light neutrino mass matrix via the standard seesaw mechanism. However, this contribution can be neglected compared to the type II seesaw contribution from the remaining terms if $\Lambda \lesssim 3 m_1 M_{GUT}^2/m_t^2 \approx 10^{18} \left(m_1/(10^{-2}\text{eV}) \right) \text{GeV}$ coming from the bound on θ_{13}. In the following, we neglect the standard contribution. This can be also achieved by introducing

[1] The Planck mass is given by $M_{pl} \sim 1.2 \cdots 10^{19}$ GeV [46].

additional gauge singlets s transforming in the same way under $S_4 \times Z_N \times Z_N$ as $\bar{\Delta}_1\psi$, and by replacing the term $y_R\psi\bar{\Delta}_1\bar{\Delta}_1\psi/\Lambda$ with $y_s\psi\bar{\Delta}_1 s$. Hence, the left-handed conjugate neutrinos form pseudo-Dirac particles with s. The type II seesaw contribution is of the form of Eq.(6.14) with $m_0 = \left\langle\bar{\Delta}_2\right\rangle^2/\Lambda$ as well as $a = y^\nu_{1,1,1}\left\langle\phi_{1,1,1}\right\rangle/\Lambda$ and $b = y^\nu_1\left\langle\phi_1\right\rangle/\Lambda$. m_ν is diagonalized by the tri-bimaximal mixing matrix and the neutrino masses are given by $\left\langle\bar{\Delta}_2\right\rangle^2/\Lambda^2\,(3a+b, b, 3a-b)$. As the structure of the charged lepton matrix Eq.(6.25c) is connected to the down-type mass matrix M_d and the CKM mixing is mainly generated by M_d, there is a correction to the tri-bimaximal mixing matrix which results in a small deviation from tri-bimaximal mixing

$$s^2_{12} = \frac{1}{3} - \frac{2\lambda_c}{9} + \frac{\lambda_c^2}{54},\; s^2_{13} = \frac{\lambda_c^2}{18},\; s^2_{23} = \frac{1}{2} - \frac{\lambda_c^2}{36} \tag{6.27}$$

with $s^2_{ij} = \sin^2\theta_{ij}$ and λ_c being the Cabibbo angle. Depending on the absolute scale of the neutrino masses, the angles are further corrected by renormalization group evolution. However, we can neglect it in case of a hierarchical spectrum [206].
Finally, we have to show that all flavons can obtain a VEV. After introducing the charge conjugate field $\bar{\varphi}$ for each field φ, the resulting superpotential of the zero modes of the flavons is given by

$$\mathrm{W}_f = \sum_{\varphi\in\{\phi_i,\varphi_i,\chi_i\}} m_\varphi(\bar{\tilde{\varphi}}\tilde{\varphi}) \;+ \sum_{\varphi_{1,2}\in\{\phi_i,\varphi_i,\chi_i\}} \frac{\lambda_{\varphi_1\varphi_2}}{\Lambda}(\bar{\tilde{\varphi}}_1\tilde{\varphi}_1)(\bar{\tilde{\varphi}}_2\tilde{\varphi}_2)\,. \tag{6.28}$$

As it can be easily checked, there is a region of parameter space where all flavons obtain finite VEVs.

In this chapter, we have presented the idea of combining the breaking of a GUT by boundary conditions on an orbifold with the breaking of a flavor symmetry arising from the orbifold. All possible VEV alignments of the two- and three-dimensional representations of S_4 have been summarized in Table 6.3. Finally, we gave a simple example in the context of $SO(10) \times S_4$, which the smallness of neutrino masses is obtained by the type-II seesaw mechanism and the neutrino mixing is tri-bimaximal. Moreover, we have also shown that the model can fit the quark sector and charged lepton masses. We state that the VEV alignment mechanism can be also used for flavor symmetries arising from different orbifolds as well as for models with flavored Higgs fields. In conclusion, the flavored orbifold GUT is a simple and promising possibility to obtain the required fermion mass structures.

Chapter 7

Confronting Flavor Symmetries with Lepton Flavor Violation

In this chapter we study the difficulties arising when one tries to combine a model with an extended scalar sector with a discrete flavor symmetry. The key point is that there are actually strong constraints on models with extended scalar sectors. Since, however, the Yukawa sector of a theory is in most of the cases poorly known (meaning that there are a lot of free parameters), such a model can usually not be excluded easily, because of internal cancellations between several of the parameters that may cause some observables to nearly vanish. If, on the other hand, some additional structure is imposed on the model (by, e.g., a discrete flavor symmetry), then additional relations between some of the parameters can easily rule out the corresponding model or to at least restrict its parameters to very narrow ranges.

This chapter is organized as follows: In Section 7.1, we introduce the argumentation which lead us to our statement that models with extended scalar sectors may get into trouble by the introduction of an additional flavor symmetry. This is exemplified in Section 7.2, where we present two particular models for which our logic clearly works. The numerical results that we have obtained are presented and discussed in Section 7.3.

7.1 The General Arguments

A natural way to extend the SM is to add further scalar particles, which have not yet been discovered. These could, e.g., be additional $SU(2)$-singlets [207], doublets (Two Higgs doublet model, THDM), or triplets [208]. Depending on the model, it can then be the case that more than one Higgs field contribute to the masses of all particles, or that certain Higgses only give masses to a particular choice of particles [209]. These models will then, however, generically lead to FCNCs [210] and hence to lepton flavor violation (LFV) [211], which are quite strongly constrained [212]. It is, however, also not easy to rule them out that way, since they will in general yield complex 3×3 Yukawa coupling matrices, which hold a lot of freedom in their 18 parameters. So, in most of the cases, such a model will be able to fit all neutrino data without any problems, even if it is strongly constrained.

On the other hand, as it has been discussed in the former chapters, imposing a non-abelian discrete flavor symmetry on the SM leads to more structure in the Yukawa coupling matrices in the sense that we obtain relations between different entries of the Yukawa matrices. From

this, we can obtain the neutrino oscillation parameters as well as the charged lepton masses as functions of only a few parameters, which can then be checked on whether they are in accordance with data, or not. We note that we assume that the flavor symmetry is broken at a high energy scale, so the flavons are decoupled from the model at low energy.

We now apply the following logic:

1. We impose a flavor symmetry and decouple the flavons in order to end up with an effective low energy model with a scalar sector that is slightly extended compared to the SM. This could, e.g., be a THDM or something similar.

2. Since we have gained predictivity by imposing the flavor symmetry, we can fit the model to neutrino data, which allows us to extract certain ranges for the model parameters.

3. The model has additional scalars compared to the SM, which will be able to mediate LFV-processes, whose branching ratios can be predicted using the fitted parameter values.

4. If this prediction does not fit with present (future) LFV-bounds, we are (will be) able to exclude the particular flavor symmetry imposed (in a certain scenario). Note that this logic will also hold in the non-decoupling case if no extreme fine-tuning is involved.

In principle, this could work for any model with a slightly extended scalar sector. If the structure of the model is not extremely peculiar, which is rarely the case in the scalar sector of a theory, the additional scalars (compared to the SM) will unavoidably lead to LFV-processes, which are already strongly constrained. The key point is that these constraints are so strong, that imposing some more structure by adding a flavor symmetry can easily destroy the consistency of the model with all data.

Here, we want to present such an analysis for one particular example, namely for Ma's scotogenic model [6], as this consists of a very minimal extension of the SM. Furthermore, it does not have too many possible LFV-diagrams, so that our logic is not shadowed by a heavy calculational apparatus. In this model, one can see immediately the effect of certain symmetries: Without imposing a flavor symmetry, one constrains quantities like

$$|h^*_{11}h_{21} + h^*_{12}h_{22} + h^*_{13}h_{23}| \tag{7.1}$$

by LFV-processes like $\mu \to e\gamma$ [213], where h is the Yukawa coupling matrix involved. Such a combination can easily become zero for unfortunate values of some phases, exactly as the effective neutrino mass in neutrino-less double beta processes [214]. Imposing relations between certain elements of h hinders such cancellations to appear, and the term in Eq.(7.1) will generically be much larger than zero.

We want to stress, however, that this particular model is just an example and that our approach works for a much wider class of models.

7.2 Constraining Particular Models

7.2.1 One Possible Example: The Scotogenic Model

There are a lot of different models for neutrino mass generation on the market [7]. A difficult task for all of them is to explain the smallness of neutrino masses compared to other particles we know in Nature.

One way is to forbid a tree-level mass term for neutrinos and generate neutrino masses only by radiative corrections, as done in several models [6–11]. Out of those, Ma's "scotogenic" model [6] (that we call "Ma-model" for simplicity) is particularly attractive: By adding only one additional Higgs doublet and 3 heavy left-handed conjugate neutrinos to the SM, as well as imposing an additional Z_2-symmetry, it allows for sufficiently small neutrino masses. These masses are generated radiatively, because the additional neutral Higgs does not obtain a VEV that could lead to a tree-level neutrino mass term. Furthermore, due to the Z_2-symmetry, this model also provides a stable dark matter candidate, namely the lightest of the heavy neutrinos [215] or the lightest neutral scalar [216]. Constraints on the model arise from various different sources as, e.g., lepton flavor violation or the dark matter abundance [213]. In that sense, this model is very "complete".

The basic ingredients apart from the SM are:

- 3 heavy left-handed conjugate (Majorana) neutrinos N_k, which are singlets under $SU(2)$ and have no hypercharge
- a second Higgs doublet η with SM-like quantum numbers that does not obtain a VEV
- an additional Z_2-parity under which all SM-particles are even, while N_k as well as η are odd

The corresponding Higgs potential looks like

$$V = m_1^2\phi^\dagger\phi + m_2^2\eta^\dagger\eta + \frac{\lambda_1}{2}(\phi^\dagger\phi)^2 + \frac{\lambda_2}{2}(\eta^\dagger\eta)^2 + \lambda_3(\phi^\dagger\phi)(\eta^\dagger\eta) + \lambda_4(\phi^\dagger\eta)(\eta^\dagger\phi) + \frac{\lambda_5}{2}\left[(\phi^\dagger\eta)^2 + h.c.\right], \tag{7.2}$$

where ϕ is the SM-Higgs. If $m_1^2 < 0$ and $m_2^2 > 0$, then only ϕ^0 will obtain a VEV $v = 174$ GeV, while $\langle\eta^0\rangle = 0$. Then, the Yukawa Lagrangian is given by

$$\mathcal{L}_Y = f_{ij}(\phi^-\nu_i + (\phi^0)^* l_i)e_j^c + h_{ij}(\eta^0\nu_i - \eta^+ l_i)N_j + h.c., \tag{7.3}$$

which does not lead to a tree-level neutrino mass term due to the vanishing VEV of η^0. The neutrino masses can, however, be generated radiatively, which gives a natural suppression of the neutrino mass eigenvalues and can exploit the heaviness of the N_k (with masses M_k) as well. The mass matrix of the light neutrinos reads

$$(M_\nu)_{ij} = \sum_{k=1}^{3} h_{ik}h_{jk}\Lambda_k, \tag{7.4}$$

where

$$\Lambda_k = \frac{M_k}{16\pi^2}\left[\frac{m^2(H^0)}{m^2(H^0) - M_K^2}\ln\left(\frac{m^2(H^0)}{M_K^2}\right) - \frac{m^2(A^0)}{m^2(A^0) - M_K^2}\ln\left(\frac{m^2(A^0)}{M_K^2}\right)\right]. \tag{7.5}$$

Note that we have named the Higgses like in the general THDM, with $\alpha = \beta = m_{12} = \lambda_{6,7} = 0$ [217]. The resulting Higgs masses are given by

$$m^2(h^0) = 2\lambda_1 v^2,\ m^2(H^0) = m_2^2 + (\lambda_3 + \lambda_4 + \lambda_5)v^2,\ m^2(A^0) = m_2^2 + (\lambda_3 + \lambda_4 - \lambda_5)v^2,$$
$$\text{and } m^2(H^\pm) = m_2^2 + \lambda_3 v^2. \tag{7.6}$$

Field	$l_{1,2,3}$	e_1^c	e_2^c	e_3^c	$N_{1,2,3}$	ϕ	η	φ_S	φ_T	χ
A_4	$\underline{\mathbf{3}}$	$\underline{\mathbf{1}}$	$\underline{\mathbf{1}}''$	$\underline{\mathbf{1}}'$	$\underline{\mathbf{3}}$	$\underline{\mathbf{1}}$	$\underline{\mathbf{1}}$	$\underline{\mathbf{3}}$	$\underline{\mathbf{3}}$	$\underline{\mathbf{1}}$
Z_4	i	i	i	i	-1	1	1	i	-1	i

Table 7.1: The particle content of model 1: The SM particles are the three left-handed lepton $SU(2)_L$ doublets l_i, the left-handed conjugate charged leptons e_i^c, and the SM-Higgs ϕ. The BSM particles are the left-handed conjugate neutrinos N_i, the second Higgs doublet η (which does not obtain a VEV), and the flavons φ_S, φ_T, and χ, that only transform under $A_4 \times Z_4$.

7.2.2 The Flavor Symmetries Considered

In the following, we will present two models which constrain the structure of the Yukawa coupling matrix h in Eq.(7.3), without discussing a particular mechanism for vacuum alignment. [1] The first one, based on [119], represents the class of models which predicts tri-bimaximal mixing. The second one represents the class which predicts $\mu - \tau$ symmetry.

The A_4-Model (Model 1)

The particle content of this model is given in Table 7.1. We note that the group theory of A_4 can be found in Appendix A.3. The Lagrangian which is invariant under the flavor symmetry $A_4 \times Z_4$ reads[2]

$$\begin{aligned}\mathcal{L}_l &= y_1^e \frac{\phi}{\Lambda}(l_1\varphi_{T1} + l_2\varphi_{T3} + l_3\varphi_{T2})e_1^c + y_2^e \frac{\phi}{\Lambda}(l_3\varphi_{T3} + l_1\varphi_{T2} + l_2\varphi_{T1})e_2^c \\ &+ y_3^e \frac{\phi}{\Lambda}(l_2\varphi_{T2} + l_1\varphi_{T3} + l_3\varphi_{T1})e_1^c + \frac{\eta}{\Lambda}\Big[y_1[(2l_1N_1 - l_2N_3 - l_3N_2)\varphi_{S1} \\ &+ (2l_3N_3 - l_1N_2 - l_2N_1)\varphi_{S3} + (2l_2N_2 - l_1N_3 - l_3N_1)\varphi_{S2}] \\ &+ y_2(l_1N_1 + l_2N_3 + l_3N_2)\chi\Big] + M(N_1N_1 + N_2N_3 + N_3N_2). \end{aligned} \tag{7.7}$$

Let us assume that the flavons obtain their VEVs as follows,

$$\begin{pmatrix} \langle\varphi_{S1}\rangle \\ \langle\varphi_{S2}\rangle \\ \langle\varphi_{S3}\rangle \end{pmatrix} = w_S \begin{pmatrix} 1 \\ 1 \\ 1 \end{pmatrix}, \quad \begin{pmatrix} \langle\varphi_{T1}\rangle \\ \langle\varphi_{T2}\rangle \\ \langle\varphi_{T3}\rangle \end{pmatrix} = w_T \begin{pmatrix} 1 \\ 0 \\ 0 \end{pmatrix}, \quad \text{and} \quad \langle\chi\rangle = u\,, \tag{7.8}$$

and the SM Higgs gets the VEV $\langle\phi\rangle = v$. Then, the Yukawa coupling matrix and the left-handed conjugate neutrino mass matrix for model 1 can be written as

$$h = \begin{pmatrix} 2a+b & -a & -a \\ -a & 2a & b-a \\ -a & b-a & 2a \end{pmatrix}, \text{and} \quad M_R = M \begin{pmatrix} 1 & 0 & 0 \\ 0 & 0 & 1 \\ 0 & 1 & 0 \end{pmatrix}, \tag{7.9}$$

[1] In general, the vacuum alignment can be achieved by a minimization of the scalar potential.

[2] Here, we neglect the anti-symmetric part of the coupling between l and N, or assume that the anti-symmetric coupling vanishes, which is done similarly in [119, 218].

where $a = y_1 \frac{w_S}{\Lambda}$ and $b = y_2 \frac{u}{\Lambda}$.
The charged lepton mass matrix in this model is diagonal,

$$m_e = \frac{v}{\Lambda} y_1^e w_T,\ m_\mu = \frac{v}{\Lambda} y_2^e w_T,\ m_\tau = \frac{v}{\Lambda} y_3^e w_T. \tag{7.10}$$

Here, the hierarchies in the charged lepton masses are determined by the Yukawa couplings. Assuming that the Yukawa coupling of the τ, y_3^e, is of $\mathcal{O}(1)$ and the Higgs VEV v is 174 GeV, we can determine the ratio of the flavon over the cutoff scale Λ ($\frac{\langle f \rangle}{\Lambda}$) as being of the order of the Cabibbo angle squared, $\lambda^2 \sim 0.04$.

In order to make the discussion easier, we go to the basis where the left-handed conjugate neutrino mass matrix is diagonal. The matrix $M_R M_R^\dagger$ is diagonalized by the unitary matrix U_r,

$$U_r = \begin{pmatrix} 0 & 0 & 1 \\ 0 & 1 & 0 \\ 1 & 0 & 0 \end{pmatrix}. \tag{7.11}$$

Note that the left-handed conjugate neutrino masses are degenerate, $M_{1,2,3} = M$.
The Yukawa coupling in this basis reads

$$h' = h U_r = \begin{pmatrix} -a & -a & 2a+b \\ b-a & 2a & -a \\ 2a & b-a & -a \end{pmatrix}. \tag{7.12}$$

Using Eq.(7.4), the neutrino mass matrix can be written as

$$M_\nu = \Lambda_{1,2,3} \begin{pmatrix} (6a^2+4ab+b^2) & -a(3a+2b) & -a(3a+2b) \\ -a(3a+2b) & (6a^2-2ab+b^2) & a(-3a+4b) \\ -a(3a+2b) & a(-3a+4b) & (6a^2-2ab+b^2) \end{pmatrix}, \tag{7.13}$$

where $\Lambda_{1,2,3} = \Lambda_1 = \Lambda_2 = \Lambda_3$, and the neutrino masses are given by the eigenvalues of $M_\nu M_\nu^\dagger$:

$$m_1^2 = (3a+b)^4 \Lambda_{1,2,3}^2,\ \ m_2^2 = b^4 \Lambda_{1,2,3}^2,\ \text{ and } m_3^2 = (-3a+b)^4 \Lambda_{1,2,3}^2, \tag{7.14}$$

which correspond to the eigenvectors $(-2,1,1)^T/\sqrt{6}$, $(1,1,1)^T/\sqrt{3}$, and $(0,-1,1)^T/\sqrt{2}$, respectively. In this model, the neutrino masses obey normal mass ordering.

The neutrino mixing observables look like:

$$\Delta m_\odot^2 = (b^4 - (3a+b)^4)\Lambda_{1,2,3}^2,\ \Delta m_A^2 = -24ab(9a^2+b^2)\Lambda_{1,2,3}^2,\ \tan\theta_{12} = \frac{1}{\sqrt{2}},\ \theta_{13} = 0,\ \text{and } \theta_{23} = \frac{\pi}{4}. \tag{7.15}$$

In this model, we have only three free parameters (a, b, M) to fit all observables. Therefore, this model is quite predictive (and hence harder to fit).

The D_4-Model (Model 2)

The particle content of this model is given in Table 7.2. We note that the group theory of A_4 can be found in Section 3.1.1. The Lagrangian which is invariant under the flavor symmetry

Field	l_1	$l_{2,3}$	e_1^c	$e_{2,3}^c$	N_1	N_2	N_3	ϕ	η	φ_e	χ_e	φ_ν	$\psi_{1,2}$
D_4	$\underline{\mathbf{1_1}}$	$\underline{\mathbf{2}}$	$\underline{\mathbf{1_3}}$	$\underline{\mathbf{2}}$	$\underline{\mathbf{1_3}}$	$\underline{\mathbf{1_2}}$	$\underline{\mathbf{1_4}}$	$\underline{\mathbf{1_1}}$	$\underline{\mathbf{1_1}}$	$\underline{\mathbf{1_3}}$	$\underline{\mathbf{1_4}}$	$\underline{\mathbf{1_3}}$	$\underline{\mathbf{2}}$
Z_2	1	1	1	1	-1	-1	-1	1	1	1	1	-1	-1

Table 7.2: The particle content of model 2: Th SM particles are the three left-handed lepton $SU(2)_L$ doublets l_i, the left-handed conjugate charged leptons e_i^c, and the SM-Higgs ϕ. The BSM particles are the left-handed conjugate neutrinos N_i, second Higgs doublet η (which does not obtain a VEV),and the flavons φ_e, χ_e, φ_ν, and ψ_i, that only transform under $D_4 \times Z_2$.

$D_4 \times Z_2$ reads

$$\begin{aligned}\mathcal{L}_l &= y_1^e l_1 e_1^c \frac{\phi}{\Lambda}\varphi_e + y_2^e(l_2 e_2^c + l_3 e_3^c)\frac{\phi}{\Lambda}\varphi_e + y_3^e(l_2 e_2^c - l_3 e_3^c)\frac{\phi}{\Lambda}\chi_e \\ &+ y_1 l_1 N_1 \frac{\eta}{\Lambda}\varphi_\nu + y_2(l_2\psi_1 + l_3\psi_2)N_1\frac{\eta}{\Lambda} + y_3(l_2\psi_2 - l_3\psi_1)N_2\frac{\eta}{\Lambda} + y_4(l_2\psi_1 - l_3\psi_2)N_3\frac{\eta}{\Lambda} \\ &+ \frac{1}{2}M_1 N_1 N_1 + \frac{1}{2}M_2 N_2 N_2 + \frac{1}{2}M_3 N_3 N_3. \end{aligned} \tag{7.16}$$

Let us assume that the flavons obtain their VEVs as follows:

$$\langle\varphi_e\rangle = u_e,\ \ \langle\chi_e\rangle = -w_e,\ \ \langle\varphi_\nu\rangle = u\ ,\ \text{ and }\ \begin{pmatrix}\langle\psi_1\rangle\\ \langle\psi_2\rangle\end{pmatrix} = w\begin{pmatrix}1\\ -1\end{pmatrix}, \tag{7.17}$$

and the SM Higgs gets the VEV $\langle\phi\rangle = v$. Then, the Yukawa coupling matrix for model 2 can be written as

$$h = \begin{pmatrix} a & 0 & 0\\ b & -c & d\\ -b & -c & d\end{pmatrix}, \tag{7.18}$$

where $a = y_1\frac{u}{\Lambda}$, $b = y_2\frac{w}{\Lambda}$, $c = y_3\frac{w}{\Lambda}$, and $d = y_4\frac{w}{\Lambda}$.

The charged lepton and left-handed conjugate neutrino mass matrices in this model are diagonal,

$$m_e = \frac{v}{\Lambda}y_1^e u_e,\ m_\mu = \frac{v}{\Lambda}(y_2^e u_e - y_3^e w_e),\ m_\tau = \frac{v}{\Lambda}(y_2^e u_e + y_3^e w_e). \tag{7.19}$$

Here, the hierarchy between the masses of e and (μ,τ) arises from the smallness of the Yukawa coupling y_1^e. As we did for model 1, we assume that the ratio $(\frac{\langle f\rangle}{\Lambda})$ is of order $\lambda^2 \sim 0.04$.

Using Eq.(7.4), the neutrino mass matrix can be written as

$$M_\nu = \begin{pmatrix} a^2\Lambda_1 & ab\Lambda_1 & -ab\Lambda_1\\ ab\Lambda_1 & b^2\Lambda_1 + c^2\Lambda_2 + d^2\Lambda_3 & -b^2\Lambda_1 + c^2\Lambda_2 + d^2\Lambda_3\\ -ab\Lambda_1 & -b^2\Lambda_1 + c^2\Lambda_2 + d^2\Lambda_3 & b^2\Lambda_1 + c^2\Lambda_2 + d^2\Lambda_3\end{pmatrix}. \tag{7.20}$$

The neutrino masses are given by the eigenvalues of $M_\nu M_\nu^\dagger$,

$$m_1^2 = 0,\ \ m_2^2 = (a^2 + 2b^2)^2\Lambda_1^2,\ \text{ and } m_3^2 = 4(c^2\Lambda_2 + d^2\Lambda_3)^2, \tag{7.21}$$

Scenario	$m(h^0)$	$m(H^0)$	$m(A^0)$	$m(H^\pm)$
α	120.0	32.9	84.5	93.0
β	120.0	60.4	101.5	111.5
γ	120.0	946.8	950.0	950.3
δ	120.0	548.9	549.4	550.6

Table 7.3: The Higgs masses (in GeV) for the different scenarios defined in Eq.(7.27).

Quantity	$\Delta m^2_\odot$	$(\Delta m^2_A)_{\text{nor.}}$	θ_{12}	θ_{13}	θ_{23}
Best-fit	$7.67 \cdot 10^{-5}$ eV^2	$2.46 \cdot 10^{-3}$ eV^2	$34.5°$	$0.0°$	$42.3°$
1σ	$2.15 \cdot 10^{-6}$ eV^2	$0.15 \cdot 10^{-3}$ eV^2	$1.4°$	$7.9°$	$4.2°$

Table 7.4: The neutrino mixing parameters (best-fit values and symmetrized 1σ-ranges) obtained by a global fit [219].

which correspond to the eigenvectors

$$\frac{a}{\sqrt{2(a^2+2b^2)}}(2b/a,-1,1)^T,\ \frac{b}{\sqrt{2(a^2+2b^2)}}(-b/a,1,1)^T,\ \text{and}\ (0,1,1)^T/\sqrt{2}, \tag{7.22}$$

respectively.
In this model, the neutrino masses will obey normal ordering. The neutrino mixing observables look like:

$$\Delta m^2_\odot = (a^2+2b^2)^2\Lambda_1^2,\ \Delta m^2_A = 4(c^2\Lambda_2 + d^2\Lambda_3)^2,\ \tan\theta_{12} = \frac{a}{\sqrt{2}b},\ \theta_{13}=0,\ \text{and}\ \theta_{23}=\frac{\pi}{4}. \tag{7.23}$$

In this model, we have 7 free parameters $(a, b, c, d, M_1, M_2, M_3)$ to fit all neutrino observables. This makes model 2 much easier to fit, but we of course pay the price of losing predictivity.

7.2.3 Phenomenological Analysis

The General Procedure

In this section, we describe the analysis procedure we have applied. The first thing to say is that there are constraints that are required for a THDM like in Eq.(7.2) ($\lambda_1 > 0$, $\lambda_2 > 0$, $\lambda_3 > -\sqrt{\lambda_1\lambda_2}$, and $\lambda_3 + \lambda_4 - |\lambda_5| > -\sqrt{\lambda_1\lambda_2}$; they keep the potential stable) as well as consistency conditions for a Ma-like model ($m_1^2 < 0$ and $m_2^2 > 0$; these are necessary in order for ϕ^0 to obtain a VEV, while η^0 obtains none). Furthermore, there are limits from direct searches at collider experiments [220]: $m(h^0) > 112.9$ GeV and $m(H^\pm) > 78.6$ GeV, both at 95% confidence level.[3] Further constraints arise from the W- and Z-boson decay widths, namely $m(H^\pm)+m(H^0), m(H^\pm)+m(A^0) > M_W$ and $2m(H^\pm), m(H^0)+m(A^0) > M_Z$, as well as from the requirement of perturbativity for the Higgs potential, $\lambda_2 < 1$ and $\lambda_3^2 + (\lambda_3+\lambda_4)^2 + \lambda_5^2 < 12\lambda_1^2$ [216].

[3]Note that these constraints do not apply to the "inert" Higgses H^0 and A^0. They are constrained much less severely by the current limits, differently from a normal THDM.

Strong constraints also come from the correction to the ρ-parameter [221]. The explicit formula for this correction reads

$$\Delta\rho = \frac{\alpha(M_Z)}{16\pi s_W^2 M_W^2} \cdot \left[F(m_2^2, m^2(H^0)) + F(m_2^2, m^2(A^0)) - F(m^2(H^0), m^2(A^0))\right], \tag{7.24}$$

where

$$F(x,y) = \begin{cases} \frac{x+y}{2} - \frac{xy}{x-y}\ln\frac{x}{y}, & \text{for } x \neq y, \\ 0, & \text{for } x = y, \end{cases} \tag{7.25}$$

and $\alpha(M_Z) = 1/127.9$. The experimental constraint is [46]

$$\Delta\rho = -0.0006 \pm 0.0008, \tag{7.26}$$

which cuts the allowed parameter space for the Ma-model. Since we want to focus on neutrino physics and lepton flavor violation, we do not try to fit the Higgs sector as well, but rather use four different benchmark scenarios that all fulfill the consistency conditions, as well as the experimental bounds from direct searches and from the measurement of the correction to the ρ-parameter (at 3σ). In the form $(m_1, m_2, \lambda_1, \lambda_2, \lambda_3, \lambda_4, \lambda_5)$, these scenarios are:

$$\begin{aligned} \alpha: &\quad (100i\text{GeV}, 75\text{GeV}, 0.24, 0.10, 0.10, -0.15, -0.10), \\ \beta: &\quad (100i\text{GeV}, 98.5\text{GeV}, 0.24, 0.30, 0.09, -0.18, -0.11), \\ \gamma: &\quad (100i\text{GeV}, 950\text{GeV}, 0.24, 0.50, 0.02, -0.12, -0.10), \\ \delta: &\quad (100i\text{GeV}, 550\text{GeV}, 0.24, 0.30, 0.02, -0.05, -0.01). \end{aligned} \tag{7.27}$$

The corresponding Higgs masses are given in Table 7.3. We have chosen these four scenarios such that they are also consistent with the 3σ-range of WMAP-data for H^0 being the dark matter candidate, which cuts the allowed parameter space significantly [216]. This leads to some more consistency conditions, as H^0 has to be the lightest of all scalars and it also has to be lighter than the heavy left-handed conjugate neutrinos.

For all these scenarios, we do the following:

1. First, the models are fitted to neutrino oscillation data, i.e., mixing angles and mass square differences [219]. This is done by the χ^2-function

$$\chi^2 = \sum_{i=1}^{N} \frac{(q_i - q_i^{\text{exp}})^2}{\sigma_i^2}, \tag{7.28}$$

   where q_i are the observables obtained from neutrino oscillations (θ_{12}, θ_{13}, θ_{23}, Δm_A^2, $\Delta m_\odot^2$), which are calculated in terms of the model parameters (see Section 7.2.2). q_i^{exp} are their measured counterparts and σ_i are the corresponding (symmetrized) standard deviations. The best-fit model parameters are determined by a minimization of the χ^2-function. By projection on the different directions in the parameter space, we determine the 1σ- and 3σ-ranges of the model parameters.

2. Next, we calculate the maximum and minimum values of the quantities measured in different LFV-experiments ($\mu \to e\gamma$, $\tau \to \mu\gamma$, $\tau \to e\gamma$, and μ-e conversion for four different nuclei) by varying the model parameters within their 1σ- and 3σ-ranges.

3. Finally, we compare how well different past and future LFV-experiments are able to constrain or exclude the particular model in the four scenarios.

The χ^2-Fit

After outlining the general points, we will explain the procedure in more detail using scenario α (see Eq.(7.27)) in connection with model 1 (see Section 7.2.2) as example.

The χ^2-function has already been given in Eq.(7.28) and the experimental values and errors of the neutrino observables are summarized in Table 7.4. These observables in terms of model parameters have been given in Eq.(7.15). The minimization of the χ^2-function then yields the following best-fit values for the three parameters:

$$a = 0.0189,\ b = -0.691,\ M = 2.42 \cdot 10^6 \text{ GeV}. \tag{7.29}$$

Note that the parameter b is negative to fit the normal mass ordering, see Eq.(7.15). In the minimization we have required $M_{1,2,3} > m(H^0)$ and $M_{1,2,3} > M_Z/2$ for consistency reasons.

The 1σ-(3σ-) values for the model parameters are obtained by inserting all values from Eq.(7.29) into the χ^2-function, except for the one parameter that is to be constrained, and by determining the intersections of the remaining 1-dimensional function $\Delta\chi^2 \equiv \chi^2 - \chi^2_{\text{min}}$ with 1(9). For the above parameters, this yields in the form $^{+1\sigma,+3\sigma}_{-1\sigma,-3\sigma}$:

$$\begin{aligned} a: &\quad {}^{+0.0003,+0.0009}_{-0.0003,-0.0009}, \\ b: &\quad {}^{+0.003,+0.009}_{-0.003,-0.009}, \\ M: &\quad {}^{+0.02,+0.05}_{-0.02,-0.05} \cdot 10^6 \text{ GeV}. \end{aligned} \tag{7.30}$$

These are the ranges that we will use in the subsequent analysis. Note that in this model, they are already quite narrow, which is a manifestation of the fact that this model holds a lot of structure.

Predictions for Various LFV-Experiments

The most important types of LFV-experiments are rare lepton decays, $e_i \to e_j\gamma$, as well as conversions of a bound muon to an electron for some nucleus N, $\mu N \to eN$. In a Ma-like model, the decisive quantities for both types of processes are [222] ($ij = e_i \to e_j\gamma/e_i$-$e_j$-conversion):

$$\sigma_{ij} \equiv \frac{-i}{2m^2(H^\pm)} \sum_{k=1}^{3} h^*_{jk} h_{ik} \left[(m_i + m_j) I_a\left(\frac{M_k^2}{m^2(H^\pm)}\right) + M_k I_b\left(\frac{M_k^2}{m^2(H^\pm)}\right)\right], \tag{7.31}$$

where

$$I_a(t) = \frac{1}{16\pi^2}\left[\frac{2t^2+5t-1}{12(t-1)^3} - \frac{t^2 \ln t}{2(t-1)^4}\right] \text{ and } I_b(t) = \frac{1}{16\pi^2}\left[\frac{t+1}{2(t-1)^2} - \frac{t\ln t}{(t-1)^3}\right]. \tag{7.32}$$

Using these, the branching ratios for the processes are given by

$$\text{Br}(e_i \to e_j\gamma) = \frac{m_i^3}{8\pi} \frac{|\sigma_{ij}|^2}{\Gamma(e_i \to e_j \nu_i \overline{\nu}_j)} \text{ and } \text{Br}(\mu N \to eN) = \frac{\pi^2}{2^5 m_\mu^2} \frac{D_N^2}{\omega_{\text{capt}}(N)} |\sigma_{\mu e}|^2. \tag{7.33}$$

In the first formula, we have neglected the final state lepton mass. The quantities D_N and $\omega_{\text{capt}}(N)$, as well as a general expression for the second formula are given in [223].

Experiment	Status	Process	BR-Limit/Sensitivity
MEGA	Past	$\mu \to e\gamma$	$1.2 \cdot 10^{-11}$
MEG	Future	$\mu \to e\gamma$	$1.0 \cdot 10^{-13}$
BELLE	Past	$\tau \to \mu\gamma$	$4.5 \cdot 10^{-8}$
Babar	Past	$\tau \to e\gamma$	$1.1 \cdot 10^{-7}$
MECO	Cancelled	$\mu\mathrm{Al} \to e\mathrm{Al}$	$2.0 \cdot 10^{-17}$
SINDRUM II	Past	$\mu\mathrm{Ti} \to e\mathrm{Ti}$	$6.1 \cdot 10^{-13}$
PRISM/PRIME	Future	$\mu\mathrm{Ti} \to e\mathrm{Ti}$	$5.0 \cdot 10^{-19}$
SINDRUM II	Past	$\mu\mathrm{Au} \to e\mathrm{Au}$	$7.0 \cdot 10^{-13}$
SINDRUM II	Past	$\mu\mathrm{Pb} \to e\mathrm{Pb}$	$4.6 \cdot 10^{-11}$

Table 7.5: Limits on the branching ratios for several past and future LFV-experiments [212].

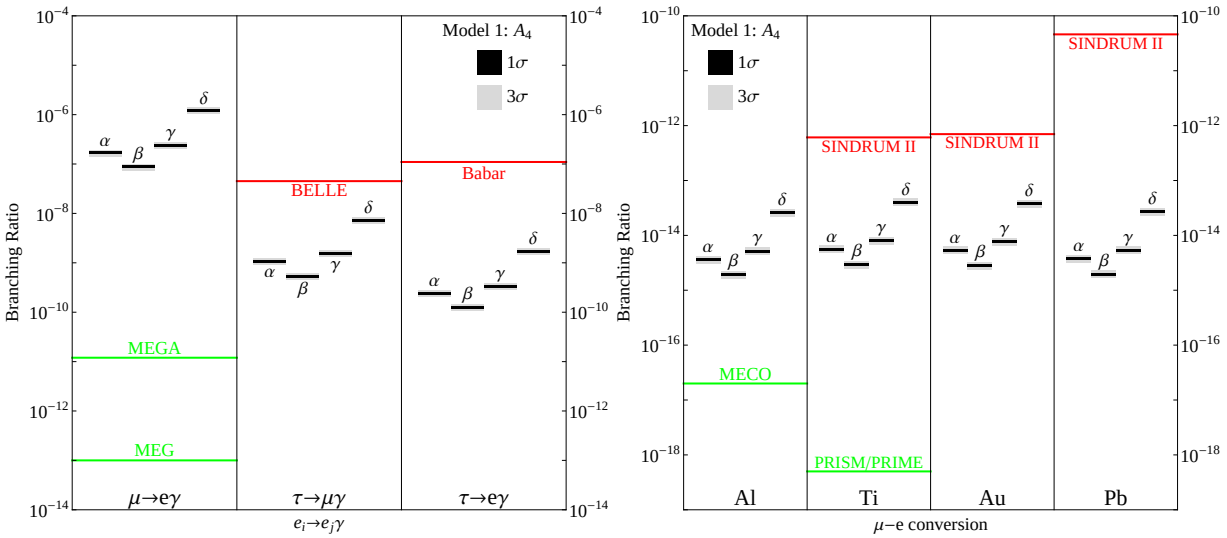

Figure 7.1: The numerical results of our analysis for model 1.

Past and Future LFV-Experiments for Model 1

We then use the parameter ranges from Eq.(7.30) to make predictions with Eq.(7.33). The result is included in Figure 7.1. Furthermore, we have put in the limits/sensitivities of several past/future experiments, all listed in Table 7.5. A further discussion of the results will be given in the next section.

7.3 Results

We will now discuss how the general conflict between an extended scalar sector and flavor symmetries looks in our example models. Let us first start with model 1. The numerical results can be seen in Figure 7.1: On the left panel, we present the 1σ (black) and 3σ (gray) predictions of model 1 for the processes $\mu \to e\gamma$, $\tau \to \mu\gamma$, and $\tau \to e\gamma$, as well as different present and future bounds from several experiments, see Table 7.5. The right panel shows

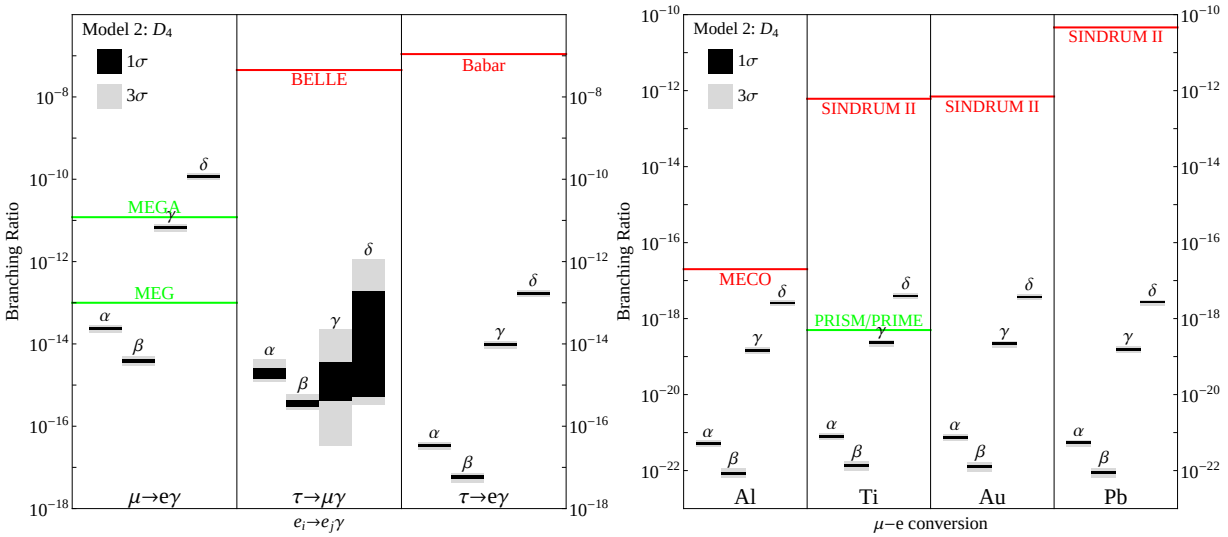

Figure 7.2: The numerical results of our analysis for model 2.

the same for μ-e conversion on the elements Al, Ti, Au, and Pb.

Model 1 is the prime example that our logic works: As explained in Section 7.2.2, there are only 3 free parameters in the model. Still, it is able to fit the neutrino data well. Actually, the only deviations from a perfect fit arise from the very accurate prediction of the mixing angles (e.g., the experimental best-fit value of θ_{23} is not exactly maximal; see Eq.(7.15) and Table 7.4). The obtained parameter ranges are, however, quite narrow, as can be seen from the example given in Section 7.2.3. This is exactly the point, where the experimental limits on LFV-processes get really powerful: Because of the stiffness in the model parameter space, the prediction of, e.g., the branching ratio $\mu \to e\gamma$ is so clear, that only a very narrow window is left for parameter variations. Accordingly, this model is actually already excluded by the past MEGA experiment (see Figure 7.1) for all four Higgs scenarios from Eq.(7.27). We want to stress again, that these four scenarios belong to the few regions in parameter space that are indeed consistent with all the data and constraints mentioned in Section 7.2.3. The branching ratios for μ-e conversion are in general lower, and pass all current constraints. However, in this sector PRISM/PRIME will provide another future bound that will be able to exclude this model.

The remaining questions is how far we can stretch this logic for models with less and less predictivity. As example for that case we can use model 2, which has seven free parameters to fit the data (see Section 7.2.2). This more than doubles the degrees of freedom in the fit.

The numerical results for this model are given in Figure 7.2. First of all, it may look odd that here, all 1σ and 3σ regions are somehow narrow, except for $\tau \to \mu\gamma$. This is simply because all branching ratios are essentially functions of the product $|ab|$ (where a and b are model parameters), while the one for $\tau \to \mu\gamma$ is given by the sum of three contributions, which are proportional to $|b|^2$, $|c|^2$, and $|d|^2$, respectively. This numerical example nicely shows how more freedom blows up the regions which are predicted by a certain model. Turning this argumentation around, a certain limit on some observable will be weaker the more free parameters there are that influence the observable in question.

However, even this model with much less predictivity than the one before can be excluded

for some scenarios: Scenario δ has already been excluded by the MEGA-experiment and scenario γ can be tested by MEG. This shows the strength of our considerations: Even for a model that has a lot of freedom our logic still applies in suitable settings, which are here given by the scenarios γ and δ. Actually, even the scenarios α and β are not that far below the future MEG-bound, and especially a hypothetical future experiment aiming at $\tau \to \mu\gamma$ might be very suitable to exclude this particular model.

In this chapter we have studied the conflict arising in models with an extended scalar sector and discrete flavor symmetries when confronted with LFV-bounds. We have illustrated this using two examples based on the Ma-model, one with an A_4 and one with a D_4 symmetry. Since the first model exhibits a relatively rigid structure (only three free parameters), it is already excluded for all four scenarios by existing bounds. Even though the second model has more than twice as many free parameters, it can still be strongly constrained and two of the scenarios can either be excluded or tested in the near future. We want to stress, however, that our considerations are not at all restricted to Ma-like models, but should apply to a much wider class of theories. Models with a lot of structure (meaning few parameters) may easily be excluded by existing or future LFV-bounds although they have no problems without the flavor symmetry. Even models with many parameters can at least be strongly constrained, if not excluded as well.

Chapter 8

Radiative Transmission of Lepton Flavor Hierarchies

In this chapter, we present a bottom-up one-loop scheme in the left-right symmetric (LR) model ($G_{LR} \times Z_4$) which leads to an effective Ma-model ($G_{SM} \times Z_2$), discussed in the last Chapter, after the left-right symmetry is broken. Therefore, we call this model the LR-extension of the Ma-model. We obtain the following seesaw-like formula even though the Dirac mass matrix vanishes to all orders in perturbation theory:

$$M_\nu \;=\; \frac{2\lambda_5}{16\pi^2} M_l^{\rm diag} \tilde{M}_N^{-1} M_l^{\rm diag} \,, \tag{8.1}$$

where $M_l^{\rm diag}$ is the diagonal charged lepton mass matrix $M_\ell^{diag} = {\rm diag}(m_e, m_\mu, m_\tau)$ and λ_5 is a Higgs self coupling. As a result, the flavor structure of the RH neutrino mass matrix is completely determined. We find a stronger hierarchy in the RH neutrino sector compared to the charged leptons. Thus the radiative corrections transmit the charged lepton mass hierarchy into the RH neutrino sector (radiative transmission of lepton flavor hierarchies). Furthermore the hierarchy in the RH sector is such that it can be easily obtained from a simple $U(1)_H$ family assignment. As an application, we study the phenomenology of the model.

We also discuss how the quark sector can be made realistic since the Z_4 symmetry leads to vanishing down quark masses at tree-level. Two ways to generate realistic down quark masses and CKM angles are: (model 1) introduction of color triplet isospin singlet fields that give radiative masses to down quarks or (model 2) the addition of three isospin singlet vector-like down quarks which generate a tree-level masses for the down quarks.

This chapter is organized as follows: In Section 8.1, we discuss the neutrino sector of the model. In Section 8.2, lepton flavor violation (LFV) of the model is investigated. In Section 8.3, we discuss lepton number violation (LNV) of the model. In Section 8.4, we discuss two models of down quark masses and also their consequences to flavor changing neutral currents (FCNCs). We note that the discussion of the Higgs sector can be found in Appendix C.

8.1 Neutrino Masses and Mixing

We construct a model based on the left-right symmetric group [224–226] $SU(2)_L \times SU(2)_R \times U(1)_{B-L}$ supplemented by a discrete symmetry group Z_4. The quarks and leptons are assigned

Field	Q_L	Q_R	L_L	L_R	ϕ	$\tilde{\phi} = \sigma_2 \phi^* \sigma_2$	Δ_L	Δ_R
G_{LR}	$(2, 1, \frac{1}{3})$	$(1, 2, \frac{1}{3})$	$(2, 1, -1)$	$(1, 2, -1)$	$(2, 2, 0)$	$(2, 2, 0)$	$(3, 1, 2)$	$(1, 3, 2)$
Z_4	1	$-i$	1	i	i	$-i$	1	-1

Table 8.1: The particle content of the model.

as in the minimal LR model to left-right symmetric doublets. The symmetry breaking is implemented also as in the minimal LR model by the Higgs fields $\phi(2, 2, 0)$ and $\Delta_R(1, 3, +2) \oplus \Delta_L(3, 1, +2)$.

In the leptonic sector of the model, the $SU(2)_R \times U(1)_{B-L}$ breaking by the right-handed triplet with $B - L = 2$ gives large Majorana masses to the RH neutrinos [227]. Unlike in the usual implementation of the seesaw formula, however, in our model, the Dirac mass for neutrinos vanishes to all orders in perturbation theory due to the Z_4 symmetry. The particle content of the model is given in Table 8.1. The gauge invariant Yukawa couplings of the above Z_4 supplemented LR model are

$$\begin{aligned} \mathcal{L}_Y &= \left(\bar{Q}_L \phi h_q Q_R \; + \; \bar{L}_L \tilde{\phi} h_l L_R + h.c.\right) + \\ &\quad + \left[f_{ab} \left((L_R)_a^T C^{-1} (i\sigma^2 \Delta_R)(L_R)_b + (L_L)_a^T C^{-1} (i\sigma^2 \Delta_L)(L_L)_b\right) \; + \; h.c.\right] \end{aligned} \tag{8.2}$$

where f and $\tilde{f}$ are symmetric 3×3 matrices in flavor space.
The most general potential for the LR model has been discussed in the literature before [228]. The presence of the Z_4 symmetry in our model forbids terms linear in the invariant $\mathrm{Tr}(\tilde{\phi}^\dagger \phi)$ in the potential, so that the minimum energy configuration corresponds to the following VEV for the ϕ field (instead of the general one in [224–226]):

$$\langle \phi \rangle \; = \; \begin{pmatrix} v_1 & 0 \\ 0 & 0 \end{pmatrix}. \tag{8.3}$$

For the $\Delta_{L,R}$ fields we have:

$$\langle \Delta_R \rangle \; = \; \begin{pmatrix} 0 & 0 \\ v_R & 0 \end{pmatrix}, \; \langle \Delta_L \rangle \; = \; 0. \tag{8.4}$$

After the $SU(2)_R \times U(1)_{B-L}$ breaking by the right-handed triplet with $B - L = 2$, the particle

content with respect to $(SU(2)_L, U(1)_Y)_{Z_2=\pm}$ is given by

$$\begin{aligned}
Q_L = \begin{pmatrix} u_L \\ d_L \end{pmatrix} &\rightarrow (2, 1/6)_+ \\
Q_R = \begin{pmatrix} u_R \\ d_R \end{pmatrix} &\rightarrow \begin{pmatrix} (1, \frac{2}{3})_+ \\ (1, -\frac{1}{3})_- \end{pmatrix} \\
L_L = \begin{pmatrix} \nu_L \\ e_L \end{pmatrix} &\rightarrow (2, -1/2)_+ \\
L_R = \begin{pmatrix} N_R \\ e_R \end{pmatrix} &\rightarrow \begin{pmatrix} (1, 0)_- \\ (1, 1)_+ \end{pmatrix} \\
\phi = \begin{pmatrix} \phi_2 \\ \phi_1 \end{pmatrix}_R &\rightarrow \begin{pmatrix} (2, \frac{1}{2})_- \\ (2, -\frac{1}{2})_+ \end{pmatrix} \\
\Delta_L = \begin{pmatrix} \delta_L^{++} \\ \delta_L^{+} \\ \delta_L^{0} \end{pmatrix} &\rightarrow (3, 1)_+ \\
\Delta_R = \begin{pmatrix} \delta_R^{++} \\ \delta_R^{+} \\ \delta_R^{0} \end{pmatrix} &\rightarrow \begin{pmatrix} (1, 2)_+ \\ (1, 1)_- \\ (1, 0)_+ \end{pmatrix}
\end{aligned} \tag{8.5}$$

The generators from $G_{LR} \times Z_4$ to $SM \times Z_2$ are

$$e^{iT_{3L}\gamma_L} e^{iT_{3L}\alpha_R} e^{i(B-L)\beta} e^{k\pi} \rightarrow e^{iT_{3L}\gamma_L} e^{i\beta' Y} e^{i(T_{3R}+k)\pi}, \tag{8.6}$$

where $\beta' = 2\beta$, $Y = T_{3R} + (B-L)/2$ and the electrical charge is defined as $Q = T_{3L} + Y$.

Note that the bi-doublet can be written in the 2×2 matrix form as

$$\phi = \begin{pmatrix} \phi_1^{0*} & \phi_2^{+} \\ \phi_1^{-} & \phi_2^{0} \end{pmatrix} = \begin{pmatrix} \phi^{0*} & \eta^{+} \\ \phi^{-} & \eta^{0} \end{pmatrix}, \tag{8.7}$$

where $\begin{pmatrix} \phi^{0*} \\ \phi^{-} \end{pmatrix} \sim (2, -\frac{1}{2})_+$ and $\begin{pmatrix} \eta^{+} \\ \eta^{0} \end{pmatrix} \sim (2, \frac{1}{2})_-$ (under $(SU(2)_L, U(1)_Y)_{Z_2}$) are similar to the two Higgs doublets from the Ma-model (see Section 7.2.1).

By an appropriate choice of the basis, we can choose both $h_{q,l}$ to be diagonal matrices without loss of generality. It is easy to see that, with the above assignment, we get the Dirac neutrino mass $m_D = 0$ and the diagonal Yukawa coupling matrix h_l is given by $h_l = \text{diag}(m_e, m_\mu, m_\tau)/v_1$. We also note that there is no type II seesaw [229–232] contribution to the neutrino masses unlike in usual LR models due to the vanishing VEV of Δ_L in Eq.(8.4). Moreover, the diagonal Yukawa coupling matrix h_q can be written as $h_q = \text{diag}(m_u, m_c, m_t)/v_1$, and the down quark masses are vanished due to the Z_4 symmetry.

8.1.1 A Seesaw-like Formula for Neutrino Masses

The tree-level neutrino Dirac mass vanishes. The neutrinos pick up their masses at one-loop level from the diagram in Figure 8.1. The light neutrino mass matrix is given by the one-loop

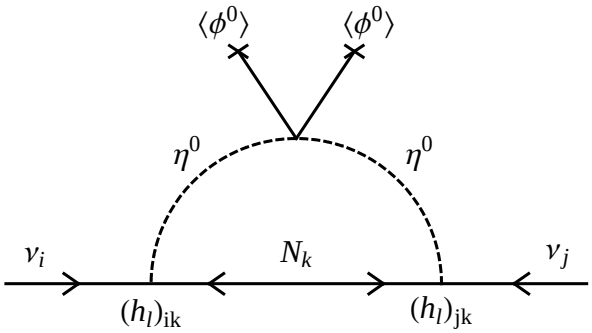

Figure 8.1: The diagrams responsible for neutrino masses in a Ma-like model [6]. We note that this diagram is given in the right-handed neutrino mass basis.

formula

$$M_{\nu,ij} \;=\; M_{l,i}^{\rm diag}\Lambda_{ij}(\lambda_5, M_{N,ij})M_{l,j}^{\rm diag}, \tag{8.8}$$

where $M_l^{\rm diag} = {\rm diag}(m_e, m_\mu, m_\tau)$ and Λ_{ij} [1] is given by $\frac{M_{N,ij}}{16\pi^2}$ times

$$\left[\frac{m^2(\sqrt{2}\Re\eta^0)}{m^2(\sqrt{2}\Re\eta^0) - M_{N,ij}^2}\log\left(\frac{m^2(\sqrt{2}\Re\eta^0)}{M_{N,ij}^2}\right) - \frac{m^2(\sqrt{2}\Im\eta^0)}{m^2(\sqrt{2}\Im\eta^0) - M_{N,ij}^2}\log\left(\frac{m^2(\sqrt{2}\Im\eta^0)}{M_{N,ij}^2}\right)\right] \tag{8.9}$$

and M_N is the heavy neutrino mass matrix. The Higgs masses are given by [2]

$$\begin{aligned} &m^2(\sqrt{2}\Re\phi^0) = 2\lambda_1 v_1^2,\; m^2(\sqrt{2}\Re\eta^0) = m_2^2 + (\lambda_3+\lambda_4+\lambda_5)v_1^2, \\ &m^2(\sqrt{2}\Im\eta^0) = m_2^2 + (\lambda_3+\lambda_4-\lambda_5)v_1^2, \text{ and } m^2(\eta^\pm) = m_2^2 + \lambda_3 v_1^2. \end{aligned} \tag{8.10}$$

Note that these couplings λ_i are the effective couplings which we get at the low energy when the left-right symmetry is broken, see Section 7.2.1 and Appendix C.3.

We assume that $m^2(\sqrt{2}\Re\eta^0) \ll M_{N,ij}^2$, $\Lambda_{ij}(\lambda_5, M_{N,ij}) \simeq 2\frac{\lambda_5}{M_{N,ij}^2}\log(M_{N,ij}^2/m_{\eta^0}^2)$ [6], where $m_{\eta^0}^2 = \frac{1}{2}(m^2(\sqrt{2}\Re\phi^0) + m^2(\sqrt{2}\Im\eta^0))$. Then, the light neutrino mass matrix can be written as

$$M_{\nu,ij} \;=\; \frac{2\lambda_5}{16\pi^2}M_{l,i}^{\rm diag}\left(\tilde{M}_N^{-1}\right)_{ij}M_{l,j}^{\rm diag}, \tag{8.11}$$

where $\left(\tilde{M}_N^{-1}\right)_{ij} = \log(M_{N,ij}^2/m_{\eta^0}^2)/\left(M_{N,ij}\right)$.

8.1.2 Reconstructing the Heavy Neutrino Mass Matrix

Since we have a rough idea about the form of the neutrino mass matrix in the limit of zero CP phase and small reactor angle θ_{13}, we can use it to get an idea about the elements of the RH neutrino mass matrix. It is interesting that all elements of this mass matrix can be determined, up to an overall constant.

[1] Λ_{ij} is similar to Λ_k in Eq.(7.5) except for being in different basis.

[2] We assume $\alpha_3 \simeq 0$ for a phenomenological reason, see Appendix C.1.

To see analytically why this happens, let us try to reconstruct M_N from the tri-bimaximal form for the PMNS-matrix given in Eq.(2.26). Using this and Eq.(8.11), we can write down $\left(\tilde{M}_N^{-1}\right)_{ij}$ as function of λ_5 and of the light neutrino mass eigenvalues $m_{1,2,3}$. It is given by $\frac{4\pi^2}{3\lambda_5}$ times

$$\begin{pmatrix} 2(2m_1+m_2)/(m_e^2) & 2(m_2-m_1)/(m_e m_\mu) & 2(m_2-m_1)/(m_e m_\tau) \\ 2(m_2-m_1)/(m_e m_\mu) & (m_1+2m_2+3m_3)/(m_\mu^2) & (m_1+2m_2-3m_3)/(m_\mu m_\tau) \\ 2(m_2-m_1)/(m_e m_\tau) & (m_1+2m_2-3m_3)/(m_\mu m_\tau) & (m_1+2m_2+3m_3)/(m_\tau^2) \end{pmatrix}, \tag{8.12}$$

The form of $\left(\tilde{M}_N^{-1}\right)$ is hence roughly given by

$$\frac{4\pi^2\mathcal{O}(m_\nu)}{3\lambda_5}\begin{pmatrix} \mathcal{O}(m_e^{-2}) & \mathcal{O}((m_e m_\mu)^{-1}) & \mathcal{O}((m_e m_\tau)^{-1}) \\ \mathcal{O}((m_e m_\mu)^{-1}) & \mathcal{O}(m_\mu^{-1}) & \mathcal{O}((m_\mu m_\tau)^{-1}) \\ \mathcal{O}((m_e m_\tau)^{-1}) & \mathcal{O}((m_\mu m_\tau)^{-1}) & \mathcal{O}(m_\tau^{-1}) \end{pmatrix}. \tag{8.13}$$

We can calculate $M_{N,ij}$ by solving the equation $\log(M_{N,ij}^2/m_{\eta^0}^2)/M_{N,ij} = (\tilde{M}_N^{-1})_{ij}$.

In order to demonstrate the size of the right-handed neutrinos, we assume the normal hierarchy, $m_1 = 10^{-4}$ eV, $m_2 = \sqrt{m_1^2 + \Delta m_{21}^2}$, and $m_3 = \sqrt{m_1^2 + |\Delta m_{31}|^2}$, where $\Delta m_{21}^2 = 7.65 \times 10^{-5}$ eV^2, $|\Delta m_{31}^2| = 2.40 \times 10^{-3}$ eV^2 [47]. Assuming that $\lambda_5 = 1$ and $m(\sqrt{2}\Re\eta^0) = 300$ GeV leads to $m_{\eta^0} \simeq 244.39$ GeV and the right-handed neutrino mass matrix reads

$$(M_N)_{NH} = \begin{pmatrix} 7632.44 & 4.68 \times 10^6 & 1.03 \times 10^8 \\ \times & 1.36 \times 10^8 & -3.64 \times 10^9 \\ \times & \times & 5.61 \times 10^{10} \end{pmatrix} \text{ GeV}. \tag{8.14}$$

The right-handed neutrino masses can be calculated as

$$M_{N1} = 1.41 \times 10^5 \text{ GeV}, \quad M_{N2} = 9.96 \times 10^7 \text{ GeV}, \quad \text{and } M_{N3} = 5.64 \times 10^{10} \text{ GeV}. \tag{8.15}$$

For the inverse hierarchy, we use $m_1 = \sqrt{m_3^2 + \Delta m_{31}^2}$, $m_2 = \sqrt{m_1^2 + \Delta m_{21}^2}$, and $m_3 = 10^{-4}$ eV. The right-handed neutrino mass matrix then reads

$$(M_N)_{IH} = \begin{pmatrix} 664.31 & 6.63 \times 10^7 & 1.39 \times 10^9 \\ \times & 1.52 \times 10^8 & 3.15 \times 10^9 \\ \times & \times & 6.24 \times 10^{10} \end{pmatrix} \text{ GeV}. \tag{8.16}$$

The right-handed neutrino masses can be calculated as

$$M_{N1} = 6.48 \times 10^6 \text{ GeV}, \quad M_{N2} = 3.13 \times 10^7 \text{ GeV}, \quad \text{and } M_{N3} = 6.26 \times 10^{10} \text{ GeV}. \tag{8.17}$$

Here, we see that there is a strong hierarchy in the RH neutrino sector in a way similar to the charged lepton sector. This is what we label as the radiative transmission of hierarchy, from charged leptons to the RH neutrinos. Note that this mechanism, given a certain form of M_N (with small mixings), naturally allows for large mixing angles in the SM lepton sector that are not necessarily maximal. This is different from many other models, where in most cases only zero or maximal mixing is predicted. Note, however, that there are also exceptions to this:

E.g., the size of the mixing angle could be determined by underlying discrete symmetries [86], or it could arise from an anarchical pattern of the neutrino mass matrix [233].

These mass matrices for RH neutrinos have a structure that can be easily obtained from the Froggat-Nielsen (FN) mechanism [50] with a $U(1)_H$ family symmetry with H charges $(0, 1, 2)$ for the third, second, and the first generation right handed lepton doublets. The left-right and $U(1)_H$ invariant Yukawa couplings in this case can be written as

$$\begin{aligned}\mathcal{L}_{Y,H} &= h_{l,3}\bar{L}_{3,L}\tilde{\phi}L_{3,R} + h_{l,2}\bar{L}_{2,L}\tilde{\phi}L_{2,R}\frac{\varphi}{M} + h_{l,1}\bar{L}_{1,L}\tilde{\phi}L_{1,R}\left(\frac{\varphi}{M}\right)^2 \\ &+ \left[\sum_{a,b=1,2,3} f_{ab}L_{a,R}^T C^{-1}(i\sigma^2\Delta_R)L_{b,R}\left(\frac{\varphi}{M}\right)^{6-(a+b)} + h.c.\right],\end{aligned} \tag{8.18}$$

where φ is the SM singlet with the H charge (-1). For an appropriate choice of $\frac{<\varphi>}{M}$ (roughly $1/20$ in the normal hierarchy case), we get the desired hierarchy in both the charged lepton masses as well as in the RH neutrino sector. This hierarchy then translates into a structure of the light neutrino mass matrix that naturally yields large mixing angles.

8.2 Lepton Flavor Violation

The main ingredients of the model that induce lepton flavor violation are the additional Higgs triplets $\Delta_{L,R}$. The most important process is $\mu^\pm \to e^\pm e^\mp e^\mp$, which is already mediated at tree-level. Further processes are $e_i \to e_j\gamma$ and the related μ-e conversion, which is less strongly constrained as long as it only consists of the diagram for $\mu \to e\gamma$ attached to the nucleus. Therefore, we will only study the $\mu \to 3e$ and $\mu \to e\gamma$ in more detail here.

8.2.1 $\mu \to 3e$

The $\mu \to 3e$ process is depicted in Figure 8.2. The corresponding couplings might arise through terms in Eq.(8.2):

$$f_{ab}(L_{L,R})_a^T C^{-1}(i\sigma^2\Delta_{L,R})(L_{L,R})_b \supset f_{ab}\delta_{L,R}^{++}(e_{L,R})_a^T C^{-1}(e_{L,R})_b. \tag{8.19}$$

Taking $m_\delta \approx m(\delta_{L,R}^{\pm\pm})$ (see Eq.(C.15)) and applying the standard Feynman rules, it is easy to work out the expression for the decay width, which is given by

$$\Gamma(\mu \to 3e) \simeq \frac{m_\mu^5}{2^7 \cdot 3\pi^3} \cdot \frac{|f_{e\mu}|^2|f_{ee}|^2}{m_\delta^4}. \tag{8.20}$$

The corresponding branching ratio,

$$\mathrm{Br}(\mu \to 3e) \simeq \frac{|f_{e\mu}|^2|f_{ee}|^2}{2G_F^2 m_\delta^4}, \tag{8.21}$$

is known experimentally to be less than $1.0 \cdot 10^{-12}$ [234], which leads to a bound on $m_\delta \gtrsim 2 \cdot 10^5$ GeV for Yukawa couplings of $|f| \approx 0.1$.

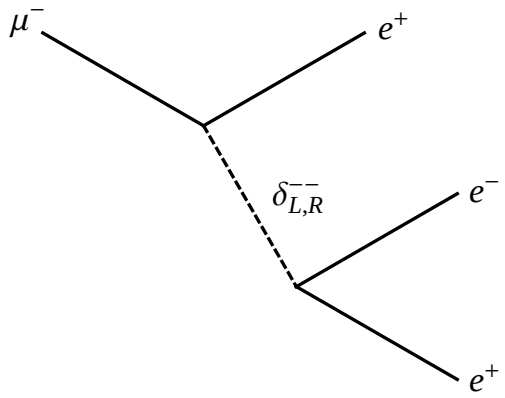

Figure 8.2: The LFV-diagram for $\mu \to 3e$.

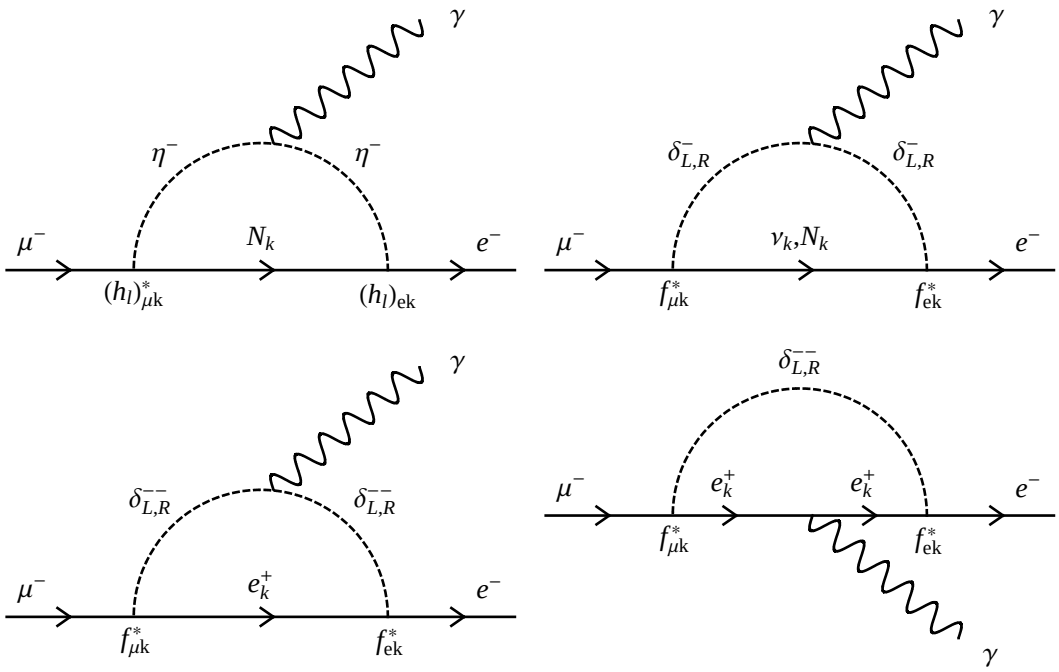

Figure 8.3: The LFV-diagrams for $\mu \to e\gamma$.

8.2.2 $\mu \to e\gamma$

The $\mu \to e\gamma$ process does, differently from $\mu \to 3e$, already occur in the Ma-model itself (see Section 7.2.3). In the LR-symmetric extension, however, there are more diagrams that can contribute, see Figure 8.3. A model-independent treatment of $e_i \to e_j\gamma$ (and related processes) is given in [222]. Let us concentrate on $\mu \to e\gamma$ here, as this process is much more strongly constrained by experiments, and let us focus on specific limiting cases. The loop-functions resulting from the diagrams in Figure 8.3 depend on the ratios of the squared mass of the internal fermion to the squared mass of the internal scalar that are involved. Going through all examples, these ratios are

$$\begin{aligned} t_A &\equiv \frac{m^2(N_i)}{m^2(\eta^-)} && \text{(upper left diagram)},\\ t_B &\equiv \frac{m^2(\nu_i)}{m^2(\delta_L^-)} && \text{(upper right diagram)},\\ t_C &\equiv \frac{m^2(N_i)}{m^2(\delta_R^-)} && \text{(upper right diagram)},\\ t_D &\equiv \frac{m^2(e_i^+)}{m^2(\delta_L^{--})} && \text{(lower diagrams), and}\\ t_E &\equiv \frac{m^2(e_i^+)}{m^2(\delta_R^{--})} && \text{(lower diagrams).} \end{aligned} \tag{8.22}$$

As all these diagrams lead to the same final state, the corresponding amplitudes have to be summed before squaring the total amplitude.

From the known masses of the charged leptons and from the bounds on the light neutrino mass scale, as well as the bounds on the scale of the heavy neutrinos and scalars involved, we can easily conclude that $t_{B,D,E} \approx 0$ and only t_A and t_C are sizable. Using [222], it is easy to see that the current limit of $1.2 \cdot 10^{-11}$ [235] on the branching ratio for $\mu \to e\gamma$ translates into

$$|\epsilon_L|^2 + |\epsilon_R|^2 \lesssim 3 \cdot 10^{-11}/\text{GeV}^4, \tag{8.23}$$

where (taking m_δ to simply denote the mass scale of all the δ's and similar for m_N and m_η)

$$\begin{aligned} \epsilon_L &\equiv \frac{1}{m_\delta^2} \cdot \left[1 + 6 \cdot \left(-\bar{c}(t) + \frac{3}{2}\bar{d}(t)\right)|_{t=m_N^2/m_\delta^2}\right], \text{ and}\\ \epsilon_R &\equiv \frac{3}{2m_\delta^2} + \frac{10}{m_\eta^2} \cdot \left(-\bar{c}(t) + \frac{3}{2}\bar{d}(t)\right)|_{t=m_N^2/m_\eta^2}. \end{aligned} \tag{8.24}$$

The exact definitions of $\bar{c}$ and $\bar{d}$ can be found in [222]. Depending on the sizes of the different mass scales one can have several limiting cases that lead to different bounds:

- light Ma-scale (less realistic, N too light): $m_\eta \lesssim m_N \ll m_\delta$
  This yields $\epsilon_L \approx \frac{3}{2m_\delta^2} \ll \epsilon_R \approx \frac{5}{3m_\eta^2}$ and hence a limit of $m_{\eta,N} \gtrsim 300$ GeV.
- intermediate N-scale (realistic): $m_\eta \ll m_N \ll m_\delta$
  This yields $\epsilon_L \approx \frac{3}{2m_\delta^2} \ll \epsilon_R \approx \frac{5}{3m_N^2}$ and hence a limit of $m_N \gtrsim 550$ GeV.
- N at the LR-scale (realistic): $m_\eta \ll m_N \approx m_\delta$
  This yields $\epsilon_L \approx \frac{5}{4m_\delta^2} \sim \epsilon_R \approx \frac{19}{6m_\delta^2}$ and hence a limit of $m_{\delta,N} \gtrsim 800$ GeV.

- heavy N-scale (unrealistic, N too heavy): $m_\eta \ll m_\delta \ll m_N$
  This yields $\epsilon_L \approx \frac{1}{m_\delta^2} \sim \epsilon_R \approx \frac{3}{2m_\delta^2}$ and hence a limit of $m_\delta \gtrsim 600$ GeV.

We note that since the Higgs triplets do not appear in the pure Ma-model, the chance to detect these particles lead to a way to discriminate the pure Ma-model from the LR-extension of the Ma-model.

8.3 Lepton Number Violation

There are also lepton number violating processes that can be mediated via the Higgs triplets.

8.3.1 Neutrino-less Double Beta Decay

The first possibility one might think of when talking about LNV is neutrino-less double beta decay. The doubly charged components of the scalar triplets could indeed contribute to this process. An expression for the effective neutrino mass in case of the triplet-mediated mechanism is given by [236],

$$|m_{ee}| = \mu f_{ee} \frac{v^2}{m_\delta^2}, \tag{8.25}$$

where μ is the effective coupling of the triplet to two W-bosons and m_δ is the mass of the doubly charged triplet component. The only origin of a coupling μ can come from the Higgs potential itself, and the only terms that could potentially do this job are the ones proportional to α_3 and β_1 in Eq.(C.1) and Eq.(C.19), which do, however, not yield any term of the form $v_R \phi^+ \phi^+ \Delta_{L,R}^{--}$ (as $\langle \Delta_L \rangle = 0$), and hence $\mu = 0$ in our case. Neutrino-less double beta decay will not be changed by our model.

8.3.2 μ-Decay

Another LNV-contribution is from μ-decay. Actually, one would assume this decay to be lepton number conserving. However, by taking a look at the couplings of the Higgs triplets in Eq.(8.2), one can see that the corresponding decay (see Figure 8.4) is actually given by

$$\mu^- \to \overline{\nu}_\mu e^- \nu_e \ . \tag{8.26}$$

The decay rate of this process reads

$$\Gamma(\mu^- \to \overline{\nu}_\mu e^- \nu_e) \simeq \frac{m_\mu^5}{2^8 \cdot 3\pi^3} \cdot \frac{|f_{\mu\mu}|^2 |f_{ee}|^2}{m_\delta^4} \ , \tag{8.27}$$

where explicit expressions for the mass scale $m_\delta = m_\delta(\delta_L^-)$ can be found in Eq.(C.13). Comparing this to the rate for ordinary μ-decay yields a correction to the Fermi constant, which amounts to

$$(G_F')^2 = G_F^2 + \frac{|f_{\mu\mu}|^2 |f_{ee}|^2}{4 m_\delta^4}. \tag{8.28}$$

Experimentally, the Fermi constant is determined to be [46]

$$G_F^2 = 1.16637(1) \cdot 10^{-5} \text{ GeV}^{-2}, \tag{8.29}$$

which leads to an uncertainty of $\delta(G_F) \equiv |G_F' - G_F| = 10^{-10}$ GeV^{-2}. Taking the Yukawa couplings to be both around 0.1, this yields a lower bound on the triplet mass of $m_\delta \gtrsim$ 400 GeV.

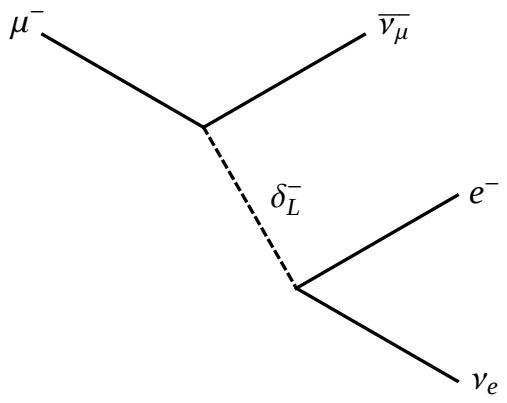

Figure 8.4: The LNV-diagram for μ-decay.

8.3.3 N-Decay

Decays of heavy neutrinos N are among the most interesting processes in the Ma-model in what concerns phenomenology [213]. When considering the LR-extension of the model, it might be that there are additional decay modes, driven by the Yukawa couplings of the Higgs triplets in Eq.(8.2). We can treat them by simply integrating out the heavy triplets, as the dominant decay modes are tree-level processes, and although the triplet contributions are also not loop-suppressed, they are small because of the large triplet masses. Integrating out the triplets yields the following effective operator:

$$\mathcal{L} = \frac{1}{2M^2(\delta_R^\pm)} \left(\overline{N}_i f_{ik}^* (1-\gamma_5) e_k^c\right) \left(\overline{e^c}_l f_{lj} (1+\gamma_5) N_j\right). \tag{8.30}$$

The corresponding decay would look like

$$N_i \to N_j e_k^+ e_l^-, \tag{8.31}$$

with $m(N_i) > m(N_j)$, which would only yield another heavy neutrino, which is barely detectable. On the other hand, the charged lepton pair (that does not necessarily have to have the same flavor!) plus missing energy might be an interesting collider signature. Other decays like $N_i \to \eta^0 \nu_j$ or $N_i \to \eta^\pm e_j^\mp$ are sufficiently treated in [213] and are, of course, also present in the LR-extension of the Ma-model.

8.3.4 Leptogenesis

According to Ma, the normal leptogenesis is possible in the pure Ma-model [237,238]. In order to see whether the leptogenesis is possible or not in the LR-extension of the Ma-model, we calculate the CP-violation and the baryon asymmetry using the fitting parameters in Section 8.1.2. We assume the neutrino mixing matrix is nearly tri-bimaximal, but θ_{13} and the CP phase δ are not fixed.

The CP-asymmetry from the decay of the lightest right-handed neutrino can be calculated by [239]

$$\epsilon_{N_1} = -\frac{3M_{N1}}{16\pi} \sum_{i=2,3} \frac{Im[(h_l^\dagger h_l)_{1i}^2]}{(h_l^\dagger h_l)_{11}} \frac{1}{M_{Ni}}, \tag{8.32}$$

Field	ω_L	ω_R
G_{LR}	$(1,1,-\frac{2}{3})$	$(1,1,-\frac{2}{3})$
Z_4	1	-1

Table 8.2: The particle content of model 1. Note that $\omega_{L,R}$ are triplets under $SU(3)_c$

where the Yukawa coupling between the left-handed lepton and the right-handed neutrino in the right-handed neutrino basis is $h_l = (M_l^{\rm diag}/v_1)U_R$, and U_R is the unitary matrix which diagonalizes M_N. Inserting the fitting parameters, we obtain $|\epsilon_{N_1}| = 2.99 \times 10^{-12}$ for normal hierarchy and $|\epsilon_{N_1}| = 3.38 \times 10^{-10}$ for inverse hierarchy. The baryon asymmetry relative to the entropy density can be written as

$$Y_{\Delta B} =\simeq \frac{n_{N_1}}{s} C_{sphal} \chi_{N_1} |\epsilon_{N_1}|, \tag{8.33}$$

where $\frac{n_{N_1}}{s}$ is of order 4×10^{-3}, $C_{sphal} = \frac{28}{79}$ and the efficiency factor $0 < \eta < 1$. We see that the CP-violation we get is too small to explain the observed baryon asymmetry of the Universe ($Y_{\Delta B}^{obs} = (8.75 \pm 0.23) \times 10^{-11}$) [239].

Note that in the pure Ma-model, the Yukawa couplings h_l are not fixed, so we can vary them to increase the CP-violation. This is, however, not possible in our case because the Yukawa coupling h_l is already determined by the masses of the charged leptons due to left-right symmetry.

8.4 Masses for The *d* Quarks and Their Consequences

8.4.1 Model 1

Masses for The *d* Quarks

The problem is that the term $h_q \bar{Q}_L^T \phi Q_R$ from Eq.(8.2) does not lead to a down-quark mass term due to Eq.(8.3). This can be cured by introducing the scalar color triplets $\omega_{L,R}$ and using part of the Z_2 soft breaking term. The quantum numbers of the scalar color triplets are given in Table 8.2. The Yukawa couplings between the scalar color triplets and the quarks read

$$\mathcal{L}_Y = \tilde{f}_{ab}((Q_L)_a^T C^{-1}(i\sigma^2)(Q_L)_b \omega_L + (Q_R)_a^T C^{-1}(i\sigma^2)(Q_R)_b \omega_R) + h.c.\,, \tag{8.34}$$

where $i\sigma^2$ acts on $SU(2)_{L,R}$ space.
After the LR symmetry is broken, the quantum numbers of the scalar color triples with respect to $(SU(2)_L, U(1)_Y)_{Z_2}$ read

$$\begin{aligned} \omega_L &\rightarrow (1,-1/3)_+ \\ \omega_R &\rightarrow (1,-1/3)_-. \end{aligned} \tag{8.35}$$

Another important ingredient of the model is the Z_2 soft breaking mass terms of the scalar color triplets,

$$V_{\rm soft} = \delta m_\omega^2 [\bar{\omega}_L \omega_L + \bar{\omega}_R \omega_R] + \delta m_{\omega,\rm m}^2 [\bar{\omega}_L \omega_R + \bar{\omega}_R \omega_L]. \tag{8.36}$$

Both these contributions are necessary for two reasons: First, it would be highly unnatural to forbid only one of them and second, both contributions are necessary lead to non-degenerate ω mass eigenstates (whose mass squares are proportional to $\delta m_\omega^2 \pm \delta m_{\omega,\mathrm{m}}^2$), which is required for a non-zero d-quark mass.

The mass eigenstates $\omega_{1,2}$ are given by

$$\begin{pmatrix}\omega_1\\ \omega_2\end{pmatrix} = \frac{1}{\sqrt{2}}\begin{pmatrix}1 & 1\\ -1 & 1\end{pmatrix}\begin{pmatrix}\omega_L\\ \omega_R\end{pmatrix}. \tag{8.37}$$

Note that the the minus sign is crucial for the cancellation of the divergent parts of the diagrams between ω_1 and ω_2. The way how the ω's can generate a mass for the d-like quarks is shown in Figure 8.5. By the structure of the diagram (namely by the complex conjugations), this cancellation does not appear between real and imaginary part, as, e.g., for the light neutrino mass. Note that, at both vertices, the Yukawa coupling is just given by the symmetric matrix $\tilde{f}$ from Eq.(8.34). We note that there is no factor of three to be added, since the ω's form a color triplet as well as the quarks themselves. The result for the d-quark mass matrix is given by

$$(M_d)_{ij} = \frac{1}{16\pi^2}\tilde{f}_{ik}\tilde{f}^*_{jk}(m_u)_k\left[\frac{(m_u)_k^2\log(m_u)_k^2 - (m_u)_k^2 + M_{\omega_1}^2 - M_{\omega_1}^2\log\left(M_{\omega_1}^2\right)}{(m_u)_k^2 - M_{\omega_1}^2} - (\omega_2)\right], \tag{8.38}$$

with $(m_u)_{1,2,3} = m_{u,c,t}$. We would actually get a factor of two as we add the diagrams for real and imaginary parts, but this factor is exactly canceled by the mixing angle contribution $\left(\frac{1}{\sqrt{2}}\right)^2$ from Eq.(8.37), as it should (it does not matter if we imagine one complex scalar or two real ones propagating). Since the ω's are colored, one can derive a mass of $M_\omega = \mathcal{O}(\mathrm{TeV}) \gg m_{u,c,t}$ from hadronic FCNC limits (B- and K-mixing, see Section 8.4.3). Using this, one can simplify Eq.(8.38) to

$$(M_d)_{ij} = \frac{L}{16\pi^2}\tilde{f}_{ik}\tilde{f}^*_{jk}(m_u)_k, \text{ where } L = \log\left(\frac{M_{\omega_1}^2}{M_{\omega_2}^2}\right) \simeq \frac{\Delta M_\omega}{M_\omega}. \tag{8.39}$$

If strictly $M_{\omega_1}^2 = M_{\omega_2}^2$, then M_d will be zero since $L = 0$, so there must be a difference in the masses of the real and imaginary parts (this statement is trivial, since for both masses being identical we would need $\delta m_{\omega,\mathrm{m}}^2 = 0$, in which case the above diagram does not exist). If there is such a difference, the log-term in Eq.(8.39) will be of $\mathcal{O}(0.1-1)$, or so. Note that the loop suppression factor $1/16\pi^2$ renders it natural for the down quarks to be lighter than those of the the up quarks.

The d quark mass matrix can be written as

$$M_d = \frac{L}{16\pi^2}\tilde{f}D_u\tilde{f}^*, \tag{8.40}$$

where $D_u = \mathrm{diag}(m_u, m_c, m_t)$.
Using the down quark masses and CKM matrix given in Eq.(2.6), the symmetric Yukawa coupling $\tilde{f}$ can be calculated as

$$\tilde{f} = \begin{pmatrix}1.4558 & 0.0613 & 0.0005\\ \times & 0.2809 & 0.0063\\ \times & \times & 0.1564\end{pmatrix}\frac{16\pi^2}{L}, \tag{8.41}$$

where we neglect the CP phase in V_{CKM} and L is taken from Eq.(8.39).

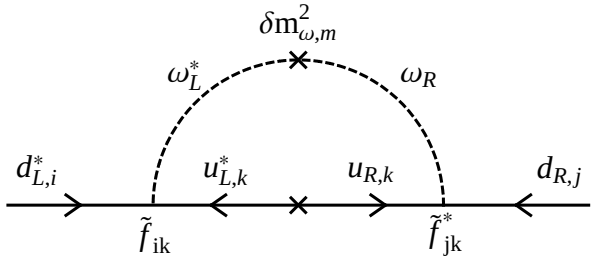

Figure 8.5: The diagram giving mass to the down quarks due to soft Z_2-breaking.

The Resulting Correction for The Neutrino Mass

The diagram leading to the masses of the down quarks can actually translate into a Z_2-breaking correction to the neutrino mass depicted on the left panel of Figure 8.6. This correction could be potentially dangerous, if it was larger than the 1-loop correction to a zero neutrino mass at tree-level coming from the Ma-model itself [6].

When calculating this diagram, one can take the effective version drawn on the right panel of Figure 8.6, where simply a massive d-like quark propagates leading to an effective VEV of the η^0. Note that this diagram can actually exist, no matter if we exchange the scalar or the pseudo-scalar part of η^0, leading to a complex VEV. The correction to the self-energy of the neutrinos looks like

$$\begin{aligned} -i\Sigma_{ij}(0) &= 2\cdot\frac{-i}{\sqrt{2}}(h_l)_{ij}\frac{i}{0^2-m^2(\sqrt{2}\Re(\eta^0))}\cdot 3\cdot(-1)\cdot\sum_{q=d,s,b}\frac{-i}{\sqrt{2}}(h_q)_{qq}\int\frac{d^4k}{(2\pi)^4}\frac{i(\not{k}+m_q)}{k^2-m_q^2} \\ &\quad -(\Im(\eta^0)\text{-part}), \end{aligned} \tag{8.42}$$

where the factor 2 in front originates from the different structure of the Majorana mass term compared to a Dirac mass term, 3 is the color factor that has to be included, and (-1) comes from the fermion loop. The integral over the loop momentum can be calculated easily by performing a Wick-rotation and introducing a cutoff Λ. As the Z_2-breaking is assumed to be soft, the quadratically divergent part will not contribute to the physical correction, and what remains amounts to (taking only into account the dominant b-quark contribution)

$$|\Sigma_{ij}(0)| \approx \frac{3(h_l)_{ij}(h_q)_{33}m_b^3}{2^4\pi^2}\log\left(1+\frac{\Lambda^2}{m_b^2}\right)\left(\frac{1}{m^2(\sqrt{2}\Re(\eta^0))}-\frac{1}{m^2(\sqrt{2}\Im(\eta^0))}\right). \tag{8.43}$$

Assuming a cutoff of $\Lambda \sim M_\omega \sim 10^6$ GeV, Yukawa couplings of $\mathcal{O}(0.1)$, a Higgs mass scale of $m_\eta \sim 100$ GeV, and no fine-tuning between the mass of the real and imaginary part, which is more or less an upper limit on this correction, the resulting contribution to the neutrino mass is roughly $\mathcal{O}(10^{-7}\text{eV})$, and hence completely negligible.

8.4.2 Model 2

Masses for The d Quarks

There is another possibility to obtain the down quark masses without introducing the Z_2 soft breaking terms as in model 1. We extend the model by adding the three heavy quarks

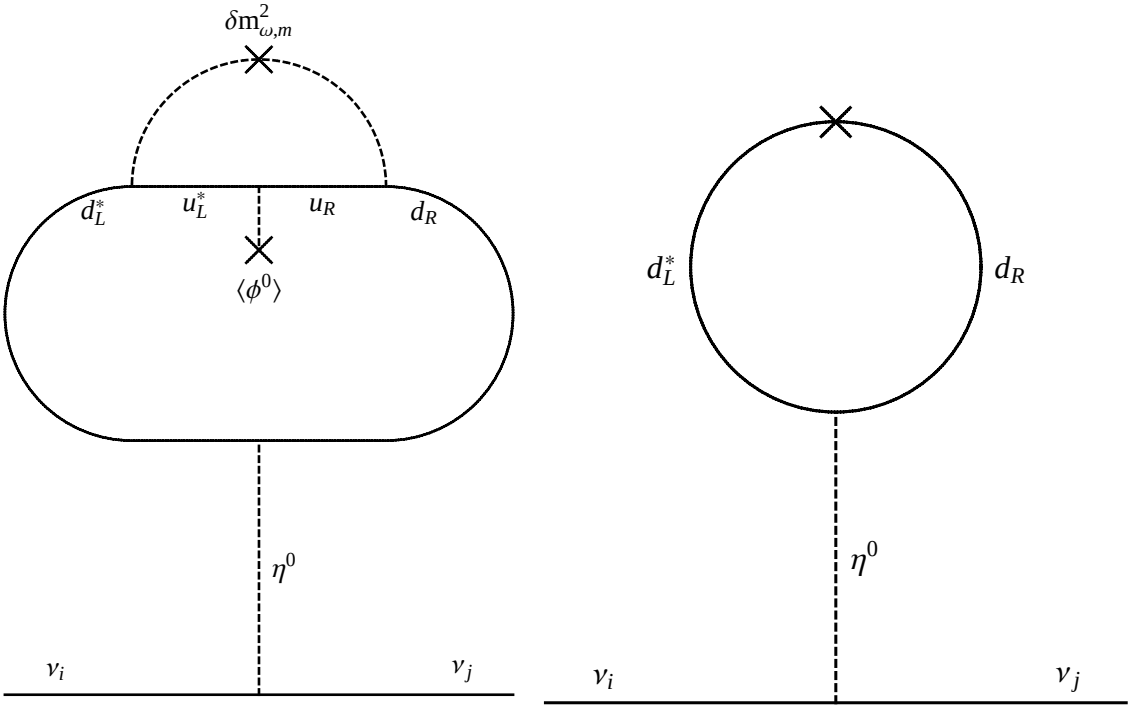

Figure 8.6: The translation of Figure 8.5 into a correction for the neutrino mass, in its fundamental (left) and effective (right) version.

Field	$Q_L = \begin{pmatrix} u_L \\ d_L \end{pmatrix}$	$Q_R = \begin{pmatrix} u_R \\ D_R \end{pmatrix}$	d_R	D_L	$\chi_L = \begin{pmatrix} \chi_L^+ \\ \chi_L^0 \end{pmatrix}$	$\chi_R = \begin{pmatrix} \chi_R^+ \\ \chi_R^0 \end{pmatrix}$
G_{LR}	$(2,1,\frac{1}{3})$	$(1,2,\frac{1}{3})$	$(1,1,-\frac{2}{3})$	$(1,1,-\frac{2}{3})$	$(2,1,1)$	$(1,2,1)$
Z_4	1	$-i$	1	$-i$	1	1

Table 8.3: The particle content of model 2.

(denoted by $D_{L,R}$) and two Higgs doublets under the $SU(2)_{L,R}$ group with $B-L=1$ (denoted by $\chi_{L,R}$). The heavy down quark D_R is the second component of the $SU(2)_R$ quark doublet Q_R where the down quark d_R is considered as $SU(2)_{L,R}$ singlet. Under the Z_4 symmetry, the $\chi_{L,R}$ and d_R are invariant, whereas $D_L \to -iD_L$. The particle content of this model is given in Table 8.3.

It is easy to write down a potential for $\chi_{L,R}$ with asymmetric mass terms for them so that they have non-equal VEVs. Since the discrete symmetry does not permit the term $\chi_L^\dagger \phi \chi_R$ term in the potential, the additional fields do not destabilize the ϕ VEV pattern assumed in the bulk of the paper.

The Yukawa interaction that is invariant under Z_4 and gauge symmetry is given by

$$\mathcal{L} \;=\; f_D(\bar{Q}_L \chi_L d_R + \bar{Q}_R \chi_R D_L) + h.c. \tag{8.44}$$

After spontaneous symmetry breaking the down quarks have masses proportional to the VEV of χ_L. And the heavy down quarks are also obtained masses proportional to the VEV of χ_R which is supposed to be at the LR-breaking scale. The mass of D is in the 10 to 100 TeV range. We emphasize that there is no direct mass term between D_L and D_R. We also note that after the LR symmetry is broken, the Z_4 symmetry is broken down to Z_2 symmetry in the lepton sector (see Eq.(8.5) and Eq.(8.6)) and the Z_4' symmetry in the quark sector where the additional Higgs doublets transform as

$$\begin{aligned} \chi_L = \begin{pmatrix} \chi_L^+ \\ \chi_L^0 \end{pmatrix} &\;\to\; (2,1/2)_{+1} \\ \chi_R = \begin{pmatrix} \chi_R^+ \\ \chi_R^0 \end{pmatrix} &\;\to\; \begin{pmatrix} (1,1)_{+i} \\ (1,0)_{-i} \end{pmatrix}. \end{aligned} \tag{8.45}$$

Using the down quark masses and CKM matrix given in Eq.(2.6), the Yukawa coupling reads[3]

$$f_D = \begin{pmatrix} 0.89 & 24.7 & 14.1 \\ \times & 106.5 & 169.9 \\ \times & \times & 4192.9 \end{pmatrix} \frac{1}{v_L}, \tag{8.46}$$

where v_L is the VEV of χ_L and the CP phase in V_{CKM} is neglected.

New Heavy Hadrons

Note that the existence of the heavy D quarks in model 2 leads to new heavy hadrons. It is easy to see from Eq.(8.44) that the mass terms for the heavy D quarks are (after LR breaking)

[3]Here, we assume that the Yukawa coupling is symmetric.

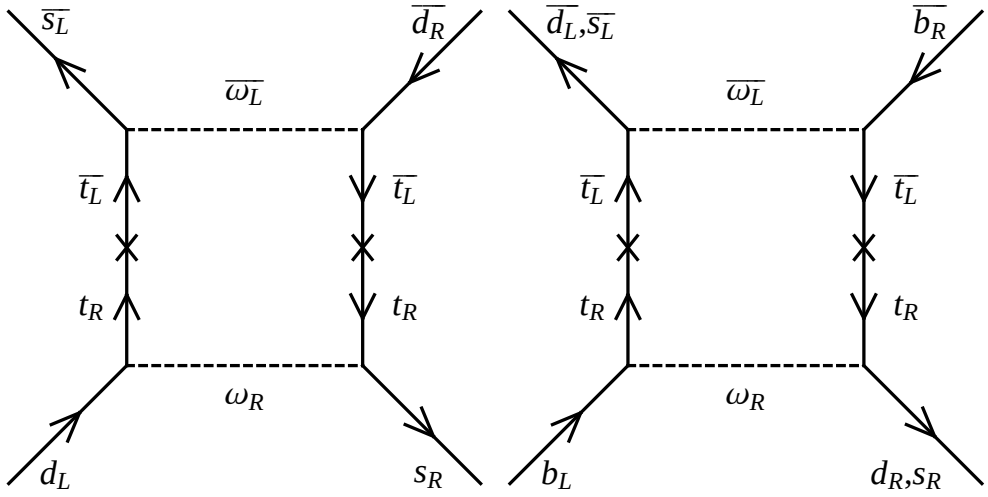

Figure 8.7: The diagrams for K-, B_d-, and B_s-mixing.

given by

$$\mathcal{L}_{\text{heavy}} = \bar{D_R} w_R f_D D_L + h.c. \tag{8.47}$$

If w_R is assumed to be at the LR breaking scale, $\mathcal{O}(10^5\text{GeV})$, and $f_D \sim 0.1$, then the mass scale of the heavy new quarks (and hence of the heavy new hadrons) will be $\mathcal{O}(10^4\text{GeV})$, as there is a binding force stronger than strong interactions themselves.

The particle spectrum will consist of all physical combinations that can appear. As all quarks in the model are triplets under $SU(3)$, we can form any of the usual mesons and baryons by replacing down quarks by their heavy counterparts, as long as the resulting particle has an integer electric charge. Completely neutral possibilities are, e.g., $\bar{D}_{L,R} D_{L,R}$ (heavy pions or ρ mesons) or $u_R D_R D_R$ (heavy neutrons and hyperons). Note that some of those particles might not only carry electric charge, but might also be non-singlets under Z_4. Detecting these states would be a clear signal of model 2 that is well in the range of LHC.

8.4.3 Hadronic FCNCs

Model 1

The colored scalars $\omega_{L,R}$ will, of course, in general transmit flavor-changing processes in the hadron sector. As example for this (and because they are well investigated experimentally), we consider oscillations of K- and $B_{d,s}$-mesons. The diagrams arising from $\omega_{L,R}$-exchange are drawn in Figure 8.7.

Let us start by considering $K^0 - \bar{K}^0$ oscillations. Assuming $M_{\omega_1} \simeq M_{\omega_2}$ and dominance of the top mass, the transition amplitude can be read off from the diagrams as

$$\begin{aligned} i\mathcal{M}_K &= 8|f'_{13}|^2|f'_{23}|^2 \int \frac{d^4k}{2\pi^4} [\bar{v}(s) P_L \frac{i(k+m_t)}{k^2-m_t^2} P_L u(d)][\bar{u}(s) P_R \frac{i(k+m_t)}{k^2-m_t^2} P_R v(d)] \left(\frac{i}{k^2-M_\omega^2}\right)^2 \\ &= 8|f'_{13}|^2|f'_{23}|^2 I(m_t, m_\omega) Q_K, \end{aligned} \tag{8.48}$$

where $f'_{ij} = \sqrt{2} f_{ij}$, $I(m_t, m_\omega) = \int \frac{d^4k}{2\pi^4} \frac{m_t^2}{(k^2-m_t^2)^2(k^2-M_\omega^2)^2} \simeq i \frac{m_t^2}{16\pi^2 M_\omega^2}$, and $Q_K = [\bar{v}(s) P_L u(d)][\bar{u}(s) P_R v(d)]$.

The factor 8 is the total number of the contributing diagrams.[4]

From Eq.(8.37), one can see easily that $\omega_{L,R}$ can be decomposed in terms of mass eigenstates as

$$\begin{aligned}\omega_L &= \frac{1}{\sqrt{2}}(\omega_1-\omega_2),\\ \omega_R &= \frac{1}{\sqrt{2}}(\omega_1+\omega_2).\end{aligned} \tag{8.49}$$

The transition amplitude reads

$$\mathcal{M}_K = \frac{2m_t^2}{\pi^2 M_\omega^4}|f_{13}|^2|f_{23}|^2 Q_K. \tag{8.50}$$

The mass difference of K_L–K_S is given by [240]

$$\Delta m_K = 2Re[\langle K^0|H^{\Delta S=2}|\bar{K}^0\rangle] = \frac{4m_t^2}{\pi^2 M_\omega^4}|f_{13}|^2|f_{23}|^2 Re[\langle Q_K\rangle], \tag{8.51}$$

where $H^{\Delta S=2}=\mathcal{M}_K$ and

$$\langle Q_K\rangle = \langle K^0|[\bar{v}(s)P_L u(d)][\bar{u}(s)P_R v(d)]|\bar{K}^0\rangle = \langle K^0|[\bar{s}P_L d][\bar{s}P_R d]|\bar{K}^0\rangle. \tag{8.52}$$

The matrix element $\langle Q_K\rangle$ can be written as [240]

$$\langle Q_K\rangle = \langle Q_2^{LR}(\mu)\rangle = \frac{1}{4}\Big(\frac{m_K}{m_s(\mu)+m_d(\mu)}\Big)^2 m_K F_K^2 B_2^{LR}(\mu). \tag{8.53}$$

Using $F_K = 155.74$ MeV [5], $m_K = 498$ MeV [46], and $[B_2^{LR}(\mu=2\text{GeV})]_{LRI} = 1.03$ [240][6], we obtain $\langle Q_K\rangle = 0.064\text{GeV}^3$. The mass of the scalar triplet is constrained by

$$M_\omega > \sqrt[4]{\frac{4m_t^2}{\pi^2\Delta m_K}|f_{13}|^2|f_{23}|^2\langle Q_K\rangle} = 38.3754\times\frac{16\pi^2}{|L|}\ \text{GeV}, \tag{8.54}$$

where we have used $\Delta m_K = 3.483\times10^{-12}$ MeV [46].

In the same way, we can also calculate the $B_d-\bar{B}_d$ and the $B_s-\bar{B}_s$ oscillations. The transition amplitudes are given by

$$\begin{aligned} i\mathcal{M}_{B_d} &= 8|f'_{13}|^2|f'_{33}|^2 I(m_t,m_\omega)Q_{B_d},\\ i\mathcal{M}_{B_s} &= 8|f'_{23}|^2|f'_{33}|^2 I(m_t,m_\omega)Q_{B_s},\end{aligned} \tag{8.55}$$

with

$$\langle Q_{B_q}\rangle = \langle B_q|[\bar{q}P_L b\bar{q}P_R d]|\bar{B}_q\rangle = \frac{1}{4}\Big(\frac{m_{B_q}}{m_b(\mu)+m_q(\mu)}\Big)^2 m_{B_q}F_{B_q}^2 B_4^q(\mu), \tag{8.56}$$

[4] Two from the rotated part and four from all possible combinations of $\omega'_{1,2}$.
[5] $F_K = 1.198\times F_\pi = 1.198\times 130$ MeV.
[6] LRI stands for Landau RI scheme.

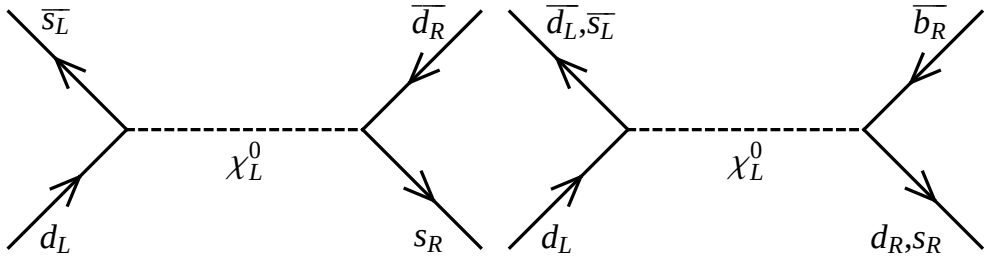

Figure 8.8: The diagrams for K-, B_d-, and B_s-mixing.

where we have made use of the formulae from Ref. [241].

The decay constants have been calculated using lattice QCD: $f_{B_d} = 216$ MeV, $f_{B_s} = 1.20 f_{B_d}$ [242, 243] and the non-perturbative B-factors are $B_4^d = 1.16$ and $B_4^s = 1.17$ [244].

The mass difference Δm_{B_q} is given by [240]

$$\Delta m_{B_q} = 2|\langle B_q|H_q^{\Delta B=2}|\bar{B}_q\rangle| = \frac{4m_t^2}{\pi^2 M_\omega^4}|f_{i3}|^2|f_{33}|^2|\langle Q_{B_q}\rangle|, \tag{8.57}$$

where $i = 1$ for B_d and $i = 2$ for B_s.
The experimental values are [46]

$$\begin{aligned} \Delta m_{B_d} &= 3.337 \times 10^{-10} \text{ MeV}, \\ \Delta m_{B_s} &= 1.17 \times 10^{-10} \text{ MeV}, \\ m_{B_d} &= 5279.50 \text{ MeV}, \\ m_{B_s} &= 5366.3 \text{ MeV}, \end{aligned} \tag{8.58}$$

so the constraints on the ω masses arising from B_d and B_s mixings are given by

$$\begin{aligned} (M_\omega)_{B_d} &> 70.4 \times \frac{16\pi^2}{|L|} \text{ GeV}, \\ (M_\omega)_{B_s} &> 356.6 \times \frac{16\pi^2}{|L|} \text{ GeV}, \end{aligned} \tag{8.59}$$

whose second line yields the strongest constraint. Assuming a typical value of $|L| \approx 0.1$, one can derive a lower limit of $M_\omega \gtrsim 6 \cdot 10^5$ GeV.

Model 2

In this model, we have new contributions to $K^0 - \bar{K}^0$ oscillations from χ_L^0 exchange at tree-level which dominate over other loop diagrams[7]. Note that $\chi_L^0 = \frac{1}{\sqrt{2}}(\chi_L^{0r} + i\chi_L^{0i})$. The diagrams arising from χ_L^0-exchange are drawn in Figure 8.8.

[7] We also have another contribution from $\chi_{R,L}^0$ exchange at loop-level, but we do not consider it here as it is small compared to the tree-level contribution. Apart from the $K^0 - \bar{K}^0$ oscillations, we can also have $D^0 - \bar{D}^0$ oscillations due to the exchange of the charged Higgses $\chi_{R,L}^+$ in the loop.

The transition amplitude can be read off from the diagrams as

$$\begin{aligned} i\mathcal{M}_K &= 4\left|\frac{f_{D,12}}{\sqrt{2}}\right|^2 [\bar{v}(s)P_R u(d)][\bar{u}(s)P_R v(d)]\left(\frac{i}{k^2 - M^2_{\chi^0_L}}\right) \\ &\simeq -2|f_{D,12}|^2\left(\frac{i}{M^2_{\chi^0_L}}\right) Q_K, \end{aligned} \tag{8.60}$$

where $Q_K = [\bar{v}(s)P_R u(d)][\bar{u}(s)P_R v(d)]$ and at low energy we assume that $M^2_{\chi^0_L} >> k^2$. The factor 4 is the total number of the contributing diagrams[8].

The transition amplitude reads

$$\mathcal{M}_K = -2|f_{D,12}|^2\left(\frac{1}{M^2_{\chi^0_L}}\right) Q_K. \tag{8.61}$$

The mass difference of K_L–K_S is given by [240]

$$\Delta m_K = 2Re[\langle K^0|H^{\Delta S=2}|\bar{K}^0\rangle] = -4|f_{D,12}|^2\left(\frac{1}{M^2_{\chi^0_L}}\right) Re[\langle Q_K\rangle], \tag{8.62}$$

where $H^{\Delta S=2} = \mathcal{M}_K$ and

$$\langle Q_K\rangle = \langle K^0|[\bar{v}(s)P_R u(d)][\bar{u}(s)P_R v(d)]|\bar{K}^0\rangle = \langle K^0|[\bar{s}P_R d][\bar{s}P_R d]|\bar{K}^0\rangle = \langle(\bar{s}_L d_R)(\bar{s}_L d_R)\rangle. \tag{8.63}$$

The matrix element $\langle Q_K\rangle$ can be written as [240]

$$\langle Q_K\rangle = \langle Q_1^{SLL}(\mu)\rangle = -\frac{5}{24}\Big(\frac{m_K}{m_s(\mu) + m_d(\mu)}\Big)^2 m_K F_K^2 B_1^{SLL}(\mu). \tag{8.64}$$

Using $F_K = 155.74$ MeV, $m_K = 498$ MeV [46], and $[B_1^{SLL}(\mu = 2\text{GeV})]_{LRI} = 0.66$ [240], we obtain $\langle Q_K\rangle = \text{GeV}^3$. The mass of χ^0_L is constrained by

$$M_{\chi^0_L} > 1.55 \times 10^8 \frac{1}{w_L}\ \text{GeV}^2, \tag{8.65}$$

where we have used $\Delta m_K = 3.483 \times 10^{-12}$ MeV [46].
In the same way, we can also calculate the $B_d - \bar{B}_d$ and the $B_s - \bar{B}_s$ oscillations. The transition amplitudes are given by

$$\begin{aligned} i\mathcal{M}_{B_d} &\simeq -2|f_{D,13}|^2\left(\frac{i}{M^2_{\chi^0_L}}\right) Q_{B_d}, \\ i\mathcal{M}_{B_s} &\simeq -2|f_{D,23}|^2\left(\frac{i}{M^2_{\chi^0_L}}\right) Q_{B_s}, \end{aligned} \tag{8.66}$$

[8]Two from the rotated part and two from the interchange of real and imaginary part of χ^0_L.

with $Q_{B_d} = (\bar{b}_L d_R)(\bar{b}_L d_R)$ and $Q_{B_s} = (\bar{b}_L s_R)(\bar{b}_L s_R)$.
The matrix elements of the operators Q_{B_d} and Q_{B_d} are given by[9]

$$\langle Q_{B_q} \rangle = \langle B_q | [\bar{b} P_R q \bar{b} P_R q] | \bar{B}_q \rangle = -\frac{5}{24} \Big(\frac{m_{B_q}}{m_b(\mu) + m_q(\mu)} \Big)^2 m_{B_q} F_{B_q}^2 B_2^q(\mu), \tag{8.67}$$

where we have made use of the formulae from Ref. [241].

The decay constants have been calculated using lattice QCD: $f_{B_d} = 216$ MeV, $f_{B_s} = 1.20 f_{B_d}$ [242, 243] and the non-perturbative B-factors are $B_2^d = 0.82$ and $B_2^s = 0.83$ [244].

The mass difference Δm_{B_q} is given by [240]

$$\Delta m_{B_q} = 2 |\langle B_q | H_q^{\Delta B=2} | \bar{B}_q \rangle| = -4 |f_{D,i3}|^2 \left(\frac{1}{M_{\chi_L^0}^2} \right) \langle Q_{B_d} \rangle, \tag{8.68}$$

where $i = 1$ for B_d and $i = 2$ for B_s.
The experimental values are [46]

$$\begin{aligned} \Delta m_{B_d} &= 3.337 \times 10^{-10} \text{ MeV}, \\ \Delta m_{B_s} &= 1.17 \times 10^{-10} \text{ MeV}, \\ m_{B_d} &= 5279.50 \text{ MeV}, \\ m_{B_s} &= 5366.3 \text{ MeV}, \end{aligned} \tag{8.69}$$

so the constraints from B_d and B_s mixings are given by

$$\begin{aligned} (M_{\chi_L^0})_{B_d} &> 2.8 \times 10^7 \frac{1}{w_L} \text{ GeV}^2, \\ (M_{\chi_L^0})_{B_s} &> 6.1 \times 10^8 \frac{1}{w_L} \text{ GeV}^2, \end{aligned} \tag{8.70}$$

whose second line yields the best constraint. Assuming the VEV of χ_L^0 as, $w_L \approx 100$ GeV, one can derive a lower limit of $M_{\chi_L}^0 \gtrsim \mathcal{O}(10^6 \text{ GeV})$.

In this chapter, we have constructed an LR symmetric model for the radiative neutrino masses. The neutrinos obtain their mass at one-loop level. Assuming that the charged lepton mass matrix is diagonal, the hierarchy structure in the charged lepton mass matrix is transfered to the right-handed neutrino mass matrix. We called this observation: Radiative Transmission of Lepton Flavor Hierarchy. We have also discussed the phenomenological aspects of the model such as lepton flavor violation and lepton number violation. Moreover, in order to make a realistic model that includes non-zero down quark masses, we have extended the model in two ways: (model 1) introduction of color triplet isospin singlet fields that give radiative masses to down quarks or (model 2) the addition of three isospin singlet vector-like down quarks, which generate a tree-level mass for the down quarks. These two models lead to an interesting phenomenology which might show up at the LHC. In model 1, the hierarchy between up quark and down quark masses is explained, and the scalar color triplets can contribute to the new heavy bound states such as $\omega QQ, \bar{\omega}\omega, \omega\omega\omega$, etc. The generic feature of

[9] Their structure is the same as the Q_2 given in [241].

model 1 is that the masses of the scalar color triplets are not determined by the symmetry breaking scale (normally, the mass of particle is corresponding to the symmetry breaking scale) and seem to be the free parameters which have to be constrained by experiments. In model 2, the additional particle content (d_R and D_L) does not lead to a new anomaly. However, it leads to a new source of the FCNCs, which can be used for constraining the parameter space of this model.

Chapter 9

Conclusions

In this thesis, we have discussed two important problems of the Standard Model of Particle Physics, which are the flavor problem and the reason for the smallness of neutrino masses.

After discussing some aspects of model building in Chapter 2, we have presented two flavor models based on non-abelian discrete flavor symmetries. The first model was constructed based on D_4 flavor symmetry, which predicts the $\mu-\tau$ symmetry in the neutrino mass matrix leading to maximal atmospheric mixing $\theta_{23} = \pi/4$ and vanishing θ_{13}. The second model was based on D_{10} flavor symmetry, which leads the golden ratio prediction for solar neutrino mixing, i.e. $\cos(\theta_{12}) = \varphi/2$, with the golden ratio $\varphi = \varphi^2 - 1 = \frac{1}{2}(1+\sqrt{5})$, and also vanishing θ_{13}. In order for the flavor symmetries to give these predictions for the neutrino mixing, they have to be broken by flavons with a certain VEV structure, which arise as the result of the minimization of a scalar potential. We have also investigated the flavon superpotential of these models, and showed that these VEV structures are obtained. Furthermore, we have observed the connection between the mismatch of subgroups and the neutrino mixing prediction, i.e., a neutrino mixing pattern is a result of the breaking of the flavor symmetry down to different preserved subgroups in charged lepton and neutrino sectors.

As the SM is constructed based on two important symmetries, i.e., gauge symmetry and space-time symmetry, therefore, it might be an interesting task to embed the non-abelian discrete flavor symmetry into one of these symmetries. In Chapter 4, we have discussed the case where a non-abelian discrete flavor symmetry might arise as a subgroup of a continuous symmetry, i.e., $SU(2)$ or $SU(3)$. We have considered all possible cases, where the continuous symmetry is broken by the small representations of the flavons, which can couple directly to the three generations of fermions at leading order. As a result of this, the only non-abelian discrete group which can arise as a residual symmetry is the quaternion group D_2', which cannot be used for predicting very specific mixing patterns, such as tri-bimaximal mixing. In Chapter 5, we have investigated the possible origin of non-abelian discrete flavor symmetries from an orbifold compactification. We have discussed all possible 2-dimensional orbifolds, which are $T^2/Z_2, T^2/Z_3, T^2/Z_4$, and T^2/Z_6. We have found out that all non-abelian discrete flavor symmetries that can arise from these orbifolds are A_4, S_4, D_4, D_3, and D_6, which have been widely used for flavor model building. We note that the first two, A_4 and S_4 have already been discussed in [28]. Moreover, we have shown that all representations of these groups can be realized as their localization on the orbifold fixed points. In Chapter 6, we have pursued the idea of an orbifold compactification further. We have discussed that not only the non-abelian discrete flavor symmetries can arise from the orbifold compactification, but they can

be broken by the orbifolding as well. Moreover, if we combine this model with an orbifold GUT, the GUT group can also be broken by the orbifold. We called this idea: the flavored orbifold GUT. We have demonstrate this idea by constructing the model based on SUSY $SO(10) \times S_4$ in 6-dimensions. $SO(10)$ is broken to $G_{SM'} = SU(3) \times SU(2) \times U(1)_Y \times U(1)_X$ by a certain choice of the orbifold parities, where the additional $U(1)_X$ was broken further by the left-handed conjugate Majorana neutrino mass term. We have shown that in the same way non-abelian discrete flavor symmetries can be broken by the orbifold. By choices of the orbifold parities, the VEV alignment of flavons can be determined without dealing with a complicated flavon potential. We have discussed all possible VEV alignments of the two- and three-dimensional representations of S_4, which have been listed in Table 6.3. Eventually, we have shown that this model leads to the smallness of neutrino masses by the type-II seesaw mechanism and predicts the tri-bimaximal mixing. We also note that the model can fit the quark sector and charged lepton masses.

In Chapter 7, we have performed a study on a model with an extended scalar sector and a flavor symmetry. The extended scalar sector model leads to lepton flavor violation (LFV), which results in the constraints on the parameter space of Physics Beyond Standard Model. However, when we impose a flavor symmetry to generate a certain structure of the mass matrices leading to the prediction of the neutrino mixing, the extended scalar model might be ruled out by the LFV constraint. We have illustrated this using two examples based on the Ma-model, one with an A_4 and one with a D_4 symmetry. For the Higgs sector of the models, we have used the four different benchmark scenarios that all fulfill the consistency conditions, as well as the experimental bounds from direct searches and from the measurement of the correction to the ρ-parameter (at 3σ). Since the first model exhibits a relatively rigid structure (only three free parameters), it is already excluded for all four scenarios by existing bounds. Even though the second model has more than twice as many free parameters, it can still be strongly constrained and two of the scenarios can either be excluded or tested in the near future. We want to stress that our considerations are not at all restricted to Ma-like models, but should apply to a much wider class of theories. Models with a lot of structure (meaning few parameters) may easily be excluded by existing or future LFV-bounds although they have no problems without the flavor symmetry. Even models with many parameters can at least be strongly constrained, if not excluded as well.

In Chapter 8, we have proposed a one-loop neutrino mass model in the left-right symmetric framework. The model leads to the effective Ma-model after the LR symmetry is broken. Assuming that the charged lepton mass matrix is diagonal, the hierarchy structure in the charged lepton mass matrix is transfered to the right-handed neutrino mass matrix. We called this observation: Radiative Transmission of Lepton Flavor Hierarchy. We have also discussed the phenomenological aspects of the model such as lepton flavor violation and lepton number violation. In the lepton sector, we have found out that the strongest constraint of the scale of the LR symmetry breaking stems from the lepton flavor violating process, $\mu^{\pm} \to e^{\pm}e^{\mp}e^{\mp}$, mediated by the Higgs triplets. Assuming the couplings between charged leptons and the Higgs triplets are of order $\mathcal{O}(0.1)$, it leads to a constraint on the masses of the Higgs triplets as $m_\delta \gtrsim 2 \cdot 10^5$ GeV, which can be considered as the LR symmetry breaking scale. We have also discussed leptogenesis in our model and found out that it does not work in our model because of the constraint on the Dirac Yukawa coupling. In the quark sector, the up quark masses are obtained at leading order, however, the down quark masses are forbidden due to a Z_4 symmetry. Therefore, we have extended the model in two ways: (model 1) introduction of color triplet isospin singlet fields that give radiative masses to down quarks or (model 2)

the addition of three isospin singlet vector-like down quarks, which generate a tree-level mass for the down quarks. These two models lead to an interesting phenomenology which might show up at the LHC. In model 1, the down quark masses are obtained at one-loop, therefore, the hierarchy between up quark and down quark masses is explained. Moreover, the scalar color triplets can contribute to the new heavy bound states such as $\omega QQ, \bar{\omega}\omega, \omega\omega\omega$, etc. We have also studied flavor changing neutral current processes such as $K^0 - \bar{K}^0$, $B_d - \bar{B}_d$ and $B_s - \bar{B}_s$ oscillations induced by the exchange of the scalar color triplets. Assuming a typical value of $|L| \simeq |\frac{\Delta M_\omega}{M_\omega}| \approx 0.1$, we obtained a lower limit on the mass of the scalar color triplet as $M_\omega \gtrsim 6 \cdot 10^5$ GeV. In model 2, we have introduced two additional Higgs doublets, $\chi_{L,R}$, which obtain VEVs and give masses to the light (d) and heavy (D) down quarks respectively. The additional Higgs χ_L leads to the flavor changing neutral current processes at tree-level. Considering these processes, we have obtained a constraint for the mass of the Higgs χ_L as $M^0_{\chi_L} \gtrsim \mathcal{O}(10^6$ GeV). Moreover, we also have new heavy hadrons due to the existence of the heavy (D) quarks in this model, which might be detected at the LHC. Combining the constraint from the lepton sector and the quark sector, the LR symmetry breaking scale in model 2 is of order $\mathcal{O}(10^6$ GeV).

In summary, two important problems of the SM have been investigated. The first problem has been discussed in the context of non-abelian discrete flavor symmetries and their origins. We have shown that a promising origin of non-abelian discrete flavor symmetries is the orbifold compactification. Moreover, we have shown that the idea of a flavored orbifold GUT is a simple and promising possibility to obtain the required fermion mass structures. Since orbifolds often appear in heterotic string theory model building, it might be an interesting task to embed the flavored orbifold GUT into the string context. The second problem is concerning the reason for the smallness of neutrino masses. We have proposed a one-loop neutrino mass model in the LR symmetric framework, which leads to an interesting observation, which we called: Radiative Transmission of Lepton Flavor Hierarchy. The result of this observation stems from the fact that the Dirac Yukawa coupling of neutrinos are embedded into a bigger gauge group, in this case LR symmetry. Therefore, it might be an outlook of this study to consider other classes of models, in which this observation might show up. Moreover, the model has provided a dark matter candidate, and many interesting phenomenological aspects at the LHC.

List of Abbreviations

- BSM: Physics Beyond the Standard Model
- CKM: Cabibbo-Kobayashi-Maskawa
- FCNCs: Flavor Changing Neutral Currents
- FN: Froggat-Nielsen
- IH: Inverse Hierarchy
- LFV: Lepton Flavor Violation
- LHC: Large Hadron Collider
- LNV: Lepton Number Violation
- LR: Left-Right Symmetric
- MSSM: Minimal Supersymmetric Standard Model
- NH: Normal Hierarchy
- PMNS: Pontecorvo-Maki-Nagakawa-Sakata
- SM: The Standard Model of Particle Physics
- SUSY: Supersymmetry
- THDM: Two Higgs Doublet Model
- VEV: Vacuum Expectation Value

Acknowledgements

First of all, I would like to thank my supervisor Manfred Lindner for accepting me as his PhD student. I would like to thank him for spending his time with me to discuss many interesting topics in physics. Moreover, I would like to thank him also for giving many opportunities to attend PSI Zuoz Summerschool 2008, Workshops, and Conferences, which I have learned a lot.

It is a good pleasure for me to acknowledge the support of the following people:

- Michael G. Schmidt and Werner Rodejohann for being my co-advisors.
- My thesis referees: Manfred Lindner and Michael G. Schmidt for taking the time to read my thesis.
- Ulrich Uwer and Eberhard Grün for taking the time to be my examiners.
- Alexander Blum, Alexander Merle, and Michael A. Schmidt for spending a lot of time with me to discuss many interesting aspects in physics.
- Alexander Blum, Claudia Hagedorn, Manfred Lindner, Alexander Merle, Rabindra N. Mohapatra, Werner Rodejohann, and Michael A. Schmidt for the fruitful collaborations.
- Alexander Merle and Michael A. Schmidt for the proofreading of my thesis and also for giving useful comments.
- Michael A. Schmidt for his kindly help for translating my abstract to German.
- Andreas Hohenegger for giving comments on my abstract.
- Our secretary Anja Berneiser for taking care of all administration tasks.
- My office mate Alexander Kartavtsev for his help to keep my computer running.
- For the nice atmosphere in our group: Evgeny Akhmedov, James Barry, Anja Berneiser, Fedor Bezrukov, Alexander Blum, Alexander Dueck, Michael Duerr, Peihong Gu, Claudia Hagedorn, Frank Hartmann, Julia Haser, Julian Heeck, Hans Hettmansperger, Andreas Hohenegger, Martin Holthausen, Felix Kahlhoefer, Alexander Kartavtsev, Hendrik Kienert, Joachim Kopp, Nico Kronberg, Sebastian Lindemann, Werner Maneschg, Manfred Lindner, Werner Rodejohann, Daniel Schmidt, Angnis Schmidt-May, Michael A. Schmidt, Thomas Schwetz-Mangold, Alexander Merle, Viviana Niro, Ryo Takahashi, Thomas E. J. Underwood, Hideki Watanabe, and the whole division of "particle and astroparticle physics" at MPI-K.

Finally, I would like to thank my family: Supat, Vanpen, and Apivat Adulpravitchai for their love and support.

Appendix A

Group Theory

A.1 Group Theory of Dihedral Groups D_n

In this section, we briefly discuss the group theory of dihedral groups, D_n. For more detail discussion, we refer to [184, 195, 196]. The dihedral group is the group of regular two-sided polygon with n corner and n edges. If the index n is even, the group D_n has four one-dimensional representations denoted by $\underline{\mathbf{1}}_{1,2,3,4}$ and $\frac{n}{2}-1$ two-dimensional representations denoted by $\underline{\mathbf{2}}_j$, where $j = 1, ..., \frac{n}{2}-1$. If the index n is odd, the group D_n has only two one-dimensional representations denoted by $\underline{\mathbf{1}}_{1,2}$ and $\frac{n-1}{2}$ two-dimensional representations denoted by $\underline{\mathbf{2}}_j$, where $j = 1, ..., \frac{n-1}{2}$. The $\underline{\mathbf{1}}_1$ is always the trivial one. The order of the D_n group is $2n$. The D_n group is generated by two generators, A and B, where the one-dimensional representations transform as:

- $\underline{\mathbf{1}}_1$: $A = 1, B = 1$
- $\underline{\mathbf{1}}_2$: $A = 1, B = -1$
- $\underline{\mathbf{1}}_3$: $A = -1, B = 1$
- $\underline{\mathbf{1}}_4$: $A = -1, B = -1$.

The generators of the two-dimensional representations are given by [183]

$$A = \begin{pmatrix} e^{(\frac{2\pi i}{n})j} & 0 \\ 0 & e^{-(\frac{2\pi i}{n})j} \end{pmatrix} \text{ , and } B = \begin{pmatrix} 0 & 1 \\ 1 & 0 \end{pmatrix} , \tag{A.1}$$

where j is the index of a two dimensional representation $\underline{\mathbf{2}}_j$.
The generator relations are given by

$$A^n = 1 \ , \ B^2 = 1 \ , \text{ and } ABA = A. \tag{A.2}$$

A.2 Group Theory of D_{10}

The group D_{10} is a group which describes the symmetry of a ten-sided polygon. It has two generators, A and B, which fulfill the relations

$$A^{10} = B^2 = 1 \quad \text{and} \quad ABA = B. \tag{A.3}$$

$\times$	$\underline{\mathbf{1}}_\mathbf{1}$	$\underline{\mathbf{1}}_\mathbf{2}$	$\underline{\mathbf{1}}_\mathbf{3}$	$\underline{\mathbf{1}}_\mathbf{4}$
$\underline{\mathbf{1}}_\mathbf{1}$	$\underline{\mathbf{1}}_\mathbf{1}$	$\underline{\mathbf{1}}_\mathbf{2}$	$\underline{\mathbf{1}}_\mathbf{3}$	$\underline{\mathbf{1}}_\mathbf{4}$
$\underline{\mathbf{1}}_\mathbf{2}$	$\underline{\mathbf{1}}_\mathbf{2}$	$\underline{\mathbf{1}}_\mathbf{1}$	$\underline{\mathbf{1}}_\mathbf{4}$	$\underline{\mathbf{1}}_\mathbf{3}$
$\underline{\mathbf{1}}_\mathbf{3}$	$\underline{\mathbf{1}}_\mathbf{3}$	$\underline{\mathbf{1}}_\mathbf{4}$	$\underline{\mathbf{1}}_\mathbf{1}$	$\underline{\mathbf{1}}_\mathbf{2}$
$\underline{\mathbf{1}}_\mathbf{4}$	$\underline{\mathbf{1}}_\mathbf{4}$	$\underline{\mathbf{1}}_\mathbf{3}$	$\underline{\mathbf{1}}_\mathbf{2}$	$\underline{\mathbf{1}}_\mathbf{1}$

$\times$	$\underline{\mathbf{2}}_\mathbf{1}$	$\underline{\mathbf{2}}_\mathbf{2}$	$\underline{\mathbf{2}}_\mathbf{3}$	$\underline{\mathbf{2}}_\mathbf{4}$
$\underline{\mathbf{2}}_\mathbf{1}$	$\underline{\mathbf{1}}_\mathbf{1} + \underline{\mathbf{1}}_\mathbf{2} + \underline{\mathbf{2}}_\mathbf{2}$	$\underline{\mathbf{2}}_\mathbf{1} + \underline{\mathbf{2}}_\mathbf{3}$	$\underline{\mathbf{2}}_\mathbf{2} + \underline{\mathbf{2}}_\mathbf{4}$	$\underline{\mathbf{1}}_\mathbf{3} + \underline{\mathbf{1}}_\mathbf{4} + \underline{\mathbf{2}}_\mathbf{3}$
$\underline{\mathbf{2}}_\mathbf{2}$	$\underline{\mathbf{2}}_\mathbf{1} + \underline{\mathbf{2}}_\mathbf{3}$	$\underline{\mathbf{1}}_\mathbf{1} + \underline{\mathbf{1}}_\mathbf{2} + \underline{\mathbf{2}}_\mathbf{4}$	$\underline{\mathbf{1}}_\mathbf{3} + \underline{\mathbf{1}}_\mathbf{4} + \underline{\mathbf{2}}_\mathbf{1}$	$\underline{\mathbf{2}}_\mathbf{2} + \underline{\mathbf{2}}_\mathbf{4}$
$\underline{\mathbf{2}}_\mathbf{3}$	$\underline{\mathbf{2}}_\mathbf{2} + \underline{\mathbf{2}}_\mathbf{4}$	$\underline{\mathbf{1}}_\mathbf{3} + \underline{\mathbf{1}}_\mathbf{4} + \underline{\mathbf{2}}_\mathbf{1}$	$\underline{\mathbf{1}}_\mathbf{1} + \underline{\mathbf{1}}_\mathbf{2} + \underline{\mathbf{2}}_\mathbf{4}$	$\underline{\mathbf{2}}_\mathbf{1} + \underline{\mathbf{2}}_\mathbf{3}$
$\underline{\mathbf{2}}_\mathbf{4}$	$\underline{\mathbf{1}}_\mathbf{3} + \underline{\mathbf{1}}_\mathbf{4} + \underline{\mathbf{2}}_\mathbf{3}$	$\underline{\mathbf{2}}_\mathbf{2} + \underline{\mathbf{2}}_\mathbf{4}$	$\underline{\mathbf{2}}_\mathbf{1} + \underline{\mathbf{2}}_\mathbf{3}$	$\underline{\mathbf{1}}_\mathbf{1} + \underline{\mathbf{1}}_\mathbf{2} + \underline{\mathbf{2}}_\mathbf{2}$

$$\underline{\mathbf{1}}_{\mathbf{1,2}} \times \underline{\mathbf{2}}_\mathbf{j} = \underline{\mathbf{2}}_\mathbf{j} \;,\quad \underline{\mathbf{1}}_{\mathbf{3,4}} \times \underline{\mathbf{2}}_\mathbf{j} = \underline{\mathbf{2}}_{\mathbf{5\text{-}j}}$$

Table A.1: Multiplication rules for the dihedral group D_{10}, which has four two-dimensional and four 1-dimensional irreducible representations.

The multiplication rules for the Kronecker products are given in Table A.1. For $s_i \sim \underline{\mathbf{1}}_\mathbf{i}$ and $(a_1, a_2)^T \sim \underline{\mathbf{2}}_\mathbf{j}$ we find

$$\begin{pmatrix} s_1 a_1 \\ s_1 a_2 \end{pmatrix} \sim \underline{\mathbf{2}}_\mathbf{j} \;,\quad \begin{pmatrix} s_2 a_1 \\ -s_2 a_2 \end{pmatrix} \sim \underline{\mathbf{2}}_\mathbf{j} \;,\quad \begin{pmatrix} s_3 a_2 \\ s_3 a_1 \end{pmatrix} \sim \underline{\mathbf{2}}_{\mathbf{5\text{-}j}} \;,\quad \text{and} \quad \begin{pmatrix} s_4 a_2 \\ -s_4 a_1 \end{pmatrix} \sim \underline{\mathbf{2}}_{\mathbf{5\text{-}j}} \;.$$

The Clebsch-Gordan coefficients for the product of $(a_1, a_2)^T$ with $(b_1, b_2)^T$, both in $\sim \underline{\mathbf{2}}_\mathbf{i}$, read

$$a_1 b_2 + a_2 b_1 \sim \underline{\mathbf{1}}_\mathbf{1} \;,\quad a_1 b_2 - a_2 b_1 \sim \underline{\mathbf{1}}_\mathbf{2} \;,$$
$$\begin{pmatrix} a_1 b_1 \\ a_2 b_2 \end{pmatrix} \sim \underline{\mathbf{2}}_\mathbf{j} \quad \text{or} \quad \begin{pmatrix} a_2 b_2 \\ a_1 b_1 \end{pmatrix} \sim \underline{\mathbf{2}}_\mathbf{j} \,,$$

depending on whether $\mathrm{i} = 1, 2$ or $\mathrm{i} = 3, 4$. For the two doublets $(a_1, a_2)^T \sim \underline{\mathbf{2}}_\mathbf{i}$ and $(b_1, b_2)^T \sim \underline{\mathbf{2}}_\mathbf{j}$ we find for $\mathrm{i} + \mathrm{j} \neq 5$

$$\begin{pmatrix} a_1 b_2 \\ a_2 b_1 \end{pmatrix} \sim \underline{\mathbf{2}}_\mathbf{k} \quad (\mathrm{k} = \mathrm{i} - \mathrm{j}) \quad \text{or} \quad \begin{pmatrix} a_2 b_1 \\ a_1 b_2 \end{pmatrix} \sim \underline{\mathbf{2}}_\mathbf{k} \quad (\mathrm{k} = \mathrm{j} - \mathrm{i}) \,,$$
$$\begin{pmatrix} a_1 b_1 \\ a_2 b_2 \end{pmatrix} \sim \underline{\mathbf{2}}_\mathbf{l} \quad (\mathrm{l} = \mathrm{i} + \mathrm{j}) \quad \text{or} \quad \begin{pmatrix} a_2 b_2 \\ a_1 b_1 \end{pmatrix} \sim \underline{\mathbf{2}}_\mathbf{l} \quad (\mathrm{l} = 10 - (\mathrm{i} + \mathrm{j})) \,.$$

If $\mathrm{i} + \mathrm{j} = 5$ holds the covariants read

$$a_1 b_1 + a_2 b_2 \sim \underline{\mathbf{1}}_\mathbf{3} \;,\quad a_1 b_1 - a_2 b_2 \sim \underline{\mathbf{1}}_\mathbf{4} \;,$$
$$\begin{pmatrix} a_1 b_2 \\ a_2 b_1 \end{pmatrix} \sim \underline{\mathbf{2}}_\mathbf{k} \quad \text{or} \quad \begin{pmatrix} a_2 b_1 \\ a_1 b_2 \end{pmatrix} \sim \underline{\mathbf{2}}_\mathbf{k} \,.$$

Again, the first case is relevant for $\mathrm{k} = \mathrm{i} - \mathrm{j}$, while the second one is valid for $\mathrm{k} = \mathrm{j} - \mathrm{i}$.

A.3 Group Theory of A_4

In this section, we use the A_4 basis given in [104]. The group A_4 is a group which describes even permutations of four objects. It has two generators, S and T, that fulfill the relations

$$S^2 = (ST)^3 = T^3 = 1. \tag{A.1}$$

The group has four inequivalent irreducible representations, $\underline{\mathbf{1}}, \underline{\mathbf{1}}', \underline{\mathbf{1}}''$, and $\underline{\mathbf{3}}$, which transform under the generators, S and T as follows:

$$\begin{aligned} \underline{\mathbf{1}}: &\quad S = 1, \;\; T = 1, \\ \underline{\mathbf{1}}': &\quad S = 1, \;\; T = \omega^2, \\ \underline{\mathbf{1}}'': &\quad S = 1, \;\; T = \omega, \end{aligned} \tag{A.2}$$

$$\underline{\mathbf{3}}: \quad T = \begin{pmatrix} 1 & 0 & 0 \\ 0 & \omega^2 & 0 \\ 0 & 0 & \omega \end{pmatrix}, \quad S = \frac{1}{3}\begin{pmatrix} -1 & 2 & 2 \\ 2 & -1 & 2 \\ 2 & 2 & -1 \end{pmatrix}, \tag{A.3}$$

where $\omega = e^{i2\pi/3}$ (which implies $\omega^4 = \omega$).
The product rules for the singlets are the following:

$$\underline{\mathbf{1}}' \times \underline{\mathbf{1}}' = \underline{\mathbf{1}}'', \quad \underline{\mathbf{1}}' \times \underline{\mathbf{1}}'' = \underline{\mathbf{1}}, \quad \underline{\mathbf{1}}'' \times \underline{\mathbf{1}}'' = \underline{\mathbf{1}}', \quad \underline{\mathbf{1}} \times \underline{\mathbf{1}} = \underline{\mathbf{1}}, \quad \underline{\mathbf{1}} \times \underline{\mathbf{1}}' = \underline{\mathbf{1}}', \quad \underline{\mathbf{1}} \times \underline{\mathbf{1}}'' = \underline{\mathbf{1}}''. \tag{A.4}$$

Consider now two triplets:

$$a = (a_1, a_2, a_3)^T, \quad b = (b_1, b_2, b_3)^T. \tag{A.5}$$

The product of these two triplets can be decomposed as

$$\underline{\mathbf{3}} \times \underline{\mathbf{3}} = \underline{\mathbf{1}} + \underline{\mathbf{1}}' + \underline{\mathbf{1}}'' + \underline{\mathbf{3}}_s + \underline{\mathbf{3}}_a, \tag{A.6}$$

where

$$\begin{aligned} \underline{\mathbf{1}} &= (ab) = a_1b_1 + a_2b_3 + a_3b_2, \\ \underline{\mathbf{1}}' &= (ab)' = a_3b_3 + a_1b_2 + a_2b_1, \\ \underline{\mathbf{1}}'' &= (ab)'' = a_2b_2 + a_1b_3 + a_3b_1, \end{aligned} \tag{A.7}$$

and

$$\begin{aligned} \underline{\mathbf{3}}_s &= (ab)_s = \frac{1}{2}(2a_1b_1 - a_2b_3 - a_3b_2, 2a_3b_3 - a_1b_2 - a_2b_1, 2a_2b_2 - a_1b_3 - a_3b_1)^T, \\ \underline{\mathbf{3}}_a &= (ab)_a = \frac{1}{2}(a_2b_3 - a_3b_2, a_1b_2 - a_2b_1, a_1b_3 - a_3b_1)^T. \end{aligned} \tag{A.8}$$

	n	h	χ_1	$\chi_{1'}$	χ_2	χ_3	$\chi_{3'}$	Example
$\mathcal{C}_1$	1	1	1	1	2	3	3	1
$\mathcal{C}_2$	3	2	1	1	2	-1	-1	S^2
$\mathcal{C}_3$	8	3	1	1	-1	0	0	T
$\mathcal{C}_4$	6	2	1	-1	0	1	-1	ST^2
$\mathcal{C}_5$	6	4	1	-1	0	-1	1	S

Table A.2: Character table of S_4. $\mathcal{C}_i$ are the conjugacy classes, n the number of elements in each class, h the smallest value for which $\chi^h = 1$. In the last column we have reported an example of the elements for each class.

A.4 Group Theory of S_4

In this section, we use the S_4 basis given in [204]. The character table of the group S_4 is given in Table A.4
The generators, S and T, obey to the following rules

$$S^4 = T^3 = (ST^2)^2 = 1 \tag{A.9}$$

and can be written in the different representations as

representation $\underline{\mathbf{1}}_\mathbf{1}$: $S = 1, T = 1$

representation $\underline{\mathbf{1}}_\mathbf{2}$: $S = -1, T = 1$

representation $\underline{\mathbf{2}}$: $S = \begin{pmatrix} 0 & 1 \\ 1 & 0 \end{pmatrix}, T = \begin{pmatrix} \omega & 0 \\ 0 & \omega^2 \end{pmatrix}$

representation $\underline{\mathbf{3}}_\mathbf{1}$: $S = \frac{1}{3}\begin{pmatrix} -1 & 2\omega & 2\omega^2 \\ 2\omega & 2\omega^2 & -1 \\ 2\omega^2 & -1 & 2\omega \end{pmatrix}, T = \begin{pmatrix} 1 & 0 & 0 \\ 0 & \omega^2 & 0 \\ 0 & 0 & \omega \end{pmatrix}$

representation $\underline{\mathbf{3}}_\mathbf{2}$: $S = \frac{1}{3}\begin{pmatrix} 1 & -2\omega & -2\omega^2 \\ -2\omega & -2\omega^2 & 1 \\ -2\omega^2 & 1 & -2\omega \end{pmatrix}, T = \begin{pmatrix} 1 & 0 & 0 \\ 0 & \omega^2 & 0 \\ 0 & 0 & \omega \end{pmatrix}$.

The 24 elements of the group belong to five conjugacy classes

$$\begin{aligned}
\mathcal{C}_1 :&\quad 1 \\
\mathcal{C}_2 :&\quad S^2,\, TS^2T^2,\, S^2TS^2T^2 \\
\mathcal{C}_3 :&\quad T,\, T^2,\, S^2T,\, S^2T^2,\, STST^2,\, STS,\, S^TS^2,\, S^3TS \\
\mathcal{C}_4 :&\quad ST^2,\, T^2S,\, TST,\, TSTS^2,\, STS^2,\, S^2TS \\
\mathcal{C}_5 :&\quad S,\, TST^2,\, ST,\, TS,\, S^3,\, S^3T^2 \,.
\end{aligned}$$

In the two-dimensional representation the elements are

$$\mathcal{C}_{1,2}: \quad \begin{pmatrix} 1 & 0 \\ 0 & 1 \end{pmatrix},$$

$$\mathcal{C}_3: \quad \begin{pmatrix} \omega & 0 \\ 0 & \omega^2 \end{pmatrix}, \begin{pmatrix} \omega^2 & 0 \\ 0 & \omega \end{pmatrix},$$

$$\mathcal{C}_{4,5}: \quad \begin{pmatrix} 0 & 1 \\ 1 & 0 \end{pmatrix}, \begin{pmatrix} 0 & \omega \\ \omega^2 & 0 \end{pmatrix}, \begin{pmatrix} 0 & \omega^2 \\ \omega & 0 \end{pmatrix},$$

while for the three-dimensional representation $\underline{\mathbf{3}}_{\mathbf{1}}$ the elements are

$$\mathcal{C}_1: \quad \begin{pmatrix} 1 & 0 & 0 \\ 0 & 1 & 0 \\ 0 & 0 & 1 \end{pmatrix},$$

$$\mathcal{C}_2: \quad \frac{1}{3}\begin{pmatrix} -1 & 2 & 2 \\ 2 & -1 & 2 \\ 2 & 2 & -1 \end{pmatrix}, \frac{1}{3}\begin{pmatrix} -1 & 2\omega & 2\omega^2 \\ 2\omega^2 & -1 & 2\omega \\ 2\omega & 2\omega^2 & -1 \end{pmatrix}, \frac{1}{3}\begin{pmatrix} -1 & 2\omega^2 & 2\omega \\ 2\omega & -1 & 2\omega^2 \\ 2\omega^2 & 2\omega & -1 \end{pmatrix},$$

$$\mathcal{C}_3: \quad \begin{pmatrix} 1 & 0 & 0 \\ 0 & \omega^2 & 0 \\ 0 & 0 & \omega \end{pmatrix}, \begin{pmatrix} 1 & 0 & 0 \\ 0 & \omega & 0 \\ 0 & 0 & \omega^2 \end{pmatrix},$$
$$\frac{1}{3}\begin{pmatrix} -1 & 2\omega^2 & 2\omega \\ 2 & -\omega^2 & 2\omega \\ 2 & 2\omega^2 & -\omega \end{pmatrix}, \frac{1}{3}\begin{pmatrix} -1 & 2\omega & 2\omega^2 \\ 2 & -\omega & 2\omega^2 \\ 2 & 2\omega & -\omega^2 \end{pmatrix}, \frac{1}{3}\begin{pmatrix} -1 & 2 & 2 \\ 2\omega^2 & -\omega^2 & 2\omega^2 \\ 2\omega & 2\omega & -\omega \end{pmatrix},$$
$$\frac{1}{3}\begin{pmatrix} -1 & 2\omega^2 & 2\omega \\ 2\omega^2 & -\omega & 2 \\ 2\omega & 2 & -\omega^2 \end{pmatrix}, \frac{1}{3}\begin{pmatrix} -1 & 2\omega & 2\omega^2 \\ 2\omega & -\omega^2 & 2 \\ 2\omega^2 & 2 & -\omega \end{pmatrix}, \frac{1}{3}\begin{pmatrix} -1 & 2 & 2 \\ 2\omega & -\omega & 2\omega \\ 2\omega^2 & 2\omega^2 & -\omega^2 \end{pmatrix},$$

$$\mathcal{C}_4: \quad \frac{1}{3}\begin{pmatrix} -1 & 2\omega^2 & 2\omega \\ 2\omega & 2 & -\omega^2 \\ 2\omega^2 & -\omega & 2 \end{pmatrix}, \frac{1}{3}\begin{pmatrix} -1 & 2\omega & 2\omega^2 \\ 2\omega^2 & 2 & -\omega \\ 2\omega & -\omega^2 & 2 \end{pmatrix}, \frac{1}{3}\begin{pmatrix} -1 & 2 & 2 \\ 2 & 2 & -1 \\ 2 & -1 & 2 \end{pmatrix},$$
$$\begin{pmatrix} 1 & 0 & 0 \\ 0 & 0 & 1 \\ 0 & 1 & 0 \end{pmatrix}, \begin{pmatrix} 1 & 0 & 0 \\ 0 & 0 & \omega \\ 0 & \omega^2 & 0 \end{pmatrix}, \begin{pmatrix} 1 & 0 & 0 \\ 0 & 0 & \omega^2 \\ 0 & \omega & 0 \end{pmatrix},$$

$$\mathcal{C}_5: \quad \frac{1}{3}\begin{pmatrix} -1 & 2\omega & 2\omega^2 \\ 2\omega & 2\omega^2 & -1 \\ 2\omega^2 & -1 & 2\omega \end{pmatrix}, \frac{1}{3}\begin{pmatrix} -1 & 2\omega^2 & 2\omega \\ 2 & 2\omega^2 & -\omega \\ 2 & -\omega^2 & 2\omega \end{pmatrix}, \frac{1}{3}\begin{pmatrix} -1 & 2 & 2 \\ 2\omega & 2\omega & -\omega \\ 2\omega^2 & -\omega^2 & 2\omega^2 \end{pmatrix},$$
$$\frac{1}{3}\begin{pmatrix} -1 & 2\omega & 2\omega^2 \\ 2 & 2\omega & -\omega^2 \\ 2 & -\omega & 2\omega^2 \end{pmatrix}, \frac{1}{3}\begin{pmatrix} -1 & 2\omega^2 & 2\omega \\ 2\omega^2 & 2\omega & -1 \\ 2\omega & -1 & 2\omega^2 \end{pmatrix}, \frac{1}{3}\begin{pmatrix} -1 & 2 & 2 \\ 2\omega^2 & 2\omega^2 & -\omega^2 \\ 2\omega & -\omega & 2\omega \end{pmatrix},$$

and finally for the 3three-dimensional representation $\underline{\mathbf{3_2}}$, the matrices representing the elements of the group can be found from those just listed for the representation $\underline{\mathbf{3_1}}$: for $\mathcal{C}_{1,2,3}$ are the same, while for $\mathcal{C}_{4,5}$ are the opposite. It is connected with the generator S, which changes sign in the $\underline{\mathbf{3_1}}$ and $\underline{\mathbf{3_2}}$ representations: the elements in $\mathcal{C}_{1,2,3}$ contain an even number of S, while those in $\mathcal{C}_{4,5}$ contain an odd number of it.

We now report the Clebsch-Gordan coefficients for our basis. In the following we use α_i to indicate the elements of the first representation of the product and β_i to indicate those of the second representation.
We start with all the multiplication rules which include the 1-dimensional representations:

$$\underline{\mathbf{1_1}} \otimes \eta = \eta \otimes \underline{\mathbf{1_1}} = \eta \quad \text{with } \eta \text{ any representation}$$

$$\underline{\mathbf{1_2}} \otimes \underline{\mathbf{1_2}} = \underline{\mathbf{1_1}} \sim \alpha\beta$$

$$\underline{\mathbf{1_2}} \otimes \underline{\mathbf{2}} = \underline{\mathbf{2}} \sim \begin{pmatrix} \alpha\beta_1 \\ -\alpha\beta_2 \end{pmatrix}$$

$$\underline{\mathbf{1_2}} \otimes \underline{\mathbf{3_1}} = \underline{\mathbf{3_2}} \sim \begin{pmatrix} \alpha\beta_1 \\ \alpha\beta_2 \\ \alpha\beta_3 \end{pmatrix}$$

$$\underline{\mathbf{1_2}} \otimes \underline{\mathbf{3_2}} = \underline{\mathbf{3_1}} \sim \begin{pmatrix} \alpha\beta_1 \\ \alpha\beta_2 \\ \alpha\beta_3 \end{pmatrix}$$

The multiplication rules with the two-dimensional representation are the following:

$$\underline{\mathbf{2}} \otimes \underline{\mathbf{2}} = \underline{\mathbf{1}}_{\mathbf{1}} \oplus \underline{\mathbf{1}}_{\mathbf{2}} \oplus \underline{\mathbf{2}} \qquad \text{with} \quad \begin{cases} \underline{\mathbf{1}}_{\mathbf{1}} \sim \alpha_1\beta_2 + \alpha_2\beta_1 \\ \underline{\mathbf{1}}_{\mathbf{2}} \sim \alpha_1\beta_2 - \alpha_2\beta_1 \\ \underline{\mathbf{2}} \sim \begin{pmatrix} \alpha_2\beta_2 \\ \alpha_1\beta_1 \end{pmatrix} \end{cases}$$

$$\underline{\mathbf{2}} \otimes \underline{\mathbf{3}}_{\mathbf{1}} = \underline{\mathbf{3}}_{\mathbf{1}} \oplus \underline{\mathbf{3}}_{\mathbf{2}} \qquad \text{with} \quad \begin{cases} \underline{\mathbf{3}}_{\mathbf{1}} \sim \begin{pmatrix} \alpha_1\beta_2 + \alpha_2\beta_3 \\ \alpha_1\beta_3 + \alpha_2\beta_1 \\ \alpha_1\beta_1 + \alpha_2\beta_2 \end{pmatrix} \\ \underline{\mathbf{3}}_{\mathbf{2}} \sim \begin{pmatrix} \alpha_1\beta_2 - \alpha_2\beta_3 \\ \alpha_1\beta_3 - \alpha_2\beta_1 \\ \alpha_1\beta_1 - \alpha_2\beta_2 \end{pmatrix} \end{cases}$$

$$\underline{\mathbf{2}} \otimes \underline{\mathbf{3}}_{\mathbf{2}} = \underline{\mathbf{3}}_{\mathbf{1}} \oplus \underline{\mathbf{3}}_{\mathbf{2}} \qquad \text{with} \quad \begin{cases} \underline{\mathbf{3}}_{\mathbf{1}} \sim \begin{pmatrix} \alpha_1\beta_2 - \alpha_2\beta_3 \\ \alpha_1\beta_3 - \alpha_2\beta_1 \\ \alpha_1\beta_1 - \alpha_2\beta_2 \end{pmatrix} \\ \underline{\mathbf{3}}_{\mathbf{2}} \sim \begin{pmatrix} \alpha_1\beta_2 + \alpha_2\beta_3 \\ \alpha_1\beta_3 + \alpha_2\beta_1 \\ \alpha_1\beta_1 + \alpha_2\beta_2 \end{pmatrix} \end{cases}$$

The multiplication rules with the three-dimensional representations are the following:

$$\underline{\mathbf{3}}_{\mathbf{1}} \otimes \underline{\mathbf{3}}_{\mathbf{1}} = \underline{\mathbf{3}}_{\mathbf{2}} \otimes \underline{\mathbf{3}}_{\mathbf{2}} = \underline{\mathbf{1}}_{\mathbf{1}} \oplus \underline{\mathbf{2}} \oplus \underline{\mathbf{3}}_{\mathbf{1}} \oplus \underline{\mathbf{3}}_{\mathbf{2}} \qquad \text{with} \quad \begin{cases} \underline{\mathbf{1}}_{\mathbf{1}} \sim \alpha_1\beta_1 + \alpha_2\beta_3 + \alpha_3\beta_2 \\ \underline{\mathbf{2}} \sim \begin{pmatrix} \alpha_2\beta_2 + \alpha_1\beta_3 + \alpha_3\beta_1 \\ \alpha_3\beta_3 + \alpha_1\beta_2 + \alpha_2\beta_1 \end{pmatrix} \\ \underline{\mathbf{3}}_{\mathbf{1}} \sim \begin{pmatrix} 2\alpha_1\beta_1 - \alpha_2\beta_3 - \alpha_3\beta_2 \\ 2\alpha_3\beta_3 - \alpha_1\beta_2 - \alpha_2\beta_1 \\ 2\alpha_2\beta_2 - \alpha_1\beta_3 - \alpha_3\beta_1 \end{pmatrix} \\ \underline{\mathbf{3}}_{\mathbf{2}} \sim \begin{pmatrix} \alpha_2\beta_3 - \alpha_3\beta_2 \\ \alpha_1\beta_2 - \alpha_2\beta_1 \\ \alpha_3\beta_1 - \alpha_1\beta_3 \end{pmatrix} \end{cases}$$

$$\underline{\mathbf{3}}_{\mathbf{1}} \otimes \underline{\mathbf{3}}_{\mathbf{2}} = \underline{\mathbf{1}}_{\mathbf{2}} \oplus \underline{\mathbf{2}} \oplus \underline{\mathbf{3}}_{\mathbf{1}} \oplus \underline{\mathbf{3}}_{\mathbf{2}} \qquad \text{with} \quad \begin{cases} \underline{\mathbf{1}}_{\mathbf{2}} \sim \alpha_1\beta_1 + \alpha_2\beta_3 + \alpha_3\beta_2 \\ \\ \underline{\mathbf{2}} \sim \begin{pmatrix} \alpha_2\beta_2 + \alpha_1\beta_3 + \alpha_3\beta_1 \\ -\alpha_3\beta_3 - \alpha_1\beta_2 - \alpha_2\beta_1 \end{pmatrix} \\ \\ \underline{\mathbf{3}}_{\mathbf{1}} \sim \begin{pmatrix} \alpha_2\beta_3 - \alpha_3\beta_2 \\ \alpha_1\beta_2 - \alpha_2\beta_1 \\ \alpha_3\beta_1 - \alpha_1\beta_3 \end{pmatrix} \\ \\ \underline{\mathbf{3}}_{\mathbf{2}} \sim \begin{pmatrix} 2\alpha_1\beta_1 - \alpha_2\beta_3 - \alpha_3\beta_2 \\ 2\alpha_3\beta_3 - \alpha_1\beta_2 - \alpha_2\beta_1 \\ 2\alpha_2\beta_2 - \alpha_1\beta_3 - \alpha_3\beta_1 \end{pmatrix} \end{cases}$$

Appendix B

Mode Expansion

The possible boundary conditions of functions on the orbifold $T^2/(Z_2^I \times Z_2^{PS} \times Z_2^{GG})$ defined in Eq.(6.1) are characterized by three parities [245], $(a, b = +, -)$,

$$\begin{aligned} \phi_{\pm ab}(-z) &= \pm\phi_{\pm ab}(z)\ , \\ \phi_{a\pm b}(-z+z_1) &= \pm\phi_{a\pm b}(z+z_1)\ , \\ \phi_{ab\pm}(-z+z_3) &= \pm\phi_{ab\pm}(z+z_3)\ . \end{aligned} \tag{B.1}$$

The mode expansion of functions with the boundary conditions given in Eq.(B.1) reads

$$\phi_{+++}(x,z) = \frac{2}{\sqrt{2^{\delta_{n,0}\delta_{m,0}} L_5 L_6 \sin\theta}} \left[\delta_{0,m}\sum_{n=0}^{\infty} + \sum_{m=1}^{\infty}\sum_{n=-\infty}^{\infty}\right] \phi_{+++}^{(2m,2n)}(x) \times \cos\left(\frac{2m\pi}{L_5}(x_5 - \frac{x_6}{\tan\theta}) + \frac{2n\pi}{L_6\sin\theta}x_6\right), \tag{B.2a}$$

$$\phi_{++-}(x,z) = \frac{2}{\sqrt{L_5 L_6 \sin\theta}} \left[\delta_{0,m}\sum_{n=0}^{\infty} + \sum_{m=1}^{\infty}\sum_{n=-\infty}^{\infty}\right] \phi_{++-}^{(2m,2n+1)}(x) \times \cos\left(\frac{2m\pi}{L_5}(x_5 - \frac{x_6}{\tan\theta}) + \frac{(2n+1)\pi}{L_6\sin\theta}x_6\right), \tag{B.2b}$$

$$\phi_{+-+}(x,z) = \frac{2}{\sqrt{L_5 L_6 \sin\theta}} \left[\sum_{m=0}^{\infty}\sum_{n=-\infty}^{\infty}\right] \phi_{+-+}^{(2m+1,2n)}(x) \times \cos\left(\frac{(2m+1)\pi}{L_5}(x_5 - \frac{x_6}{\tan\theta}) + \frac{2n\pi}{L_6\sin\theta}x_6\right), \tag{B.2c}$$

$$\phi_{+--}(x,z) = \frac{2}{\sqrt{L_5 L_6 \sin\theta}} \left[\sum_{m=0}^{\infty}\sum_{n=-\infty}^{\infty}\right] \phi_{+--}^{(2m+1,2n+1)}(x) \times \cos\left(\frac{(2m+1)\pi}{L_5}(x_5 - \frac{x_6}{\tan\theta}) + \frac{(2n+1)\pi}{L_6\sin\theta}x_6\right), \tag{B.2d}$$

$$\phi_{-++}(x,y) = \frac{2}{\sqrt{L_5 L_6 \sin\theta}} \left[\sum_{m=0}^{\infty}\sum_{n=-\infty}^{\infty}\right] \phi_{-++}^{(2m+1,2n+1)}(x) \times \sin\left(\frac{(2m+1)\pi}{L_5}(x_5 - \frac{x_6}{\tan\theta}) + \frac{(2n+1)\pi}{L_6\sin\theta}x_6\right), \tag{B.2e}$$

$$\phi_{-+-}(x,y) = \frac{2}{\sqrt{L_5 L_6 \sin\theta}} \left[\sum_{m=0}^{\infty}\sum_{n=-\infty}^{\infty}\right] \phi_{-+-}^{(2m+1,2n)}(x) \times \sin\left(\frac{(2m+1)\pi}{L_5}(x_5 - \frac{x_6}{\tan\theta}) + \frac{2n\pi}{L_6\sin\theta}x_6\right), \tag{B.2f}$$

$$\phi_{--+}(x,y) = \frac{2}{\sqrt{L_5 L_6 \sin\theta}} \left[\delta_{0,m}\sum_{n=0}^{\infty} + \sum_{m=1}^{\infty}\sum_{n=-\infty}^{\infty}\right] \phi_{++-}^{(2m,2n+1)}(x) \times \sin\left(\frac{2m\pi}{L_5}(x_5 - \frac{x_6}{\tan\theta}) + \frac{(2n+1)\pi}{L_6\sin\theta}x_6\right), \tag{B.2g}$$

$$\phi_{---}(x,y) = \frac{2}{\sqrt{L_5 L_6 \sin\theta}} \left[\delta_{0,m}\sum_{n=0}^{\infty} + \sum_{m=1}^{\infty}\sum_{n=-\infty}^{\infty}\right] \phi_{---}^{(2m,2n)}(x) \times \sin\left(\frac{2m\pi}{L_5}(x_5 - \frac{x_6}{\tan\theta}) + \frac{2n\pi}{L_6\sin\theta}x_6\right), \tag{B.2h}$$

where $\theta = \pi/3$, $L_5 = L_6 = 2\pi R$, and the wave functions are normalized by integrating over the fundamental region.

Appendix C

The Higgs Sector

In this appendix, we discuss the Higgs sector of the models where the formulae we use can be found in [228] and [242].

C.1 Model 1

The Higgs Potential

The Higgs potential in model 1 can be written as

$$\begin{aligned} V &= -\mu_1^2[\mathrm{Tr}(\phi^\dagger\phi)] - \mu_3^2[\mathrm{Tr}(\Delta_L\Delta_L^\dagger) + \mathrm{Tr}(\Delta_R\Delta_R^\dagger)] + \tilde{\lambda}_1[\mathrm{Tr}(\phi^\dagger\phi)]^2 \\ &+\tilde{\lambda}_2\{[\mathrm{Tr}(\tilde{\phi}\phi^\dagger)]^2 + [\mathrm{Tr}(\tilde{\phi}^\dagger\phi)]^2\} + \tilde{\lambda}_3[\mathrm{Tr}(\tilde{\phi}\phi^\dagger)\mathrm{Tr}(\tilde{\phi}^\dagger\phi)] \\ &+\rho_1\{[\mathrm{Tr}(\Delta_L\Delta_L^\dagger)]^2 + [\mathrm{Tr}(\Delta_R\Delta_R^\dagger)]^2\} + \rho_2[\mathrm{Tr}(\Delta_L\Delta_L)\mathrm{Tr}(\Delta_L^\dagger\Delta_L^\dagger) + \mathrm{Tr}(\Delta_R\Delta_R)\mathrm{Tr}(\Delta_R^\dagger\Delta_R^\dagger)] \\ &+\rho_3[\mathrm{Tr}(\Delta_L\Delta_L^\dagger)\mathrm{Tr}(\Delta_R\Delta_R^\dagger)] + \rho_4[\mathrm{Tr}(\Delta_L\Delta_L)\mathrm{Tr}(\Delta_R^\dagger\Delta_R^\dagger) + \mathrm{Tr}(\Delta_L^\dagger\Delta_L^\dagger)\mathrm{Tr}(\Delta_R\Delta_R)] \\ &+\alpha_1\mathrm{Tr}(\phi^\dagger\phi)[\mathrm{Tr}(\Delta_L\Delta_L^\dagger) + \mathrm{Tr}(\Delta_R\Delta_R^\dagger)] + \alpha_3[\mathrm{Tr}(\phi\phi^\dagger\Delta_L\Delta_L^\dagger) + \mathrm{Tr}(\phi^\dagger\phi\Delta_R\Delta_R^\dagger)] \\ &+\beta_1[\mathrm{Tr}(\phi\Delta_R\phi^\dagger\Delta_L^\dagger) + \mathrm{Tr}(\phi^\dagger\Delta_L\phi\Delta_R^\dagger)] \\ &+\gamma_1[\mathrm{Tr}(\tilde{\phi}\phi^\dagger) + \mathrm{Tr}(\tilde{\phi}^\dagger\phi)][\bar{\omega}_L\omega_R + \bar{\omega}_R\omega_L] + V_{\mathrm{soft}}. \end{aligned} \tag{C.1}$$

The general formula of Higgs potential for the LR model with two additional Higgs triplets is given in [228] (in this model, some terms are forbidden due to the additional Z_4 symmetry: $\mu_2 = \tilde{\lambda}_4 = \alpha_2 = \beta_2 = \beta_3 = 0$). V_{soft} breaks the remnant Z_2 softly (see Section 8.4.1). We note that the triplets, $\Delta_{L,R}$, can be written as

$$\Delta_{L,R} = \begin{pmatrix} \delta^+_{L,R} & \delta^{++}_{L,R} \\ \delta^0_{L,R} & -\delta^+_{L,R} \end{pmatrix}. \tag{C.2}$$

The Higgs Masses

- **The Neutral Scalar Higgs Mass Matrix**

In the basis $\{\sqrt{2}\Re\phi^0, \sqrt{2}\Re\eta^0, \sqrt{2}\Re\delta_R^0, \sqrt{2}\Re\delta_L^0\}$ the mass matrix can be written as

$$\begin{pmatrix} A_R & 0 & 2\alpha_1 v_1 v_R & 0 \\ 0 & B_R & 0 & \beta_1 v_1 v_R \\ 2\alpha_1 v_1 v_R & 0 & C_R & 0 \\ 0 & \beta_1 v_1 v_R & 0 & D_R \end{pmatrix}, \tag{C.3}$$

where $A_R = 6\tilde{\lambda}_1 v_1^2 + \alpha_1 v_R^2 - \mu_1^2$, $B_R = 2(\tilde{\lambda}_1 + 4\tilde{\lambda}_2 + 2\tilde{\lambda}_3)v_1^2 + (\alpha_1 + \alpha_3)v_R^2 - \mu_1^2$, $C_R = 6\rho_1 v_R^2 + \alpha_1 v_1^2 - \mu_3^2$, and $D_R = \rho_3 v_R^2 + \alpha_1 v_1^2 - \mu_3^2$. Already anticipating the results from the next point, these expressions can be simplified to look like

$$\begin{aligned} A_R &= 4\tilde{\lambda}_1 v_1^2, \\ B_R &= 4(2\tilde{\lambda}_2 + \tilde{\lambda}_3)v_1^2 + \alpha_3 v_R^2, \\ C_R &= 4\rho_1 v_R^2, \text{ and} \\ D_R &= (\rho_3 - 2\rho_1)v_R^2. \end{aligned} \tag{C.4}$$

- **The Neutral Pseudo-Scalar Higgs Mass Matrix**

  In the basis $\{\sqrt{2}\Im\phi^0, \sqrt{2}\Im\eta^0, \sqrt{2}\Im\delta_R^0, \sqrt{2}\Im\delta_L^0\}$ the mass matrix can be written as

$$\begin{pmatrix} A_I & 0 & 0 & 0 \\ 0 & B_I & 0 & \beta_1 v_1 v_R \\ 0 & 0 & C_I & 0 \\ 0 & \beta_1 v_1 v_R & 0 & D_I \end{pmatrix}, \tag{C.5}$$

  where $A_I = 2\tilde{\lambda}_1 v_1^2 + \alpha_1 v_R^2 - \mu_1^2$, $B_I = 2(\tilde{\lambda}_1 - 4\tilde{\lambda}_2 + 2\tilde{\lambda}_3)v_1^2 + (\alpha_1 + \alpha_3)v_R^2 - \mu_1^2$, $C_I = 2\rho_1 v_R^2 + \alpha_1 v_1^2 - \mu_3^2$, and $D_I = \rho_3 v_R^2 + \alpha_1 v_1^2 - \mu_3^2$. Looking at the matrix in Eq.(C.5), one can immediately see that $\sqrt{2}\Im\phi^0$ and $\sqrt{2}\Im\delta_R^0$ are already mass eigenstates with quantum numbers corresponding to the Z- and Z'-gauge bosons after symmetry breaking. Consequently, these fields must be the corresponding Goldstone bosons that are eaten by the gauge fields, and their masses must be equal to zero. This leads to equations for μ_1^2 and μ_3^2:

$$\mu_1^2 = 2\tilde{\lambda}_1 v_1^2 + \alpha_1 v_R^2, \ \mu_3^2 = 2\rho_1 v_R^2 + \alpha_1 v_1^2, \tag{C.6}$$

  which in turn yield:

$$\begin{aligned} A_I &= 0, \\ B_I &= -4(2\tilde{\lambda}_2 - \tilde{\lambda}_3)v_1^2 + \alpha_3 v_R^2, \\ C_I &= 0, \text{ and} \\ D_I &= (\rho_3 - 2\rho_1)v_R^2. \end{aligned} \tag{C.7}$$

- **The Singly Charged Higgs Mass Matrix**

  In the basis $\{\phi^+, \eta^+, \delta_R^+, \delta_L^+\}$ the mass matrix can be written as

$$\begin{pmatrix} A_+ & 0 & 0 & 0 \\ 0 & B_+ & \alpha_3 v_1 v_R & \beta_1 v_1 v_R \\ 0 & \alpha_3 v_1 v_R & C_+ & \beta_1 v_1^2 \\ 0 & \beta_1 v_1 v_R & \beta_1 v_1^2 & D_+ \end{pmatrix}, \tag{C.8}$$

where $A_+ = 2\tilde{\lambda}_1 v_1^2 + \alpha_1 v_R^2 - \mu_1^2$, $B_+ = 2\tilde{\lambda}_1 v_1^2 + (\alpha_1 + \alpha_3) v_R^2 - \mu_1^2$,$C_+ = 4\rho_1 v_R^2 + 2(\alpha_1 + \frac{\alpha_3}{2}) v_1^2 - 2\mu_3^2$, and $D_+ = 2\rho_3 v_R^2 + 2(\alpha_1 + \frac{\alpha_3}{2}) v_1^2 - 2\mu_3^2$. Using Eq.(C.6), one obtains:

$$\begin{aligned} A_+ &= 0, \\ B_+ &= \alpha_3 v_R^2, \\ C_+ &= \alpha_3 v_1^2, \text{ and} \\ D_+ &= 2(\rho_3 - 2\rho_1) v_R^2 + \alpha_3 v_1^2. \end{aligned} \tag{C.9}$$

This already yields one massless Goldstone boson ϕ^+ that gives mass to the W. There is no second Goldstone boson yet for the W', but the δ_R^+-entry of the matrix is significantly smaller than the others (EW scale vs. LR scale). By diagonalizing the matrix, it turns out that one gets another massless Goldstone boson that consists mainly of δ_R^+ and gives mass to the W'.

- **The Doubly Charged Higgs Mass Matrix**

  In the basis $\{\delta_R^{++}, \delta_L^{++}\}$ the mass matrix can be written as

$$\begin{pmatrix} 2(\rho_1 + 2\rho_2) v_R^2 + (\alpha_1 + \alpha_3) v_1^2 - \mu_3^2 & 0 \\ 0 & \rho_3 v_R^2 + (\alpha_1 + \alpha_3) v_1^2 - \mu_3^2 \end{pmatrix}. \tag{C.10}$$

  Using Eq.(C.6) yields:

$$\begin{pmatrix} 4\rho_2 v_R^2 + \alpha_3 v_1^2 & 0 \\ 0 & (\rho_3 - 2\rho_1) v_R^2 + \alpha_3 v_1^2 \end{pmatrix}. \tag{C.11}$$

- **The Physical Higgs Masses**

  It is easy to diagonalize the squared mass matrices from Eqs. (C.3), (C.5), (C.8), and (C.10). All rotations are small and result in admixtures of $\mathcal{O}\left(\frac{v_1}{v_R}\right) \lesssim 10^{-3}$. We name the physical Higgses accordingly to their dominant components, adding a prime to make clear that they are mass eigenstates. Moreover, for phenomenological reasons (namely for the radiative transmission to work), we assume $\alpha_3 \simeq 0$ in order for the masses of the scalar Higgs $(\sqrt{2}\Re\eta^0)'$ and $(\sqrt{2}\Im\eta^0)'$ to be at the electroweak scale. This yields the following physical scalar Higgs masses:

$$\begin{aligned} m^2[(\sqrt{2}\Re\phi^0)'] &= v_1^2 \left(\left(4\tilde{\lambda}_1 - \frac{\alpha_1^2}{\rho_1} \right) + \mathcal{O}\left(\frac{v_1^2}{v_R^2} \right) \right), \\ m^2[(\sqrt{2}\Re\eta^0)'] &= v_1^2 \left(\left(-\frac{\beta_1^2}{(\rho_3 - 2\rho_1)} + 8\tilde{\lambda}_2 + 4\tilde{\lambda}_3 \right) + \mathcal{O}\left(\frac{v_1^2}{v_R^2} \right) \right), \\ m^2[(\sqrt{2}\Re\delta_R^0)'] &= 4\rho_1 v_R^2 + v_1^2 \left(\left(\frac{\alpha_1^2}{\rho_1} \right) + \mathcal{O}\left(\frac{v_1^2}{v_R^2} \right) \right), \text{ and} \\ m^2[(\sqrt{2}\Re\delta_L^0)'] &= (\rho_3 - 2\rho_1) v_R^2 + v_1^2 \left((\rho_3 - 2\rho_1) v_R^2 + \left(\frac{\beta_1^2}{(\rho_3 - 2\rho_1)} \right) + \mathcal{O}\left(\frac{v_1^2}{v_R^2} \right) \right). \end{aligned} \tag{C.12}$$

After having got rid of the Goldstone bosons, we remain with two neutral pseudoscalar and two singly charged Higgses, which are physical. Their masses are given by

$$\begin{aligned} m^2[(\sqrt{2}\Im\eta^0)'] &= v_1^2\left(\left(-\frac{\beta_1^2}{(\rho_3-2\rho_1)}-8\tilde{\lambda}_2+4\tilde{\lambda}_3\right)+\mathcal{O}\left(\frac{v_1^2}{v_R^2}\right)\right), \\ m^2[(\eta^+)'] &= v_1^2\left(\frac{1}{2}\left(-\frac{\beta_1^2}{(\rho_3-2\rho_1)}\right)+\mathcal{O}\left(\frac{v_1^2}{v_R^2}\right)\right), \\ m^2[(\sqrt{2}\Im\delta_L^0)'] &= (\rho_3-2\rho_1)v_R^2+v_1^2\left(\left(\frac{\beta_1^2}{(\rho_3-2\rho_1)}\right)+\mathcal{O}\left(\frac{v_1^2}{v_R^2}\right)\right), \\ m^2[(\delta_L^+)'] &= 2(\rho_3-2\rho_1)v_R^2+2v_1^2\left(\frac{1}{2}\left(\frac{\beta_1^2}{(\rho_3-2\rho_1)}\right)+\mathcal{O}\left(\frac{v_1^2}{v_R^2}\right)\right). \end{aligned} \tag{C.13}$$

Note that, for the Ma-model, $(\sqrt{2}\Re\eta^0)'$ and $(\sqrt{2}\Im\eta^0)'$ must have different masses (the loop-induced neutrino mass would vanish if the masses of the scalar and the pseudoscalar η^0 were exactly equal, see Ref. [6]). Here, their masses are naturally split at $\mathcal{O}\left(\frac{v_1^4}{v_R^2}\right)$:

$$\Delta m^2(\eta) \equiv m^2((\sqrt{2}\Re\eta^0)') - m^2((\sqrt{2}\Im\eta^0)') = v_1^2\left(16\tilde{\lambda}_2 - \frac{16\tilde{\lambda}_2\beta_1^2}{(2\rho_1-\rho_3)^2}\frac{v_1^2}{v_R^2}+\mathcal{O}\left(\frac{v_1^4}{v_R^4}\right)\right). \tag{C.14}$$

Keeping this difference non-zero in particular requires $\tilde{\lambda}_2 \neq 0$, exactly as in the pure Ma-model. The doubly charged Higgs masses finally can be read off directly from Eq.(C.11):

$$\begin{aligned} m^2[(\delta_R^{++})'] &= 4\rho_2 v_R^2 \quad \text{and} \\ m^2[(\delta_L^{++})'] &= (\rho_3-2\rho_1)v_R^2. \end{aligned} \tag{C.15}$$

ρ-Parameter and EW-Boson Masses

A general formula for ρ-parameter in multi-Higgs models is given by [208]

$$\rho = \frac{m_W^2}{m_Z^2\cos^2\theta_W} = \frac{\sum_{T,Y}[T(T+1)-Y^2]|v_{T,Y}|^2 c_{T,Y}}{\sum_{T,Y}2Y^2|v_{T,Y}|^2}, \tag{C.16}$$

where $c_{T,Y}=1$ for a complex scalar and $c_{T,Y}=1/2$ for a real scalar ($Y=0$).

The corresponding W-mass is

$$m_W^2 = g^2\sum_{T,Y}[T(T+1)-Y^2]|v_{T,Y}|^2 c_{T,Y} \tag{C.17}$$

and Z-mass is

$$m_Z^2 = (g^2+g'^2)\sum_{T,Y}2Y^2|v_{T,Y}|^2. \tag{C.18}$$

In this model, the VEV of Δ_R does not modify the ρ-parameter and also the W-boson mass due to the fact that $(Y,T)_{\sqrt{2}\Re\delta_R^0} = (0,0)$ after LR breaking. Also the second Higgs doublet (which is identified with the η from the Ma-model) and the Δ_L have no effect due to their vanishing VEVs.

C.2 Model 2

The Higgs Potential

The Higgs potential in model 2 can be written as

$$\begin{aligned}
V &= -\mu_1^2[\mathrm{Tr}(\phi^\dagger\phi)] - \mu_3^2[\mathrm{Tr}(\Delta_L\Delta_L^\dagger) + \mathrm{Tr}(\Delta_R\Delta_R^\dagger)] + \tilde{\lambda}_1\{[\mathrm{Tr}(\phi^\dagger\phi)]^2\} \\
&\quad +\tilde{\lambda}_2\{[\mathrm{Tr}(\tilde{\phi}\phi^\dagger)]^2 + [\mathrm{Tr}(\tilde{\phi}^\dagger\phi)]^2\} + \tilde{\lambda}_3[\mathrm{Tr}(\tilde{\phi}\phi^\dagger)\mathrm{Tr}(\tilde{\phi}^\dagger\phi)] \\
&\quad +\rho_1\{[\mathrm{Tr}(\Delta_L\Delta_L^\dagger)]^2 + [\mathrm{Tr}(\Delta_R\Delta_R^\dagger)]^2\} + \rho_2[\mathrm{Tr}(\Delta_L\Delta_L)\mathrm{Tr}(\Delta_L^\dagger\Delta_L^\dagger) + \mathrm{Tr}(\Delta_R\Delta_R)\mathrm{Tr}(\Delta_R^\dagger\Delta_R^\dagger)] \\
&\quad +\rho_3[\mathrm{Tr}(\Delta_L\Delta_L^\dagger)\mathrm{Tr}(\Delta_R\Delta_R^\dagger)] + \rho_4[\mathrm{Tr}(\Delta_L\Delta_L)\mathrm{Tr}(\Delta_R^\dagger\Delta_R^\dagger) + \mathrm{Tr}(\Delta_L^\dagger\Delta_L^\dagger)\mathrm{Tr}(\Delta_R\Delta_R)] \\
&\quad +\alpha_1\mathrm{Tr}(\phi^\dagger\phi)[\mathrm{Tr}(\Delta_L\Delta_L^\dagger) + \mathrm{Tr}(\Delta_R\Delta_R^\dagger)] + \alpha_3[\mathrm{Tr}(\phi\phi^\dagger\Delta_L\Delta_L^\dagger) + \mathrm{Tr}(\phi^\dagger\phi\Delta_R\Delta_R^\dagger)] \\
&\quad +\beta_1[\mathrm{Tr}(\phi\Delta_R\phi^\dagger\Delta_L^\dagger) + \mathrm{Tr}(\phi^\dagger\Delta_L\phi\Delta_R^\dagger)] \\
&\quad -\mu_\chi^2(\chi_L^\dagger\chi_L + \chi_R^\dagger\chi_R) + \lambda_{\chi_1}\mathrm{Tr}(\phi^\dagger\phi)(\chi_L^\dagger\chi_L + \chi_R^\dagger\chi_R) \\
&\quad +\lambda_{\chi_2}[\mathrm{Tr}(\Delta_L\Delta_L^\dagger) + \mathrm{Tr}(\Delta_R\Delta_R^\dagger)](\chi_L^\dagger\chi_L + \chi_R^\dagger\chi_R). \qquad \text{(C.19)}
\end{aligned}$$

Note that we have also added the two Higgs doublets $\chi_{L,R}$ to the model.

The Higgs Masses

Because of the VEVs of the additional Higgs doublets, the parameters μ_1^2, μ_3^2 are shifted as $\mu_1^2 \to \mu_1^2 - \lambda_{\chi_1}(v_L^2 + w_R^2) = \tilde{\mu}_1^2$ and $\mu_3^2 \to \mu_3^2 - \lambda_{\chi_2}(v_L^2 + w_R^2) = \tilde{\mu}_3^2$.

- **The Neutral Scalar Higgs Masses**

  The mass matrix for the scalar Higgses looks exactly as the one from Eq.(C.3), except for $\mu_{1,3} \to \tilde{\mu}_{1,3}$ and for an additional diagonal block corresponding to $\sqrt{2}\Re\chi_R^0$ and $\sqrt{2}\Re\chi_L^0$. The masses of these two new physical Higgses are given by

  $$m^2(\sqrt{2}\Re\chi_{R,L}^0) = \lambda_{\chi_1}v_1^2 + \lambda_{\chi_2}v_R^2 - \mu_\chi^2, \qquad \text{(C.20)}$$

  while the other masses do not change compared to Eq.(C.12).

- **The Neutral Pseudo-Scalar Higgs Masses**

  Also here, the diagonalization is in principle the same as in Eq.(C.5). The physical masses of $\sqrt{2}\Im\chi_{R,L}^0$ are the same as the ones of $\sqrt{2}\Re\chi_{R,L}^0$. The other physical pseudoscalars have the same masses as the ones given in Eq.(C.13).

- **The Singly Charged Higgs Masses**

  Again there are no changes compared to Eq.(C.13) and the singly charged scalars $\chi_{R,L}^+$ have the same masses as $\sqrt{2}\Re\chi_{R,L}^0$.

- **The Doubly Charged Higgs Masses**

  These masses are the same as the ones from Eq.(C.15).

ρ-Parameter and EW-Boson Masses

In this model, the VEVs of Δ_R, χ_R do not modify the ρ-parameter (see Eq.(C.16)) and also the W-boson mass due to the fact that $(Y,T)_{\sqrt{2}\Re\delta_R^0} = (0,0)$ after LR breaking. Also the second Higgs doublet (which is identified with the η from the Ma-model) and the Δ_L have no effect due to their vanishing VEVs.

Although the VEV of χ_L does not modify the ρ-parameter, it modifies the mass formulae for W-boson, Eq.(C.17), and Z-boson, Eq.(C.18):

$$m_W^2 = \frac{g^2}{2}(v_1^2 + w_L^2),\ m_Z^2 = \frac{g^2+g'^2}{2}(v_1^2 + w_L^2). \tag{C.21}$$

C.3 The Correspondence to The Ma-model

Writing the ϕ-part of Eq.(C.1) and Eq.(C.19) and comparing it to the potential of the Ma-model given in Eq.(7.2), one can derive the correspondence of the Ma-model parameters $m_{1,2}^2$ and $\lambda_{1,2,3,4,5}$ with the ones in the LR symmetric potential (model 1: μ_1 and $\tilde{\lambda}_{1,2,3}$; model 2: $\tilde{\mu}_1$ and $\tilde{\lambda}_{1,2,3}$). The result is, at the LR breaking scale and above:

$$m_{1,2}^2 = -\mu_1^2\ \ (-\tilde{\mu}_1^2),\ \lambda_{1,2,3} = 2\tilde{\lambda}_1,\ \lambda_4 = 4\tilde{\lambda}_3,\ \text{and}\ \lambda_5 = 8\tilde{\lambda}_2. \tag{C.22}$$

Of course, these parameters have to run down to the low energy scale, which will lead to some changes. m_1 and m_2 will evolve differently, which is required by the Ma-model itself, as we need $m_1^2 < 0$ and $m_2^2 > 0$ in order for the SM-Higgs to obtain a VEV, while the η gets none. As the Higgses do not take part in strong interactions, one can expect the change of their masses due to the running to be moderate. Since m_1^2 and m_2^2 need, however, a different sign, it is natural to assume them to be relatively small. Going back to Eq.(C.6), this requires a very small α_1 for μ_1^2 to be small. Also $\lambda_{1,2,3}$ are equal at the LR breaking scale and should hence have similar values at the electroweak scale. λ_4 and λ_5 can, however, have different values.

Bibliography

[1] R. N. Mohapatra and A. Y. Smirnov, *Neutrino Mass and New Physics*, Ann. Rev. Nucl. Part. Sci. **56** (2006), 569–628, hep-ph/0603118.

[2] G. Altarelli and F. Feruglio, *Models of neutrino masses and mixings*, New J. Phys. **6** (2004), 106, hep-ph/0405048.

[3] G. Altarelli, *Theoretical Models of Neutrino Mixing: Recent Developments*, (2009), 0905.2350.

[4] P. Minkowski, $\mu \to e\gamma$ *at a Rate of One Out of 1-Billion Muon Decays?*, Phys. Lett. **B67** (1977), 421.

[5] R. N. Mohapatra and G. Senjanovic, *Neutrino mass and spontaneous parity nonconservation*, Phys. Rev. Lett. **44** (1980), 912.

[6] E. Ma, *Verifiable radiative seesaw mechanism of neutrino mass and dark matter*, Phys. Rev. **D73** (2006), 077301, hep-ph/0601225.

[7] E. Ma, *Neutrino Mass: Mechanisms and Models*, (2009), 0905.0221.

[8] A. Zee, *A Theory of Lepton Number Violation, Neutrino Majorana Mass, and Oscillation*, Phys. Lett. **B93** (1980), 389.

[9] K. S. Babu and E. Ma, *Natural Hierarchy of Radiatively Induced Majorana Neutrino Masses*, Phys. Rev. Lett. **61** (1988), 674.

[10] A. Zee, *Quantum Numbers of Majorana Neutrino Masses*, Nucl. Phys. **B264** (1986), 99.

[11] K. S. Babu, *Model of 'Calculable' Majorana Neutrino Masses*, Phys. Lett. **B203** (1988), 132.

[12] T. Fukuyama and H. Nishiura, *Mass matrix of Majorana neutrinos*, (1997), hep-ph/9702253.

[13] A. Datta, F.-S. Ling, and P. Ramond, *Correlated hierarchy, Dirac masses and large mixing angles*, Nucl. Phys. **B671** (2003), 383–400, hep-ph/0306002.

[14] Y. Kajiyama, M. Raidal, and A. Strumia, *The golden ratio prediction for the solar neutrino mixing*, Phys. Rev. **D76** (2007), 117301, 0705.4559.

[15] L. L. Everett and A. J. Stuart, *Icosahedral A_5 Family Symmetry and the Golden Ratio Prediction for Solar Neutrino Mixing*, Phys. Rev. **D79** (2009), 085005, 0812.1057.

[16] W. Rodejohann, *Unified Parametrization for Quark and Lepton Mixing Angles*, Phys. Lett. **B671** (2009), 267–271, 0810.5239.

[17] P. F. Harrison, D. H. Perkins, and W. G. Scott, *Tri-bimaximal mixing and the neutrino oscillation data*, Phys. Lett. **B530** (2002), 167, hep-ph/0202074.

[18] A. Adulpravitchai, A. Blum, and M. Lindner, *Non-Abelian Discrete Groups from the Breaking of Continuous Flavor Symmetries*, JHEP **09** (2009), 018, 0907.2332.

[19] G. Etesi, *Spontaneous Symmetry Breaking in SO(3) Gauge Theory to Discrete Subgroups*, J. Math. Phys. **37** (1996), 1596–1602, hep-th/9706029.

[20] J. Berger and Y. Grossman, *Model of leptons from $SO(3) \to A_4$*, (2009), 0910.4392.

[21] T. Kobayashi, S. Raby, and R.-J. Zhang, *Searching for realistic 4d string models with a Pati-Salam symmetry: Orbifold grand unified theories from heterotic string compactification on a Z(6) orbifold*, Nucl. Phys. **B704** (2005), 3–55, hep-ph/0409098.

[22] T. Kobayashi, H. P. Nilles, F. Ploger, S. Raby, and M. Ratz, *Stringy origin of non-Abelian discrete flavor symmetries*, Nucl. Phys. **B768** (2007), 135–156, hep-ph/0611020.

[23] P. Ko, T. Kobayashi, J.-h. Park, and S. Raby, *String-derived D_4 flavor symmetry and phenomenological implications*, Phys. Rev. **D76** (2007), 035005, 0704.2807.

[24] H. Abe, K.-S. Choi, T. Kobayashi, and H. Ohki, *Non-Abelian Discrete Flavor Symmetries from Magnetized/Intersecting Brane Models*, Nucl. Phys. **B820** (2009), 317–333, 0904.2631.

[25] H. Abe, K.-S. Choi, T. Kobayashi, and H. Ohki, *Flavor structure from magnetic fluxes and non-Abelian Wilson lines*, (2010), 1001.1788.

[26] T. Watari and T. Yanagida, *Geometric origin of large lepton mixing in a higher dimensional spacetime*, Phys. Lett. **B544** (2002), 167–175, hep-ph/0205090.

[27] T. Watari and T. Yanagida, *Higher dimensional supersymmetry as an origin of the three families for quarks and leptons*, Phys. Lett. **B532** (2002), 252–258, hep-ph/0201086.

[28] G. Altarelli, F. Feruglio, and Y. Lin, *Tri-bimaximal neutrino mixing from orbifolding*, Nucl. Phys. **B775** (2007), 31–44, hep-ph/0610165.

[29] A. Adulpravitchai, A. Blum, and M. Lindner, *Non-Abelian Discrete Flavor Symmetries from T^2/Z_N Orbifolds*, JHEP **07** (2009), 053, 0906.0468.

[30] Y. Kawamura, *Gauge symmetry reduction from the extra space S^1/Z_2*, Prog. Theor. Phys. **103** (2000), 613–619, hep-ph/9902423.

[31] Y. Kawamura, *Triplet-doublet splitting, proton stability and extra dimension*, Prog. Theor. Phys. **105** (2001), 999–1006, hep-ph/0012125.

[32] Y. Kawamura, *Split multiplets, coupling unification and extra dimension*, Prog. Theor. Phys. **105** (2001), 691–696, hep-ph/0012352.

[33] G. Altarelli and F. Feruglio, *SU(5) grand unification in extra dimensions and proton decay*, Phys. Lett. **B511** (2001), 257–264, hep-ph/0102301.

[34] L. J. Hall and Y. Nomura, *Gauge unification in higher dimensions*, Phys. Rev. **D64** (2001), 055003, hep-ph/0103125.

[35] J. Scherk and J. H. Schwarz, *Spontaneous Breaking of Supersymmetry Through Dimensional Reduction*, Phys. Lett. **B82** (1979), 60.

[36] J. Scherk and J. H. Schwarz, *How to Get Masses from Extra Dimensions*, Nucl. Phys. **B153** (1979), 61–88.

[37] T. J. Burrows and S. F. King, *A_4 Family Symmetry from SU(5) SUSY GUTs in 6d*, (2009), 0909.1433.

[38] N. Haba, A. Watanabe, and K. Yoshioka, *Twisted flavors and tri/bi-maximal neutrino mixing*, Phys. Rev. Lett. **97** (2006), 041601, hep-ph/0603116.

[39] G. Seidl, *Unified model of fermion masses with Wilson line flavor symmetry breaking*, Phys. Rev. **D81** (2010), 025004, 0811.3775.

[40] T. Kobayashi, Y. Omura, and K. Yoshioka, *Flavor Symmetry Breaking and Vacuum Alignment on Orbifolds*, Phys. Rev. **D78** (2008), 115006, 0809.3064.

[41] A. Adulpravitchai, A. Blum, and C. Hagedorn, *A Supersymmetric D_4 Model for $\mu - \tau$ Symmetry*, JHEP **03** (2009), 046, 0812.3799.

[42] A. Adulpravitchai, A. Blum, and W. Rodejohann, *Golden Ratio Prediction for Solar Neutrino Mixing*, New J. Phys. **11** (2009), 063026, 0903.0531.

[43] A. Adulpravitchai, M. Lindner, and A. Merle, *Confronting Flavour Symmetries and extended Scalar Sectors with Lepton Flavour Violation Bounds*, Phys. Rev. **D80** (2009), 055031, 0907.2147.

[44] A. Adulpravitchai, M. Lindner, A. Merle, and R. N. Mohapatra, *Radiative Transmission of Lepton Flavor Hierarchies*, Phys. Lett. **B680** (2009), 476–479, 0908.0470.

[45] A. Adulpravitchai and M. A. Schmidt, *Flavored Orbifold GUT*, (2010), 1001.3172.

[46] Particle Data Group, C. Amsler et al., *Review of particle physics*, Phys. Lett. **B667** (2008), 1.

[47] T. Schwetz, M. A. Tortola, and J. W. F. Valle, *Three-flavour neutrino oscillation update*, New J. Phys. **10** (2008), 113011, 0808.2016.

[48] S. Weinberg, *Baryon and Lepton Nonconserving Processes*, Phys. Rev. Lett. **43** (1979), 1566–1570.

[49] S. Antusch, J. Kersten, M. Lindner, M. Ratz, and M. A. Schmidt, *Mixing Parameter Tools 1.0 Documentation*, found at url: http://users.physik.tu-muenchen.de/rge/MPT/index.html.

[50] C. D. Froggatt and H. B. Nielsen, *Hierarchy of Quark Masses, Cabibbo Angles and CP Violation*, Nucl. Phys. **B147** (1979), 277.

[51] N. Irges, S. Lavignac, and P. Ramond, *Predictions from an anomalous U(1) model of Yukawa hierarchies*, Phys. Rev. **D58** (1998), 035003, hep-ph/9802334.

[52] J. M. Mira, E. Nardi, and D. A. Restrepo, *A $SU(3)_c \times SU(2)_L \times U(1)_Y \times U(1)_H$ gauge model of flavor*, Phys. Rev. **D62** (2000), 016002, hep-ph/9911212.

[53] R. Barbieri, L. J. Hall, S. Raby, and A. Romanino, *Unified theories with U(2) flavor symmetry*, Nucl. Phys. **B493** (1997), 3–26, hep-ph/9610449.

[54] R. Barbieri, L. Giusti, L. J. Hall, and A. Romanino, *Fermion masses and symmetry breaking of a U(2) flavour symmetry*, Nucl. Phys. **B550** (1999), 32–40, hep-ph/9812239.

[55] S. F. King, *Predicting neutrino parameters from SO(3) family symmetry and quark-lepton unification*, JHEP **08** (2005), 105, hep-ph/0506297.

[56] S. F. King and G. G. Ross, *Fermion masses and mixing angles from SU(3) family symmetry*, Phys. Lett. **B520** (2001), 243–253, hep-ph/0108112.

[57] S. F. King and G. G. Ross, *Fermion masses and mixing angles from SU(3) family symmetry and unification*, Phys. Lett. **B574** (2003), 239–252, hep-ph/0307190.

[58] I. de Medeiros Varzielas, S. F. King, and G. G. Ross, *Tri-bimaximal neutrino mixing from discrete subgroups of SU(3) and SO(3) family symmetry*, Phys. Lett. **B644** (2007), 153–157, hep-ph/0512313.

[59] J. Kubo, *Majorana phase in minimal S_3 invariant extension of the standard model*, Phys. Lett. **B578** (2004), 156–164, hep-ph/0309167.

[60] J. Kubo, A. Mondragon, M. Mondragon, and E. Rodriguez-Jauregui, *The flavor symmetry*, Prog. Theor. Phys. **109** (2003), 795–807, hep-ph/0302196.

[61] S.-L. Chen, M. Frigerio, and E. Ma, *Large neutrino mixing and normal mass hierarchy: A discrete understanding*, Phys. Rev. **D70** (2004), 073008, hep-ph/0404084.

[62] S. Morisi and M. Picariello, *The flavor physics in unified gauge theory from an $S_3 * P$ discrete symmetry*, Int. J. Theor. Phys. **45** (2006), 1267–1277, hep-ph/0505113.

[63] L. Lavoura and E. Ma, *Two predictive supersymmetric $S_3 \times Z_2$ models for the quark mass matrices*, Mod. Phys. Lett. **A20** (2005), 1217–1226, hep-ph/0502181.

[64] R. Dermisek and S. Raby, *Bi-large neutrino mixing and CP violation in an SO(10) SUSY GUT for fermion masses*, Phys. Lett. **B622** (2005), 327–338, hep-ph/0507045.

[65] F. Caravaglios and S. Morisi, *Neutrino masses and mixings with an S_3 family permutation symmetry*, (2005), hep-ph/0503234.

[66] F. Caravaglios and S. Morisi, *Fermion masses in E_6 grand unification with family permutation symmetries*, (2005), hep-ph/0510321.

[67] W. Grimus and L. Lavoura, *$S_3 \times Z_2$ model for neutrino mass matrices*, JHEP **08** (2005), 013, hep-ph/0504153.

[68] W. Grimus, *Realizations of mu - tau interchange symmetry*, (2006), hep-ph/0610158.

[69] Y. Koide, *Permutation symmetry S_3 and VEV structure of flavor- triplet Higgs scalars*, Phys. Rev. **D73** (2006), 057901, hep-ph/0509214.

[70] T. Teshima, *Flavor mass and mixing and S_3 symmetry: An S_3 invariant model reasonable to all*, Phys. Rev. **D73** (2006), 045019, hep-ph/0509094.

[71] N. Haba and K. Yoshioka, *Discrete flavor symmetry, dynamical mass textures, and grand unification*, Nucl. Phys. **B739** (2006), 254–284, hep-ph/0511108.

[72] M. Tanimoto and T. Yanagida, *A higher-dimensional origin of the inverted mass hierarchy for neutrinos*, Phys. Lett. **B633** (2006), 567–572, hep-ph/0511336.

[73] Y. Koide, *Seesaw mass matrix model of quarks and leptons with flavor-triplet Higgs scalars*, Eur. Phys. J. **C48** (2006), 223–228, hep-ph/0508301.

[74] S. Morisi, *S_3 family permutation symmetry and quark masses: A model independent approach*, (2006), hep-ph/0604106.

[75] M. Picariello, *Neutrino CP violating parameters from nontrivial quark- lepton correlation: A $S_3 \times$ GUT model*, Int. J. Mod. Phys. **A23** (2008), 4435–4448, hep-ph/0611189.

[76] R. N. Mohapatra, S. Nasri, and H.-B. Yu, *Grand unification of mu - tau symmetry*, Phys. Lett. **B636** (2006), 114–118, hep-ph/0603020.

[77] R. N. Mohapatra, S. Nasri, and H.-B. Yu, *S_3 symmetry and tri-bimaximal mixing*, Phys. Lett. **B639** (2006), 318–321, hep-ph/0605020.

[78] S. Kaneko, H. Sawanaka, T. Shingai, M. Tanimoto, and K. Yoshioka, *Flavor Symmetry and Vacuum Aligned Mass Textures*, Prog. Theor. Phys. **117** (2007), 161–181, hep-ph/0609220.

[79] Y. Koide, *S_3 symmetry and neutrino masses and mixings*, Eur. Phys. J. **C50** (2007), 809–816, hep-ph/0612058.

[80] C.-Y. Chen and L. Wolfenstein, *Consequences of Approximate S_3 Symmetry of the Neutrino Mass Matrix*, Phys. Rev. **D77** (2008), 093009, 0709.3767.

[81] F. Feruglio and Y. Lin, *Fermion Mass Hierarchies and Flavour Mixing from a Minimal Discrete Symmetry*, Nucl. Phys. **B800** (2008), 77–93, 0712.1528.

[82] W. Grimus, A. S. Joshipura, S. Kaneko, L. Lavoura, and M. Tanimoto, *Lepton mixing angle $\theta_{13} = 0$ with a horizontal symmetry D_4*, JHEP **07** (2004), 078, hep-ph/0407112.

[83] H. Ishimori et al., *D_4 Flavor Symmetry for Neutrino Masses and Mixing*, Phys. Lett. **B662** (2008), 178–184, 0802.2310.

[84] H. Ishimori et al., *Soft supersymmetry breaking terms from $D_4 \times Z_2$ lepton flavor symmetry*, Phys. Rev. **D77** (2008), 115005, 0803.0796.

[85] C. Hagedorn, M. Lindner, and F. Plentinger, *The discrete flavor symmetry D(5)*, Phys. Rev. **D74** (2006), 025007, hep-ph/0604265.

[86] A. Blum, C. Hagedorn, and A. Hohenegger, θ_C *from the Dihedral Flavor Symmetries* D_7 *and* D_14, JHEP **03** (2008), 070, 0710.5061.

[87] A. Blum and C. Hagedorn, *The Cabibbo Angle in a Supersymmetric D14 Model*, Nucl. Phys. **B821** (2009), 327–353, 0902.4885.

[88] E. Ma and G. Rajasekaran, *Softly broken* A_4 *symmetry for nearly degenerate neutrino masses*, Phys. Rev. **D64** (2001), 113012, hep-ph/0106291.

[89] E. Ma, *Quark Mass Matrices in the* A_4 *Model*, Mod. Phys. Lett. **A17** (2002), 627–630, hep-ph/0203238.

[90] K. S. Babu, E. Ma, and J. W. F. Valle, *Underlying* A_4 *symmetry for the neutrino mass matrix and the quark mixing matrix*, Phys. Lett. **B552** (2003), 207–213, hep-ph/0206292.

[91] M. Hirsch, J. C. Romao, S. Skadhauge, J. W. F. Valle, and A. Villanova del Moral, *Phenomenological tests of supersymmetric* A_4 *family symmetry model of neutrino mass*, Phys. Rev. **D69** (2004), 093006, hep-ph/0312265.

[92] E. Ma, A_4 *origin of the neutrino mass matrix*, Phys. Rev. **D70** (2004), 031901, hep-ph/0404199.

[93] E. Ma, *Non-Abelian discrete symmetries and neutrino masses: Two examples*, New J. Phys. **6** (2004), 104, hep-ph/0405152.

[94] E. Ma, *Non-Abelian discrete family symmetries of leptons and quarks*, (2004), hep-ph/0409075.

[95] E. Ma, *Aspects of the tetrahedral neutrino mass matrix*, Phys. Rev. **D72** (2005), 037301, hep-ph/0505209.

[96] E. Ma, *Tetrahedral family symmetry and the neutrino mixing matrix*, Mod. Phys. Lett. **A20** (2005), 2601–2606, hep-ph/0508099.

[97] E. Ma, *Tribimaximal neutrino mixing from a supersymmetric model with* A_4 *family symmetry*, Phys. Rev. **D73** (2006), 057304, hep-ph/0511133.

[98] E. Ma, *Suitability of* A_4 *as a Family Symmetry in Grand Unification*, Mod. Phys. Lett. **A21** (2006), 2931–2936, hep-ph/0607190.

[99] E. Ma, *Supersymmetric* $A_4 X Z_3$ *and* A_4 *Realizations of Neutrino Tribimaximal Mixing Without and With Corrections*, Mod. Phys. Lett. **A22** (2007), 101–106, hep-ph/0610342.

[100] S.-L. Chen, M. Frigerio, and E. Ma, *Hybrid seesaw neutrino masses with* A_4 *family symmetry*, Nucl. Phys. **B724** (2005), 423–431, hep-ph/0504181.

[101] K. S. Babu and X.-G. He, *Model of geometric neutrino mixing*, (2005), hep-ph/0507217.

[102] A. Zee, *Obtaining the neutrino mixing matrix with the tetrahedral group*, Phys. Lett. **B630** (2005), 58–67, hep-ph/0508278.

[103] G. Altarelli and F. Feruglio, *Tri-bimaximal neutrino mixing from discrete symmetry in extra dimensions*, Nucl. Phys. **B720** (2005), 64–88, hep-ph/0504165.

[104] G. Altarelli and F. Feruglio, *Tri-Bimaximal Neutrino Mixing, A_4 and the Modular Symmetry*, Nucl. Phys. **B741** (2006), 215–235, hep-ph/0512103.

[105] X.-G. He, Y.-Y. Keum, and R. R. Volkas, *A_4 flavour symmetry breaking scheme for understanding quark and neutrino mixing angles*, JHEP **04** (2006), 039, hep-ph/0601001.

[106] B. Adhikary, B. Brahmachari, A. Ghosal, E. Ma, and M. K. Parida, *A_4 symmetry and prediction of U_{e3} in a modified Altarelli-Feruglio model*, Phys. Lett. **B638** (2006), 345–349, hep-ph/0603059.

[107] L. Lavoura and H. Kuhbock, *Predictions of an A_4 model with a five-parameter neutrino mass matrix*, Mod. Phys. Lett. **A22** (2007), 181, hep-ph/0610050.

[108] S. F. King and M. Malinsky, *A_4 family symmetry and quark-lepton unification*, Phys. Lett. **B645** (2007), 351–357, hep-ph/0610250.

[109] S. Morisi, M. Picariello, and E. Torrente-Lujan, *A model for fermion masses and lepton mixing in $SO(10) \times A_4$*, Phys. Rev. **D75** (2007), 075015, hep-ph/0702034.

[110] F. Yin, *Neutrino mixing matrix in the 3-3-1 model with heavy leptons and A_4 symmetry*, Phys. Rev. **D75** (2007), 073010, 0704.3827.

[111] F. Bazzocchi, S. Kaneko, and S. Morisi, *A SUSY A_4 model for fermion masses and mixings*, JHEP **03** (2008), 063, 0707.3032.

[112] F. Bazzocchi, S. Morisi, and M. Picariello, *Embedding A_4 into left-right flavor symmetry: Tribimaximal neutrino mixing and fermion hierarchy*, Phys. Lett. **B659** (2008), 628–633, 0710.2928.

[113] B. Brahmachari, S. Choubey, and M. Mitra, *The A_4 flavor symmetry and neutrino phenomenology*, Phys. Rev. **D77** (2008), 073008, 0801.3554.

[114] F. Bazzocchi, S. Morisi, M. Picariello, and E. Torrente-Lujan, *Embedding A_4 into $SU(3) \times U(1)$ flavor symmetry: Large neutrino mixing and fermion mass hierarchy in $SO(10)$ GUT*, J. Phys. **G36** (2009), 015002, 0802.1693.

[115] P. H. Frampton and S. Matsuzaki, *Renormalizable A_4 Model for Lepton Sector*, (2008), 0806.4592.

[116] M. Honda and M. Tanimoto, *Deviation from tri-bimaximal neutrino mixing in A_4 flavor symmetry*, Prog. Theor. Phys. **119** (2008), 583–598, 0801.0181.

[117] G. Altarelli, F. Feruglio, and C. Hagedorn, *A SUSY SU(5) Grand Unified Model of Tri-Bimaximal Mixing from A_4*, JHEP **03** (2008), 052–052, 0802.0090.

[118] Y. Lin, *A predictive A_4 model, Charged Lepton Hierarchy and Tri- bimaximal Sum Rule*, Nucl. Phys. **B813** (2009), 91–105, 0804.2867.

[119] M.-C. Chen and S. F. King, *A_4 See-Saw Models and Form Dominance*, JHEP **06** (2009), 072, 0903.0125.

[120] P. H. Frampton and T. W. Kephart, *Simple nonAbelian finite flavor groups and fermion masses*, Int. J. Mod. Phys. **A10** (1995), 4689–4704, hep-ph/9409330.

[121] A. Aranda, C. D. Carone, and R. F. Lebed, *U(2) flavor physics without U(2) symmetry*, Phys. Lett. **B474** (2000), 170–176, hep-ph/9910392.

[122] A. Aranda, C. D. Carone, and R. F. Lebed, *Maximal neutrino mixing from a minimal flavor symmetry*, Phys. Rev. **D62** (2000), 016009, hep-ph/0002044.

[123] P. D. Carr and P. H. Frampton, *Group theoretic bases for tribimaximal mixing*, (2007), hep-ph/0701034.

[124] A. Aranda, *Neutrino mixing from the double tetrahedral group T'*, Phys. Rev. **D76** (2007), 111301, 0707.3661.

[125] P. H. Frampton and T. W. Kephart, *Flavor Symmetry for Quarks and Leptons*, JHEP **09** (2007), 110, 0706.1186.

[126] P. H. Frampton and S. Matsuzaki, *$T^{'}$ Predictions of PMNS and CKM Angles*, Phys. Lett. **B679** (2009), 347–349, 0902.1140.

[127] G.-J. Ding, *Fermion Mass Hierarchies and Flavor Mixing from T' Symmetry*, Phys. Rev. **D78** (2008), 036011, 0803.2278.

[128] F. Feruglio, C. Hagedorn, Y. Lin, and L. Merlo, *Tri-bimaximal neutrino mixing and quark masses from a discrete flavour symmetry*, Nucl. Phys. **B775** (2007), 120–142, hep-ph/0702194.

[129] M.-C. Chen and K. T. Mahanthappa, *CKM and Tri-bimaximal MNS Matrices in a $SU(5) \times T^{(d)}$ Model*, Phys. Lett. **B652** (2007), 34–39, 0705.0714.

[130] M.-C. Chen, K. T. Mahanthappa, and F. Yu, *A Viable Randall-Sundrum Model for Quarks and Leptons with T' Family Symmetry*, Phys. Rev. **D81** (2010), 036004, 0907.3963.

[131] S. Pakvasa and H. Sugawara, *Mass of the t Quark in $SU(2) \times U(1)$*, Phys. Lett. **B82** (1979), 105.

[132] Y. Yamanaka, H. Sugawara, and S. Pakvasa, *Permutation Symmetries and The Fermion Mass Matrix*, Phys. Rev. **D25** (1982), 1895.

[133] T. Brown, N. Deshpande, S. Pakvasa, and H. Sugawara, *CP Nonconservation and Rare Processes in S_4 Model of Permutation Symmetry*, Phys. Lett. **B141** (1984), 95.

[134] T. Brown, S. Pakvasa, H. Sugawara, and Y. Yamanaka, *Neutrino Masses, Mixing and Oscillations in S_4 Model of Permutation Symmetry*, Phys. Rev. **D30** (1984), 255.

[135] D.-G. Lee and R. N. Mohapatra, *An $SO(10) \times S_4$ scenario for naturally degenerate neutrinos*, Phys. Lett. **B329** (1994), 463–468, hep-ph/9403201.

[136] E. Ma, *Neutrino mass matrix from S_4 symmetry*, Phys. Lett. **B632** (2006), 352–356, hep-ph/0508231.

[137] C. Hagedorn, M. Lindner, and R. N. Mohapatra, *S_4 flavor symmetry and fermion masses: Towards a grand unified theory of flavor*, JHEP **06** (2006), 042, hep-ph/0602244.

[138] Y. Cai and H.-B. Yu, *An SO(10) GUT Model with S_4 Flavor Symmetry*, Phys. Rev. **D74** (2006), 115005, hep-ph/0608022.

[139] F. Caravaglios and S. Morisi, *Gauge boson families in grand unified theories of fermion masses: E_6^4 x S_4* , Int. J. Mod. Phys. **A22** (2007), 2469–2492, hep-ph/0611078.

[140] H. Zhang, *Flavor $S_4 \times Z_2$ symmetry and neutrino mixing*, Phys. Lett. **B655** (2007), 132–140, hep-ph/0612214.

[141] Y. Koide, *S_4 Flavor Symmetry Embedded into SU(3) and Lepton Masses and Mixing*, JHEP **08** (2007), 086, 0705.2275.

[142] M. K. Parida, *Intermediate left-right gauge symmetry, unification of couplings and fermion masses in SUSY $SO(10) \times S_4$*, Phys. Rev. **D78** (2008), 053004, 0804.4571.

[143] C. S. Lam, *The Unique Horizontal Symmetry of Leptons*, Phys. Rev. **D78** (2008), 073015, 0809.1185.

[144] F. Bazzocchi and S. Morisi, *S_4 as a natural flavor symmetry for lepton mixing*, Phys. Rev. **D80** (2009), 096005, 0811.0345.

[145] H. Ishimori, Y. Shimizu, and M. Tanimoto, *S_4 Flavor Symmetry of Quarks and Leptons in SU(5) GUT*, Prog. Theor. Phys. **121** (2009), 769–787, 0812.5031.

[146] F. Bazzocchi, L. Merlo, and S. Morisi, *Phenomenological Consequences of See-Saw in S_4 Based Models*, Phys. Rev. **D80** (2009), 053003, 0902.2849.

[147] G. Altarelli, F. Feruglio, and L. Merlo, *Revisiting Bimaximal Neutrino Mixing in a Model with S_4 Discrete Symmetry*, JHEP **05** (2009), 020, 0903.1940.

[148] H. Ishimori, Y. Shimizu, and M. Tanimoto, *S_4 Flavor Model of Quarks and Leptons*, Prog. Theor. Phys. Suppl. **180** (2010), 61–71, 0904.2450.

[149] W. Grimus, L. Lavoura, and P. O. Ludl, *Is S_4 the horizontal symmetry of tri-bimaximal lepton mixing?*, J. Phys. **G36** (2009), 115007, 0906.2689.

[150] G.-J. Ding, *Fermion Masses and Flavor Mixings in a Model with S_4 Flavor Symmetry*, Nucl. Phys. **B827** (2010), 82–111, 0909.2210.

[151] D. Meloni, *A See-Saw S_4 model for fermion masses and mixings*, (2009), 0911.3591.

[152] B. Dutta, Y. Mimura, and R. N. Mohapatra, *An SO(10) Grand Unified Theory of Flavor*, (2009), 0911.2242.

[153] S. Morisi and E. Peinado, *An S_4 model for quarks and leptons with maximal atmospheric angle*, (2010), 1001.2265.

[154] I. de Medeiros Varzielas, S. F. King, and G. G. Ross, *Neutrino tri-bi-maximal mixing from a non-Abelian discrete family symmetry*, Phys. Lett. **B648** (2007), 201–206, hep-ph/0607045.

[155] E. Ma, *Near Tribimaximal Neutrino Mixing with* $\Delta(27)$ *Symmetry*, Phys. Lett. **B660** (2008), 505–507, 0709.0507.

[156] W. Grimus and L. Lavoura, *A model for trimaximal lepton mixing*, JHEP **09** (2008), 106, 0809.0226.

[157] C. Luhn, S. Nasri, and P. Ramond, *Simple Finite Non-Abelian Flavor Groups*, J. Math. Phys. **48** (2007), 123519, 0709.1447.

[158] F. Bazzocchi and I. de Medeiros Varzielas, *Tri-bi-maximal mixing in viable family symmetry unified model with extended seesaw*, Phys. Rev. **D79** (2009), 093001, 0902.3250.

[159] S. F. King and C. Luhn, *A new family symmetry for SO(10) GUTs*, Nucl. Phys. **B820** (2009), 269–289, 0905.1686.

[160] S. F. King and C. Luhn, *A Supersymmetric Grand Unified Theory of Flavour with PSL(2,7) x SO(10)*, (2009), 0912.1344.

[161] C. Luhn, S. Nasri, and P. Ramond, *Tri-Bimaximal Neutrino Mixing and the Family Symmetry* $Z_7 \rtimes Z_3$, Phys. Lett. **B652** (2007), 27–33, 0706.2341.

[162] C. Hagedorn, M. A. Schmidt, and A. Y. Smirnov, *Lepton Mixing and Cancellation of the Dirac Mass Hierarchy in SO(10) GUTs with Flavor Symmetries T7 and Sigma(81)*, Phys. Rev. **D79** (2009), 036002, 0811.2955.

[163] K.-S. Choi and J. E. Kim, *Quarks and leptons from orbifolded superstring*.

[164] T. Fukuyama, A. Ilakovac, T. Kikuchi, S. Meljanac, and N. Okada, *SO(10) group theory for the unified model building*, J. Math. Phys. **46** (2005), 033505, hep-ph/0405300.

[165] J. Kopp, M. Lindner, V. Niro, and T. E. J. Underwood, *On the Consistency of Perturbativity and Gauge Coupling Unification*, Phys. Rev. **D81** (2010), 025008, 0909.2653.

[166] M.-C. Chen and K. T. Mahanthappa, *Fermion masses and mixing and CP-violation in SO(10) models with family symmetries*, Int. J. Mod. Phys. **A18** (2003), 5819–5888, hep-ph/0305088.

[167] H. Georgi and C. Jarlskog, *A New Lepton - Quark Mass Relation in a Unified Theory*, Phys. Lett. **B86** (1979), 297–300.

[168] S. Dimopoulos and F. Wilczek, *Incomplete Multiplets in Supersymmetric Unified Models*, Print-81-0600 (SANTA BARBARA).

[169] Z. Chacko and R. N. Mohapatra, *A new doublet-triplet splitting mechanism for supersymmetric SO(10) and implications for fermion masses*, Phys. Rev. Lett. **82** (1999), 2836–2839, hep-ph/9810315.

[170] D.-G. Lee and R. N. Mohapatra, *Automatically R conserving supersymmetric SO(10) models and mixed light Higgs doublets*, Phys. Rev. **D51** (1995), 1353–1361, hep-ph/9406328.

[171] M. Quiros, *New ideas in symmetry breaking*, (2003), hep-ph/0302189.

[172] R. Dermisek and A. Mafi, *SO(10) grand unification in five dimensions: Proton decay and the mu problem*, Phys. Rev. **D65** (2002), 055002, hep-ph/0108139.

[173] H. D. Kim and S. Raby, *Unification in 5D SO(10)*, JHEP **01** (2003), 056, hep-ph/0212348.

[174] B. Kyae and Q. Shafi, *GUT scale and leptogenesis from 5D inflation*, Phys. Lett. **B556** (2003), 97–104, hep-ph/0211059.

[175] B. Kyae and Q. Shafi, *Inflation and leptogenesis with five dimensional SO(10)*, Phys. Rev. **D69** (2004), 046004, hep-ph/0212331.

[176] T. Asaka, W. Buchmuller, and L. Covi, *Gauge unification in six dimensions*, Phys. Lett. **B523** (2001), 199–204, hep-ph/0108021.

[177] L. J. Hall, Y. Nomura, T. Okui, and D. Tucker-Smith, *SO(10) unified theories in six dimensions*, Phys. Rev. **D65** (2002), 035008, hep-ph/0108071.

[178] L. J. Hall, J. March-Russell, T. Okui, and D. Tucker-Smith, *Towards a theory of flavor from orbifold GUTs*, JHEP **09** (2004), 026, hep-ph/0108161.

[179] C. H. Albright and S. M. Barr, *Lifting a realistic SO(10) grand unified model to five dimensions*, Phys. Rev. **D67** (2003), 013002, hep-ph/0209173.

[180] R. Kitano and T.-j. Li, *Flavor hierarchy in SO(10) grand unified theories via 5- dimensional wave-function localization*, Phys. Rev. **D67** (2003), 116004, hep-ph/0302073.

[181] Q. Shafi and Z. Tavartkiladze, *Neutrino democracy and other phenomenology from 5D SO(10)*, Nucl. Phys. **B665** (2003), 469–486, hep-ph/0303150.

[182] W. Grimus and L. Lavoura, *A discrete symmetry group for maximal atmospheric neutrino mixing*, Phys. Lett. **B572** (2003), 189–195, hep-ph/0305046.

[183] J. S. Lomont, *Applications of Finite Groups*.

[184] A. Blum, C. Hagedorn, and M. Lindner, *Fermion Masses and Mixings from Dihedral Flavor Symmetries with Preserved Subgroups*, Phys. Rev. **D77** (2008), 076004, 0709.3450.

[185] A. Merle and W. Rodejohann, *The elements of the neutrino mass matrix: Allowed ranges and implications of texture zeros*, Phys. Rev. **D73** (2006), 073012, hep-ph/0603111.

[186] M. Maltoni, T. Schwetz, M. A. Tortola, and J. W. F. Valle, *Status of global fits to neutrino oscillations*, New J. Phys. **6** (2004), 122, hep-ph/0405172.

[187] S. Hannestad, *Primordial Neutrinos*, Ann. Rev. Nucl. Part. Sci. **56** (2006), 137–161, hep-ph/0602058.

[188] C. Aalseth et al., *Neutrinoless double beta decay and direct searches for neutrino mass*, (2004), hep-ph/0412300.

[189] V. M. Lobashev, *The search for the neutrino mass by direct method in the tritium beta-decay and perspectives of study it in the project KATRIN*, Nucl. Phys. **A719** (2003), 153–160.

[190] W. Maneschg, A. Merle, and W. Rodejohann, *Statistical Analysis of future Neutrino Mass Experiments including Neutrino-less Double Beta Decay*, Europhys. Lett. **85** (2009), 51002, 0812.0479.

[191] S. Pascoli and S. T. Petcov, *The SNO solar neutrino data, neutrinoless double-beta decay and neutrino mass spectrum*, Phys. Lett. **B544** (2002), 239–250, hep-ph/0205022.

[192] S. Pascoli and S. T. Petcov, *Addendum: The SNO Solar Neutrino Data, Neutrinoless Double Beta-Decay and Neutrino Mass Spectrum*, Phys. Lett. **B580** (2004), 280–289, hep-ph/0310003.

[193] S. Pascoli, S. T. Petcov, and T. Schwetz, *The Absolute Neutrino Mass Scale, Neutrino Mass Spectrum, Majorana CP-Violation and Neutrinoless Double-Beta Decay*, Nucl. Phys. **B734** (2006), 24–49, hep-ph/0505226.

[194] S. Antusch, S. F. King, M. Malinsky, L. Velasco-Sevilla, and I. Zavala, *Flavon Inflation*, Phys. Lett. **B666** (2008), 176–180, 0805.0325.

[195] C. Hagedorn, *Flavored model building*, Ph.D. thesis, Technische Universität München, München, jan 2008.

[196] A. S. Blum, *Dihedral flavor symmetries*, Ph.D. thesis, Ruprecht-Karls Universität, Heidelberg, Germany, jun 2009.

[197] P. H. Frampton and A. Rasin, *Nonabelian discrete symmetries, fermion mass textures and large neutrino mixing*, Phys. Lett. **B478** (2000), 424–433, hep-ph/9910522.

[198] W. Grimus and G. Ecker, *Basic transformations in generation space and a criterion for the existence of standard forms for unitarily congruent matrices*, J. Phys. **A21** (1988), 2825.

[199] M. Frigerio, S. Kaneko, E. Ma, and M. Tanimoto, *Quaternion family symmetry of quarks and leptons*, Phys. Rev. **D71** (2005), 011901, hep-ph/0409187.

[200] T. Asaka, W. Buchmuller, and L. Covi, *Exceptional coset spaces and unification in six dimensions*, Phys. Lett. **B540** (2002), 295–300, hep-ph/0204358.

[201] A. Hebecker and J. March-Russell, *The structure of GUT breaking by orbifolding*, Nucl. Phys. **B625** (2002), 128–150, hep-ph/0107039.

[202] T. Asaka, W. Buchmuller, and L. Covi, *Bulk and brane anomalies in six dimensions*, Nucl. Phys. **B648** (2003), 231–253, hep-ph/0209144.

[203] E. A. Mirabelli and M. E. Peskin, *Transmission of supersymmetry breaking from a 4-dimensional boundary*, Phys. Rev. **D58** (1998), 065002, hep-th/9712214.

[204] F. Bazzocchi, L. Merlo, and S. Morisi, *Fermion Masses and Mixings in a S_4-based Model*, Nucl. Phys. **B816** (2009), 204–226, 0901.2086.

[205] B. Dutta, Y. Mimura, and R. N. Mohapatra, *Origin of Quark-Lepton Flavor in SO(10) with Type II Seesaw*, Phys. Rev. **D80** (2009), 095021, 0910.1043.

[206] S. Antusch, J. Kersten, M. Lindner, and M. Ratz, *Running neutrino masses, mixings and CP phases: Analytical results and phenomenological consequences*, Nucl. Phys. **B674** (2003), 401–433, hep-ph/0305273.

[207] V. Barger, P. Langacker, M. McCaskey, M. J. Ramsey-Musolf, and G. Shaughnessy, *LHC Phenomenology of an Extended Standard Model with a Real Scalar Singlet*, Phys. Rev. **D77** (2008), 035005, 0706.4311.

[208] J. F. Gunion, H. E. Haber, G. L. Kane, and S. Dawson, *The Higgs Hunter's Guide*, SCIPP-89/13.

[209] H. E. Haber and D. O'Neil, *Basis-independent methods for the two-Higgs-doublet model. II: The significance of tan(beta)*, Phys. Rev. **D74** (2006), 015018, hep-ph/0602242.

[210] R. Diaz, R. Martinez, and J. A. Rodriguez, *Lepton flavor violation in the two Higgs doublet model type III*, Phys. Rev. **D63** (2001), 095007, hep-ph/0010149.

[211] A. Blum and A. Merle, *General Conditions for Lepton Flavor Violation at Tree- and 1-Loop Level*, Phys. Rev. **D77** (2008), 076005, 0709.3294.

[212] M. Raidal et al., *Flavour physics of leptons and dipole moments*, Eur. Phys. J. **C57** (2008), 13–182, 0801.1826.

[213] D. Aristizabal Sierra, J. Kubo, D. Restrepo, D. Suematsu, and O. Zapata, *Radiative seesaw: Warm dark matter, collider and lepton flavour violating signals*, Phys. Rev. **D79** (2009), 013011, 0808.3340.

[214] M. Lindner, A. Merle, and W. Rodejohann, *Improved limit on θ_{13} and implications for neutrino masses in neutrino-less double beta decay and cosmology*, Phys. Rev. **D73** (2006), 053005, hep-ph/0512143.

[215] D. Suematsu, T. Toma, and T. Yoshida, *Reconciliation of CDM abundance and $\mu \to e\gamma$ in a radiative seesaw model*, Phys. Rev. **D79** (2009), 093004, 0903.0287.

[216] E. M. Dolle and S. Su, *The Inert Dark Matter*, Phys. Rev. **D80** (2009), 055012, 0906.1609.

[217] D. Eriksson, J. Rathsman, and O. Stal, *2HDMC - Two-Higgs-Doublet Model Calculator Physics and Manual*, Comput. Phys. Commun. **181** (2010), 189–205, 0902.0851.

[218] M. Hirsch, S. Morisi, and J. W. F. Valle, *Tri-bimaximal neutrino mixing and neutrinoless double beta decay*, Phys. Rev. **D78** (2008), 093007, 0804.1521.

[219] M. C. Gonzalez-Garcia and M. Maltoni, *Phenomenology with Massive Neutrinos*, Phys. Rept. **460** (2008), 1–129, 0704.1800.

[220] A. Raspereza, *Higgs search results*, (2002), hep-ex/0209021.

[221] W. Grimus, L. Lavoura, O. M. Ogreid, and P. Osland, *A precision constraint on multi-Higgs-doublet models*, J. Phys. **G35** (2008), 075001, 0711.4022.

[222] L. Lavoura, *General formulae for $f_1 \to f_2\gamma$*, Eur. Phys. J. **C29** (2003), 191–195, hep-ph/0302221.

[223] R. Kitano, M. Koike, and Y. Okada, *Detailed calculation of lepton flavor violating muon electron conversion rate for various nuclei*, Phys. Rev. **D66** (2002), 096002, hep-ph/0203110.

[224] J. C. Pati and A. Salam, *Lepton Number as the Fourth Color*, Phys. Rev. **D10** (1974), 275–289.

[225] R. N. Mohapatra and J. C. Pati, *Left-Right Gauge Symmetry and an Isoconjugate Model of CP Violation*, Phys. Rev. **D11** (1975), 566–571.

[226] G. Senjanovic and R. N. Mohapatra, *Exact Left-Right Symmetry and Spontaneous Violation of Parity*, Phys. Rev. **D12** (1975), 1502.

[227] R. N. Mohapatra and G. Senjanovic, *Neutrino Masses and Mixings in Gauge Models with Spontaneous Parity Violation*, Phys. Rev. **D23** (1981), 165.

[228] N. G. Deshpande, J. F. Gunion, B. Kayser, and F. I. Olness, *Left-right symmetric electroweak models with triplet Higgs*, Phys. Rev. **D44** (1991), 837–858.

[229] W. Konetschny and W. Kummer, *Nonconservation of Total Lepton Number with Scalar Bosons*, Phys. Lett. **B70** (1977), 433.

[230] T. P. Cheng and L.-F. Li, *Neutrino Masses, Mixings and Oscillations in $SU(2) \times U(1)$ Models of Electroweak Interactions*, Phys. Rev. **D22** (1980), 2860.

[231] G. Lazarides, Q. Shafi, and C. Wetterich, *Proton Lifetime and Fermion Masses in an SO(10) Model*, Nucl. Phys. **B181** (1981), 287.

[232] J. Schechter and J. W. F. Valle, *Neutrino Masses in $SU(2) \times U(1)$ Theories*, Phys. Rev. **D22** (1980), 2227.

[233] N. Haba and H. Murayama, *Anarchy and hierarchy*, Phys. Rev. **D63** (2001), 053010, hep-ph/0009174.

[234] SINDRUM II., C. Dohmen et al., *Test of lepton flavor conservation in $\mu \to e$ conversion on titanium*, Phys. Lett. **B317** (1993), 631–636.

[235] MEGA, M. L. Brooks et al., *New Limit for the Family-Number Non-conserving Decay $\mu^+ \to e^+\gamma$*, Phys. Rev. Lett. **83** (1999), 1521–1524, hep-ex/9905013.

[236] H. V. Klapdor-Kleingrothaus and U. Sarkar, *Neutrinoless double beta decay with scalar bilinears*, Phys. Lett. **B554** (2003), 45–50, hep-ph/0211274.

[237] E. Ma, *Neutrino mass, dark matter, and leptogenesis*, Nucl. Phys. Proc. Suppl. **168** (2007), 347–349, hep-ph/0611181.

[238] P.-H. Gu and U. Sarkar, *Pathways to testable leptogenesis*, (2008), 0811.0956.

[239] S. Davidson, E. Nardi, and Y. Nir, *Leptogenesis*, Phys. Rept. **466** (2008), 105–177, 0802.2962.

[240] A. J. Buras, S. Jager, and J. Urban, *Master formulae for $\Delta F = 2$ NLO-QCD factors in the standard model and beyond*, Nucl. Phys. **B605** (2001), 600–624, hep-ph/0102316.

[241] D. Becirevic et al., *$B_d - \bar{B}_d$ mixing and the $B_d \to J/\psi K_s$ asymmetry in general SUSY models*, Nucl. Phys. **B634** (2002), 105–119, hep-ph/0112303.

[242] Y. Zhang, H. An, X. Ji, and R. N. Mohapatra, *General CP Violation in Minimal Left-Right Symmetric Model and Constraints on the Right-Handed Scale*, Nucl. Phys. **B802** (2008), 247–279, 0712.4218.

[243] N. Tantalo, *Lattice calculations for B and K mixing*, (2007), hep-ph/0703241.

[244] D. Becirevic, V. Gimenez, G. Martinelli, M. Papinutto, and J. Reyes, *B-parameters of the complete set of matrix elements of $\Delta B = 2$ operators from the lattice*, JHEP **04** (2002), 025, hep-lat/0110091.

[245] W. Buchmuller, R. Catena, and K. Schmidt-Hoberg, *Small Extra Dimensions from the Interplay of Gauge and Supersymmetry Breaking*, Nucl. Phys. **B804** (2008), 70–89, 0803.4501.